Université Libre de Bruxelles

Faculté des Sciences appliquées

Tomsk State University

Physics faculty

Investigation of the dynamics of physical systems by supersymmetric quantum mechanics

Thèse présentée en vue de l'obtention du titre
de Docteur en Sciences de l'Ingénieur par

Andrey M Pupasov

April 2010

Contents

Foreword

This thesis was written under a joint PhD work supervision. I was registered as a PhD student in both the Tomsk State University in Russia and the Université Libre de Bruxelles in Belgium. Boris Samsonov and Jean-Marc Sparenberg were my PhD directors at TSU and ULB, respectively. One of the main reasons for such a collaboration was our desire to combine the notably theoretical style of the Russian part and the high physical experience of the Belgian part.

According to the joint PhD agreement there are two versions of the thesis: one in Russian, one in English. The English version contains all subjects included in the Russian version, but it is not a direct translation. I slightly modified the structure of the thesis trying to improve the text.

The results of the thesis were reported and discussed at the seminar of the Departments of Theoretical Physics and Quantum Field Theory, Tomsk State University. The main results were communicated at the following international conferences and seminars.
Oral presentations:
1. Six international conference "Symmetry in nonlinear mathematical physics", Kiev, Ukraine, 2005,
2. International school-seminar "Recent problems of theoretical and mathematical physics, Volga XV", Kazan, Russia, 2006,
3. International school-seminar "Quantum Field Theory and Gravity", Tomsk, Russia, 2007,
4. BRIX workshop, Mol, Belgium, 2008,
5. XXVII International colloquium on group theoretical methods in physics, Yerevan, Armenia, 2008,
6. BPS General Scientific Meeting, Universiteit Hasselt, Belgium, 2009.
Co-author:
1. International Workshop "Pseudo-Hermitian Hamiltonians in Quantum Physics", Istanbul, Turkey, 2005,
2. International Conference on Inverse Quantum Scattering Theory, Siofok, Hungary, 2007,

There were ten papers published during my work on the thesis which contain all essential results [1–10].

Introduction

Recently, the interest for the low energy quantum systems has increased due to the impressive experimental progress in condensed matter physics (BEC [11–13], cold atom-atom collisions [14,15]), nuclear physics (low energy nuclear collisions, investigation of exotic nuclei, nuclear astrophysics [16–19]), quantum optics [20] and quantum computing [21]. In many important cases it is possible to investigate the corresponding physical problem in terms of the one particle Schrödinger equation with an effective potential. For example, consider a collision of two compound particles, say an atom-atom collision. The full quantum mechanical description should include all possible configurations of constituents, but in a first approximation we may consider these atoms like two point particles which interacts through a potential. This last problem may be transformed into a set of radial Schrödinger equations by performing a partial wave decomposition. Next, the internal structure of colliding particles leads to different possible asymptotic states (so-called channels) which in our example correspond to the different excited states. Only a few channels and partial waves a play role at low energies. An outgoing asymptotic state may differ from the ingoing one, which means that the collision process leads to the modification of the internal structure. This situation corresponds to coupled channels. Many low energy quantum processes can be described by the system of N coupled radial Schrödinger equations [22, 23]. In this thesis, we will work with such Schrödinger equations ($N = 1, 2, \ldots$) bearing in mind the physical interpretation given above.

One of the important theoretical problems concerns the studying of the dynamics or the time evolution of a system described by such a Schrödinger equation. For example, one may try to find how wave packets propagate in a given potential [24, 25]. Mathematically, it is necessary to solve the Cauchy problem for the time-dependent Schrödinger equation, for instance, by finding the corresponding propagator [26, 27].

Often, such a detailed description of the evolution is not necessary. It is sufficient to know the so-called scattering matrix which contains transition amplitudes from the initial to the final scattering states [22, 23]. As far as scattering is concerned we should distinguish two equally interesting and important problems. On the one hand, the calculation of the scattering matrix (or any analogous object) for a given interaction potential is called the direct scattering problem [22, 23]. On the other hand, the inverse scattering problem consists in restoring the potential from given scattering properties (e.g., scattering matrix) [28].

Let us stress the importance of exact analytical solutions of the Cauchy problem and of both the direct and the inverse scattering problems in quantum mechanics. Exact analytical results are important for a better understanding of the underlying quantum phenomena. These analytical results may also be useful in order to test existing numerical methods [29, 30], especially in the multi-channel case [31].

In this thesis we will study propagators of the time-dependent Schrödinger equation and investigate coupled-channel scattering problems with the help of algebraic technique emerged in so-called supersymmetric quantum mechanics. Let us first describe in words these three subjects. The rigorous mathematical definitions will be given in the first chapter.

Propagators in quantum mechanics

The space-time evolution of a quantum mechanical system is governed by its Schrödinger equation and in its most complete form it is encoded in the propagator [26]. To be precise we should note

that we use the term propagator for the Green function of the time-dependent Schrödinger equation to distinguish it from the term Green function which is used for the stationary Schrödinger equation. Both the propagator and the Green function are the fundamental solutions of the time-dependent and stationary Schrödinger equations, respectively.

The propagator defines the probability amplitude for a particle to move from one point of the space to another in a given time. Similar to propagators in relativistic field theories, it provides a global picture of the causal structure of a quantum system which goes beyond the information contained in a single wave function. Propagators play an essential role in solving the probability related Cauchy problem of Quantum Mechanics [26, 27]. Moreover, with the aid of the propagator one can obtain other important objects. For instance, applying Wick rotation $t \to i\beta$ to a propagator leads to the statistical sum of the underlying system thus providing a link between quantum and statistical mechanics. The exact expression for the propagator may be used to obtain pq, qp and Weyl symbols of the evolution operator [32].

There are several methods to calculate propagators. The straightforward technique is based on the decomposition of the propagator in terms of a basis. This method leads to two problems: how to find the coefficients and how to calculate the sum. Another method is based on the path-integral representation of the propagator. Roughly speaking, path integration gives the exact answer for the case of quadratic Hamiltonians, whereas for the general case one should use the perturbative technique. The first order correction coincides with the result obtained from the well-known WKB method [26]. To calculate exact propagators one can use symmetry properties of the system. The corresponding general method was developed in [33], where the exact propagators for quadratic Hamiltonians were calculated as an illustration. The vast literature on propagators, summarized e.g. in [34], lists mainly explicit expressions of propagators for Schrödinger equations in one space dimension which are reducible to hypergeometric differential equations or their confluent forms.

The interest in new exact propagators is less motivated by their mere existence or their technical subtleties than by their applicability to concrete physical problems. For example, in [35] exact propagators for quadratic systems were applied to study multi-dimensional systems and magnetic properties of ideal gases. As far as applications are concerned, propagation of a short laser pulse in the paraxial approximation may be described by time-dependent Schrödinger equation [36,37]. The propagator is also used to study the behaviour of light in meta materials [25]. Exact propagators for non-Hermitian Hamiltonians may be interested in view of decaying systems [38].

It is known that the propagator of the time-dependent Schrödinger equation is related to the Green function of the stationary Schrödinger equation by Fourier transformation. The Green functions are used in different quantum problems. For instance, inhomogeneous Schrödinger equations may be treated by using Green functions. Inhomogeneous equations cover two important classes of problems. The first class is the perturbation theory. The second class deals with reactions (creation and annihilation of particles). In this case inhomogeneity plays the role of a source (outlet) of particles [39]. Note that the method of the Green function is an important ingredient in the quantum field theory also. In this work we restrict ourselves to Green functions of the stationary Schrödinger equation.

Coupled-channel scattering problems

Almost all low-energy collisions of microparticles with an internal structure (i.e., atom-atom,

nucleus-nucleus, etc) include inelastic processes such as excitations of internal degrees of freedom of colliding particles or processes with rearrangements of their constituent parts. These processes can be described by a matrix (more precisely multichannel) Schrödinger equation with a local matrix potential [22, 23] in the framework of the coupled-channel scattering theory. The main idea of the scattering theory is that the colliding particles are supposed to move freely at large distances. This asymptotic behavior is encoded by the ingoing and outgoing states. Roughly speaking, to describe the collision process one should find the operator which transforms ingoing states into outgoing states. This operator is nothing but the scattering matrix S mentioned above.

The widespread point about the scattering matrix is that its poles (for negative energies $E < 0$) correspond to the bound states of the system. It is actually not always true. To establish whether a pole corresponds to a bound state or not we should either solve the Schrödinger equation at this energy to look at the wave function or decompose the scattering matrix in terms of the so-called Jost matrix, $S(k) \sim F^{-1}(k)F(-k)$, where k is the momentum. Then, the zeros of the Jost matrix determinant correspond to the bound states of the system, whereas poles of the Jost matrix elements do not. The Jost matrix can be found independently of the scattering matrix. In the thesis, we will use the Jost matrix as a basic object.

One can distinguish the coupled-channel scattering with different and equal thresholds. An example of the coupled-channel scattering with different channel thresholds is the scattering of atoms of alkali metal in a background magnetic field. The presence of the magnetic field results in different energies for the different possible spin-configurations of the outer s-electron and the nucleus. Thus channels with different threshold energies appear. Low energy neutron-proton scattering gives an example of two-channel scattering with equal thresholds, because one should take into account uncoupled channels ${}^1S_0$, ${}^1P_1$, ..., and coupled channels ${}^3S_1 - {}^3D_1$, ${}^3P_2 - {}^3F_2$, ... These two examples will be considered in details in the third and fourth chapters, respectively.

In principle, the scattering matrix may be defined from the collision experiments. Hence, one can raise the inverse scattering problem about determination of the interacting potential [28]. Part of the problem was solved in works of Gelfand, Levitan, Marchenko, Jost. They formulated prescriptions for both the single- and coupled-channel cases of how to construct the integral equation which allows to find the potential from the Jost or the scattering matrix [40–43]. They also found some exact solutions of the equation, in particular, for single-channel problems in the case of separable kernel. The search of alternative approaches to the inversion continues, especially for the coupled-channel problems [44, 45].

Regarding the coupled-channel inverse scattering problem we should mention one important result that serves as an intermediate point in developing any inversion technique. In [46] Cox derives an exactly-solvable coupled-channel potential with threshold differences, two remarkable features of which are the compact expressions provided both for the potential and for its Jost matrix. Since the Jost matrix completely defines the bound- and scattering-state properties of a potential model [23, 47], such an analytical expression seems very promising in the context of the scattering inverse problem.

The work of Cox has however received little attention, probably because it is plagued by two problems. First, the way of getting the potential is rather complicated and mysterious: the paper mostly consists in a check that the provided analytical expression for the solutions satisfies the coupled-channel Schrödinger equation with the provided analytical expression for the potential. Not much information is given on how these expressions were obtained, which makes any generalization of the method impossible. The second problem, already stressed in [46], is that, despite the compact

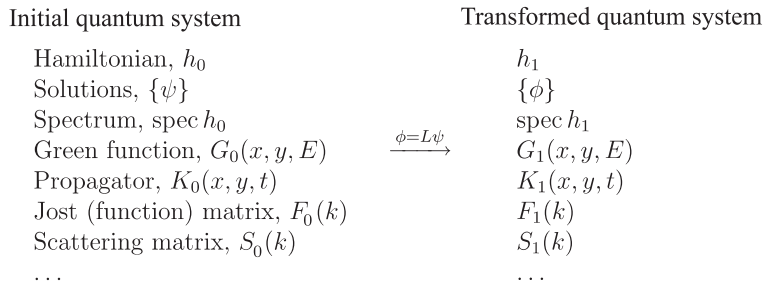

Figure 1: The diagram illustrates the principle of supersymmetric transformations

expression of the Jost matrix, calculating the corresponding bound- and resonant-state properties is a difficult task because these states correspond to zeros of the determinant of the Jost matrix in the intricate structure of the energy Riemann sheet, which has a multiplicity 2^N for N channels.

The first problem was solved recently, when it was realized that the Cox potential, at least in its simplest form ($q = 1$ in [46]), can be obtained by a single supersymmetric transformation of the zero potential [48, 49]. It is not exaggerated to say that this result was one of the main impulse for my work in the coupled-channel inversion by supersymmetric quantum mechanics. Now we are in a position to get acquainted with this remarkable method.

Supersymmetric quantum mechanics (SUSY QM)

In general, physical systems are described by differential equations. This raises the problem of finding their solutions. One of the natural idea about solving is to transform equations with unknown solutions to a much simpler form and in the ideal case to an equation with known solutions. Particulary, studying of the transformations which preserve the equation gives us information about its symmetries. This information helps a lot in finding the solutions.

Note that we can invert this logic. Consider a set of all one-dimensional Schrödinger equations. A representative of this set is totally determined by the potential. Starting from a given exactly solvable potential we may apply all possible transformations (maybe with a fixed type, like differential transformations) modifying this potential. As a result we find the class of potentials associated with the given exactly solvable problem. If we can describe this class in some general and foreseeable terms, then we know all equations reducible to the initial exactly solvable equation.

In this thesis we will use the method of supersymmetric quantum mechanics which is entirely based on the idea of differential transformations. Historically, SUSY QM was introduced by Witten [50] as a simple QFT model to study supersymmetry breaking. A little bit later, the links between SUSY QM, Darboux transformations [51] and the factorization method of Infeld and Hull [52, 53] were established [54, 55]. Many exactly solvable quantum models were discovered in the framework of SUSY QM [56–59].

Supersymmetric quantum mechanics gives us useful lessons of the "quantum intuition". We learn how to modify a potential to make very precise spectrum modification. We also learn how to modify transition and reflection coefficients, scattering phases etc. Boris Zahariev is known as the popularizer of the conception of quantum intuition (see for example book [60] and references therein).

In figure 1 we give the general diagram of the supersymmetric transformations in quantum

mechanics. The differential operator L transforms the solutions of the initial Schrödinger equation into the solutions of the final Schrödinger equation. This transformation induces definite relations between Hamiltonians, its spectra and other auxiliary objects. We will distinguish conservative and non-conservative SUSY transformations. Conservative SUSY transformations map wave functions to wave functions, whereas non-conservative SUSY transformations always map wave functions to some unphysical solutions. As a result, spectra of the initial and transformed systems are almost identical for the conservative SUSY. The other way round, non-conservative SUSY changes the spectrum totally. More precisely, no one spectral point of the initial Hamiltonian belongs to the spectrum of the transformed Hamiltonian. As a result, a supersymmetry algebra, which is always present in the case of conservative SUSY transformations, cannot actually be constructed here and the word 'SUSY transformation' is only a formal heritage from the previous conservative case. Previously, more attention was payed to the conservative transformation only.

Obviously, we can use Hamiltonian h_1 (see figure 1) as the initial Hamiltonian for a new SUSY transformation. Thus we obtain chains of SUSY transformations. These chains lead to quantum models with so-called polynomial super algebras [57, 61–63]. Some deformed SUSY algebras and its applications were considered in [64–67]. An interesting class of potentials appearing in SUSY QM is called shape invariant potentials [68]. For the moment ten shape-invariant potentials are known [56]. All these potentials are widely used in mathematical physics. Most of the works in the field of SUSY QM deals with the one dimensional case. Note that a multi-dimensional generalization of SUSY QM was constructed in works [54, 69] using the formalism of the superspace.

Another exotic field where SUSY QM is effectively applied is known as $\mathcal{CPT}$ quantum mechanics (or the complex generalization of quantum mechanics). It was presumed that SUSY QM may become an essential ingredient of the infant complex quantum mechanics because of its nice property to convert a non-diagonalizable Hamiltonian into diagonalizable forms and to delete spectral singularities from the continuous spectrum of a non-Hermitian Hamiltonian [70–76].

As we mentioned above, SUSY transformations induce relations between corresponding auxiliary objects (see figure 1). The study of these objects was very unbalanced. For instance, the transformation properties of the fundamental solutions like the propagators and the Green functions were not studied in details.

Regarding propagators, probably there was only one work by Jauslin [77] who constructed a general integral transformation scheme simultaneously for propagators of the Schrödinger equations and for heat equations, but who did not provide a discussion of convergency and divergency of the derived expressions. Moreover his expressions are rather involved, which implies that he can only calculate explicitly the propagator of the so-called one-soliton potential generated by the first order SUSY. For the sake of convergency he applied his technique to the heat-equation-type Fokker-Planck equation only. In general, this result may be extended via Wick rotation to propagators for Schrödinger equations of a free particle and a particle moving through transparent potentials. But the question of convergency and with it the question of solvability remains to be clarified. Another indication that the problem may be solvable has been provided by Refs [1, 2] where a similar model has been analyzed at the level of Green functions of stationary Schrödinger equations. Approximate methods to calculate propagators in SUSY QM were proposed in [78, 79].

In the case of the SUSY transformation which removes the ground state of the initial Hamiltonian, Sukumar has studied an integral relation between the Green functions for SUSY partners. He has formulated conditions leading to the vanishing of some matrix elements of a Hamiltonian and related this property to a hidden supersymmetry of the system [80]. The transformation of

the Green function is not explicitly discussed in that paper.

Speaking about the applications of supersymmetric transformations, we should mention quantum scattering theory [22, 23]. Supersymmetric transformations are a powerful tool to manipulate the scattering properties of one-dimensional (single-channel) quantum systems. Briefly speaking, this possibility appears due to the simple transformation of the scattering matrix under a SUSY transformation. The scattering matrix is multiplied by a rational function of the momentum [81–85]. The iteration of SUSY transformations may be used to solve the inverse scattering problem. This idea was proposed in works of Sukumar [81]. The effectiveness of SUSY transformations in the inversion of scattering data is demonstrated in [83–85]. This approach to the scattering inversion is more efficient [85] comparing with the integral transformations of Gelfand-Levitan and Marchenko just because of the differential character of the transformation.

There are several papers devoted to supersymmetric transformations for multichannel problems [48, 86–92]. Arbitrary chains of first-order SUSY transformations in the case of the matrix Schrödinger equation are studied in [93]. There, a compact expressions for both the transformed matrix potential and solutions were obtained.

It should be noted that methods based on a direct generalization of the SUSY technique to the multichannel case are not able to provide an easy control of the scattering properties for all channels simultaneously. For instance, in the two-channel case, the S-matrix is parameterized by the eigenphase shifts $\delta_1(k)$, $\delta_2(k)$ and mixing parameter $\epsilon(k)$, where k is the wave number. Usual SUSY transformations modify these three quantities in a complicated way, which makes their individual control difficult. We believe that this is the reason why SUSY transformations did not find a wide application to multichannel scattering inversion.

An important ingredient of the supersymmetric inversion technique are the phase-equivalent SUSY transformations, which are based on two-fold, or second-order, differential operators. These are described in [94–96] for the single-channel case and in [91, 92] for the coupled-channel case. Such transformations keep the scattering matrix unchanged and simultaneously allow to reproduce given bound state properties. However these intermediate results are still far from an effective SUSY-based inversion in the coupled-channel case.

A full review of SUSY QM and of its applications goes beyond this introduction. However, the areas mentioned above, where SUSY QM is effectively applied, indicate the great potential of the approach. In the present work, we use the advantages of SUSY-based methods to investigate the dynamics of quantum systems both in the single- and multi-channel cases. We will concentrate on the following questions. First of all, we will study SUSY transformations of the Green functions and propagators of the single-channel Schrödinger equation. Besides usual time-independent SUSY partner potentials we will consider non-stationary potentials and non-Hermitian potentials. Note that open and dissipative systems may be described by the Schrödinger equation with non-Hermitian Hamiltonian [97].

Secondly, we pay attention to the coupled-channel models in the framework of SUSY QM. We will study SUSY transformations between diagonal matrix Hamiltonians (trivial coupling) and coupled Hamiltonians. Thus several new nontrivially coupled potentials will be obtained. The spectral and the scattering properties of the transformed models will also be studied in details.

Structure of the thesis

In the first chapter, we make all the necessary preparations. In the first section, we introduce notations and recall some important properties of the single- and coupled-channel Schrödinger equations. The definitions of the propagator, the Green function, the scattering and the Jost matrices are given. The other sections are devoted to a review of the SUSY transformations in quantum mechanics. The SUSY transformations are introduced in the standard framework of the differential transformation operators. This approach is very convenient when one works with the polynomial generalization of SUSY transformations. The first and the second order transformations are building blocks for high-order transformations, therefore these cases are considered in details. We also consider SUSY transformations of the time-dependent Schrödinger equation. The end of the chapter is devoted to the explicit construction of exactly solvable models which will be treated below.

In the second chapter, we consider SUSY transformations of the fundamental solutions (Green functions and propagators) for the single-channel problems. First of all, we deduce relations between Green functions for the potentials interrelated by the first and the second order SUSY transformations. Moreover, we recalculate the Sukumar "trace formula" obtained in [80]. In the case of scattered potentials we have found a correction to this formula [80]. We give a simple interpretation of this correction in terms of the norm of the scattering states.

In the second section, we formulate and prove several theorems about propagators for SUSY partner potentials. We begin with the relations between propagators induced by the simplest first order SUSY transformation. Then we generalize this result to the case of N-th order SUSY transformation.

In the third section, these results are used to calculate explicit expressions for propagators and a number of new exact Green functions. We consider models in the finite interval, the soliton potentials and potentials with the quasi-equidistant spectrum. Calculations of propagators for non-Hermitian and time-dependent potentials are demonstrated in simple examples of the time-dependent soliton potential and a complex isospectral deformation of the harmonic oscillator.

The third chapter is devoted to the coupled-channel problems with different thresholds. In this chapter, we restrict our consideration by s-wave only. The case of different thresholds requires non-conservative SUSY transformations [48] which lead to a new derivation of the Cox potential [46]. We give a qualitative analysis of its spectrum for arbitrary number of channels and find the exact spectrum for two channels thus correcting Cox' wrong statement about the spectrum of this model. Our analysis is based on the analytical expressions for the Jost and scattering matrices obtained through SUSY transformations. The information about the spectrum and scattering properties allows us to construct a model of magnetic-induced Feshbach resonance for the atoms of alkali metals.

In the fourth chapter, coupled-channel problems with equal thresholds and arbitrary partial waves are studied. We start with the most general first order (conservative) SUSY transformation and study the properties of the transformed model in details. This analysis allows us to conclude that at least second order SUSY transformations are needed. As a result, we introduce new *eigenphase preserving* SUSY transformations. It is necessary to stress the difference between this new kind of transformation and the well-known phase-equivalent transformations mentioned above. A phase-equivalent transformation does not modify the scattering matrix at all, whereas the eigen-

phase preserving transformation modifies the mixing between channels. An important consequence of that is the possibility to use single-channel SUSY transformations to fit experimental values of the eigenphase shifts. Afterwards, the mixing parameter can be fitted without further modification of the eigenphase shifts. This approach to the inversion is demonstrated by constructing a phenomenological neutron-proton potential.

In the conclusion, we summarize the main results, discuss possible applications of the presented methods and formulate some feasible lines of future investigations.

Chapter 1

Supersymmetry of the Schrödinger equation

1.1 The Schrödinger equation

1.1.1 Single-channel case

We are interested in the non-relativistic quantum mechanics. Hence, we work with the Schrödinger equation. Let us start with the simplest one dimensional time-dependent Schrödinger equation in the reduced units

$$(i\partial_t - h_0)\Psi(x,t) = 0\,, \qquad x \in (a,b)\,, \tag{1.1.1}$$

where $h_0 = -\partial_x^2 + V_0(x,t)$ is the Hamiltonian. This equation describes a quantum particle which moves in the potential $V_0(x,t)$ inside the interval (a,b). In the present work, we will consider both stationary, $V_0(x)$, and time-dependent, $V_0(x,t)$, potentials. Usually in quantum mechanics one works with Hermitian Hamiltonians only. This implies that potential V_0 is a real function (this holds through the whole text, except for section 2.2.7). The wave function $\Psi(x,t)$ defines the probability distribution for the particle in (a,b)

$$\rho(x,t) = |\Psi(x,t)|^2\,. \tag{1.1.2}$$

Using (1.1.1) and complex conjugated equation (note that V_0 is real) one can find that the total probability is conserved

$$\frac{\partial}{\partial t}\int_a^b |\Psi(x,t)|^2 dx = 0\,,$$

hence, we can normalize the wave function to get unit probability, $\int_a^b \rho(x,t)dx = 1$.

Assume for simplicity that the potential is stationary (we work with time-dependent potentials in section 2.2.6, where corresponding changes in the formalism are considered in details). As a result the energy of the particle is conserved.

The Cauchy problem for the time-dependent equation (1.1.1) is to find the wave function $\Psi(x,t)$ evolving from an initial configuration $\Psi(x,0) = \Psi_0(x)$. The solution of this problem may be given with the help of the so-called propagator $K_0(x,y,t)$ of the time-dependent Schrödinger equation

$$\Psi(x,t) = \int_a^b K_0(x,y,t)\Psi(y,0)dy\,.$$

The propagator (integration kernel) satisfies a differential equation with the Dirac delta function as initial condition

$$[i\partial_t - h_0(x)]K_0(x,y;t) = 0 \qquad K_0(x,y;0) = \delta(x-y)\,. \tag{1.1.3}$$

For non-dissipative systems, like in our case, the propagator $K_0(x,y;t)$ can be interpreted as the coordinate representation of the unitary evolution operator $U_0(t)$: $K_0(x,y;t) = \langle x|U_0(t)|y\rangle$, where unitarity implies the symmetry $K_0^*(x,y;-t) = K_0(y,x;t)$. It should be noted that the propagator may be calculated by path-integration [27].

Subsequently, we will mainly work with a spectral decomposition of propagators in terms of complete basis sets of eigenfunctions. Let us consider the main ingredients of this decomposition. In the case of a stationary potential, the evolution equation (1.1.1) reduces, via the standard substitution $\Psi(x,t) = \psi(x)\mathrm{e}^{-iEt}$ and properly chosen boundary conditions, to the spectral problem for the stationary Schrödinger equation (in what follows we refer to this equation as *the Schrödinger equation* and use term *time-dependent Schrödinger equation* for (1.1.1))

$$h_0\psi = E\psi\,. \tag{1.1.4}$$

Let us define requirements for the mathematical environment more precisely. We assume the real-valued potential $V_0(x)$ to be continuous and bounded from below so that the differential expression $h_0 = -\partial_x^2 + V_0(x)$ defines a Sturm-Liouville operator which is symmetric with respect to the usual $\mathcal{L}^2(a,b)$ inner product $\langle\psi|\phi\rangle = \int_a^b \psi^*(x)\phi(x)dx$. The corresponding functions $\psi \in \mathcal{L}^2(a,b)$ are additionally assumed sufficiently smooth[1], e.g. $\psi \in C^2(a,b)$, over the interval $(a,b) \subseteq \mathbb{R}$. Almost everywhere in the text we choose real-valued solutions of equation (1.1.4). This is always possible when $V_0(x)$ is a real-valued function and the spectral parameter E is real also. We will mention when complex-valued solutions and spectral parameters will be used.

Concentrating on physically relevant cases, we restrict our attention to the following three types of setups [98]:

A: The interval (a,b) is finite ,$|a|, |b| < \infty$, so that h_0 has a non-degenerate purely discrete spectrum (see e.g. [99]).

B: For spectral problems on the half-line, $(a = 0, b = \infty)$, we consider the so-called scattering (or short-ranged) potentials

$$\int_0^\infty x|V_0(x)|dx < \infty\,, \tag{1.1.5}$$

which decrease at infinity faster than any finite power of x and have a continuous spectrum filling the positive semi-axis and a finite number of discrete levels; the whole spectrum is non-degenerate. This spectral problem may be interpreted as a radial problem for a 3-dimensional quantum system. Therefore in this case it is convenient to replace the coordinate variable x by the radial coordinate $r \in (0,\infty)$.

C: For spectral problems on the whole real line, $(a = -\infty, b = \infty)$, we consider confining as well as scattering potentials. Confining potentials produce purely discrete non-degenerate spectra (see e.g. [32]), whereas scattering potentials lead to two-fold degenerate continuous spectra filling the whole real line and to a finite number of non-degenerate discrete levels (see e.g. [99]).

The spectrum is determined by imposing Dirichlet boundary conditions (BCs) for the bound state eigenfunctions of h_0. The eigenvalues E_n of h_0 are interpreted as the energies of the stationary

[1] As usual, $C^2(a,b)$ denotes the space of twice continuously differentiable functions.

states. The operator h_0 is assumed to be essentially self-adjoint (with a closure that we denote by the same symbol h_0, for details see, e.g., [100]) in domain

$$\mathcal{D}(h_0) := \{\psi : \psi \in \mathcal{L}^2(a,b) \cap C^2(a,b),\, \psi(a) = \psi(b) = 0\}\,. \tag{1.1.6}$$

As usual, the eigenfunctions $\psi_k(x)$,

$$h_0\psi_k(x) = k^2\psi_k(x)\,, \qquad E = k^2\,, \tag{1.1.7}$$

which correspond to the continuous spectrum $E > 0$ of h_0, are supposed to have the oscillating asymptotic behavior at spatial infinity. Here k denotes the momentum.

The eigenfunctions of Hamiltonian h_0 form a basis in the Hilbert space $\mathcal{L}^2(a,b)$

$$\sum_{n=0}^{M} \psi_n(x)\psi_n^*(y) + \int dk\, \psi_k(x)\psi_k^*(y) = \delta(x-y)\,, \quad \langle\psi_n|\psi_m\rangle = \delta_{nm}\,, \quad \langle\psi_k|\psi_{k'}\rangle = \delta(k-k')\,. \tag{1.1.8}$$

For the spectral problem on the whole real axis (case **C**) the continuous spectrum is two-fold degenerate and the integral over k runs from minus infinity to plus infinity and for the problem on a half line (case **B**) it runs from zero to infinity. For a finite interval (case **A**) or confining potentials the integral is absent and the sum runs over infinite number of discrete levels, $M = \infty$. This agreement about integration and summation is assumed in what follows. For example, using this basis one can calculate the propagator in the following form

$$K_0(x,y;t) = \sum_{n=0}^{M} \Psi_n(x,t)\psi_n^*(y) + \int dk\, \Psi_k(x,t)\psi_k^*(y)\,, \tag{1.1.9}$$

$$\Psi_n(x,t) = \psi_n(x)\mathrm{e}^{-iE_nt}\,, \qquad \Psi_k(x,t) = \psi_k(x)\mathrm{e}^{-ik^2t}\,.$$

By "physical" solutions we mean solutions belonging to the domain $\mathcal{D}(h_0)$ (1.1.6) and scattering states belonging to the continuous spectrum. All solutions $\psi \notin \mathcal{D}(h_0)$ corresponding to a spectral parameter E outside the continuous spectrum are interpreted as "unphysical". Such solutions appear when we consider the Schrödinger equation just as a differential equation. Then the solution space at a given spectral parameter E is the two-dimensional linear space $\mathbb{H}_{0,E} = \mathrm{span}(\psi, \tilde\psi)$, i.e., $(h_0 - E)(a\psi + \tilde a\tilde\psi) \equiv 0$, $\forall a, \tilde a \in \mathbb{C}$. The two solutions ψ and $\tilde\psi$ are linearly independent. One can see from the Schrödinger equation (1.1.4) that the Wronskian of these solutions is a constant,

$$W[\psi,\tilde\psi] \equiv \psi\tilde\psi' - \psi'\tilde\psi = \mathrm{const}\,, \tag{1.1.10}$$

where the prime denotes the derivative with respect to x (or r in case **B**). We define the Green function as the kernel of the operator $(h_0 - E)^{-1}$ (see e.g. [98, 101]). It is well-defined for all $E \notin \mathrm{spec}\, h_0$. This Green function has two different but equivalent representations. The first representation is obtained with the help of two real solutions, f_{l0} and f_{r0} (''left" and ''right" solutions), of the equation

$$h_0 f_{l,r0}(x,E) := -f''_{l,r0}(x,E) + V_0(x) f_{l,r0}(x,E) = E f_{l,r0}(x,E)\,, \qquad x \in (a,b)\,, \qquad E \notin \mathrm{spec} h_0\,. \tag{1.1.11}$$

In case **A** these solutions satisfy zero boundary conditions at one of the boundaries only

$$f_{l0}(a,E) = 0\,, \qquad f_{r0}(b,E) = 0\,. \tag{1.1.12}$$

In case **B** the left solution vanishes at the origin, the right solution has the exponential asymptotics

$$f_{l0}(0,E)=0\,,\qquad f_{r0}(r\to\infty,E)\to \mathrm{e}^{ikr}\,,\qquad E=k^2\,,\qquad \mathrm{Im}k>0\,. \tag{1.1.13}$$

In this case, f_{l0} is a regular solution at the origin, and f_{r0} is proportional to the so-called Jost solution (we will discuss the Jost solutions in the next subsection). In case **C** both the left and the right solutions have the exponential asymptotics at the right (and the left) infinity

$$f_{l0}(x,E)\to \mathrm{e}^{-ikx}\,,\qquad f_{r0}(x,E)\to \mathrm{e}^{ikx}\,,\qquad E=k^2\,,\qquad \mathrm{Im}k>0\,,\qquad x\to\infty\,, \tag{1.1.14}$$

$$f_{l0}(x,E)\to \mathrm{e}^{ikx}\,,\qquad f_{r0}(x,E)\to \mathrm{e}^{-ikx}\,,\qquad E=k^2\,,\qquad \mathrm{Im}k>0\,,\qquad x\to-\infty\,. \tag{1.1.15}$$

Since these solutions correspond to the same spectral parameter, their Wronskian $W_0=W[f_{r0},f_{l0}]$ does not depend on x and is a function of E only. The Green function then reads

$$G_0(x,y,E)=f_{l0}(x,E)f_{r0}(y,E)/W_0\,,\quad x<y\,, \tag{1.1.16}$$

$$G_0(y,x,E)=G_0(x,y,E)\,. \tag{1.1.17}$$

These formulae are clearly equivalent to

$$G_0(x,y,E)=[f_{l0}(x,E)f_{r0}(y,E)\Theta(y-x)+f_{l0}(y,E)f_{r0}(x,E)\Theta(x-y)]/W_0\,, \tag{1.1.18}$$

where Θ is the Heaviside step function.

The second representation of the Green function may be constructed in terms of the complete basis set of h_0's eigenfunctions as follows:

$$G_0(x,y,E)=\sum_{n=0}^{M}\frac{\psi_n(x)\psi_n^*(y)}{E_n-E}+\int\frac{\psi_k(x)\psi_k^*(y)}{k^2-E}dk\,. \tag{1.1.19}$$

The propagator and the Green function of the corresponding stationary Schrödinger equation are related as follows [35]:

$$G_0(x,y,E)=i\int\limits_0^\infty K_0(x,y,t)\mathrm{e}^{iEt}dt\,,\qquad \mathrm{Im}E>0\,.$$

1.1.2 Coupled-channel case

In the equations considered above, the wave function was a scalar function. This means that the corresponding particle does not have internal degrees of freedom. We can generalize the one-dimensional Schrödinger equation to the case of particles with internal degrees of freedom. The internal states may be associated, for example, with the spin or with the excited states of a composite particle. In this case, the Hilbert space of the system is the direct product $\mathcal{L}^2(a,b)\times\mathbb{C}^N$. The wave function depends on a discrete variable, say j, which determines the internal state. In other words, the state of the system is determined by a set of functions $\psi=\psi(x,j)$, $j=\overline{1,N}$. Thus, the wave function is a vector- (or spinor-) valued function. The scalar product modifies as follows

$$\langle\phi|\psi\rangle=\sum_{j=1}^{N}\int\limits_a^b\phi^*(x,j)\psi(x,j)dx\,.$$

Such systems naturally appear after a partial wave decomposition of a three-dimensional Schrödinger equation in the context of scattering theory [22]. Note that in this case $(a, b) = (0, \infty)$ and we replace x by $r \in (0, \infty)$. Different values of the discrete variable j correspond to different asymptotic states called channels.

Let us first summarize the notations used below for the coupled-channel scattering theory [22, 23, 47]. We consider a system of coupled radial Schrödinger equations that in reduced units reads

$$h_0\psi(k,r) = K^2\psi(k,r)\,, \qquad h_0 = -I_N\frac{\partial^2}{\partial r^2} + V_0(r)\,, \qquad r \in (0,\infty)\,, \tag{1.1.20}$$

$$V_0 = l(l+I_N)r^{-2} + \bar{V}_0(r)\,, \tag{1.1.21}$$

where $V_0(r)$ is an $N \times N$ real symmetric matrix, I_N is the $N \times N$ identity matrix, and ψ may be either a vector-valued solution or a matrix-valued solution combined from the vector solutions. From the context it will always be clear what type of the potential V is considered: matrix or scalar. Potential $V_0(r)$ combines the centrifugal term $l(l + I_N)/r^2$, $l = \mathrm{diag}(l_1, \ldots, l_N)$, $l_j = 0, 1, \ldots$, and a short ranged interaction $\bar{V}_0(r)$. Here and in what follows we also denote $l \pm 1$ (and $\nu \pm 1$ below) matrix $l \pm I_N$ ($\nu \pm I_N$). Matrix l defines the asymptotic behaviour of the potential at large distances

$$V_0(r \to \infty) = r^{-2}l(l+1) + \mathrm{o}(r^{-2}) \tag{1.1.22}$$

which is typical for coupled channels involving various partial waves. We denote by ν the matrix which determines the singularity of the potential at the origin

$$V_0(r \to 0) = r^{-2}\nu(\nu+1) + \mathrm{O}(1)\,, \quad \nu = \mathrm{diag}\,[\nu_1, \nu_2, \ldots, \nu_N]\,, \quad \nu_j = 0, 1, \ldots\,. \tag{1.1.23}$$

Note that V does not contain a Coulomb-like r^{-1} singularity by our conjecture.

In the multi-channel case, by k we denote a point in the space $\mathbb{C}^N$, $k = \{k_1, \ldots, k_N\}$, $k_i \in \mathbb{C}$. A diagonal matrix with non-vanishing entries k_i is written as $K = \mathrm{diag}(k) = \mathrm{diag}(k_1, \ldots, k_N)$. The components of this matrix are nothing but the momenta corresponding to the different channels (channel momenta). The complex wave numbers k_i are related to the center-of-mass energy E and the channel thresholds $\Delta_1, \ldots, \Delta_N$ by the "threshold condition"

$$k_j^2 = E - \Delta_j\,, \qquad \Delta_1 = 0\,. \tag{1.1.24}$$

The thresholds $\Delta = \mathrm{diag}(\Delta_1, \ldots, \Delta_N)$ correspond to the excitation energies of the interacting particles. We assume here that $\Delta_1 = 0$ and the different channels have equal reduced masses, a case to which the general situation can always be formally reduced [23]. In the case of equal thresholds all channel momenta coincide $k_j^2 = E$, therefore it is sufficient to use only one momentum k.

Depending on the presence of the centrifugal term and the thresholds one may distinguish three essentially different types of problem: s-wave scattering with different thresholds $\Delta_{i(\neq j)} \neq \Delta_j$, $l \equiv 0$; arbitrary partial waves with equal thresholds $\Delta \equiv 0$; arbitrary partial waves with different thresholds $\Delta_{i(\neq j)} \neq \Delta_j$, $l \neq 0$. In this work we consider only the first and the second cases.

We define the regular $N \times N$ matrix solution $\varphi(k, r)$ of (1.1.20) according to [23]

$$\begin{aligned} \varphi(k, r \to 0) &\to \mathrm{diag}(r^{\nu_1+1}/(2\nu_1+1)!!, \ldots, r^{\nu_N+1}/(2\nu_N+1)!!) \\ &=: r^{\nu+1}[(2\nu+1)!!]^{-1}\,. \end{aligned} \tag{1.1.25}$$

The Jost solution $f(k, r)$ is the matrix solution which has the exponential asymptotic behaviour at large distances

$$f(k, r \to \infty) \to \mathrm{diag}[e^{ik_1 r}, \ldots, e^{ik_N r}] := e^{ikr}\,. \tag{1.1.26}$$

The Jost solutions $f(k,r)$ and $f(-k,r)$ form a basis in the matrix solution space. The regular solution is expressed in terms of the Jost solutions as

$$\varphi(k,r) = \frac{i}{2}\left[f(-k,r)K^{-1}F(k) - f(k,r)K^{-1}F(-k)\right], \tag{1.1.27}$$

where $F(k)$ is known as the Jost matrix. The Jost matrix plays an important role in the non-relativistic scattering theory [102]. From (1.1.25) and (1.1.27) it follows that

$$F(k) = \lim_{r\to 0}\left[f^T(k,r)r^\nu\right]\left[(2\nu-1)!!\right]^{-1}. \tag{1.1.28}$$

Introducing the Wronskian of two matrix functions u, v as

$$\mathrm{W}[u,v](r) \equiv u^T(r)v'(r) - u^{T'}(r)v(r), \tag{1.1.29}$$

we can rewrite (1.1.27) in the following form

$$F(k) = \mathrm{W}[f(k,r),\varphi(k,r)]. \tag{1.1.30}$$

Note, that the Wronskian (1.1.29) of two linearly independent matrix solutions corresponding to the same energy is a constant matrix in the full analogy with the single channel case (1.1.10).

Zeros of the Jost-matrix determinant define positions of the bound/virtual states and the resonances. Thus, to find these positions we have to solve the following equation

$$\det F(k) = 0, \tag{1.1.31}$$

taking into account the threshold conditions (1.1.24).

The physical solution, which appears in the partial wave decomposition of the stationary scattering state, behaves as

$$\Psi(k, r\to\infty) \propto e^{il\frac{\pi}{2}-iKr} - e^{-il\frac{\pi}{2}+iKr}K^{-1/2}S(k)K^{1/2}. \tag{1.1.32}$$

The scattering matrix $S(k)$ is expressed in terms of the Jost matrix as

$$S(k) = e^{il\frac{\pi}{2}}K^{-1/2}F(-k)F^{-1}(k)K^{1/2}e^{il\frac{\pi}{2}}. \tag{1.1.33}$$

Note that the Jost and scattering matrices may also be defined for the single channel case by the same relations with obvious changes.

Since the scattering matrix is unitary and symmetric there exists an orthogonal transformation $R(k)$ diagonalizing this matrix. More precisely, just the sub-matrix which corresponds to the open channels is unitary. Open channels correspond to the real channel momenta. In the two-channel case, assuming that both channels are open (or $\Delta_1 = \Delta_2$), we get

$$R^T(k)\begin{pmatrix} S_{11}(k) & S_{12}(k) \\ S_{12}(k) & S_{22}(k)\end{pmatrix}R(k) = \begin{pmatrix} e^{2i\delta_1(k)} & 0 \\ 0 & e^{2i\delta_2(k)}\end{pmatrix}. \tag{1.1.34}$$

The rotation matrix $R(k)$ is parameterized by a mixing angle $\epsilon = \epsilon(k)$,

$$R(k) = \begin{pmatrix} \cos\epsilon(k) & -\sin\epsilon(k) \\ \sin\epsilon(k) & \cos\epsilon(k)\end{pmatrix}, \tag{1.1.35}$$

which is expressed in terms of S-matrix entries as

$$\tan 2\epsilon(k) = \frac{2S_{12}(k)}{S_{11}(k) - S_{22}(k)}. \tag{1.1.36}$$

Note that an opposite sign definition for the mixing angle could have been chosen; moreover, the order of the eigenphase shifts is arbitrary: exchanging them while adding $\pm\pi/2$ to the mixing angle keeps the scattering matrix unchanged. From a physical motivation, a natural order of the eigenphase shifts corresponds to the mixing parameter vanishing at zero energy (at the threshold).

In the next sections, we present the method of SUSY transformations which allows one to generate new non-trivial exactly solvable models described by the Schrödinger equations discussed here. We start with the most general SUSY transformations of the single-channel stationary Schrödinger equation. Then we consider how this general scheme works in particular cases of the first and the second order transformations. In the case of the first order transformation, we generalize the method to the multi-channel problems. The first order SUSY transformation for the time-dependent Schrödinger equation will also be considered.

1.2 SUSY transformations of the stationary Schrödinger equation

Let us consider the simplest two-component system of Witten's non-relativistic supersymmetric quantum mechanics [50, 103] described by the Schrödinger equation

$$H\mathbf{\Psi}(x) = E\mathbf{\Psi}(x)\,, \qquad x \in (a,b)\,, \tag{1.2.1}$$

where H is a diagonal super-Hamiltonian consisting of the two (single-channel) super-partners h_0 and h_N as components

$$H = \begin{pmatrix} h_0 & 0 \\ 0 & h_N \end{pmatrix}, \qquad h_{0,N} = -\partial_x^2 + V_{0,N}(x)\,, \tag{1.2.2}$$

and $\mathbf{\Psi}(x) = (\psi(x), \phi(x))^T$.

We assume that the partner Hamiltonians h_0 and h_N are intertwined by an Nth-order differential operator L with the following properties:

1. intertwining relations

$$Lh_0 = h_N L \qquad h_0 L^+ = L^+ h_N \tag{1.2.3}$$

2. factorization rule

$$\begin{aligned} &L^+L = P_N(h_0) \qquad LL^+ = P_N(h_N) \\ &P_N(x) = (x-\alpha_0)\dots(x-\alpha_{N-1}) \\ &\mathrm{Im}\,(\alpha_i) = 0 \qquad \alpha_i \neq \alpha_{k\neq i} \qquad i,k = 0,\dots,N-1\,. \end{aligned} \tag{1.2.4}$$

Here, the adjoint operation is understood in the sense of Laplace (i.e. as formally adjoint with the property $\partial_x^+ = -\partial_x$, $(AB)^+ = B^+A^+$ and $i^+ = -i$) and the roots α_i of the polynomial P_N are called factorization constants. For simplicity we assume that the polynomial P_N has only simple roots. The intertwining relations together with the factorization rule can be represented in terms of the polynomial super-algebra [57, 104, 105]

$$Q^2 = (Q^+)^2 = 0 \qquad [Q,H] = [Q^+,H] = 0 \qquad QQ^+ + Q^+Q = P_N(H) \tag{1.2.5}$$

with nilpotent super-charges

$$Q = \begin{pmatrix} 0 & 0 \\ L & 0 \end{pmatrix} \qquad Q^+ = \begin{pmatrix} 0 & L^+ \\ 0 & 0 \end{pmatrix}.$$

Although the component Hamiltonians h_0 and h_N enter the super-Hamiltonian (1.2.2) in an algebraically symmetric way, we consider h_0 as a given Hamiltonian with known spectral properties and h_N as a derived Hamiltonian with a still undefined spectrum.

The intertwiner L is completely described by a set of N transformation functions $u_n(x)$, which are solutions of the stationary Schrödinger equation with h_0 as Hamiltonian:

$$h_0 u_n = \alpha_n u_n \quad n = 0,\dots,N-1\,.$$

Note that transformation functions may be unphysical solutions.

In our case of a polynomial $P_N(x)$ with simple roots (i.e. $\alpha_i \neq \alpha_k$) the action of the intertwiner L on a function ψ is given by the Crum-Krein formula [106, 107]

$$\phi = L\psi = \frac{W(u_0, u_1, \ldots, u_{N-1}, \psi)}{W(u_0, u_1, \ldots, u_{N-1})} \tag{1.2.6}$$

with W denoting the Wronskian

$$W = W(u_0, u_1, \ldots, u_{N-1}) = \begin{vmatrix} u_0 & u_1 & \ldots & u_{N-1} \\ u_0' & u_1' & \ldots & u_{N-1}' \\ \ldots & \ldots & \ldots & \ldots \\ u_0^{(N-1)} & u_1^{(N-1)} & \ldots & u_{N-1}^{(N-1)} \end{vmatrix} . \tag{1.2.7}$$

It links the solutions ϕ and ψ of the Schrödinger equations with h_N and h_0 as Hamiltonians by the relation $\phi = L\psi$. Furthermore, the determinant structure (1.2.6) of the operator L leads to the immediate implication that it has a nontrivial kernel space Ker$L$ spanned by the set of transformation functions u_n:

$$\mathrm{Ker}L = \mathrm{span}\{u_0, \ldots, u_{N-1}\} \qquad \dim(\mathrm{Ker}L) = \dim(\mathrm{Ker}L^+) = N\,.$$

The solutions v_n of the equation $h_N v_n = \alpha_n v_n$ are elements of the kernel space of the adjoint operator L^+ and can be obtained as

$$v_n = \frac{W_n(u_0, u_1, \ldots, u_{N-1})}{W(u_0, u_1, \ldots, u_{N-1})} \qquad n = 0, \ldots, N-1 \tag{1.2.8}$$

$$\mathrm{Ker}L^+ = \mathrm{span}\{v_0, \ldots, v_{N-1}\}$$

where W_n denotes the Wronskian built as a determinant of the $(N-1)\times(N-1)$ matrix with the u_n-related column omitted $W_n = W(u_0, u_1, \ldots, u_{n-1}, u_{n+1}, \ldots, u_{N-1})$. The potential V_N of the Hamiltonian h_N can be expressed as [106, 107]

$$V_N = V_0 - 2\left[\ln W(u_0, u_1, \ldots, u_{N-1})\right]'' . \tag{1.2.9}$$

In general, it is not excluded that the transformation operator L may move a solution of h_0 out of $\mathcal{H}_0 = \mathcal{L}^2(a, b)$ thus transforming a physical solution of h_0 into an unphysical solution of h_N. Moreover the inverse scenario is also possible, i.e. L may transform an unphysical solution of h_0 into a physical solution of h_N. In such cases the point spectrum of h_N will differ from that of h_0. Subsequently, we will mostly use the conservative transformations L, which leave most of the original spectrum invariant with exception of a finite number of spectral points — a characteristic feature of differential intertwining operators L leaving the boundary behavior of the solutions of the Schrödinger equation and positions of singularities of the potential unchanged. Recently in [61] a conjecture has been proven, which was originally formulated in [108] and which states that any Nth-order differential transformation L can be constructed as a superposition from only first- and second-order transformations. In this case it is possible to show [57] that for problems formulated over the whole $\mathbb{R}$ (for infinite values of a and b) V_N behaves asymptotically like V_0. Therefore the operator h_N is also essentially self-adjoint and "lives" in the same Hilbert space $\mathcal{H}$ as h_0. Moreover, since the point spectrum of the self-adjoint Sturm-Liouville problems that we consider is non-degenerate there is no way to create a new discrete level at the position of an already existing discrete level and by this means to increase the geometric multiplicity of that level.

According to [106] the necessary condition for an Nth-order transformation to produce an essentially self-adjoint operator h_N is[2]

$$(E-\alpha_0)\dots(E-\alpha_{N-1}) \geqslant 0 \qquad \forall E \in \operatorname{spec} h_0\,. \tag{1.2.10}$$

This criterion ensures the conservativeness of the transformation L leading only to changes in maximally N spectral points (of the point spectrum). Specifically, the spectrum of h_N may contain p points more and q points less than $\operatorname{spec}(h_0)$, where necessarily $p+q \leqslant N$.

In the present work we will consider the following possibilities.

- The spectrum of h_0 is a subset of the spectrum of h_N. A new energy level may be created in the spectrum of h_N if and only if the corresponding transformation function $u(x)$ is such that $1/u(x) \in \mathcal{D}(h_N)$, i.e., in particular, that $1/u(x)$ is $\mathcal{L}^2-$integrable and satisfies the Dirichlet BCs.

- The spectrum of h_N is a subset of the spectrum of h_0. An energy level may be removed from the spectrum of h_0 if and only if the corresponding transformation function $u(x)$ coincides with the h_0-eigenfunction of this level, i.e. when $u(x)$ satisfies the Dirichlet BCs.

- The spectrum of h_0 coincides with the spectrum of h_N. In this case neither the transformation functions $u_n(x)$ nor $1/u_n(x)$ should be square integrable or satisfy Dirichlet BCs on both ends of the interval (a,b). This property should be fulfilled for all transformation functions $u_n(x)$ from which the transformation operator is built.

- The spectra of h_0 and h_N do not have common points. In this case the transformation functions $u_n(x)$ should violate Dirichlet BCs at one of the boundaries of the interval (a,b).

In all cases we assume that the transformation functions $\{u_n(x)\}_{n=0}^{N-1}$ are linearly independent from one another and their Wronskian $W(u_0,\dots,u_{N-1})$ does not vanish $\forall x \in (a,b)$.

The first and the second order transformations are building blocks for high-order transformations. One can start from the first order SUSY transformations and construct transformations of higher order iteratively. This iteration process may result in some intermediate Hamiltonians with domains of definition different from (1.1.6). Then the resulting N-th order transformation operator is called irreducible. Taking into account the second order transformations one can decompose any N-th order transformation operator in such a way, that all intermediate Hamiltonians will be defined in (1.1.6). We consider the first and the second order transformations in details in the next sections.

1.2.1 The first order SUSY transformations

According to (1.2.6) the first-order intertwiner has the form

$$L := -(\ln u)' + \partial_x = -w + \partial_x\,, \tag{1.2.11}$$

[2]The basic idea can be understood as signature preservation of Hilbert space metrics, i.e. $\forall E$ belonging to the point spectrum of h_0 the eigenfunctions ψ_E with $||\psi_E||^2 = (\psi_E,\psi_E) > 0$ should map into corresponding eigenfunctions ϕ_E of h_N with $||\phi_E||^2 = ||L\psi_E||^2 = (\psi_E, L^+L\psi_E) = (\psi_E, P_N(h_0)\psi_E) \geq 0$ what via (1.2.4) implies (1.2.10). Here, the equality takes place for those ψ_E for which the point E does not belong to the spectrum of h_N, i.e. if $P_N(E)=0$ and $\phi_E = L\psi_E \equiv 0$. A more detailed analysis of the corresponding sufficient conditions for spectral problems on the whole real line in the case of scattering potentials and of confining potentials is given in [108].

where $h_0 u = \alpha u$. The logarithmic derivative of the transformation function $w(x) = (\ln u)'$ is called the superpotential [109]. Operator L and adjoint operator $L^+ = -w - \partial_x$ factorize Hamiltonians h_0 and h_1 as follows

$$L^+ L = h_0 - \alpha\,, \qquad LL^+ = h_1 - \alpha\,. \tag{1.2.12}$$

Operator L transforms the solutions $\psi = \psi(x, E)$ of the initial Schrödinger equation with potential $V = V_0(x)$ into solutions

$$\phi(x, E) \equiv L\psi(x, E) = \psi'(x, E) - \psi(x, E)u'(x)/u(x) \tag{1.2.13}$$

of the transformed Schrödinger equation with potential

$$V_1 = V_0 - 2(\ln u)''. \tag{1.2.14}$$

To get the transformed potential with no more singularities than the initial one it is necessary to choose a non-vanishing transformation solution $u(x) \neq 0$, $\forall x \in (a, b)$.

Operators L and L^+ realize a one-to-one correspondence between two-dimensional spaces of solutions for any $E \neq \alpha$

$$\mathbb{H}_{0,E} \xrightarrow{\quad L \quad} \mathbb{H}_{1,E}\,.$$

When $E = \alpha$, $\psi = u(x)$ and $Lu = 0$, this correspondence may be established as follows. Normalizing the linearly independent solution $\tilde{u}$ by the condition $W(u, \tilde{u}) = 1$ and integrating this Wronskian we obtain

$$\tilde{u}(x) = u(x) \int_{x_0}^{x} \frac{dy}{u^2(y)}\,. \tag{1.2.15}$$

Applying the transformation operator L to $\tilde{u}$ we get

$$\tilde{v}(x) = Lu(x) \int_{x_0}^{x} \frac{dy}{u^2(y)} = 1/u(x)\,. \tag{1.2.16}$$

Finally, we restore the solution space $\mathbb{H}_{1,\alpha} = \mathrm{span}(v, \tilde{v})$ using integral (1.2.15), where u is replaced by $\tilde{v}$ which yields

$$v(x) = 1/u(x) \int_{x_0}^{x} u^2(y)dy\,. \tag{1.2.17}$$

Here we have used well-known fact about the Schrödinger equation that the Wronskian $W_0 = W(\psi, \tilde{\psi})$ does not depend on x, (1.1.10).

Lemma 1. *The Wronskian W_1 of the transformed solutions $\phi = L\psi$ and $\tilde{\phi} = L\tilde{\psi}$ is expressed from the Wronskian W_0 as follows:*

$$W_1 = (E - \alpha)W_0\,, \quad E \neq \alpha\,. \tag{1.2.18}$$

Proof. Writing Wronskian W_1 in terms of the initial solutions

$$W_1 = (L\psi)(L\tilde{\psi})' - (L\psi)'(L\tilde{\psi}) = (\psi' - w\psi)(\tilde{\psi}'' - w\tilde{\psi}' - w'\tilde{\psi}) - (\tilde{\psi}' - w\tilde{\psi})(\psi'' - w\psi' - w'\psi)\,.$$

and using $\psi'' = (V_0 - E)\psi$ we get

$$W_1 = (w^2 + w' + E - V_0)W_0\,.$$

Taking into account that $w(x) = u'/u$, and u is a solution of the initial Schrödinger equation we complete the proof. □

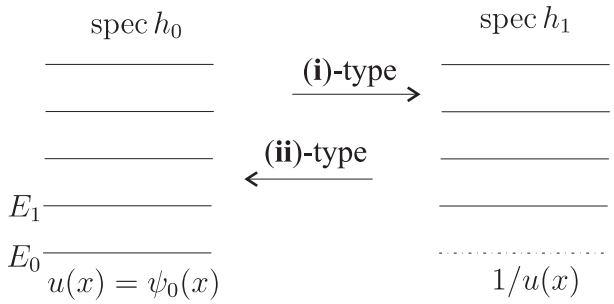

Figure 1.1: The diagram shows spectra of the initial and the transformed system for the cases **(i)** and **(ii)**.

Since we choose a non-vanishing transformation solution the choice of the factorization energy is constrained by the 'oscillation' theorem (see e.g. [32]). The factorization energy has to be less than the ground state energy $\alpha \leq E_0$. Obviously, for the scattering potentials without bound states $\alpha \leq 0$. Depending on the concrete form of the function $u(x)$ the intertwiner L may result in the following three types of relations between the spectra of the Hamiltonians h_0 and h_1 (see, e.g., [103]):
(i) for $\alpha = E_0$ and $u = \psi_0$ the ground state level E_0 of h_0 is removed from the spectrum of h_1,
(ii) h_1 has a new and deeper ground state level $E_{-1} = \alpha < E_0$ than h_0,
(iii) the spectra of h_1 and h_0 completely coincide ($\alpha < E_0$).
The first two situations are shown schematically in figure 1.1.

In order to create a potential $V_1(x)$ which is nonsingular on the whole interval $(a, b) \ni x$ the function $u(x)$ should be nodeless inside this interval. This property is evidently fulfilled for type **(i)** relations since the function $u(x)$ coincides in this case with the ground state eigenfunction $u(x) = \psi_0(x)$. In cases **(ii)** and **(iii)** the nodelessness should be ensured by an appropriate choice of $u(x)$, a choice which is always possible because of the 'oscillation' theorem (see e.g. [32]). In case **(iii)** it implies $\alpha < E_0$.

Let us consider the orthonormal basis formed by h_0 eigenfunctions $\{\psi_n, n = 0, 1, \ldots\}$. Here for simplicity we consider only confining potentials. The eigenfunctions of the Hamiltonian h_1

$$\phi_n = (E_n - \alpha)^{-1/2} L\psi_n \,, \qquad n = 0, 1, \ldots \tag{1.2.19}$$

form an orthonormal basis in the same Hilbert space in case **(iii)**. In case **(i)** the basis does not include ϕ_0 and in case **(ii)** it is necessary to include $\phi_{-1} \propto 1/u$.

In the case of the regular Sturm-Liouville problem $\psi_n'(a) \neq 0$ and $\psi_n'(b) \neq 0$ when $\psi_n \equiv \psi(x, E_n)$ is an eigenfunction. From (1.2.13) it follows that $\phi_n = L\psi_n$ is an eigenfunction if and only if $u(a) = u(b) = 0$. As a result there is only one possible transformation solution, $u(x) = \psi_0(x)$. Thus only case **(i)** may lead to a conservative SUSY transformation for the finite interval (a, b). In this case functions $\{\phi_n, n = 1, 2, \ldots\}$ belong to the discrete spectrum of h_1 and form a complete basis in the Hilbert space $\mathcal{L}^2(a, b)$. Note, that the transformed potential has singularities at the boundaries.

If the transformation function violates Dirichlet BCs (at least at one boundary), then h_0 and h_1 do not have common spectral points at all. The transformation operator L maps eigenfunctions into unphysical solutions of transformed Schrödinger equation. This is a single-channel example of the non-conservative SUSY transformation.

The first order SUSY transformations may be directly generalized to the coupled-channel case [48,49,86,87]. Which is not the case for the formula (1.2.6). With respect to the single-channel case there are additional difficulties due to the non-commutative character of matrix-valued functions. Therefore in the coupled-channel case we will use iterations of the first order transformations. The solutions of the initial Schrödinger equation (1.1.20) are mapped into the solutions of the transformed equation with the help of the differential-matrix operator L,

$$\phi(k,r) = L\psi(k,r) := \left[w(r) - I_N \frac{d}{dr}\right] \psi(k,r)\,. \tag{1.2.20}$$

The transformed Schrödinger equation has form (1.1.20) with a new potential

$$V_1(r) = V_0(r) - 2w'(r)\,. \tag{1.2.21}$$

Matrix $w(r)$, called the superpotential, is expressed in terms of a square matrix solution u of the initial Schrödinger equation

$$h_0 u(r) = -\mathcal{K}^2 u(r)\,, \tag{1.2.22}$$

as follows

$$w(r) = u'(r)u^{-1}(r)\,, \tag{1.2.23}$$

where $\mathcal{K} = \mathrm{diag}(\kappa) = \mathrm{diag}(\kappa_1, \ldots, \kappa_N)$ is a diagonal matrix called the factorization wave number, which corresponds to an energy $\mathcal{E}$ lying below all thresholds, called the factorization energy. The entries of $\mathcal{K}$, thus, satisfy $\mathcal{E} = -\kappa_i^2 + \Delta_i$; by convention, we choose them positive: $\kappa_i > 0$. Solution $u(r)$ is called the factorization solution or (matrix-valued) transformation function.

In the most general case the transformation function may be expressed in terms of the Jost solutions as follows

$$u(r) = f_0(-i\kappa, r)C + f_0(i\kappa, r)D\,, \tag{1.2.24}$$

where the real constant matrices C and D are arbitrary. To obtain a Hermitian potential after a transformation with transformation function (1.2.24) matrix $C^T D$ should be symmetric [49]

$$D^T C = C^T D\,. \tag{1.2.25}$$

Matrices C and D with a maximal number of independent parameters guaranteeing the Hermitian character of the superpotential (1.2.23) have the following canonical form,

$$C = \begin{pmatrix} I_M & 0 \\ Q & 0 \end{pmatrix}, \qquad D = \begin{pmatrix} X_0 & -Q^T \\ 0 & I_{N-M} \end{pmatrix}, \tag{1.2.26}$$

where $X_0 = X_0^T$ is a real symmetric nonsingular $M \times M$ matrix, and Q is an $(N-M) \times M$ real matrix so that $\mathrm{rank}\, C = M$. There are two particular cases: $M = N$, $C = I_N$, $D = D^T = X_0$ and $M = 0$, $C = 0$, $D = I_N$.

The SUSY transformations of the Jost and the scattering matrices crucially depend on the asymptotic behaviour of the superpotential $w_\infty := \lim\limits_{r\to\infty} w(r)$. The reason is that the Jost solution transforms as follows

$$f_1(k,r) = Lf_0(k,r)(w_\infty - iK)^{-1}\,. \tag{1.2.27}$$

The factor $(w_\infty - iK)^{-1}$ is introduced to guarantee the correct asymptotic behaviour of $f_1(k,r)$ (see (1.1.26)). Then the Jost matrix may be calculated by definition (1.1.28).

The analysis of this asymptotic behaviour in the case $\Delta \neq 0$, $l = 0$ may be found in [49]. In this case the superpotential at infinity is diagonal, $w_\infty = \mathrm{diag}(\kappa_1, \ldots, \kappa_M, -\kappa_{M+1}, \ldots, -\kappa_M)$, $0 \leqslant M \leqslant N$. Below we consider in details SUSY transformations in the case of different thresholds when $M = N$, $C = I_N$. A detailed analysis of the superpotential asymptotic behaviour in the case $\Delta = 0$, $l \neq 0$ allows us to introduce coupling SUSY transformations (i.e. the resulting potential and S-matrix will be non-diagonal whereas the initial potential is diagonal).

Let us also mention that, since $Lu(r) = 0$, the solution $\phi(i\kappa, r)$ of the transformed equation corresponding to the energy $E = -\kappa^2$ is found as the matrix $v(r) = [u^\dagger(r)]^{-1}$. Moreover, this matrix, when chosen as the transformation function for the next transformation step, cancels the previously produced potential difference. This means that it corresponds to a transformation in the opposite direction. As in the single channel case one can use chains of SUSY transformations. For our purpose it is more convenient to make SUSY transformations iteratively than to use generalized Crum-Krein Wronskian formulas obtained in [93].

1.2.2 The second order SUSY transformations

The second order SUSY transformation is determined by two transformation functions $u_1(x)$ and $u_2(x)$. One may choose both different and coinciding factorization energies $\alpha_{1,2}$. When $\alpha_2 \neq \alpha_1$ the transformed potential and solutions read (see (1.2.6) and (1.2.9))

$$V_2 = V_0 - 2(\ln W(u_1, u_2))'', \tag{1.2.28}$$

$$\phi \equiv L\psi = W(u_1, u_2, \psi)/W(u_1, u_2)\,, \tag{1.2.29}$$

$$h_2\phi = E\phi\,.$$

Here $h_0 u_{1,2} = \alpha_{1,2} u_{1,2}$ $h_0\psi = E\psi$. When $E = \alpha_1, \alpha_2$ the rhs of (1.2.29) is zero. In this case we may calculate solutions of the transformed Schrödinger equation as follows

$$v_{2,1}(x) = u_{1,2}/W(u_1, u_2)\,, \quad h_2 v_{2,1}(x) = \alpha_{2,1} v_{2,1}(x)\,. \tag{1.2.30}$$

Note that formula (1.2.18) may be easily generalized for the second order SUSY transformation

$$W_2(E) = (E - \alpha_1)(E - \alpha_2) W_0(E)\,, \quad E \neq \alpha_1, \alpha_2\,. \tag{1.2.31}$$

To analyze transformation (1.2.29) one may express second order derivatives from the Schrödinger equations $u''_{1,2} = (V_0 - \alpha_{1,2})u_{1,2}$, $\psi'' = (V_0 - E)\psi$, thus obtaining

$$\phi = [E + \frac{u'_1\alpha_2 u_2 - u'_2\alpha_1 u_1}{W(u_1, u_2)}]\psi - (\alpha_2 - \alpha_1)\frac{u_1 u_2}{W(u_1, u_2)}\psi'\,. \tag{1.2.32}$$

In the degenerate case $\alpha_1 = \alpha_2 \equiv \alpha$ we can not use (1.2.28) and (1.2.29) directly. One may try to consider this case as a limit $\alpha_2 \to \alpha_1$. Note that the limiting procedure is non-trivial. Details of this approach to the degenerate second order SUSY may be found in [110]. We will use another method based on the iterative representation of the high-order and, in particular, the second order SUSY transformation. It is necessary to consider the chain of two consecutive first order transformations. The transformation function of the second step corresponds to the same factorization energy α as the first transformation function u, $h_0 u = \alpha u$. According to (1.2.16) and (1.2.17) the general solution of the Schrödinger equation with the Hamiltonian h_1 for spectral

parameter α reads $v = [c + \int_{x_0}^{x} u^2(t)dt]/u(x)$. Constants c and x_0 should provide $c + \int_{x_0}^{x} u^2(t)dt \neq 0$ for all $x \in (a, b)$, to get the regular transformed potential V_2

$$V_2 = V_0 - 2[\ln(c + \int_{x_0}^{x} u^2(t)dt)]'' , \tag{1.2.33}$$

inside the interval (a, b). Solutions $\phi = \phi(x, E)$ then reads:

$$\phi \equiv L\psi = [\alpha - E + \frac{uu'}{c + \int_{x_0}^{x} u^2(t)dt}]\psi - \frac{u^2}{c + \int_{x_0}^{x} u^2(t)dt}\psi' . \tag{1.2.34}$$

As usual when $\psi(x, E) = u(x)$ (i.e., $E = \alpha$) the rhs of this expression is zero. Once again we should use solution linearly independent from u. As a result we get

$$\phi(x, \alpha) = \frac{u(x)}{c + \int_{x_0}^{x} u^2(t)dt} . \tag{1.2.35}$$

The wronskian of two linearly independent solutions transforms according to (1.2.31), where $\alpha_2 = \alpha_1 = \alpha$. The degenerate case presents an interest for the radial Schrödinger equation, because it allows to construct so-called iso-phase potentials with the same scattering properties and different spectra [94].

It is obvious that the second order transformation will define a regular potential V_2 if $W[u_1, u_2] \neq 0$ or $c + \int_{x_0}^{x} u^2(t)dt \neq 0$, $\forall x \in (a, b)$. Note that the behaviour of $W[u_1, u_2]$ for some important and quite general models was analyzed in [111]. Let us summarize different possibilities of spectrum modifications depending on the choice of factorization constants α_1, α_2 and asymptotical (or boundary) behaviour of the transformation solutions u_1, u_2 [111]. Transformation functions u_1 and u_2 are chosen to provide $W(u_1, u_2) \neq 0$ for all $x \in (a, b)$.

(**I**) - *Removal of two levels*

Transformations functions are neighboring eigenfunctions $u_1(x) = \psi_k(x)$ and $u_2(x) = \psi_{k+1}(x)$ with energies $\alpha_1 = E_k$ end $\alpha_2 = E_{k+1}$. It can be seen that Wronskian $W[u_1, u_2]$ is non-vanishing in (a, b) in this case [106]. We have $u_{1,2}(a) = u_{1,2}(b) = 0$, hence operator L conserves BCs for all E except $E = \alpha_1, \alpha_2$. As a result energy levels E_k and E_{k+1} are removed from the spectrum of Hamiltonian h_0

$$\operatorname{spec} h_2 \bigcup \{\alpha_1 = E_k, \alpha_2 = E_{k+1}\} = \operatorname{spec} h_0 .$$

When $k = 0$ the second order transformation is a superposition $L = L_2 L_1$ of two ''well-defined" first order transformations of **(i)**-type

$$h_0 \xrightarrow{L_1} h_1 \xrightarrow{L_2} h_2 , \tag{1.2.36}$$

where the intermediate Hamiltonian h_1 is self-adjoint. Such SUSY transformation is called completely reducible [57, 62].

(**II**) - *Reducible creation of two levels*

This case realizes when $(a, b) = \mathbb{R}$. Factorization constants lie below the ground state energy of h_0, $E_0 > \alpha_1 > \alpha_2$. The factorization solutions increase at large distances $u_{1,2}(|x| \to \infty) \to \infty$. Moreover, the inverse functions $u_{1,2}^{-1}$ belong to $\mathcal{L}^2(\mathbb{R})$. Then, the transformed Hamiltonian h_2 has two new levels $E_{-2} = \alpha_2$ and $E_{-1} = \alpha_1$ in its spectrum

$$\operatorname{spec} h_0 \bigcup \{E_{-1} = \alpha_1, E_{-2} = \alpha_2\} = \operatorname{spec} h_2 .$$

This second order SUSY transformation is completely reducible and may be presented as the pair of two first order SUSY transformations of **(ii)**-type.

(**III**) - *Irreducible creation of two levels*

Factorization constants lie between two neighboring energy levels of h_0, $E_{k+1} > \alpha_1 > \alpha_2 > E_k$. Again, if the inverse functions $u_{1,2}^{-1}$ belong to $\mathcal{L}^2(\mathbb{R})$ then the transformed Hamiltonian h_2 has two new levels $E = \alpha_2$ and $E = \alpha_1$

$$\operatorname{spec} h_0 \bigcup \{\alpha_1, \alpha_2\} = \operatorname{spec} h_2 \,.$$

Note, that the intermediate Hamiltonian h_1 is unphysical, therefore this is an irreducible second order SUSY transformation.

(**IV**) - *Isospectral transformation*

Let us consider the case when $u_1(a) = 0$, $u_1(b) \neq 0$ and $u_2(a) \neq 0$, $u_2(b) = 0$. In this case, one can see from (1.2.32) that spectra of h_0 and h_2 coincide

$$\operatorname{spec} h_0 = \operatorname{spec} h_2 \,.$$

Parameters α_1 and α_2 provide an isospectral deformation of the Hamiltonian h_2. Its spectrum is real even for complex factorization constants (and, hence, for complex potential V_2) . The intermediate Hamiltonian h_1 may also define a Sturm-Liuville problem on $[a, b]$ if $\alpha_1 < E_0$, but its spectrum radically differs from h_0's spectrum. The first order operator defined by u_1 maps the eigenfunctions of h_0 to unphysical solutions of h_1. Therefore, the full second order transformation is irreducible [2].

(**V**) - *The ground state shift*

If $\alpha_1 = E_0$, $u_1 = \psi_0$ and $\alpha_2 < E_1$, $u_2^{-1} \in \mathcal{L}^2(a, b)$ then

$$\operatorname{spec} h_0 \backslash \{E_0 = \alpha_1\} = \operatorname{spec} h_2 \backslash \{E_0' = \alpha_2 < E_1\} \,.$$

This second order transformation is completely reducible [2], it may be decomposed into two first order SUSY transformations of type **(i)** and **(ii)**.

(**VI**)/(**VII**) - *Creation/Removal of one level*

Combining two first order SUSY transformations of **(ii)**/**(i)** and **(iii)** types we may create/remove one additional level

$$\operatorname{spec} h_0 \bigcup \{E_{-1} = \alpha_1 < E_0\} = \operatorname{spec} h_2 \,, \alpha_2 < \alpha_1 \,,$$

or

$$\operatorname{spec} h_0 = \operatorname{spec} h_2 \bigcup \{E_0 = \alpha_1\} \,, \alpha_2 < E_1 \,.$$

1.2.3 Higher order SUSY transformations

In section 1.2 we defined the most general transformation operator of an arbitrary order. In the case of the stationary Schrödinger equation the N-th order SUSY transformation operator which intertwines Hamiltonians h_0 and h_N may be presented as a superposition of N first order transformations [57, 110]. It should be emphasized that one has to distinguish between chains which are completely reducible within a given Hilbert space $\mathcal{H}$ [112] and chains which are partially or completely irreducible in $\mathcal{H}$. Recall that complete reducibility means that apart from h_0 and

h_N also all intermediate first-order SUSY related Hamiltonians h_k, $k \neq 0, N$ are self-adjoint or essentially self-adjoint in the same Hilbert space $\mathcal{H}$. In case of irreducible chains[3] several or all intermediate Hamiltonians are non-self-adjoint in $\mathcal{H}$. The concepts of reducibility and irreducibility were rigourously analyzed in [110]. Below both chain types will play a role. We note that chain representations lead to extremely simplified transformation rules for higher-order intertwined propagators and allow for very efficient calculation techniques (see subsection 2.2.3 below).

In this section, we obtain an additional information on the intermediate transformation steps of Nth-order SUSY-transformations which goes beyond that presented in section 1.2. Therefore we start with a more detailed description of the transformation operators and solutions of the Schrödinger equation at each transformation step.

Let us consider a chain of N first-order transformations

$$h_N \overset{L_{N,N-1}}{\longleftarrow} h_{N-1} \overset{L_{N-1,N-2}}{\longleftarrow} \dots \overset{L_{2,1}}{\longleftarrow} h_1 \overset{L_{1,0}}{\longleftarrow} h_0$$

built from operators $L_{k+1,k}$ which intertwine neighbor Hamiltonians h_k and h_{k+1} as $L_{k+1,k}h_k = h_{k+1}L_{k+1,k}$. We assume all Hamiltonians h_k, $k = 0, \dots, N$ self-adjoint or essentially self-adjoint in the same Hilbert space $\mathcal{H}$ so that the SUSY-transformation chain itself is completely reducible. Furthermore, we assume that at each transformation step the ground state of the corresponding Hamiltonian is removed. This means that after N linear SUSY-transformations the first N states of the h_0-system are removed and the $N+1$st state of h_0 maps into the ground state of h_N. In our analysis these first $N+1$ states of h_0 will play a crucial role and we denote them by $u_{0,n}$, $n = 0, \dots, N$. Furthermore, we use a numbering for the solutions $u_{k,n}$ of the Schrödinger equations of the SUSY-chain Hamiltonians h_k, $k = 0, \dots, N$ which is "synchronized" with the level numbering of h_0, meaning that a function $u_{k,n}$ is related to the spectral parameter E_n. We have to distinguish between physical solutions, which correspond to the existing bound states of h_k and which have indices $n = k, \dots, N$, and unphysical auxiliary solutions $u_{k,n}$ with $n = 0, \dots, k-1$ which we construct below. The ground state eigenfunction of a Hamiltonian h_k is given by $u_{k,k}$ and for $k < N$ it is annihilated by the SUSY-intertwiner $L_{k+1,k}$

$$L_{k+1,k}u_{k,k} = 0\,.$$

The bound state functions $u_{k+1,n}$, $n = k+1, \dots, N$ of h_{k+1} may be obtained by acting with the SUSY-intertwiner

$$L_{k+1,k} = -u'_{k,k}/u_{k,k} + \partial_x \qquad L_{k+1,k}f = \frac{W(u_{k,k}, f)}{u_{k,k}} \tag{1.2.37}$$

on the corresponding eigenfunctions of h_k

$$L_{k+1,k}u_{k,n} = u_{k+1,n} \qquad n = k+1, \dots, N\,.$$

Next, we note that the chain of k, $(k = 2, \dots, N)$ first-order transformations is equivalent to a single kth-order transformation (1.2.6) generated by the transformation functions $u_{0,0}, u_{0,1}, \dots, u_{0,k-1}$. Furthermore, the transformation operators obey the composition rules

$$L_{k+1,\,k}L_{k,\,l} = L_{k+1,\,l} \qquad l = 0, \dots, k-1 \qquad k = 1, \dots, N-1 \tag{1.2.38}$$

so that, e.g., the second-order transformation operator $L_{k+2,k}$ intertwines the Hamiltonians h_k and h_{k+2}

$$L_{k+2,k}h_k = h_{k+2}L_{k+2,k} \qquad k = 0, \dots, N-2\,.$$

[3]For a careful analysis of different kinds of irreducible transformations we refer to [61].

The Nth-order transformation operator $L_{N,0}$ is then inductively defined as $L_{N,0} = L_{N,N-1}L_{N-1,0}$. Obviously, it annihilates the N lowest states of the original Hamiltonian h_0, i.e. $u_{0,0}, \ldots, u_{0,N-1} \in \mathrm{Ker} L_{N,0}$.

As further ingredient we need the set of unphysical auxiliary functions $u_{N,n}$, $n = 0, \ldots, N-1$. We construct them as $u_{N,n} = L_{N,0}\widetilde{u}_{0,n}$, where the functions $\widetilde{u}_{0,n}$ are the unphysical solutions of the h_0-Schrödinger equation at energies E_n which are linearly independent from the eigenfunctions $u_{0,n}$. Normalizing $\widetilde{u}_{0,n}$ by the condition $W(u_{0,n}, \tilde{u}_{0,n}) = 1$ and integrating this Wronskian gives

$$\widetilde{u}_{0,n}(x) = u_{0,n}(x) \int_{x_0}^{x} \frac{dy}{u_{0,n}^2(y)}$$

and finally

$$u_{N,n}(x) = L_{N,0}u_{0,n}(x) \int_{x_0}^{x} \frac{dy}{u_{0,n}^2(y)} \qquad n = 0, \ldots, N-1\,. \tag{1.2.39}$$

Let us derive a representation of the unphysical auxiliary solutions $u_{N,n}$, $n = 0, \ldots, N-1$ of the h_N-Schrödinger equation in terms of Wronskian fractions. The operator $L_{N,0}$ itself is constructed from the $u_{0,n}$, $n = 0, \ldots, N-1$ as transformation functions.

Below we show by induction that the unphysical solutions $u_{N,n}$ defined in (1.2.39) as

$$u_{N,n} = L_{N,0}\widetilde{u}_{0,n} = L_{N,0}u_{0,n} \int_{x_0}^{x} \frac{dy}{u_{0,n}^2(y)}$$

have the following representation in terms of Wronskian fractions

$$u_{N,n} = C_{N,n} \frac{W_n(u_{0,0}, \ldots, u_{0,N-1})}{W(u_{0,0}, \ldots, u_{0,N-1})} \tag{1.2.40}$$

$$C_{N,n} := (E_{N-1} - E_n)(E_{N-2} - E_n) \ldots (E_{n+1} - E_n) \qquad n = 0, \ldots, N-2$$

$$u_{N,N-1} = \frac{W_{N-1}(u_{0,0}, \ldots, u_{0,N-1})}{W(u_{0,0}, \ldots, u_{0,N-1})} = \frac{W(u_{0,0}, \ldots, u_{0,N-2})}{W(u_{0,0}, \ldots, u_{0,N-1})}\,. \tag{1.2.41}$$

The ground state function of h_N is obtained by acting with $L_{N,0}$ on the Nth excited state of h_0:

$$u_{N,N} = L_{N,0}u_{0,N} = \frac{W(u_{0,0}, \ldots, u_{0,N})}{W(u_{0,0}, \ldots, u_{0,N-1})}\,. \tag{1.2.42}$$

For $N = 1$ the first order transformation operator $L_{1,0}$ is constructed with the help of $u_{0,0}$. Therefore applying (1.2.13) with $\psi = \widetilde{u}_{0,0}$ yields

$$u_{1,0} = L_{1,0}\widetilde{u}_{0,0} = \frac{1}{u_{0,0}}$$

which obviously agrees with the statement. Applying (1.2.13) with $\psi = u_{0,1}$ we obtain

$$u_{1,1} = L_{1,0}u_{0,1} = \frac{W(u_{0,0}, u_{0,1})}{u_{0,0}}\,. \tag{1.2.43}$$

In order to prove the statement for $N = 2$ we build the linear SUSY-operator $L_{2,1}$ from $u_{1,1}$ and act with it on the unphysical solutions $\widetilde{u}_{1,1}$ and $u_{1,0}$. As first result we obtain

$$u_{2,1} = L_{2,1}\widetilde{u}_{1,1} = \frac{1}{u_{1,1}} = \frac{u_{0,0}}{W(u_{0,0}, u_{0,1})}$$

where (1.2.13) and (1.2.43) have been used. For the second function we find

$$\begin{aligned} u_{2,0} = L_{2,1}u_{1,0} = L_{2,1}\frac{1}{u_{0,0}} &= \frac{1}{u_{0,0}u_{1,1}}L_{1,0}^{+}u_{1,1} = \frac{1}{u_{0,0}u_{1,1}}L_{1,0}^{+}L_{1,0}u_{0,1} \\ &= (E_1 - E_0)\frac{1}{u_{0,0}u_{1,1}}u_{0,1} = (E_1 - E_0)\frac{u_{0,1}}{W(u_{0,0}, u_{0,1})}\,. \end{aligned} \tag{1.2.44}$$

Here the operator $L_{2,1} = -u'_{1,1}/u_{1,1} + \partial_x$ has been replaced by $L^+_{1,0} = -u'_{0,0}/u_{0,0} - \partial_x$ with the help of $(1/u_{0,0})' = -u'_{0,0}/u^2_{0,0}$. Moreover, we have used (1.2.43), the factorization rule $L^+_{1,0}L_{1,0} = h_0 - E_0$ and the Schrödinger equation $h_0 u_{0,1} = E_1 u_{0,1}$.

Assuming finally that the representations (1.2.40) and (1.2.41) are valid for $u_{N,n}$ and $u_{N,N-1}$ we prove them for $u_{N+1,n}$ and $u_{N+1,N}$.

We start with $u_{N,N-1} \mapsto u_{N+1,N}$. To go from h_N to h_{N+1} only the linear (one-step) SUSY transformation $L_{N+1,N}$ is required. Applying (1.2.13) and combining it with the normalization condition $W(u_{N,N}, \widetilde{u}_{N,N}) = 1$ and the Crum-Krein formula (1.2.6) [or (1.2.42)] we find the equivalence chain

$$u_{N+1,N} = L_{N+1,N}\widetilde{u}_{N,N} = \frac{W(u_{N,N}, \widetilde{u}_{N,N})}{u_{N,N}} = \frac{1}{u_{N,N}} = \frac{W(u_{0,0}, \dots, u_{0,N-1})}{W(u_{0,0}, \dots, u_{0,N})}\,.$$

Comparison with (1.2.41) shows that the proof is done.

The proof of the induction $u_{N,n} \mapsto u_{N+1,n}$ is less obvious. The linear intertwiners $L_{m+1,m}$ have been built strictly incrementally from the corresponding ground state eigenfunctions $u_{m,m}$ (of the Hamiltonians h_m) as transformation functions. Here, we need a more general non-incremental construction scheme. In order to facilitate it, we first introduce a very detailed notation for general polynomial intertwiners $L_{k,0}$ indicating explicitly the energy levels of the transformation functions from which they are built. Based on the Crum-Krein formula (1.2.6) we set

$$L^{(a_1,a_2,\dots,a_k)}_{k,0} f := \frac{W(u_{0,a_1}, u_{0,a_2}, \dots, u_{0,a_k}, f)}{W(u_{0,a_1}, u_{0,a_2}, \dots, u_{0,a_k})} \qquad a_i \neq a_{j\neq i} \tag{1.2.45}$$

with $a_i \in \mathbb{Z}^+$ being any energy level numbers of the Hamiltonian h_0. The determinant structure of (1.2.45) immediately implies the generalized kernel property

$$L^{(a_1,\dots,n,\dots,a_k)}_{k,0} u_{0,n} = 0 \tag{1.2.46}$$

and the invariance of the operator $L^{(a_1,a_2,\dots,a_k)}_{k,0}$ with regard to permutations
$(a_1, a_2, \dots, a_k) \mapsto \sigma(a_1, a_2, \dots, a_k)$

$$L^{\sigma(a_1,a_2,\dots,a_k)}_{k,0} = L^{(a_1,a_2,\dots,a_k)}_{k,0}\,. \tag{1.2.47}$$

Recalling that (1.2.45) can be built from a chain $L^{(a_k)}_{k,k-1}L^{(a_{k-1})}_{k-1,k-2}\cdots L^{(a_1)}_{1,0}$ of linear intertwiners $L^{(a_m)}_{m+1,m}$ we conclude that the ordering with regard to energy levels is inessential in the transformation chain and that we can split it into sub-chains with any permuted combination of levels

$$\begin{aligned} &\sigma(a_1, \dots, a_k) = (b_1, \dots, b_B, c_1, \dots, c_C)\,, \quad B + C = k \\ &L^{(a_1,\dots,a_k)}_{k,0} = L^{(c_1,\dots,c_C)}_{B+C,B} L^{(b_1,\dots,b_B)}_{B,0} = L^{(b_1,\dots,b_B)}_{C+B,C} L^{(c_1,\dots,c_C)}_{C,0}\,. \end{aligned} \tag{1.2.48}$$

Apart from this full commutativity of the transformations we note their associativity

$$L^{(a_3)}_{m+3,m+2}\left(L^{(a_2)}_{m+2,m+1}\,L^{(a_1)}_{m+1,m}\right) = \left(L^{(a_3)}_{m+3,m+2}\,L^{(a_2)}_{m+2,m+1}\right)L^{(a_1)}_{m+1,m}\,. \tag{1.2.49}$$

Commutativity and associativity can be used to re-arrange a sequence of transformations in any required order.

In accordance with the intertwiners L we denote eigenfunctions as

$$u^{(a_1,a_2,\dots,a_k)}_{k,n} := L^{(a_1,a_2,\dots,a_k)}_{k,0} u_{0,n}\,, \qquad a_i \neq n\,,\ i = 1, \dots, k\,. \tag{1.2.50}$$

Another ingredient that we need is the representation

$$\begin{aligned}\frac{W(u_{0,0},\ldots,u_{0,N-1})}{W_n(u_{0,0},\ldots,u_{0,N-1})} &= (-1)^{N-1-n}\frac{W(u_{0,0},\ldots,u_{0,n-1},u_{0,n+1},\ldots,u_{0,N-1},u_{0,n})}{W_n(u_{0,0},\ldots,u_{0,N-1})}\\ &= (-1)^{N-1-n}L_{N-1,0}^{(0,\ldots,n-1,n+1,\ldots,N-1)}u_{0,n}\\ &= (-1)^{N-1-n}u_{N-1,n}^{(0,\ldots,n-1,n+1,\ldots,N-1)} =: v_{N-1,n} \end{aligned} \tag{1.2.51}$$

which immediately follows from the Crum-Krein formula (1.2.45) and definition (1.2.50). From the physical solution $v_{N-1,n}$ we build the operators[4]

$$\begin{aligned} L_{N,N-1}^{(n)} &:= L_{N,N-1}^{(n)}[v_{N-1,n}] = -\frac{v'_{N-1,n}}{v_{N-1,n}} + \partial_x\\ L_{N,N-1}^{(n)+} &:= L_{N,N-1}^{(n)+}[v_{N-1,n}] = -\frac{v'_{N-1,n}}{v_{N-1,n}} - \partial_x \end{aligned} \tag{1.2.52}$$

and the corresponding Hamiltonian $h_{N-1}^{(0,\ldots,n-1,n+1,\ldots,N-1)}$ with

$$L_{N,N-1}^{(n)+}L_{N,N-1}^{(n)} = h_{N-1}^{(0,\ldots,n-1,n+1,\ldots,N-1)} - E_n\,. \tag{1.2.53}$$

We start the proof of the induction $u_{N,n} \mapsto u_{N+1,n}$ with the following transformations

$$\begin{aligned} u_{N+1,n} &= L_{N+1,N}^{(N)}\,u_{N,n} = C_{N,n}\,L_{N+1,N}^{(N)}\,\frac{W_n(u_{0,0},\ldots,u_{0,N-1})}{W(u_{0,0},\ldots,u_{0,N-1})}\\ &= C_{N,n}\,L_{N+1,N}^{(N)}\,v_{N-1,n}^{-1}\\ &= C_{N,n}\left[-\frac{u'_{N,N}}{u_{N,N}v_{N-1,n}} - \frac{v'_{N-1,n}}{v_{N-1,n}^2}\right]\\ &= C_{N,n}\frac{1}{u_{N,N}v_{N-1,n}}\,L_{N,N-1}^{(n)+}\,u_{N,N}\,. \end{aligned} \tag{1.2.54}$$

In order to obtain the operator product $L_{N,N-1}^{(n)+}L_{N,N-1}^{(n)}$ we use (1.2.42), the composition rule (1.2.48) and the Crum-Krein formula (1.2.45)

$$\begin{aligned} u_{N,N} &= L_{N,0}^{(0,1,\ldots,N-1)}u_{0,N} = \frac{W(u_{0,0},\ldots,u_{0,N})}{W(u_{0,0},\ldots,u_{0,N-1})}\\ &= L_{N,N-1}^{(n)}L_{N-1,0}^{(0,1,\ldots,n-1,n+1,\ldots,N-1)}u_{0,N}\\ &= L_{N,N-1}^{(n)}u_{N-1,N}^{(0,1,\ldots,n-1,n+1,\ldots,N-1)} \end{aligned} \tag{1.2.55}$$

where

$$\begin{aligned} u_{N-1,N}^{(0,1,\ldots,n-1,n+1,\ldots,N-1)} &= L_{N-1,0}^{(0,1,\ldots,n-1,n+1,\ldots,N-1)}u_{0,N}\\ &= \frac{W_n(u_{0,0},\ldots,u_{0,N})}{W_n(u_{0,0},\ldots,u_{0,N-1})}\,. \end{aligned} \tag{1.2.56}$$

This gives

$$\begin{aligned} u_{N+1,n} &= C_{N,n}\frac{1}{u_{N,N}v_{N-1,n}}\,L_{N,N-1}^{(n)+}\,u_{N,N}\\ &= C_{N,n}\frac{1}{u_{N,N}v_{N-1,n}}\,L_{N,N-1}^{(n)+}L_{N,N-1}^{(n)}u_{N-1,N}^{(0,1,\ldots,n-1,n+1,\ldots,N-1)}\\ &= C_{N,n}\frac{1}{u_{N,N}v_{N-1,n}}(E_N - E_n)u_{N-1,N}^{(0,1,\ldots,n-1,n+1,\ldots,N-1)}\\ &= C_{N+1,n}\frac{W_n(u_{0,0},\ldots,u_{0,N})}{W(u_{0,0},\ldots,u_{0,N})} \end{aligned} \tag{1.2.57}$$

[4]For $C \neq 0$ holds $L_{N,N-1}^{(n)}[Cv_{N,n}] = L_{N,N-1}^{(n)}[v_{N,n}]$ so that the sign factor $(-1)^{N-1-n}$ plays no role in the operator $L_{N,N-1}^{(n)}$ itself.

where the last line has been obtained by expressing $u_{N-1,N}^{(0,1,\ldots,n-1,n+1,\ldots,N-1)}$, $u_{N,N}$ and $v_{N-1,n}$ via (1.2.56), (1.2.42) and (1.2.51) in terms of their Wronskian fractions. With (1.2.57) the proof is complete.

Relations (1.2.40) and (1.2.41) coincide with the Crum-Krein formulae up to normalization factors $C_{N,n}$. These factors will be important to calculate propagators in section 2.2.3.

1.3 Supersymmetry of the time-dependent Schrödinger equation

Supersymmetric transformations of the time-dependent Schrödinger equation may be introduced in the same manner as in the case of the stationary equation, although there are some essential peculiarities [57]. In [113] it was shown that the SUSY transformation of the time-dependent Schrödinger equation may be reduced to the SUSY transformation of an ordinary second order differential equation by an appropriate change of variables. However, often it is more convenient to work with the time-dependent Schrödinger equation directly.

In this thesis, we consider only the first-order time-dependent SUSY transformations. As in the stationary case, the intertwining relation

$$L(i\partial_t - h_0) = (i\partial_t - h_1)L\,, \tag{1.3.1}$$

determines the differential operator

$$L = L_1(t)(-\frac{u_x}{u} + \partial_x)\,, \tag{1.3.2}$$

which maps solutions of the Schrödinger equation with Hamiltonian h_0 (initial equation) into solutions of the Schrödinger equation with Hamiltonian h_1 (transformed equation), $\Phi(x,t) = L\Psi(x,t)$. Adjoint operator L^+ realizes map in the opposite direction. Thus, their composition L^+L transforms solutions of the initial equation into other solutions of the same equation. Therefore operator $g_0 = L^+L + \alpha$, where α is a real constant, is a symmetry operator of the initial equation. The operator $g_1 = LL^+ + \alpha$ is a symmetry operator of the transformed equation.

The transformation operator L is determined by a solution $u(x,t)$ of the initial equation,

$$(i\partial_t - h_0)u(x,t) = 0\,,$$

and an arbitrary function $L_1(t)$. The difference between the initial and the transformed potentials reads

$$\Delta V = V_1 - V_0 = -i(\ln L_1)_t - 2(\ln u)_{xx}\,. \tag{1.3.3}$$

Having restricted ourselves by real transformed potentials we should impose the following condition

$$\ln(u/u^*)_{xxx} = 0\,, \tag{1.3.4}$$

that fixes function $L_1(t) = \exp\left(-2i\int\limits_0^t (\ln u/u^*)_{xx}dt\right)$, $L(0) = 1$. Then the transformed potential reads

$$\Delta V(x,t) = -(\ln uu^*)_{xx}\,. \tag{1.3.5}$$

Analogously to the stationary case the properties of operator L, Hamiltonians h_0, h_1 and symmetry operators g_0, g_1 may be unified in the simplest superalgebra

$$Q^2 = (Q^+)^2 = 0 \qquad [Q, iI\partial_t - H] = [Q^+, iI\partial_t - H] = 0 \qquad \{Q, Q^+\} = J - \alpha\,, \tag{1.3.6}$$

with nilpotent super-charges

$$Q = \begin{pmatrix} 0 & 0 \\ L & 0 \end{pmatrix} \qquad Q^+ = \begin{pmatrix} 0 & L^+ \\ 0 & 0 \end{pmatrix},$$

and matrix Hamiltonian $H = \mathrm{diag}(h_0, h_1)$. The symmetry operator $J = \mathrm{diag}(L^+L + \alpha, LL^+ + \alpha)$ commutes with super-charges and the Schrödinger operator

$$[Q, J] = [Q^+, J] = 0\,, \qquad [J, iI\partial_t - H] = 0\,. \tag{1.3.7}$$

Let us consider how to define a complete basis set in the Hilbert space. From the results obtained in [57] we see that the eigenfunctions of the symmetry operators g_0 and g_1

$$g_0\psi_n = \lambda_n\psi_n\,, \qquad g_1\phi_n = \lambda_n\phi_n\,, \tag{1.3.8}$$

form two (orthonormal) basis sets which are related by SUSY transformation

$$\int \psi_m^*\psi_n dx = \int \phi_m^*\phi_n dx = \delta_{m,n}\,, \qquad \phi_n = N_n L\psi_n\,. \tag{1.3.9}$$

Here N_n is a normalization factor.

Note, that

$$g_0 u = \alpha u\,, \qquad g_1 v = \alpha v\,, \qquad v = 1/\left[L_1(t)u^*(x)\right]. \tag{1.3.10}$$

As in the case of the SUSY transformation of the stationary Schrödinger equation there are three essentially different possibilities to choose the transformation function $u(x,t)$:
(i) for $\alpha = \lambda_0$, $u = \psi_0 \Longrightarrow \mathrm{spec}(g_1) = \mathrm{spec}(g_0) \setminus \{\lambda_0\}$,
(ii) for $\alpha < \lambda_0 \Longrightarrow \mathrm{spec}(g_1) = \mathrm{spec}(g_0) \cup \{\alpha\}$,
(iii) for $\alpha < \lambda_0 \Longrightarrow \mathrm{spec}(g_1) = \mathrm{spec}(g_0)$.
We skip the detailed analysis of the structure of Hilbert spaces. Such an analysis is presented in [57]. In what follows we will use the two basis sets, $\{\psi_n\}$ and $\{\phi_n\}$, bearing in mind that the spectra of the symmetry operators g_0 and g_1 coincide with the possible exception of the lowest eigenvalue.

1.4 Exactly solvable potentials generated by SUSY transformations

In this section we explicitly derive several exactly-solvable models generated by SUSY transformations [49,57,103]. In the next chapters, we calculate the Green functions and the propagators for the single-channel models constructed here and study the spectrum for the coupled-channel ones.

1.4.1 Multi-soliton potentials

The method of SUSY transformations is well known in the connection with the soliton theory [114]. A potential of the one-dimensional stationary Schrödinger equation is said to be soliton if it is the SUSY partner of the zero potential. A soliton solution of the Korteweg-de-Vries equation may be constructed using a soliton potential [114].

The term ''N-soliton potential" was introduced by Its and Matveev [115]. One of the most intriguing mathematical discoveries of XX-th century is a possibility to use the inverse scattering method for solving non-linear equations [116]. For instance, to get solutions of the Korteweg-de-Vries equation one needs to construct a family of isospectral potentials for the Schrödinger equation. Such a family may be obtained by the Gelfand-Levitan (or Marchenko) integral transformations [40,41]. An alternative way to solve this problem is based on chains of SUSY transformations [114]. Note that multi-soliton potentials are interesting by themselves, in particular, many quantum processes can be modelled by soliton potentials [117]. Below we present the explicit expression for the N-soliton potential with N non-degenerate bound states at arbitrary energies.

We start from the stationary Schrödinger equation with the zero potential $V_0(x) = 0$, $x \in \mathbb{R}$. Choosing $u(x) = \cosh(ax + b)$, $h_0 u = -a^2 u$, $a > 0$ as the transformation function we get the one-soliton potential

$$V_1(x) = -2(\ln u)'' = \frac{-2a^2}{\cosh(ax + b)^2} \tag{1.4.1}$$

with the single discrete level $E = -a^2$. The corresponding eigenfunction is $\phi_0(x) = (a/\sqrt{2})/\cosh(ax)$. To get eigenfunctions $\phi_k(x)$ from the continuous spectrum we apply the transformation operator $L = -a\tanh(ax) + \partial_x$ to the plane waves $\psi_k(x) = 1/\sqrt{2\pi}\exp(-ikx)$, $E = k^2$.

A multi-soliton potential is generated starting from the zero initial potential, $V_0(x) = 0$ by the following set of N (which is supposed to be even) transformation functions [57, 114]

$$u_{2j-1}(x) = \cosh(a_{2j-1}x + b_{2j-1})\,, \tag{1.4.2}$$

$$u_{2j}(x) = \sinh(a_{2j}x + b_{2j})\,, \qquad j = 1, 2, \ldots N/2\,. \tag{1.4.3}$$

The factorization constants $\alpha_j = -a_j^2$ define the positions of the discrete levels (point spectrum) $E_j = \alpha_j < 0$ of $h_N = -\partial_x^2 + V_N(x)$, whereas the continuous part of the spectrum of h_N fills the whole real axis. The eigenfunctions of the discrete levels normalized to unity have the form [103]

$$\varphi_n(x) = \left[\frac{a_n}{2}\prod_{j=1, j\neq n}^{N}|a_n^2 - a_j^2|\right]^{1/2} \frac{W(u_1, u_2, \ldots, u_{n-1}, u_{n+1}, \ldots, u_N)}{W(u_1, u_2, \ldots, u_N)}\,. \tag{1.4.4}$$

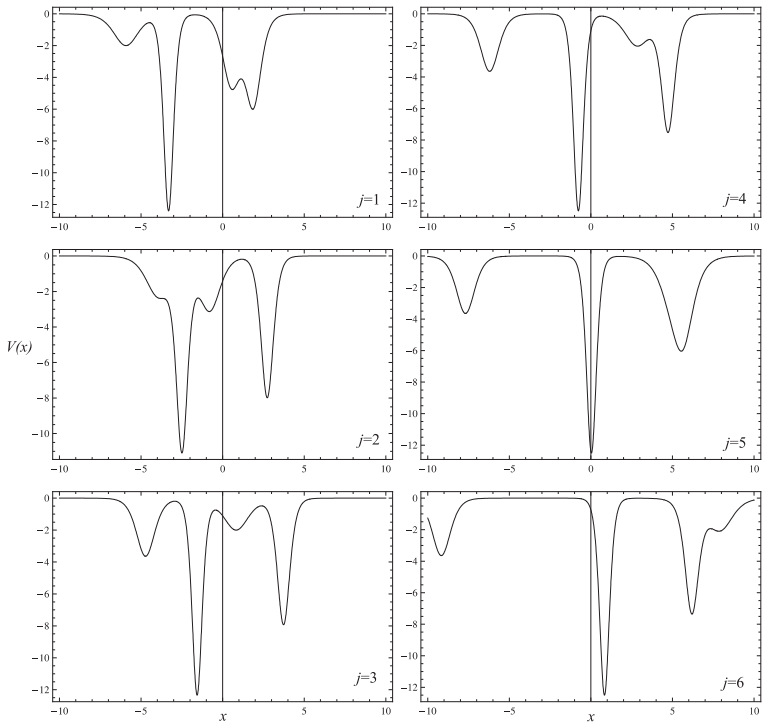

Figure 1.2: Four-soliton potential is shown. Parameters of the potential are: $a_1 = 1$, $a_2 = 1.35$, $a_3 = 2$, $a_4 = 2.5$, $b_1 = 4 + 2j$, $b_2 = 0 - 2j$, $b_3 = -1 - 2j$, $b_4 = 7 - 2j$, $j = 1, \ldots, 6$.

We also need the continuous spectrum eigenfunctions of h_N which should be found by acting with the operator L on plane waves $\psi_k(x) = 1/\sqrt{2\pi}\exp(-ikx)$, $k \in \mathbb{R}$

$$\varphi_k(x) = \frac{1}{\sqrt{(k^2 + a_1^2)(k^2 + a_2^2)\ldots(k^2 + a_N^2)}} L\psi_k(x)\,, \tag{1.4.5}$$

$$E = k^2\,, \quad \alpha_k = -a_k^2\,, \quad k = 1, \ldots, N\,.$$

The set of functions $\{\varphi_n(x),\, n = 1, \ldots, N\}$ and $\{\varphi_k(x),\, k \in \mathbb{R}\}$ forms a complete and orthonormal set in the Hilbert space of square integrable functions on the whole real line.

It is interesting to note that for particular values of the parameters a_j a multi-soliton potential may have a shape of a multi-well potential thus presenting an example of a multi-well exactly solvable potential. In figure 1.2 we plot a four-soliton potentials. The positions of minima may be changed by varying parameters b_j. One can see that solitons conserve its shape after collision. It is difficult to believe that these six potentials have coinciding spectra. Nevertheless it is exact and well-established result.

Let us consider the time-dependent Schrödinger equation. One of the possible methods to construct time-dependent multi-soliton potentials is described in [118]. Moreover, a wide range of physical applications is discussed there. In general, these potentials are complex-valued and it is necessary to impose additional constraints to make these potentials real-valued. In [119, 120] one can find a more suitable and direct approach to the real time-dependent soliton potentials. We will demonstrate the idea of this method on a particular example of the time-dependent one-soliton potential. The time-dependent transformation function $u = \exp\eta\cosh\theta$, $\eta = i(a^2 - \lambda^2)t^2 - i\lambda x$, $\theta = ax + 2a\lambda t$ leads to the following potential potential [119]

$$V(x,t) = -2a^2/\cosh^2\theta\,, \tag{1.4.6}$$

which looks like the one-soliton potential moving along x axes with a constant velocity.

The eigenfunctions of the initial symmetry operator $ig_0 = L^+L + \alpha = (i\partial_x + \lambda)^2$ coincide with the plane waves

$$\psi_k(x,t) = 1/\sqrt{2\pi}\exp\left(-ikx - ik^2t\right). \tag{1.4.7}$$

The eigenfunctions of the transformed symmetry operator $ig_1 = LL^+ + \alpha$ are obtained as follows

$$\phi_k(x,t) = (1/\sqrt{k^2+a^2})L\psi_k(x,t)\,, \qquad \phi_\alpha(x,t) = N/u^*(x,t)\,. \tag{1.4.8}$$

1.4.2 Potentials with quasi-equidistant spectra

A quasi-equidistant spectrum is an equidistant spectrum with a finite number of lacunas. Such spectrum may be obtained from an equidistant spectrum by removal of a finite number of levels. The important property of the potentials with quasi-equidistant spectra is that any wave packet moving in such a potential does not spread being a periodic function of time [121]. One can construct a potential with a quasi-equidistant spectrum using SUSY transformations of the harmonic oscillator [57].

Let us consider the family of potentials generated from the harmonic oscillator $h_0 = -\partial_x^2 + x^2/4 - 1/2$ by the second-order SUSY transformation of type (**I**), (see also [57]). Solutions of the Schrödinger equation $h_0\psi = E\psi$ are expressed in terms of parabolic cylinder functions $D_E(x)$ (see [122])

$$\psi_E(x) = C_1 D_E(x) + C_2 D_E(-x)\,, \qquad C_{1,2} = \text{const}\,,$$

for any complex E.

Wave functions should decrease at spatial infinity, $|x| \to \infty$, to be square-integrable. This requirement leads to the equidistant spectrum $E = n$, $n = 0, 1, 2, \ldots$. Wave functions are reduced to Hermite polynomials $H_n(x)$

$$\psi_n(x) = p_n(x)\exp\left(-x^2/4\right), \qquad p_n(x) = 2^{-n/2}H_n(x/\sqrt{2})\,. \tag{1.4.9}$$

There is a simple algorithm to reproduce polynomials $p_n(x)$

$$p_n(x) = n\int_0^x p_{n-1}(y)dy - p'_{n-1}(0), \qquad p'_n(x) = np_{n-1}(x), \tag{1.4.10}$$

$$p_{n+1}(x) = xp_n(x) - np_{n-1}(x)\,. \tag{1.4.11}$$

Let us write explicitly first polynomials $p_n(x)$

$$p_0(x) = 1\,, \quad p_1(x) = x\,, \quad p_2(x) = x^2 - 1\,, \quad p_3(x) = x(x^2-3)\,.$$

Choosing two neighboring eigenfunctions $u_0(x) = \psi_n(x)$, $u_1(x) = \psi_{n+1}(x)$ as the transformation functions we remove the two corresponding levels from the equidistant spectrum (**I**), [57]. Wronskian of the transformation functions, $W_{n,n+1}(x) = W(\psi_n, \psi_{n+1})$, is a polynomial multiplied by an exponential function:

$$W_{n,n+1}(x) = -Q_n(x)\exp\left(-x^2/2\right), \qquad Q_n(x) = p_{n+1}^2(x) - p_n(x)p_{n+2}(x)\,. \tag{1.4.12}$$

Potentials $V^{n,n+1}$ are calculated from (1.2.28) which yields

$$V^{n,n+1}(x) = -2\frac{Q_n''(x)}{Q_n(x)} + 2\left[\frac{Q_n'(x)}{Q_n(x)}\right]^2 + \frac{x^2}{4} + 3/2\,. \tag{1.4.13}$$

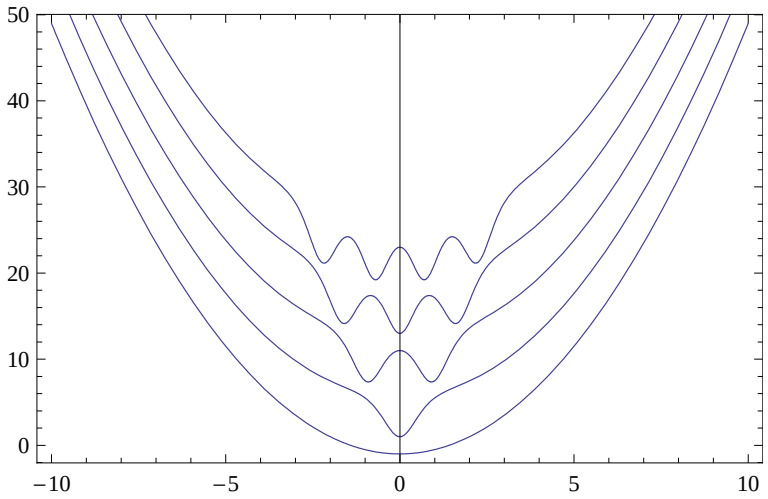

Figure 1.3: Potential of harmonic oscillator and first four potentials $V^{n,n+1}(x) + 5n$, $n = \overline{1,4}$, of family (1.4.13).

Finally we note that the potentials (1.4.13) behave asymptotically like $x^2/4$ for $|x| \to \infty$ and have n shallow minima at their bottom. This family of potentials presents an example of exactly solvable multi-well potentials [57]. We plot potential of harmonic oscillator and first four potentials in figure (1.3).

It should be noted that although the exactly solvable models considered above have been well known for a long time [57], their Green functions and propagators were not calculated.

1.4.3 Non-conservative SUSY transformations and the Cox potential

In this section, a non-conservative SUSY transformation of the coupled-channel Schrödinger equation (1.1.20) with different thresholds and $l = 0$ is studied. More precisely, we consider non-conservative SUSY transformations applied to the vanishing initial potential $V_0 = 0$, for which the Jost matrix and scattering matrix are identity, $S_0(k) = F_0(k) = I$. For a given factorization energy, the most general real symmetric superpotential depends on an N-dimensional real symmetric matrix of arbitrary parameters, i.e., on $N(N+1)/2$ real arbitrary parameters [49]. When $V_0 = 0$, the corresponding factorization solution can be written as

$$u(r) = \cosh(\kappa r) + \mathcal{K}^{-1} \sinh(\kappa r) w_0 \tag{1.4.14a}$$

$$= (2\mathcal{K})^{-1}[\exp(\kappa r)(\mathcal{K} + w_0) + \exp(-\kappa r)(\mathcal{K} - w_0)], \tag{1.4.14b}$$

which ensures that the resulting potential V_1 is regular at the origin, and where the arbitrary parameters explicitly appear as the value of the (symmetric) superpotential at the origin, $w_0 \equiv w(0)$; $\exp(\pm\kappa r)$, $\cosh(\kappa r)$ and $\sinh(\kappa r)$ are diagonal matrices with entries $\exp(\pm\kappa_i r)$, $\cosh(\kappa_i r)$ and $\sinh(\kappa_i r)$ respectively. According to Ref. [49], when $\mathcal{K} + w_0$ is invertible, the transformed Jost matrix reads

$$F_1(k) = (\mathcal{K} - iK)^{-1}(w_0 - iK). \tag{1.4.15}$$

The Jost matrix $F_1(k)$ may be obtained by definition (1.1.28), where the Jost solution is given by (1.2.27) and $w_\infty = \mathcal{K}$. We see that the coupling appear due to the non-diagonal character of w_0.

This Jost function was obtained by other means in Ref. [46] in the case $q = 1$. However, it was not realized there that the corresponding potential could be simply expressed in terms of a solution matrix u, using Eqs. (1.2.21) and (1.2.23). In that reference, a compact expression for the potential is found [see Eq. (1.4.23) below] but writing (1.4.14) and (1.2.23) is much more elegant because both the potential (1.2.21) and its Jost function (1.4.15) are expressed in terms of the same parameter matrix w_0. Nevertheless, this procedure also presents several disadvantages: calculating the potential requires several matrix operations (inversion, product, derivations); moreover, the parameters in w_0 should be chosen so that the factorization solution is invertible for all r, a condition not easily checked on Eqs. (1.4.14).

Let us now derive an alternative form for the factorization solution, which solves both these inconveniences. In Ref. [49], the possibility of rank $(\mathcal{K} + w_0) < N$ in Eq. (1.4.14b) has been studied, which leads to an interesting asymptotic behavior of the superpotential but which reduces the number of parameters in the model. Here, in order to keep the maximal number of arbitrary parameters in the potential, we choose $\mathcal{K} + w_0$ invertible. The factorization solution (1.4.14b) can then be multiplied on the right by $2(\mathcal{K} + w_0)^{-1}\mathcal{K}^{1/2}$, which leads to the factorization solution

$$u(r) = \mathcal{K}^{-1/2} \left[\exp(\kappa r) + \exp(-\kappa r) X_0\right]. \tag{1.4.16}$$

According to Eq. (1.2.23), the superpotential, and hence the transformed potential, is unaffected by this multiplication. The symmetric matrix X_0 now contains all the arbitrary parameters. The link between the two sets of parameters is given by

$$X_0 = \mathcal{K}^{-1/2}(\mathcal{K} - w_0)(\mathcal{K} + w_0)^{-1}\mathcal{K}^{1/2}, \tag{1.4.17}$$

$$w_0 = \mathcal{K}^{1/2}(I - X_0)(I + X_0)^{-1}\mathcal{K}^{1/2}. \tag{1.4.18}$$

Equation (1.4.16) can also be written as

$$u(r) = \mathcal{K}^{-1/2} \left[I + X(r)\right] \exp(\kappa r), \tag{1.4.19}$$

where

$$X(r) = \exp(-\kappa r) X_0 \exp(-\kappa r). \tag{1.4.20}$$

With respect to writing (1.4.14a) and (1.4.14b), Eq. (1.4.19) presents several advantages. First, it allows for a simple calculation of the superpotential

$$\begin{aligned} w(r) &= \mathcal{K} - 2\mathcal{K}^{1/2} X(r) [I + X(r)]^{-1} \mathcal{K}^{1/2} \\ &= -\mathcal{K} + 2\mathcal{K}^{1/2} [I + X(r)]^{-1} \mathcal{K}^{1/2}. \end{aligned} \tag{1.4.21}$$

The last expression is particularly convenient since the r dependence is limited to one factor of the second term; the potential can thus be explicitly written as

$$\begin{aligned} V_1(r) &= 4\mathcal{K}^{1/2} [I + X(r)]^{-1} X'(r) [I + X(r)]^{-1} \mathcal{K}^{1/2} \\ &= -4\mathcal{K}^{1/2} \left(e^{\kappa r} + X_0 e^{-\kappa r}\right)^{-1} (X_0 \mathcal{K} + \mathcal{K} X_0) \left(e^{\kappa r} + e^{-\kappa r} X_0\right)^{-1} \mathcal{K}^{1/2}. \end{aligned} \tag{1.4.22}$$

The last expression is exactly equivalent to Eq. (4.7) of Ref. [46] for $q = 1$, which reads

$$\begin{aligned} V_1(r) &= 2e^{-\kappa r} \left[I - A(2\mathcal{K})^{-1} e^{-2\kappa r}\right]^{-1} (A\mathcal{K} + \mathcal{K} A) \\ &\times \left[I - e^{-2\kappa r} (2\mathcal{K})^{-1} A\right]^{-1} e^{-\kappa r}, \end{aligned} \tag{1.4.23}$$

provided one defines matrix A as

$$\begin{aligned} A &= -2\mathcal{K}^{1/2} X_0 \mathcal{K}^{1/2} \\ &= -2(\mathcal{K} - w_0)(\mathcal{K} + w_0)^{-1}\mathcal{K}\,. \end{aligned} \tag{1.4.24}$$

The second advantage of writing (1.4.19) is that it easily leads to a necessary and sufficient condition on the parameters to get a potential without singularity at finite distances. This condition is positive definiteness of matrix $I + X_0$:

$$I + X_0 > 0\,. \tag{1.4.25}$$

The potential has a singularity when $u(r)$ is noninvertible, i.e., when $\det[I + X(r)]$ vanishes for some r. Using Eq. (1.4.20), we find that this is equivalent to the existence of $r_0 \geq 0$ such that $\det Y(r_0) = 0$ with $Y(r) = \exp(2\kappa r) + X_0$. Assume now that $\det Y(r) \neq 0\ \forall r \geq 0$. Since $\det Y(r) = \prod_{i=1}^{N} y_i(r)$ where $y_i(r)$ are the eigenvalues of $Y(r)$, we conclude that $y_i(r) \neq 0$ for all $i = 1, \ldots, N$ and $r \geq 0$. But since for sufficiently large r, X_0 becomes a small perturbation to $\exp(2\kappa r)$, all eigenvalues of $Y(r)$ should be positive for $r \geq 0$ and in particular at $r = 0$, thus proving the necessary character of the above condition.

The sufficiency follows from the observation that $Y(r)$ is positive definite for any $r \geq 0$, together with $Y(0) = I + X_0$. Indeed, if $Y(r)$ is positive definite, the inequality $\langle q|Y(r)|q\rangle > 0$ holds for any $q \in L_N$. Here $\langle p\,|q\rangle = \sum_{i=1}^{N} p_i^* q_i$ is the usual inner product in the N-dimensional complex linear space L_N, with p_i, q_i being coordinates of the vectors $p, q \in L_N$ with respect to an orthonormal basis. But since $\langle q|Y(r)|q\rangle = \langle q|X_0|q\rangle + \langle q|\exp(2\kappa r)|q\rangle \geq \langle q|X_0|q\rangle + \langle q|q\rangle = \langle q|X_0 + I|q\rangle$ [we recall that $r \geq 0$, $\kappa_i > 0$ and $\exp(\kappa r)$ is a diagonal matrix with entries $\exp(\kappa_i r)$], positive definiteness of $I + X_0$ implies positive definiteness of $Y(r)$ for $r \geq 0$.

Having established this condition on X_0, one can get the condition in terms of w_0, using Eq. (1.4.17). Since

$$I + X_0 = 2\mathcal{K}^{1/2}(\mathcal{K} + w_0)^{-1}\mathcal{K}^{1/2}, \tag{1.4.26}$$

the necessary and sufficient condition to get a regular potential is positive definiteness of matrix $\mathcal{K} + w_0$:

$$\mathcal{K} + w_0 > 0\,. \tag{1.4.27}$$

Since the (diagonal) elements of $\mathcal{K}$ are positive and increase when the factorization energy decreases, this condition has a simple interpretation: it just puts some upper limit on the factorization energy.

Finally, Eq. (1.4.24) shows that the condition $\det A \neq 0$ required in Ref. [46] is not required here. In Cox' paper, this condition does not appear in the potential expression, which is valid in the general case, but only in the derivation of the proof; the fact that this condition is not required here illustrates the efficiency of the supersymmetric formalism. Equation (1.4.24) also implies that $\mathrm{rank}\,(\mathcal{K} + w_0) < N$ corresponds to $\det A = \infty$, a case also not considered in Ref. [46]. The supersymmetric treatment, on the contrary, allows this case [48, 49]; our approach thus subsumes the results of Ref. [46] in several respects. The properties of the Cox potential will be studied in details in the chapter 3. The two channel Cox potential will be used to construct a model of magnetic induced Feshbach resonance.

Chapter 2

Supersymmetric transformations for the Green function and the propagator

2.1 Green functions in SUSY QM [1, 2]

2.1.1 The first and the second order SUSY transformations for the Green function

Below we give a simple formula for the Green function of the SUSY partner Hamiltonian both for confining and for scattering potentials. We restrict ourselves by the first and the second order SUSY transformarions (see sections 1.2.1 and 1.2.2).

Theorem 1. *Let $G_0(x, y, E)$ be the Green function for h_0. Then for all three cases of the first order SUSY transformation enumerated in 1.2.1 the Green function for h_1 is:*

$$G_1(x, y, E) = \frac{1}{E - \alpha}[L_x L_y G_0(x, y, E) - \delta(x - y)], \quad E \neq \alpha\,. \tag{2.1.1}$$

In case **(ii)** *it has a simple pole at $E = \alpha$. In cases* **(i)** *and* **(iii)** *it is regular at $E = \alpha$ and can be calculated as follows:*

$$G_1(x, y, \alpha) = \left[L_x L_y \frac{\partial G_0(x, y, E)}{\partial E}\right]_{E=\alpha}. \tag{2.1.2}$$

Here L_x is the operator given in (1.2.13) and L_y is the same operator where x is replaced by y.

Proof. In case **(i)** we have $u = \psi_0(x)$, and the set $\{\phi_k(x), \phi_n(x), n = 1, 2, \ldots, M\}$ is complete. Therefore

$$G_1(x, y, E) = \sum_{n=1}^{M} \frac{\phi_n(x)\phi_n^*(y)}{E_n - E} + \int \frac{\phi_k(x)\phi_k^*(y)}{k^2 - E} dk\,. \tag{2.1.3}$$

Now we replace ϕ_n using (1.2.19) which yields

$$G_1(x, y, E) = \frac{1}{\alpha - E} L_x L_y \left(\sum_{n=1}^{M} \left[\frac{1}{E_n - \alpha} - \frac{1}{E_n - E}\right] \psi_n(x)\psi_n^*(y) + \int \left[\frac{1}{k^2 - \alpha} - \frac{1}{k^2 - E}\right] \psi_k(x)\psi_k^*(y) dk\right). \tag{2.1.4}$$

The statement for $E \neq \alpha$ follows from here if in the first sum and in the first integral we express $L\psi_n$, $L\psi_k$ in terms of ϕ_n, ϕ_k, make use of the completeness condition for the set $\{\phi\}$ and formula (1.1.19) for G_0. The fact that here the sum starts from $n = 1$ and in (1.1.19) it starts from $n = 0$ cannot cause any problems since $L\psi_0(x) = 0$. For $E = \alpha$ formula (2.1.3) can be written in the form

$$G_1(x, y, \alpha) = \left[\frac{\partial}{\partial E} L_x L_y \left(\sum_{n=0}^{M} \frac{\psi_n(x)\psi_n^*(y)}{E_n - E} + \int \frac{\psi_k(x)\psi_k^*(y)}{k^2 - E} dk \right) \right]_{E=\alpha}, \tag{2.1.5}$$

from which (2.1.2) follows in this case.

In case **(ii)** let $\phi_{-1}(x, \alpha) \sim 1/u$ be the normalized ground state function of h_1 corresponding to the new discrete level $E = \alpha$. Then

$$G_1(x, y, E) = \sum_{n=0}^{M} \frac{\phi_n(x, E_n)\phi_n^*(y, E_n)}{E_n - E} + \frac{\phi_{-1}(x)\phi_{-1}^*(y)}{\alpha - E} + \int \frac{\phi_k(x)\phi_k^*(y)}{k^2 - E} dk \,. \tag{2.1.6}$$

Now the use of exactly the same transformations as in case **(i)** reduces (2.1.6) to (2.1.1).

In case **(iii)** we start from the same formula (2.1.3) with the only difference that the sum now starts from $n = 0$ and following the same line of reasoning as in the earlier cases we get formula (2.1.1). It is interesting to notice the intermediate result

$$G_1(x, y, E) = \frac{1}{\alpha - E} L_x L_y \left[G_0(x, y, \alpha) - G_0(x, y, E) \right], \tag{2.1.7}$$

which makes clear how formula (2.1.2) arises for this case by taking the limit $E \to \alpha$. The fact that in case **(ii)** function (2.1.1) has a simple pole at $E = \alpha$ is a consequence of the equivalence between (2.1.6) and (2.1.1). □

Corrolary 1. *In terms of the special solutions f_{l0} and f_{r0} of the Schrödinger equation for h_0 the Green function G_1 for all three cases listed above may be expressed as follows:*

$$G_1(x, y, E) = \frac{1}{(E - \alpha)W_0} \left[\Theta(y - x) L_x f_{l0}(x, E) L_y f_{r0}(y, E) + \Theta(x - y) L_y f_{l0}(y, E) L_x f_{r0}(x, E) \right]. \tag{2.1.8}$$

In case **(ii)** *this function has a simple pole at $E = \alpha$. In cases* **(i)** *and* **(iii)** *it is regular at $E = \alpha$ and can be calculated as follows:*

$$G_1(x, y, E) = \left[\frac{\partial}{\partial E} \frac{\Theta(y - x) L_x f_{l0}(x, E) L_y f_{r0}(y, E) + \Theta(x - y) L_y f_{l0}(y, E) L_x f_{r0}(x, E)}{W_0} \right]_{E=\alpha}. \tag{2.1.9}$$

Proof. To prove these formulae we substitute G_0 as given in (1.1.18) into (2.1.1) and (2.1.2). Taking the derivative of the theta functions in (1.1.18) gives rise to the Dirac delta function which cancels out the delta function present in (2.1.1). Formula (2.1.8) is clearly valid since the conservative SUSY transformations necessarily preserve the boundary conditions for all E except perhaps for $E = \alpha$. This implies that $f_{l1} = Lf_{l0}$ vanishes at $x = a$ and $f_{r1} = Lf_{r0}$ vanishes at $x = b$. The denominator in (1.1.18) is just the Wronskian of f_{r1} and f_{l1}. From lemma 1 and (1.2.18) follows that $W(f_{r1}, f_{l1}) = (E - \alpha)W(f_{r0}, f_{l0}) = (E - \alpha)W_0$. □

Let us consider the second order transformations described in section 1.2.2. The spectrum of the Hamiltonian $h_2 = -d^2/dx^2 + V_2$ coincides with the spectrum of h_0 except may be $E = \alpha_1, \alpha_2$.

Theorem 2. *Let $G_0(x,y,E)$ be the Green function for h_0. Then the Green function for h_2 is:*

$$G_2(x,y,E) = \frac{1}{(E-\alpha_1)(E-\alpha_2)} L_x L_y G_0(x,y,E)\,, \quad x<y\,, \quad E\neq\alpha_1,\alpha_2\,. \tag{2.1.10}$$

Proof. The (conservative) second order SUSY transformation preserves a boundary behaviour of solutions, therefore $f_{2l}(x,E) = Lf_{0l}(x,E)$ and $f_{2r}(x,E) = Lf_{0r}(x,E)$ for all E except maybe $E=\alpha_1,\alpha_2$. From (1.2.31) we obtain the wronskian of these solutions $W_2 = (E-\alpha_1)(E-\alpha_2)W_0$. As a result, from (1.1.16) immediately follows the statement of the theorem □

For the second order transformation of the Green function we prefer to use the unsymmetrized form of the Green function with $x<y$, because this form makes expressions more compact. In principle, one can express the Green function for arbitrary x and y as follows:

$$G_2(x,y,E) = \frac{1}{(E-\alpha_1)(E-\alpha_2)} L_x L_y \left[G_0(x,y,E) - (h_0 - E - \alpha_1 - \alpha_2)\delta(x-y)\right]\,. \tag{2.1.11}$$

It is the straightforward generalization of (2.1.1).

Again cases $E=\alpha_1,\alpha_2$ require an additional analysis. Consider, for example, the case $E=\alpha_1$. If $\alpha_1 \in \operatorname{spec} h_2$ (cases (**II**), (**III**) and (**IV**)) then G_2 has a pole at this energy. Otherwise, if $\alpha_1 \notin \operatorname{spec} h_2$ then one can find $G_2(x,y,\alpha_1)$ as the limit $\lim\limits_{E\to\alpha_1} G_2(x,y,E)$. For example, in case (**VI**) when both $\alpha_{1,2} \notin \operatorname{spec} h_2$ and $\alpha_{1,2} \notin \operatorname{spec} h_0$ the Green function at $E=\alpha_1$ reads

$$G_2(x,y,\alpha_1) = \frac{1}{\alpha_1-\alpha_2} L_x L_y \left[\left(\frac{\partial G_0(x,y,E)}{\partial E}\right)_{E=\alpha_1} + \frac{G_0(x,y,\alpha_2) - G_0(x,y,\alpha_1)}{\alpha_1-\alpha_2}\right]\,. \tag{2.1.12}$$

Finally we consider the case of the degenerate second order transformation when $\alpha_1=\alpha_2=\alpha$. For $E\neq\alpha$ the Green function is calculated by (2.1.10) where operator L is defined in (1.2.34),

$$G_2(x,y,E) = \frac{1}{(E-\alpha)^2} \tag{2.1.13}$$

$$\left(\alpha - E + \frac{u(x)u'(x) - u(x)^2\partial_x}{c + \int_{x_0}^x u^2(t)dt}\right)\left(\alpha - E + \frac{u(y)u'(y) - u(y)^2\partial_y}{c + \int_{x_0}^y u^2(t)dt}\right) G_0(x,y,E)\,, \tag{2.1.14}$$

$$x<y\,, \quad E\neq\alpha\,. \tag{2.1.15}$$

2.1.2 Scattering potentials and the trace formula

The trace of the Green function defined as $\int_a^b G(x,x,E)dx$ is usually divergent if the system has a continuous spectrum. It is remarkable that the trace of the difference $G_0(x,x,E) - G_1(x,x,E)$ is a finite quantity which may or may not be equal to zero [80]. In some cases this fact may be explained by another remarkable property. It may happen that the difference of infinite normalizations (they diverge as $\delta(x-y)$ when $y\to x$) of the continuous spectrum eigenfunctions of the two SUSY partners is a finite quantity.

Theorem 3. *Let G_0 and G_1 be the Green functions related by the first order SUSY transformation. Then the trace of the difference $G_0(x,x,E) - G_1(x,x,E)$ reads*

$$\Delta(E) = \int_a^b [G_0(x,x,E) - G_1(x,x,E)]dx = \frac{Q(E)}{W_0(E-\alpha)}\,. \tag{2.1.16}$$

where $Q(E)$ can be calculated by one of the following formulae:

$$Q(E) = (f_{r0}f_{l1})_{x=b} - (f_{r0}f_{l1})_{x=a} = (f_{l0}f_{r1})_{x=b} - (f_{l0}f_{r1})_{x=a} \tag{2.1.17}$$

$$= -W_0 + (f_{l0}f_{r1})_{x=b} - (f_{r0}f_{l1})_{x=a} = W_0 + (f_{r0}f_{l1})_{x=b} - (f_{l0}f_{r1})_{x=a}\,, \tag{2.1.18}$$

Proof. From Corollary 1 it follows that $G_1(x,x,E) = \frac{1}{W_0(E-\alpha)} Lf_{l0}(x)Lf_{r0}(x)$. While integrating this expression over the interval (a,b) one can transfer the derivative present in L either from f_{l0} to f_{r0} or from f_{r0} to f_{l0} which leads to one of the following integrands $f_{l0}(x)L^+Lf_{r0}(x)$ or $f_{r0}(x)L^+Lf_{l0}(x)$. In both cases the factorization property (1.2.12) may be used to reduce the integrand to $(E-\alpha)f_{l0}(x)f_{r0}(x)$. Thus we arrive at the relation

$$\int_a^b G_1(x,x,E)dx = \int_a^b f_{l0}f_{r0}dx - \frac{Q(E)}{W_0(E-\alpha)}\,, \tag{2.1.19}$$

where $Q(E)$ is given by (2.1.17). To prove (2.1.18) it is sufficient to notice that

$$f_{l0}(x,E)f_{r1}(x,E) - f_{r0}(x,E)f_{l1}(x,E) = W_0 \tag{2.1.20}$$

since $f_{r1} = W[f_{r0},u]/u$ and $f_{l1} = W[f_{l0},u]/u$. The identification of the integrand on the right hand side of (2.1.19) as $W_0G_0(x,x,E)$ then leads to the result given in (2.1.16). □

Using the first of equalities (2.1.17) one can rewrite (2.1.16) as follows:

$$\int_a^b [G_0(x,x,E) - G_1(x,x,E)]dx = \frac{1}{\alpha - E} + \frac{(f_{l0}f_{r1})_{x=b} - (f_{r0}f_{l1})_{x=a}}{W_0(E-\alpha)} \tag{2.1.21}$$

Now for case **(i)** where $\alpha = E_0$ if we compare this result with the corresponding difference which can be obtained directly from the expressions for G_0 given by (1.1.19) and for G_1 given by (2.1.3) the following feature may be noted: the first term on the right hand side of (2.1.21) arises from the contribution to Green functions from the discrete spectra and the second term, which as we show below may be different from zero, is due to the presence of the continuous spectra. This contribution was neglected in [80]. So, theorem 3 presents a generalization of the result obtained in [80] to the case where a continuous spectrum may be present. As an application of this theorem we are going to consider one particular case of scattering potential defined on the whole real line.

Theorem 4. *If h_0 is a scattering Hamiltonian with the potential V_0 satisfying for the spectral problem on the whole line the condition*

$$\int_{-\infty}^{\infty} (1+|x|)|V_0(x)|dx < \infty\,. \tag{2.1.22}$$

then for $E \neq \alpha$, $\mathrm{Im}\sqrt{E} > 0$ the following equality

$$\Delta(E) = \frac{\delta}{\kappa^2 + ia\kappa} - \frac{\delta}{\kappa^2 + a^2}\,, \tag{2.1.23}$$

*holds, where $E = \kappa^2$, $\alpha = -a^2$; $\delta = 1$ for case (**i**), $\delta = -1$ for case (**ii**) and $\delta = 0$ for case (**iii**).*

Proof. The statement readily follows from the fact that any scattering potential has a pair of solutions (Jost solutions, see e.g. [22]) with asymptotics (1.1.14) at the right infinity and similar asymptotics at the left infinity and the use of an appropriate part of equalities (2.1.17) and (2.1.18). The Wronskian W_0 for Jost solutions can easily be calculated, $W_0 = 2ik$. □

So, we see that despite the fact that for both h_0 and h_1 the continuous spectrum eigenfunctions are normalized to the Dirac delta function, i.e. that in both cases they have equal infinite norms, the difference of these infinities is a finite non-zero quantity in cases **(i)** and **(ii)** and it is zero in case **(iii)**.

For instance in case **(ii)** the following equality arises:

$$\int_{-\infty}^{\infty} \frac{P(k)dk}{k^2 - E} = R(E)\,, \qquad R(E) = \frac{-1}{\kappa^2 + ia\kappa}\,, \qquad E = \kappa^2\,, \qquad \alpha = -a^2\,, \tag{2.1.24}$$

where

$$P(k) = \int_{-\infty}^{\infty} \left[|\psi_0(x,k)|^2 - \phi_n(x,k)|^2\right] dx\,. \tag{2.1.25}$$

Equation (2.1.24) may be reduced to the Stieltjes transform and the function P may be found by the Stieltjes inversion formula (see e.g. [98]). To establish this we first notice that the integral on the left hand side of (2.1.24) is different from zero only if $P(k)$ is an even function which we assume to be the case. Therefore it can be considered only for positive ks and we can let $k^2 = \lambda$. So, (2.1.24) takes the form

$$\int_{-\infty}^{\infty} \frac{d\rho(\lambda)}{\lambda - E} = R(E)\,,$$

where the measure $\rho(\lambda)$ is continuous for $\lambda > 0$, $d\rho(\lambda) = \frac{1}{\sqrt{\lambda}} P(\lambda)d\lambda$ and such that for negative λs the integral is zero. Now the Stieltjes inversion formula yields

$$\frac{P(\lambda)}{\sqrt{\lambda}} = \frac{\mathrm{sign}\tau}{2\pi i} \lim_{\tau \to 0} [R(E) - R(E^*)]\,, \qquad E = \lambda + i\tau\,.$$

Note that because of the condition $\mathrm{Im}\sqrt{E} > 0$ the square root of E has different signs for E in the upper and lower halves of the complex E-plane. Therefore the function $R(E)$ has a cut along the real axis and the jump across this cut defines the function $P(\lambda)$. After a simple calculation one gets

$$P(\lambda) = a\pi^{-1}(\lambda^2 + a^2)^{-1}\,. \tag{2.1.26}$$

It must be noted that in the present case the interchange of the integrals over the space variable x taken in the difference of (1.1.19) and (2.1.3) at $y = x$ with the integral over the momentum k is justified.

2.1.3 Normalization of the eigenfunctions in the continuum

Let us consider a particular example of the free motion on the line, $V_0(x) = 0$, $x \in \mathbb{R}$. The Green function is

$$G_0(x,y,E) = \frac{i}{2\kappa} e^{i\kappa|x-y|}\,, \qquad \mathrm{Im}\kappa > 0\,, \qquad E = \kappa^2\,. \tag{2.1.27}$$

The simplest possible superpartner of the zero potential is the one-soliton potential (see section 1.4.1). The operator of the SUSY transformation is $L = -a\tanh(ax) + \partial_x$. The eigenfunctions of the soliton potential which belong to the continuous spectrum read as follows

$$\phi_k(x) = \frac{1}{\sqrt{2\pi}N_k} \left[-a\tanh(ax) - ik\right] \mathrm{e}^{-ikx}\,, \qquad N_k = \sqrt{k^2 + a^2}\,. \tag{2.1.28}$$

Below we calculate difference (2.1.25) for the eigenfunctions of the soliton and the zero potential directly. First, we introduce $P(k',k) = \langle\psi_{k'}|\psi_k\rangle - \langle\phi_{k'}|\phi_k\rangle$ and then consider the limit $k \to k'$:

$$P(k',k) = \lim_{A\to\infty} P(k,k',A) = \lim_{A\to\infty} \int\limits_{-A}^{A} [\psi_k^*(x)\psi_{k'}(x) - \phi_k^*(x)\phi_{k'}(x)]dx =$$

$$= \frac{1}{2\pi} \lim_{A\to\infty} \int\limits_{-A}^{A} \left(\mathrm{e}^{i(k'-k)x} - N_{k'}N_k(a^2 \frac{\sinh^2 ax}{\cosh^2 ax} + ia(k-k')\tanh ax + kk')\mathrm{e}^{i(k'-k)x} \right) dx\,.$$

One can see that $P(k,k',A)$ has the following structure $P(k,k',A) = \delta_A(k,k') - \widetilde{\delta}_A(k,k')$, where $\delta_A(k,k')$ and $\widetilde{\delta}_A(k,k')$ are two delta-like sequences

$$\delta_A(k,k') = \frac{1}{2\pi}\sin(kA)/k\,,$$

$$\widetilde{\delta}_A(k,k') = \frac{1}{2\pi} N_{k'}N_k \left[(a^2+k'k)\sin(kA)/k + 2\tanh(aA)\cos[(k'-k)A]\right]\,.$$

These sequences converge to the delta-function as $A \to \infty$,

$$\lim_{A\to\infty} \int_{-\infty}^{\infty} \delta_A(k)f(k)dk = \lim_{A\to\infty} \int_{-\infty}^{\infty} \widetilde{\delta}_A(k)f(k)dk = f(0)\,.$$

On the other hand the difference between these sequences at $k = k'$ has non-vanishing value

$$P(k) = \lim_{A\to\infty} P(k,k,A) = \frac{a}{\pi(k^2+a^2)}\,. \tag{2.1.29}$$

Thus we confirm result (2.1.26) in this simple model by direct calculations.

One may give the following interpretation of the trace formula. Difference $\Delta(E)$ is nothing but the super-trace of the matrix Green function $G = \mathrm{diag}(G_0, G_1)$. The super-trace of the Green function is related to the regularized Witten index [109], which is a topological invariant of the model. The vanishing of $\Delta(E)$ in the case (**iii**) indicates that SUSY is broken. Indeed, spectra of h_0 and h_1 coincide, therefore the ground state (vacuum) of the matrix super-hamiltonian is degenerate.

2.2 Supersymmetric transformations for propagators [3–5]

2.2.1 Propagators related by first-order intertwiners

The defining equation for the propagator of the non-stationary Schrödinger equation with super-Hamiltonian (1.2.2) can be trivially decomposed as

$$[iI\partial_t - H]\mathbf{K}(x,y;t) = 0 \qquad \mathbf{K} = \begin{bmatrix} K_0(x,y;t) & 0 \\ 0 & K_N(x,y;t) \end{bmatrix}$$
$$\mathbf{K}(x,y;0) = I\delta(x-y)\,.$$

From the structure of the SUSY induced relations between superpartner Hamiltonians it is clear that via the corresponding Schrödinger equations these relations should extend to relations between the associated propagators. The main goal of the chapter is to analyze these relations between SUSY partner propagators and to reshape them into user friendly general recipes for the construction of new propagator classes. In order to derive the corresponding technical tools we concentrate on the general approach which allows to establish the link between the propagators of any two SUSY partner Hamiltonians. By SUSY-transformations we will only induce changes in the point spectrum of h_0 so that, for simplicity, we will work with decompositions over discrete sets of basis functions (corresponding to point spectra) keeping in mind that extensions to the continuous spectrum are straightforward.

We begin with the studying of the propagators interrelated by first-order SUSY transformations. According to (1.2.6) a first-order intertwiner has the form

$$L_x = -u'(x)/u(x) + \partial_x \qquad h_0 u = \alpha u\,.$$

The intertwiner L may result in the three types of relations between the spectra of the Hamiltonians h_0 and h_1 (see discussion in section 1.2.1).

Introducing the "regularized" version of the the Green function

$$\widetilde{G}_0(z,y,E_0) = \sum_{m=1}^{\infty} \frac{\psi_m(x)\psi_m(y)}{E_m - E_0} = \lim_{E\to E_0}\left[G_0(z,y,E) - \frac{\psi_0(x)\psi_0(y)}{E_0 - E}\right]$$

the corresponding structural relations for the propagators can be summarized in the following

Theorem 5. *The propagators $K_1(x,y;t)$ and $K_0(x,y;t)$ of non-stationary Schrödinger equations with SUSY intertwined Hamiltonians h_1 and h_0 are interrelated with each other and with the Green functions $G_0(x,y;E)$ and $\widetilde{G}_0(z,y,E_0)$ in the following way:*
Type **(i)** *relation*

$$K_1(x,y,t) = L_x L_y \int_a^b K_0(x,z,t)\widetilde{G}_0(z,y,E_0)dz\,. \tag{2.2.1}$$

Type **(ii)** *relation*

$$K_1(x,y,t) = L_x L_y \int_a^b K_0(x,z,t)G_0(z,y,\alpha)dz + \phi_{-1}(x)\phi_{-1}(y)\mathrm{e}^{-i\alpha t}. \tag{2.2.2}$$

Type **(iii)** *relation*

$$K_1(x,y,t) = L_x L_y \int_a^b K_0(x,z,t)G_0(z,y,\alpha)dz\,. \tag{2.2.3}$$

Proof. We start from the type **(ii)** relation and represent the propagator $K_1(x,y;t)$ in terms of the basis functions $\phi_m(x,t)$ of the Hamiltonian h_1 (cf. (1.1.9)). We note that the explicit time-independence of h_1 implies a factorization $\phi_m(x,t) = \phi_m(x)\exp(-iE_mt)$ with $\phi_m(x)$ purely real-valued. Expressing ϕ_m in terms of the corresponding wave functions of the Hamiltonian h_0, $\phi_m = N_mL\psi_m$, with $N_m = (E-\alpha)^{-1/2}$ a normalization constant (see (1.2.19)), we arrive at

$$\begin{aligned} K_1(x,y,t) &= \sum_{m=-1}^{\infty} \phi_m(x)\phi_m(y)\mathrm{e}^{-iE_mt} \\ &= L_xL_y\sum_{m=0}^{\infty}\frac{\psi_m(x)\psi_m(y)}{E_m-\alpha}\mathrm{e}^{-iE_mt} + \phi_{-1}(x)\phi_{-1}(y)\mathrm{e}^{-i\alpha t}\,. \end{aligned}$$

Modulo a normalization factor N_{-1}, the wave function ϕ_{-1} of the new ground state is proportional to the inverse power of the transformation function $u(x)$, $\phi_{-1} = N_{-1}/u(x)$. It remains to express the time-dependent phase factor in terms of the propagator. This can be easily done using the evident property of the bound state solutions of the Schrödinger equation

$$\int_a^b K_0(x,z,t)\psi_m(z)dz = \psi_m(x)\mathrm{e}^{-iE_mt} \tag{2.2.4}$$

so that the previous equation reads

$$K_1(x,y,t) = L_xL_y\int_a^b K_0(x,z,t)\sum_{m=0}^{\infty}\frac{\psi_m(z)\psi_m(y)}{E_m-\alpha}dz + \phi_{-1}(x)\phi_{-1}(y)\mathrm{e}^{-i\alpha t}. \tag{2.2.5}$$

The sum in this relation can be identified as the Green function (1.1.19). Due to $E_m - \alpha > 0$, $\forall E_m \in \mathrm{spec}(h_0)$ this Green function is regular $\forall E_m$ and the proof for type **(ii)** transformations is complete.

The proof for type **(i)** and **(iii)** transformations follows the same scheme. The formally regularized Green function $\widetilde{G}_0(z,y,E_0)$ in **(i)** results from the fact that the ground state with energy E_0 is not present in the spectrum of h_1 so that a sum $\sum_{m>0}$ appears and the ground state contribution has to be subtracted from $G_0(x,y,\alpha=E_0)$. In case of a type **(iii)** transformation a sum $\sum_{m=0}^{\infty}$ over the complete set of eigenfunctions appears in (2.2.5) and no new state occurs. □

We conclude this section by reshaping relation (2.2.1) for the propagator of a system with removed original ground state, i.e. of a type **(i)** transformed system. The corresponding result can be formulated as

Theorem 6. *For transformations with $u(x) = \psi_0(x)$ the propagator $K_1(x,y;t)$ of the resulting system can be represented as*

$$K_1(x,y;t) = -\frac{1}{u(y)}L_x\int_a^y K_0(x,z;t)u(z)dz = \frac{1}{u(y)}L_x\int_y^b K_0(x,z;t)u(z)dz\,. \tag{2.2.6}$$

First of all we recall that $\psi_0(x)$ being the ground state function of h_0 satisfies the zero boundary conditions. To facilitate the proof of Theorem 6 we need the following two lemmas.

Lemma 2.

$$L_y\lim_{E\to E_0}\left(G_0(z,y,E) - \frac{\psi_0(z)\psi_0(y)}{E_0-E}\right) = \lim_{E\to E_0}L_yG_0(z,y,E)\,.$$

Proof. This result follows from the explicit representation of $G_0(z,y,E)$ in terms of basis functions. On the one hand, it holds

$$L_y \lim_{E\to E_0}\left(G_0(z,y,E)-\frac{\psi_0(z)\psi_0(y)}{E_0-E}\right)=\sum_{n=1}^{\infty}\frac{\psi_n(z)L_y\psi_n(y)}{E_n-E_0}$$

whereas on the other hand the kernel property (annihilation) of the ground state $L\psi_0=0$ gives

$$\lim_{E\to E_0}(L_yG_0(z,y,E))=\lim_{E\to E_0}\left(\sum_{n=1}^{\infty}\frac{\psi_n(z)L_y\psi_n(y)}{E_n-E}\right)=\sum_{n=1}^{\infty}\frac{\psi_n(z)L_y\psi_n(y)}{E_n-E_0}\,.$$

□

Lemma 3. *Let $f_l(x,E)$ and $f_r(x,E)$ satisfy the Schrödinger equation*

$$h_0f(x,E):=-f''(x,E)+V_0(x)f(x,E)=Ef(x,E)\qquad x\in(a,b) \tag{2.2.7}$$

and boundary conditions

$$f_l(a,E)=0\qquad f_r(b,E)=0\,. \tag{2.2.8}$$

Let also $E=E_0$ be the ground state level of h_0 with $\psi_0(x)$ as the ground state function (we assume that h_0 has at least one discrete level) then

$$\lim_{E\to E_0}\frac{f_l(x,E)L_yf_r(y,E)}{W(f_r,f_l)} = -\frac{\psi_0(x)\int_y^b\psi_0^2(z)dz}{\psi_0(y)\int_a^b\psi_0^2(z)dz} \tag{2.2.9}$$

$$\lim_{E\to E_0}\frac{f_r(x,E)L_yf_l(y,E)}{W(f_r,f_l)} = \frac{\psi_0(x)\int_a^y\psi_0^2(z)dz}{\psi_0(y)\int_a^b\psi_0^2(z)dz} \tag{2.2.10}$$

where $L_y=-u'(y)/u(y)+\partial_y$ with $u(y)\equiv\psi_0(y)$.

Proof. First we note that according to (1.2.13) $L_yf_r(y,E)=W(u,f_r)/u$. Next, since both $u=\psi_0$ and f_r satisfy the same Schrödinger equation (3.1.25) it holds $W'(u,f_r)=(E_0-E)uf_r$ and hence

$$W(u,f_r)=(E-E_0)\int_y^b u(z)f_r(z,E)dz \tag{2.2.11}$$

where we have used the property $W(u,f_r)_{y=b}=0$ which follows from the BCs for u and f_r. Via (2.2.11) we find

$$L_yf_r(y,E)=\frac{E-E_0}{u(y)}\int_y^b u(z)f_r(z,E)dz \tag{2.2.12}$$

and hence

$$\frac{L_yf_r(y,E)}{W(f_r,f_l)}=-\frac{E-E_0}{f_l(b,E)}\,\frac{\int_y^b u(z)f_r(z,E)dz}{f_r'(b,E)u(y)} \tag{2.2.13}$$

where it has been used that the Wronskian $W(f_r,f_l)=f_r(x,E)f_l'(x,E)-f_l(x,E)f_r'(x,E)$ is x-independent and can be calculated at $x=b$ where $f_r(b,E)=0$. Since the spectrum of h_0 is non-degenerate, the ground state function is unique up to an arbitrary constant factor and, hence, $u(x)=\psi_0(x)$, $f_r(x,E_0)$ and $f_l(x,E_0)$ have to be proportional to each other

$$f_{r,l}(x,E_0)=C_{r,l}u(x) \tag{2.2.14}$$

and for $E\to E_0$ only the first fraction in (2.2.13) remains undetermined. The l'Hospital rule gives for this limit

$$\lim_{E\to E_0}\frac{E-E_0}{f_l(b,E)}=\frac{1}{\dot f_l(b,E_0)} \tag{2.2.15}$$

where the dot denotes the derivative with respect to E. Making use of (2.2.15) and

$$\dot{f}_l(b,E_0)f_l'(b,E_0) = \int_a^b f_l^2(z,E_0)dz \tag{2.2.16}$$

(which we prove below) relation (2.2.13) yields

$$\lim_{E\to E_0} \frac{f_l(x,E)L_y f_r(y,E)}{W(f_r,f_l)} = -f_l(x,E_0)\frac{f_l'(b,E_0)}{f_r'(b,E_0)}\ \frac{\int_y^b u(z)f_r(z,E_0)dz}{u(y)\int_a^b f_l^2(z,E_0)dz} \tag{2.2.17}$$

and via (2.2.14) it leads to the result (2.2.9). The proof of (2.2.10) follows the same lines with evident changes.

Finally, it remains to derive equation (2.2.16). This is easily accomplished by multiplying the Schrödinger equation (2.2.7) for $f = f_l(x,E)$ by $\dot{f}_l(x,E)$, its derivative with respect to E by $f = f_l(x,E)$, and integrating their difference over the interval (a,b). The intermediate result

$$\begin{aligned}&\int_a^b f_l^2(x,E)dx = \\ &\dot{f}_l'(a,E)f_l(a,E) - f_l'(a,E)\dot{f}_l(a,E) - \dot{f}_l'(b,E)f_l(b,E) + f_l'(b,E)\dot{f}_l(b,E)\end{aligned}$$

reduces to (2.2.16) via BC (2.2.8) and its derivative with respect to E (what cancels the first two terms) and the limit $E = E_0$, its implication (2.2.14) and the BC for $u(x)$. □

Proof of theorem 6. For the Green function $G(x,y,E_0)$ in (2.2.1) we use the standard representation (1.1.18) in terms of two linearly independent solutions $f_{l,r}$ of the h_0-Schrödinger equation. Then relation (2.2.1) takes the form

$$\begin{aligned}&K_1(x,y,t) = \\ &L_xL_y\int_a^b K_0(x,z,t)\lim_{E\to E_0}\left[\frac{f_l(z)f_r(y)}{W(f_r,f_l)}\Theta(y-z) + \frac{f_l(y)f_r(z)}{W(f_r,f_l)}\Theta(z-y) - \frac{\psi_0(z)\psi_0(y)}{E_0-E}\right]dz\end{aligned}$$

where the step functions can be resolved to give

$$\begin{aligned}K_1(x,y,t) &= L_xL_y\int_a^y K_0(x,z,t)\lim_{E\to E_0}\left[\frac{f_l(z)f_r(y)}{W(f_r,f_l)} - \frac{\psi_0(z)\psi_0(y)}{E_0-E}\right]dz \\ &+ L_xL_y\int_y^b K_0(x,z,t)\lim_{E\to E_0}\left[\frac{f_l(y)f_r(z)}{W(f_r,f_l)} - \frac{\psi_0(z)\psi_0(y)}{E_0-E}\right]dz\,.\end{aligned}$$

The second argument of the functions $f_{l,r}$ has been omitted for notational simplicity. Explicitly acting with the differential operator L_y on the integrals with variable $y-$boundary yields

$$\begin{aligned}K_1(x,y,t) &= L_x\int_a^y K_0(x,z,t)L_y\lim_{E\to E_0}\left[\frac{f_l(z)f_r(y)}{W(f_r,f_l)} - \frac{\psi_0(z)\psi_0(y)}{E_0-E}\right]dz \\ &+ L_x\int_y^b K_0(x,z,t)L_y\lim_{E\to E_0}\left[\frac{f_l(y)f_r(z)}{W(f_r,f_l)} - \frac{\psi_0(z)\psi_0(y)}{E_0-E}\right]dz\end{aligned} \tag{2.2.18}$$

whereas via Lemma 2 the intertwiner L_y and the limit $\lim_{E\to E_0}$ can be interchanged to give

$$\begin{aligned}&K_1(x,y,t) = \\ &L_x\left\{\int_a^y K_0(x,z,t)\lim_{E\to E_0}\frac{f_l(z)L_yf_r(y)}{W(f_r,f_l)}dz + \int_y^b K_0(x,z,t)\lim_{E\to E_0}\frac{f_r(z)L_yf_l(y)}{W(f_r,f_l)}dz\right\}.\end{aligned} \tag{2.2.19}$$

Application of Lemma 3 leads to

$$K_1(x,y,t) = \frac{L_x}{\psi_0(y)\int_a^b \psi_0^2(q)dq}\left\{-\int_y^b \psi_0^2(q)dq \int_a^y K_0(x,z,t)\psi_0(z)dz \right. \\ \left. + \int_a^y \psi_0^2(q)dq \int_y^b K_0(x,z,t)\psi_0(z)dz\right\} \tag{2.2.20}$$

which we further reshape by expressing the integral with respect to q over the interval (y,b) by the difference of two integrals over the intervals (a,b) and (a,y). Substitution of $\psi_0 = u$ in the first term results in

$$K_1(x,y,t) = -\frac{1}{u(y)}L_x \int_a^y K_0(x,z,t)u(z)dz \\ +\frac{1}{\psi_0(y)\int_a^b \psi_0^2(q)dq}\int_a^y \psi_0^2(q)dq \; L_x \int_a^b K_0(x,z,t)\psi_0(z)dz\,. \tag{2.2.21}$$

The very last integral is nothing but the ground state stationary wave function $\psi_0(x,t) = u(x)\exp(-iE_0t)$. Therefore, since $L_x u(x) = 0$, we obtain the first equality in (2.2.6). The second equality results from applying a similar transformation to the second term in (2.2.20). □

The following remarks are in order. First we have to note that the integral representation (2.2.6) is only valid in the case of first-order SUSY transformations which remove the ground state level. If one wants to create a level in a problem on the whole real line one has to use a transformation function $u(x)$ which diverges for $x \to \pm\infty$ ensuring in this way the normalizability and Dirichlet BCs of the new ground state wave function $\phi_{-1}(x) \propto 1/u(x)$. An attempt to calculate the propagator K_1 via (2.2.6) would usually lead to a divergent integral. The correct approach is to use (2.2.2) in this case. Jauslin [77] using a different procedure obtained the same result (2.2.6) both for removing and creating a level, but he completely ignored questions of convergence or divergence of the corresponding integrals. In concrete calculations he avoided divergent integrals by considering the heat equation only.

2.2.2 Addition of new levels

Let us consider an Nth-order ($N = 2,3,\ldots$) polynomial supersymmetry corresponding to the appearance of N additional levels in the spectrum of h_N compared to the spectrum of h_0. In this case new levels may appear both below the ground state energy of h_0 (reducible supersymmetry) and between any two neighbor levels of h_0 (irreducible supersymmetry, see e.g. [108]). The propagator for the transformed equation can be found in the following way. We develop $K_N(x,y;t)$ over the complete orthonormal set $\{\phi_m(x,t)\}$ of eigenfunctions of h_N and express all ϕ_m with eigenvalues already contained in the spectrum of h_0 in terms of ψ_m, i.e. $\phi_m = N_m L\psi_m$. The normalization constants N_m for transformations fulfilling condition (1.2.10) have the form [57]:

$$N_m = [(E_m-\alpha_0)(E_m-\alpha_1)\ldots(E_m-\alpha_{N-1})]^{-1/2}\,.$$

All other eigenfunctions of h_N which correspond to new levels and which are not contained in spec(h_0) we keep untouched. This yields

$$K_N(x,y,t) = L_xL_y\sum_{m=0}^{\infty}\frac{\psi_m(x)\psi_m(y)}{(E_m-\alpha_0)\ldots(E_m-\alpha_{N-1})}\mathrm{e}^{-iE_mt} + \sum_{n=0}^{N-1}\phi_n(x)\phi_n(y)\mathrm{e}^{-i\alpha_nt}\,.$$

Here we interchanged the derivative operators present in $L_{x,y}$ and the summation. This interchange is justified because the propagators are understood not as usual functions but as generalized functions [123] (which, in particular, may be regular, i.e. defined with the help of locally integrable functions). It remains to express $\psi_m(x)\exp(-iE_mt)$ with the help of (2.2.4) in terms of $K_0(x,z,t)$, to make use of the identity

$$\prod_{n=0}^{N-1}\frac{1}{E-\alpha_n}=\sum_{n=0}^{N-1}\left(\prod_{j=0,j\neq n}^{N-1}\frac{1}{\alpha_j-\alpha_n}\right)\frac{1}{E-\alpha_n}$$

and to represent the sum over m in terms of the Green function $G_0(z,y,\alpha_n)$. As a result, one arrives at

$$K_N(x,y,t)=L_xL_y\sum_{n=0}^{N-1}\left(\prod_{j=0,j\neq n}^{N-1}\frac{1}{\alpha_j-\alpha_n}\right)\int_a^b K_0(x,z,t)G_0(z,y,\alpha_n)dz$$
$$+\quad\sum_{n=0}^{N-1}\phi_n(x)\phi_n(y)\mathrm{e}^{-i\alpha_nt}\,. \tag{2.2.22}$$

This representation seems to be more convenient for calculations than the recursive approach [77]. This approach is based on the formula similar to (2.2.6). The, calculation of propagator K_N in terms of K_0 involves a complicated N-fold integral

$$K_N(x,y,t)=(-1)^NL_x\int_y^\infty dz_N\int_{z_N}^\infty dz_{N-1}\ldots\int_{z_2}^\infty dz_1K_0(x,z_1,t)\prod_{i=0}^{N-1}\left(\frac{u_{ii}(z_i)}{u_{ii}(z_{i+1})}\right), \tag{2.2.23}$$

where u_{ii} is determined by (1.2.42) with N replaced by i. Formula (2.2.23) is nothing but a result of a consecutive application of (2.2.6). Note, that when SUSY creates new levels in this approach one need to regularize integral in (2.2.6), for example by considering the diffusion equation instead of the Schrödinger equation. In our approach expression (2.2.22) is well-defined and looks simpler. Moreover for some models, the integral $\int_{-\infty}^{\infty}K_0(x,z,t)G_0(z,y,\alpha)dz=I(\alpha)$ may be calculated explicitly. In the next subsection we also show that there is more convenient way to iterate relation (2.2.6).

2.2.3 Removal of levels

Within the framework described in section 1.2.3, the N first discrete levels $E_0,E_1,\ldots,E_{N-1}$ have been removed from the spectrum of h_0 by choosing the ground state functions $u_{k,k}$ of the Hamiltonians h_k as intermediate transformation functions. For such a construction the transformed propagator may be calculated according to

Theorem 7. *Let the N first eigenfunctions $u_{0,n}\equiv u_n=\psi_n$, $n=0,\ldots,N-1$ of h_0 be the SUSY transformation functions. Then the propagators $K_N(x,y;t)$ and $K_0(x,y;t)$ of the Schrödinger equations with Hamiltonians h_N and h_0 are interrelated as*

$$K_N(x,y;t) = (-1)^NL_{N,0,x}\sum_{n=0}^{N-1}(-1)^n\frac{W_n(y)}{W(y)}\int_a^y K_0(x,z;t)u_n(z)dz \tag{2.2.24}$$
$$= (-1)^{N-1}L_{N,0,x}\sum_{n=0}^{N-1}(-1)^n\frac{W_n(y)}{W(y)}\int_y^b K_0(x,z;t)u_n(z)dz\,. \tag{2.2.25}$$

Proof. The proof of these relations can be given by induction. We start with (2.2.25). For $K_1(x,y;t)$ the statement is proven in (2.2.6). Assuming that (2.2.25) holds for $K_N(x,y;t)$ we verify its validity for $K_{N+1}(x,y;t)$. The corresponding Hamiltonians h_{N+1} and h_N are intertwined by the *linear* transformation $L_{N+1,N}$ so that (2.2.6) is applicable and $K_{N+1}(x,y;t)$ can be represented as

$$K_{N+1}(x,y;t) = \frac{1}{u_{N,N}(y)} L_{N+1,N,x} \int_y^b K_N(x,z;t) u_{N,N} dz\,.$$

Replacing K_N by (2.2.25) and making use of relations (1.2.40), (1.2.41) and the composition rule (1.2.38) gives

$$\begin{aligned}(-1)^{N-1} K_{N+1}(x,y;t) &= \frac{1}{u_{N,N}(y)} L_{N+1,0,x} \\ &\times \sum_{n=0}^{N-1} (-1)^n C_{Nn}^{-1} \int_y^b dz \int_z^b dq\, u_{N,n}(z) u_{N,N}(z) K_0(x,q;t) u_{0,n}(q)\,. \end{aligned} \tag{2.2.26}$$

The integration region of the double integral is the upper triangle of the rectangle $y<z, q<b$ in the $(z,q)-$plane. We replace this double integral by the difference of two double integrals over the whole rectangle and the lower triangle, respectively,

$$\begin{aligned}(-1)^{N-1} K_{N+1}(x,y;t) &= \frac{1}{u_{N,N}(y)} L_{N+1,0,x} \sum_{n=0}^{N-1} (-1)^n C_{Nn}^{-1} \\ &\times \left[\int_y^b dz\, K_0(x,z;t) u_{0,n}(z) \int_y^b dq\, u_{N,n}(q) u_{N,N}(q) \right. \\ &\left. - \int_y^b dz\, K_0(x,z;t) u_{0,n}(z) \int_z^b dq\, u_{N,n}(q) u_{N,N}(q) \right]. \end{aligned} \tag{2.2.27}$$

Here, we reshape the two integrals of the type $\int_\xi^b dq\, u_{N,n}(q) u_{N,N}(q)$ as follows. First we note that $u_{N,n}$ and $u_{N,N}$ are solutions of the same Schrödinger equation with Hamiltonian h_N and therefore

$$\begin{aligned}\int_\xi^b dq\, u_{N,n}(q) u_{N,N}(q) &= \frac{W\left[u_{N,N}(\xi), u_{N,n}(\xi)\right]}{E_n - E_N} - W_{b,n} \\ &= \frac{u_{N,N} L_{N+1,N} u_{N,n}}{E_n - E_N} - W_{b,n} \end{aligned} \tag{2.2.28}$$

where $W_{b,n} := W\left[u_{N,N}(b), u_{N,n}(b)\right]/(E_n - E_N)$ and where the second equality was obtained via (1.2.37). Applying the general relation (1.2.40) to $L_{N+1,N} u_{N,n} = u_{N+1,n}$ leads finally to

$$\begin{aligned}\int_\xi^b dq\, u_{N,n}(q) u_{N,N}(q) &= -C_{N,n} u_{N,N} \frac{W_n(u_0,\ldots,u_N)}{W(u_0,\ldots,u_N)} - W_{b,n} \\ &=: -C_{N,n} u_{N,N}(\xi) \frac{W_n(\xi)}{W(\xi)} - W_{b,n}\,. \end{aligned} \tag{2.2.29}$$

With (2.2.29) as substitution rule the propagator (2.2.27) takes the form

$$\begin{aligned}(-1)^{N-1} K_{N+1}(x,y;t) &= -L_{N+1,0,x} \sum_{n=0}^{N-1} (-1)^n \frac{W_n(y)}{W(y)} \int_y^b K_0(x,z;t) u_{0,n}(z) dz \\ &+ \frac{1}{u_{N,N}(y)} L_{N+1,0,x} \int_y^b dz K_0(x,z;t) \frac{u_{N,N}(z)}{W(z)} \sum_{n=0}^{N-1} (-1)^n u_{0,n}(z) W_n(z)\,. \end{aligned} \tag{2.2.30}$$

(The terms containing $W_{b,n}$ exactly cancelled.) The sum

$$S_N := \sum_{n=0}^{N-1} (-1)^n u_{0,n} W_n(u_0,\ldots,u_N) \tag{2.2.31}$$

in the second term can be calculated explicitly. Comparison with the evident determinant identity

$$0 = \begin{vmatrix} u_{0,0} & \dots & u_{0,N-1} & u_{0,N} \\ u_{0,0} & \dots & u_{0,N-1} & u_{0,N} \\ \dots & \dots & \dots & \dots \\ u_{0,0}^{(N-1)} & \dots & u_{0,N-1}^{(N-1)} & u_{0,N}^{(N-1)} \end{vmatrix}$$

$$= \begin{vmatrix} u_{0,0} & \dots & u_{0,N-1} & 0 \\ u_{0,0} & \dots & u_{0,N-1} & u_{0,N} \\ \dots & \dots & \dots & \dots \\ u_{0,0}^{(N-1)} & \dots & u_{0,N-1}^{(N-1)} & u_{0,N}^{(N-1)} \end{vmatrix} + \begin{vmatrix} 0 & \dots & 0 & u_{0,N} \\ u_{0,0} & \dots & u_{0,N-1} & u_{0,N} \\ \dots & \dots & \dots & \dots \\ u_{0,0}^{(N-1)} & \dots & u_{0,N-1}^{(N-1)} & u_{0,N}^{(N-1)} \end{vmatrix} \tag{2.2.32}$$

shows that (2.2.31) coincides with the decomposition of the first determinant in the second line of (2.2.32) over the elements of its first row. Hence, it holds

$$S_N = -(-1)^N u_{0,N} W(u_{0,0}, \dots, u_{0,N-1})\,.$$

Representing the ground state eigenfunctions $u_{N,N}$ in (2.2.30) via (1.2.42) in terms of Wronskian fractions we find that

$$\frac{u_{N,N}(z)}{W(z)} \sum_{n=0}^{N-1} (-1)^n u_{0,n}(z) W_n(z) = -(-1)^N u_{0,N}(z)$$

and, hence, that the second term in (2.2.30) is nothing but the absent $n = N$ summand of the sum in the first term. As a result, we arrive at

$$K_{N+1}(x,y;t) = (-1)^N L_{N+1,0,x} \sum_{n=0}^{N} (-1)^n \frac{W_n(u_0,\dots,u_N)}{W(u_0,\dots,u_N)} \int_y^b K_0(x,z;t) u_{0,n}(z) dz$$

what completes the proof of (2.2.25). The representation (2.2.24) follows from (2.2.25) and the relations

$$\int_a^b K_0(x,z,t) u_n(z) dz = u_n(x) \exp(-iE_n t) \qquad L_{N,0,x} u_n(x) = 0\,.$$

□

We note that in formulas (2.2.24) and (2.2.25) only one-dimensional integrals are present. In this way, they may turn out more convenient for concrete calculations than similar equations derived in [77].

Furthermore, we note the following. Theorem 7 is proven for the case when the N lowest discrete levels are removed from the spectrum of h_0 starting from the ground state level. This scenario corresponds to reducible supersymmetry. In order to see which of the conditions on the transformation functions $u_{0,n}$ used for the construction of the propagator representations (2.2.24) and (2.2.25) are indeed necessary conditions one may simply insert $K_N(x,y;t)$ directly into the Schrödinger equation (1.1.3). It turns out that neither the condition of level deletion starting from the ground state nor a deletion of a level block without surviving levels inside is used. This means that equations (2.2.24) and (2.2.25) hold for any choice of transformation functions provided their Wronskian does not vanish inside the interval (a,b), i.e. it holds for reducible as well as for irreducible SUSY transformation chains. A necessary but in general not sufficient condition for the nodelessness of the Wronskian is inequality (1.2.10) (for further details see [108]).

2.2.4 Strictly isospectral transformations

Strictly isospectral transformations can be generated with the help of unphysical solutions of the Schrödinger equation as transformation functions. In this section, we extend theorem 7 to a more general set of transformation functions. We will work with models defined over the whole real line $(a,b) = (-\infty,\infty)$ and transformation functions which vanish at one of the infinities $x \to -\infty$ or $x \to \infty$ and violate the Dirichlet BCs at the opposite infinities ($x \to \infty$ or $x \to -\infty$).

In accordance with (2.2.24) and (2.2.25) we formulate the corresponding relaxed version of theorem 7 as

Theorem 8. *Let the transformation functions $u_n(x)$ vanish at only one of the infinities $x \to -\infty$ or $x \to \infty$ of the real axis $\mathbb{R}$. Then the propagators $K_N(x,y;t)$ and $K_0(x,y;t)$ of the Schrödinger equations with h_N and h_0 as Hamiltonians are related as follows:*

$$\text{for } u_n(x \to -\infty) \to 0:$$

$$K_N(x,y;t) = (-1)^N L_x \sum_{n=0}^{N-1} (-1)^n \frac{W_n(y)}{W(y)} \int_{-\infty}^{y} K_0(x,z;t) u_n(z) dz \tag{2.2.33}$$

$$\text{for } u_n(x \to \infty) \to 0:$$

$$K_N(x,y;t) = (-1)^{N-1} L_x \sum_{n=0}^{N-1} (-1)^n \frac{W_n(y)}{W(y)} \int_{y}^{\infty} K_0(x,z;t) u_n(z) dz \tag{2.2.34}$$

$$\text{for } u_k(x \to -\infty) \to 0 \quad k = 0,\ldots,M \text{ and } u_m(x \to \infty) \to 0 \quad m = M+1,\ldots,N-1:$$

$$\begin{aligned} K_N(x,y;t) &= (-1)^N L_x \sum_{k=0}^{M} (-1)^n \frac{W_k(y)}{W(y)} \int_{-\infty}^{y} K_0(x,z;t) u_k(z) dz \\ &\quad + (-1)^{N-1} L_x \sum_{m=M+1}^{N-1} (-1)^m \frac{W_m(y)}{W(y)} \int_{y}^{\infty} K_0(x,z;t) u_m(z) dz\,. \end{aligned} \tag{2.2.35}$$

Proof. We have to verify that the initial condition $K_0(x,y,0) = \delta(x-y)$ and the Schrödinger equations $(i\partial_t - h_{0x})K_0(x,y,t) = 0$ and $(i\partial_t - h_{0y})K_0(x,y,t) = 0$ fulfilled by the original propagator $K_0(x,y,t)$ map into the corresponding relations for the final propagator $K_N(x,y,t)$, i.e. that $K_N(x,y,0) = \delta(x-y)$, $(i\partial_t - h_{Nx})K_N(x,y,t) = 0$ and $(i\partial_t - h_{Ny})K_N(x,y,t) = 0$ are satisfied. We demonstrate the explicit proof for the setup with $u_k(x \to -\infty) \to 0$ omitting the technically identical considerations for the other cases.

We start by noticing that the intertwiner L_x maps solutions of the Schrödinger equation for h_0 into solutions of the Schrödinger equation for h_N and, hence, $(i\partial_t - h_{Nx})K_N(x,y,t) = 0$ is automatically satisfied.

Next, we consider the initial condition $K_N(x,y;0) = \delta(x-y)$ which should be fulfilled by the r.h.s. of (2.2.35). With $K_0(x,y,0) = \delta(x-y)$ and $\int_{-\infty}^{y} \delta(x-z)u_n(z)dz = \theta(y-x)u_n(x)$ we have from (2.2.35)

$$K_N(x,y;0) = (-1)^N \sum_{n=0}^{N-1} (-1)^n \frac{W_n(y)}{W(y)} L_x[\theta(y-x)u_n(x)]\,. \tag{2.2.36}$$

In the Crum-Krein formula (see (1.2.6))

$$L_x[\theta(x-y)u_n(x)] = \frac{W[u_0,\ldots,u_{N-1},\theta(x-y)u_n(x)]}{W(u_0,\ldots,u_{N-1})} \tag{2.2.37}$$

we represent the derivatives $\partial_x^m[\theta(y-x)u_n(x)],\ m=0,\ldots,N$ as

$$\partial_x^m[\theta(y-x)u_n(x)] = \sum_{k=0}^{m-1} C_k^m \theta_x^{(m-k)}(y-x)u_n^{(k)}(x) + \theta(y-x)u_n^{(m)}(x)\,, \tag{2.2.38}$$

$\theta_x^{(m-k)}(y-x) := \partial_x^{m-k}\theta(y-x)$. Taking into account that

$$\begin{vmatrix} u_0(x) & \ldots & u_{N-1}(x) & \theta(y-x)u_n(x) \\ u_0'(x) & \ldots & u_{N-1}'(x) & \theta(y-x)u_n'(x) \\ \ldots & \ldots & \ldots & \ldots \\ u_0^{(N)}(x) & \ldots & u_{N-1}^{(N)}(x) & \theta(y-x)u_n^{(N)} \end{vmatrix} = 0$$

and making use of the linearity properties of determinants we reshape (2.2.37) as

$$\begin{aligned} & L_x[\theta(x-y)u_n(x)] \\ = \quad & \frac{1}{W(x)} \begin{vmatrix} u_0(x) & \ldots & u_{N-1}(x) & 0 \\ u_0'(x) & \ldots & u_{N-1}'(x) & -\delta(x-y)u_n(x) \\ \ldots & \ldots & \ldots & \ldots \\ u_0^{(N)}(x) & \ldots & u_{N-1}^{(N)}(x) & \sum_{k=0}^{N-1} C_k^N \theta_x^{(N-k)}(y-x)u_n^{(k)}(x) \end{vmatrix}. \end{aligned} \tag{2.2.39}$$

Expanding this determinant with regard to the elements of the last column we find

$$L_x[\theta(x-y)u_n(x)] = \frac{(-1)^N}{W(x)} \sum_{m=1}^{N} (-1)^m W_{Nm}(x) \sum_{k=0}^{m-1} C_k^m \theta_x^{(m-k)}(y-x)u_n^{(k)}(x) \tag{2.2.40}$$

where $W_{Nm}(x)$ are corresponding minors. For the verification of the relation $K_N(x,y;0)=\delta(x-y)$ we use its representation

$$\int_{-\infty}^{\infty} K_N(x,y;0)f(x)dx = f(y) \tag{2.2.41}$$

where $f(x)$ is a sufficiently smooth test function with compact support. With (2.2.36) and (2.2.40) the l.h.s. of (2.2.41) reads

$$\sum_{n=0}^{N-1}\sum_{m=1}^{N}\sum_{k=0}^{m-1}(-1)^{n+m}C_k^m \frac{W_n(y)}{W(y)} \int_{-\infty}^{\infty} dx\, \theta_x^{(m-k)}(y-x)\, \frac{W_{Nm}(x)f(x)u_n^{(k)}(x)}{W(x)}\,. \tag{2.2.42}$$

As next step, we use $\theta_x^{(m-k)}(y-x) = -\delta^{(m-k-1)}(x-y)$ and multiple integration by parts[1] to remove the derivatives from the $\theta-$functions:

$$\text{l.h.s. of (2.2.41)} = \sum_{n=0}^{N-1}\sum_{m=1}^{N}\sum_{k=0}^{m-1}(-1)^{n-k}C_k^m \frac{W_n(y)}{W(y)}\, \partial_y^{m-k-1}\left[\frac{W_{Nm}(y)f(y)u_n^{(k)}(y)}{W(y)}\right]. \tag{2.2.43}$$

The relation

$$\frac{1}{W}\sum_{n=0}^{N-1}(-1)^n W_n u_n^{(j)} = (-1)^N \delta_{j,N-1}\,, \qquad j=0,\ldots,N-1 \tag{2.2.44}$$

reduces this multiple sum to

$$\text{l.h.s. of (2.2.41)} = (-1)^N \frac{W_{NN}(y)f(y)}{W(y)} \sum_{k=0}^{N-1}(-1)^k C_k^N \tag{2.2.45}$$

[1]For the theory of distributions (generalized functions) see, e.g., [123] (in particular vol.1 p. 26).

and because of $W_{NN}(y) = W(y)$ and $\sum_{k=0}^{N-1}(-1)^k C_k^N = (-1)^N$ (cf. 4.2.1.3 in [124]) the condition (2.2.41) is satisfied.

It remains to prove that the Schrödinger equation $(i\partial_t - h_{Ny})K_N(x,y,t) = 0$ is fulfilled too. By explicit substitution of equation (2.2.33) we have

$$\begin{aligned}
&(i\partial_t - h_{Ny})K_N(x,y,t) \\
&= (-1)^N L_x \sum_{n=0}^{N-1}(-1)^n \frac{W_n(y)}{W(y)} \int_{-\infty}^{y} i\partial_t K_0(x,z;t)u_n(z)dz \\
&+L_x \sum_{n=0}^{N-1}(-1)^n \left[\left(\frac{W_n(y)}{W(y)}\right)'' - V_N(y)\frac{W_n(y)}{W(y)}\right] \int_{-\infty}^{y} K_0(x,z;t)u_n(z)dz \\
&+L_x \sum_{n=0}^{N-1}(-1)^n \left[2\left(\frac{W_n(y)}{W(y)}\right)' u_n(y) + \frac{W_n(y)}{W(y)}(u_n(y)\partial_y + u_n'(y))\right] K_0(x,y;t)\,. \quad (2.2.46)
\end{aligned}$$

First, we note that due to relation (2.2.44) and its derivative the last sum vanishes. Taking further into account that $W_n(y)/W(y)$ is a solution of the Schrödinger equation for h_N at energy E_n (cf. (1.2.8)) and replacing $i\partial_t K_0(x,z;t) \to h_{0z}K_0(x,z;t)$ one reduces equation (2.2.46) to

$$\begin{aligned}
&(i\partial_t - h_{Ny})K_N(x,y,t) \\
= \;& (-1)^N L_x \sum_{n=0}^{N-1}(-1)^n \frac{W_n(y)}{W(y)} \int_{-\infty}^{y} [(h_{0z} - E_n)K_0(x,z;t)]u_n(z)dz\,. \quad (2.2.47)
\end{aligned}$$

Integrating by parts and making use of $(h_{0z} - E_n)u_n(z) = 0$, the asymptotical behavior $u(z \to -\infty) \to 0$, $u'(z \to -\infty) \to 0$ and relation (2.2.44) one finds that the r.h.s. in (2.2.47) vanishes and, hence, the Schrödinger equation $(i\partial_t - h_{Ny})K_N(x,y,t) = 0$ is fulfilled. □

2.2.5 General polynomial supersymmetry

The three different types of transformations considered above may be combined in various ways to produce a supersymmetry of more general type. In general, from the spectrum of the original Hamiltonian h_0 q levels may be removed and p additional levels may be added, $p+q \leq N$ producing in this way the spectral set of h_N. The inequality would correspond to SUSY transformation chains between h_0 and h_N which contain isospectral transformations. For further convenience we split the spectra of h_0 and h_N according to their transformation related contents as

$$\begin{aligned}
\mathrm{spec}(h_0) &= \{\varepsilon_i, \beta_j, E_k\} + \mathrm{spec}_c(h_0)\,,\; i = 1,\ldots,q\,;\quad j = 1,\ldots,N-(p+q+r) \\
\mathrm{spec}(h_N) &= \{\lambda_l, \beta_j, E_k\} + \mathrm{spec}_c(h_N)\,,\; l = 1,\ldots,p\,;\quad j = 1,\ldots,N-(p+q+r) \quad (2.2.48)
\end{aligned}$$

where the discrete levels E_k and the continuous spectrum $\mathrm{spec}_c(h_0) = \mathrm{spec}_c(h_N)$ are not affected by the SUSY transformations. The set of transformation constants $\{\alpha_n\}_{n=0}^{N-1} = \{\varepsilon_i, \lambda_l, \beta_j, \gamma_k\}$ corresponds to p new discrete levels $\lambda_n \in \mathrm{spec}(h_N)$ not present in $\mathrm{spec}(h_0)$, q levels $\varepsilon_i \in \mathrm{spec}(h_0)$ not present in $\mathrm{spec}(h_N)$, $N-(p+q+r)$ levels β_j present in both spectra and r constants γ_k not coinciding with any energy level of both Hamiltonians, $\gamma_k \notin \mathrm{spec}(h_0) \cup \mathrm{spec}(h_N)$. Transformations induced at constants $\alpha_n = \beta_n, \gamma_n$ are strictly isospectral.

Summarizing the previous results the following expression for the propagator $K_N(x,y,t)$ can

be given

$$K_N(x,y,t) = L_x L_y \sum_{n=0}^{N-1} \left(\prod_{j=0, j\neq n}^{N-1} \frac{1}{\alpha_n - \alpha_j} \right) \int_a^b K_0(x,z,t) \widetilde{G}_0(z,y,\alpha_n) dz \\ + \sum_{\lambda_n} \phi_{\lambda_n}(x)\phi_{\lambda_n}(y) \mathrm{e}^{-i\lambda_n t} + \sum_{\beta_n} \phi_{\beta_n}(x)\phi_{\beta_n}(y)\mathrm{e}^{-i\beta_n t} \tag{2.2.49}$$

where for $\alpha_n = \varepsilon_n, \beta_n$

$$\widetilde{G}_0(z,y,\alpha_n) = \lim_{E\to\alpha_n} \left[G_0(z,y,E) - \frac{\psi_n(x)\psi_n(y)}{\alpha_n - E} \right]$$

and $\widetilde{G}_0(z,y,\alpha_n) = G_0(z,y,\alpha_n)$ otherwise.

2.2.6 Time-dependent potentials

In the case of the time-dependent SUSY transformations, the transformed potentials are time-dependent. Therefore the time translation is not a symmetry anymore. The evolution of a system depends on both the initial and the final moments of time

$$U(t_2,t_1) \neq U(t_2+t_0, t_1+t_0)\,. \tag{2.2.50}$$

Nevertheless, due to the composition rule $U(t_3,t_2)U(t_2,t_1) = U(t_3,t_1)$ we may consider only the evolution from the fixed initial time $t=0$

$$U(t_2,t_1) = U(t_2,0)U^+(t_1,0)\,. \tag{2.2.51}$$

The matrix element of the evolution operator

$$K(x,y;t_2,t_1) = \langle x|U(t_2,t_1)|y\rangle\,, \tag{2.2.52}$$

describes the probability of the transition from an initial point y at time t_1 to a final point x at time t_2. This matrix element coincides with the propagator of the time-dependent Schrödinger equation. If the propagator $K_0(x,y;t_2,t_1)$ is known in closed form, the Cauchy problem can be solved for any initial state $\mathbf{\Psi}(y,t_1)$:

$$\mathbf{\Psi}(x,t_2) = \int_a^b K(x,y;t_2,t_1)\mathbf{\Psi}(y,t_1)dy\,. \tag{2.2.53}$$

Bearing in mind that the hamiltonian is time-dependent we slightly modify the definition of the propagator

$$[i\partial_t - h(x,t)]K(x,y;t,t_0) = 0\,, \qquad K(x,y;t_0,t_0) = \delta(x-y)\,. \tag{2.2.54}$$

According to (2.2.51) we may fix the initial time $t_0 = 0$ and consider only the propagator $\tilde{K}(x,y;t) = \langle x|U(t,0)|y\rangle$. Then the propagator which describes the evolution from an another initial moment reads

$$K(x,y;t_2,t_1) = \langle x|U(t_2,t_1)|y\rangle = \int_a^b dz \tilde{K}(x,z;t_2)\tilde{K}^*(z,y;t_1)\,. \tag{2.2.55}$$

The complete set $\psi_n(x,t) = \langle x|U(t,0)\psi_n\rangle$ determines the following decomposition

$$\tilde{K}(x,y;t) = \sum_{n=0}^{\infty} \psi_n(x,t)\psi_n^*(y)\,. \tag{2.2.56}$$

Taking into account the method of time-dependent SUSY transformations described in section 1.3 it is convenient to choose the eigenfunctions $\{|\psi_n\rangle\}$ and $\{|\phi_n\rangle\}$ of the symmetry operators g_0 and g_1 (see section 1.3) as the basis sets

$$g_0|\psi_n\rangle = \lambda_n|\psi_n\rangle\,, \qquad g_1|\phi_n\rangle = \lambda_n|\phi_n\rangle\,. \tag{2.2.57}$$

Hence, in the case **(ii)** one can express the transformed propagator as follows

$$\begin{aligned}\tilde{K}_1(x,y;t) &= \sum_{m=-1}^{\infty} \phi_m(x,t)\phi_m^*(y) \\ &= L_x(t)L_y^*(0)\sum_{m=0}^{\infty}\frac{\psi_m(x,t)\psi_m^*(y,0)}{\lambda_m-\alpha} + \phi_{-1}(x,t)\phi_{-1}^*(y)\,.\end{aligned} \tag{2.2.58}$$

Up to a normalization constant N_{-1}, the additional eigenfunction ϕ_{-1} is determined by the transformation function, $\phi_{-1} = N/\left[L_1(t)u^*(x)\right]$. The evolution of g_0's eigenfunctions is given by the initial propagator

$$\int_a^b \tilde{K}_0(x,z,t)\psi_m(z,0)dz = \psi_m(x,t)\,. \tag{2.2.59}$$

As a result (2.2.58) reads

$$\tilde{K}_1(x,y,t) = L_x(t)L_y^*(0)\int_a^b \tilde{K}_0(x,z,t)\sum_{m=0}^{\infty}\frac{\psi_m(z,0)\psi_m^*(y,0)}{\lambda_m-\alpha}dz + \phi_{-1}(x,t)\phi_{-1}^*(y). \tag{2.2.60}$$

The sum

$$G_0(x,y,\lambda;t) = \langle x|(g_0-\lambda)^{-1}|y\rangle = \sum_{m=0}^{\infty}\frac{\psi_m(x,t)\psi_m^*(y,t)}{\lambda_m-\lambda}\,, \tag{2.2.61}$$

is the resolvent of the symmetry operator. Note that the resolvent taken at the initial moment $G_0(y,z,\lambda;0) =: G_0(y,z,\lambda)$ is used in (2.2.60). This resolvent satisfies to the following inhomogeneous equation

$$(g_0(t=0)-\lambda)_x G_0(x,y,\lambda) = \delta(x-y)\,. \tag{2.2.62}$$

We can summarize this calculation in the following theorem.

Theorem 9. *The propagators $K_1(x,y;t)$ and $K_0(x,y;t)$ of non-stationary Schrödinger equations with non-stationary SUSY intertwined Hamiltonians h_1 and h_0 are interrelated with each other and with the resolvents $G_0(x,y;\lambda)$ and $\widetilde{G}_0(x,y,\alpha)$ in the following way:*
Type **(i)** *relation*

$$\tilde{K}_1(x,y,t) = L_x L_{y,t=0}^* \int_a^b \tilde{K}_0(x,z,t)\widetilde{G}_0(z,y,\alpha)dz\,, \tag{2.2.63}$$

Type **(ii)** *relation*

$$\tilde{K}_1(x,y,t) = L_x L_{y,t=0}^* \int_a^b \tilde{K}_0(x,z,t)G_0(z,y,\alpha)dz + \phi_{-1}(x,t)\phi_{-1}(y)\,, \tag{2.2.64}$$

Type **(iii)** *relation*

$$\tilde{K}_1(x,y,t) = L_x L_{y,t=0}^* \int_a^b \tilde{K}_0(x,z,t)G_0(z,y,\alpha)dz\,. \tag{2.2.65}$$

2.2.7 Non-hermitian superpartners

Recently a considerable attention has been paid to different properties of non-Hermitian Hamiltonians (see, e.g., [125]). There are several reasons to generalize the quantum mechanics by accepting non-Hermitian Hamiltonians with purely real spectrum (see, e.g., [125, 126] and references therein). For instance, some problems are simplified being reformulated in terms of a non-Hermitian Hamiltonian. On the other hand complex potentials are used in different models of nuclear physics (optical potentials) as effective interaction potentials [127].

Although the general idea how to find the superpartner's propagator is the same in the case of the one-dimensional Schrödinger equation with a complex-valued potential $V_c(x)$

$$h_c\varphi_E(x) = E\varphi_E(x)\,, \qquad h_c = -\frac{\partial^2}{\partial x^2} + V_c(x)\,, \quad x \in \mathbb{R}\,, \tag{2.2.66}$$

there is some technical difference. Therefore it is necessary to repeat (or introduce) some important definitions and conjectures.

We consider the stationary potentials $V_c(x)$. The propagator $K_c(x, y, t)$ is defined as usual through the inhomogeneous time-dependent Schrödinger equation. If $K_c(x, y, t)$ is given the function

$$\Phi(x, t) = \int_{-\infty}^{\infty} K_c(x, y; t)\varphi_0(y)dy \tag{2.2.67}$$

is a solution of the time-dependent Schrödinger equation with the initial condition $\Phi(x, 0) = \varphi_0(x)$.

First of all we note that to be able to associate the function $\Phi(x, t)$ with a state of a quantum system the integral in (2.2.67) should converge and both the function $\varphi_0(x)$ and $\Phi(x, t)$ should belong to a certain class of functions. To present our method in its simplest form we will make several assumptions which simplify essentially our presentation keeping at the same time the essence of the method. Since in (2.2.67) the usual (Lebesgue) integration is involved it is natural to suppose that both $\varphi_0(x)$ and $\Phi(x, t)$ are square integrable. This means that the Hilbert space, where the operator (non-Hermitian Hamiltonian) h_c associated with the differential expression $-\partial^2 x/\partial x^2 + V_c(x)$ 'lives', is the usual space $\mathcal{L}_2(\mathbb{R})$ and the equation (2.2.66) creates an eigenvalue problem for h_c which is defined on a dense domain from $\mathcal{L}_2(\mathbb{R})$.

Eigenvalue problems for non-Hermitian differential operators were under an intensive study by mathematicians in the Soviet Union in the period between 50th and 70th of the previous century. Results of these investigations are mainly summarized in books [106, 128] to which we refer the interested reader where he can, in particular, find the strict definition of the spectrum, eigenfunctions, associated functions, domains of definition of operators created by non-Hermitian differential expressions and many other properties of differential equations and related non-selfadjoint operators. Here we would like to mention that the first essential result in this field was obtained by Keldysh [129] who proved the completeness of the set of eigenfunctions and associated functions for a non-selfadjoint operator and results by Lidskiy [130]. In particular, Lidskiy made a deep analysis of conditions on the potential V_c leading to an operator h_c which is uniquely defined by its closure and has a purely discrete spectrum with a complete set of eigenfunctions and associated functions.

Especial role between all non-selfadjoint operators is played by pseudo-Hermitian operators first introduced by Dirac and Pauli and latter used by Lee and Wick [131–133] to overcome some difficulties related with using Hilbert spaces with an indefinite metric and their recent generalization (weak pseudo-Hermiticity) by Solombrino and Scolarici [134, 135] since there are strict indications

that these operators are the most appropriate candidates for replacing selfadjoint operators while generalizing the conventional quantum mechanics by accepting non-Hermitian operators [134–137].

Our next essential assumption is that h_c has a purely discrete spectrum, its set of associated functions is empty, it is diagonalizable, and its set of eigenfunctions $\phi_n(x)$, $n = 0, 1, \ldots$ is complete in the space $\mathcal{L}_2(\mathbb{R})$. If h_c^+ is the adjoint differential expression it creates in the Hilbert space the adjoint operator with the eigenfunctions $\widetilde{\phi}_k(x)$ which also form a complete set in $\mathcal{L}_2(\mathbb{R})$. Moreover, if E_n is an eigenvalue of h_c then E_n^* (asterisk means the complex conjugation) is an eigenvalue of h_c^+ so that $h_c^+\widetilde{\phi}_n = E_n^*\widetilde{\phi}_n$. Note that neither $\{\phi_n\}$ nor $\{\widetilde{\phi}_n\}$, $n = 0, 1, \ldots$ form orthogonal systems but functions $\widetilde{\phi}_k$ are biorthogonal with ϕ_n and they can always be normalized such that (see e.g. [128])

$$\int_{-\infty}^{\infty} \widetilde{\phi}_k^*(x)\phi_n(x)dx = \delta_{nk}\,. \tag{2.2.68}$$

The completeness of the set of eigenfunctions of h_c means that any $\phi \in L_2(\mathbb{R})$ can be developed into the Fourier series over the set $\{\phi_n\}$, $\phi(x) = \sum_{n=0}^{\infty} c_n\phi_n(x)$. Using the biorthonormality relation (2.2.68) we can find the coefficients c_n in the usual way and put them back into the same relation thus obtaining the symbolical form of the completeness condition of the set of eigenfunctions of h_c

$$\sum_{n=0}^{\infty} \widetilde{\phi}_n^*(x)\phi_n(y) = \delta(x-y)\,. \tag{2.2.69}$$

Next we assume that the spectrum of h_c is real. Therefore the adjoint eigenvalue problem coincides with the complex conjugate form of equation (2.2.66) so that $\widetilde{\phi}_n(x) = \phi_n^*(x)$. Under these assumptions equations (2.2.68) and (2.2.69) become (cf. [138])

$$\int_{-\infty}^{\infty} \phi_n(x)\phi_k(x)dx = \delta_{nk}\,, \tag{2.2.70}$$

$$\sum_{n=0}^{\infty} \phi_n(x)\phi_n(y) = \delta(x-y)\,. \tag{2.2.71}$$

From here follows the Fourier series expansion of the propagator in terms of the basis functions ϕ_n:

$$K_c(x,y;t) = \sum_{n=0}^{\infty} \phi_n(x)\phi_n(y)e^{-iE_nt}\,. \tag{2.2.72}$$

Indeed, just like in the conventional Hermitian case the initial condition $\Phi(x,0) = \varphi_0(x)$ for function (2.2.67) with K_c of form (2.2.72) follows from (2.2.71) and the fact that $\Phi(x,t)$ satisfies the time-dependent Schrödinger equation follows from the property of the functions ϕ_n to be eigenfunctions of h_c with the eigenvalues E_n.

Another useful discussion is that the form (2.2.72) for the propagator may be interpreted as the coordinate representation of the abstract evolution operator. To show this we introduce ket-vectors (kets) $|\phi_n\rangle$ as eigenvectors of h_c and bra-vectors (bras) $\langle\widetilde{\phi}_n|$ as functionals acting in the space of kets according to[2]

$$\langle\widetilde{\phi}_n|\phi_k\rangle = \delta_{nk}\,. \tag{2.2.73}$$

Kets corresponding to the previous bras are just properly normalized eigenvectors of h_c^+ which is defined by the adjoint eigenvalue problem where $V_c(x)$ is replaced by its complex conjugate $V_c^*(x)$

[2]Without going into details we note that using the system $|\phi_n\rangle$ one can construct the Hilbert space H so that the set of all finite linear combinations of ϕ_n is dense in H and formula (2.2.73) uniquely defines a functional in H, see e.g. [139].

so that (2.2.73) is nothing but the same biorthogonality condition (2.2.70) written in the abstract representation. As usual the coordinate representation of the above abstract eigenvectors are $\phi_n(x) = \langle x|\phi_n\rangle = \langle\widetilde{\phi}_n|x\rangle$ where $|x\rangle$ is an eigenvector of the coordinate operator. The completeness condition in the abstract form now reads

$$\sum_{n=0}^{\infty} |\phi_n\rangle\langle\widetilde{\phi}_n| = 1 \tag{2.2.74}$$

and the formula

$$h_c = \sum_{n=0}^{\infty} |\phi_n\rangle E_n \langle\widetilde{\phi}_n| \tag{2.2.75}$$

presents the spectral decomposition of the Hamiltonian h_c. Now in the known way [134–136] one can introduce an automorphism η to establish the property that h_c is (weakly) pseudo-Hermitian and construct a basis in which h_c takes a real form. We will not go into further details of the known properties of (weakly) pseudo-Hermitian operators since this is not the aim of this work. The interested reader can consult papers [131–136] and the recent preprint [137] where biorthogonal systems are widely used in the study of different properties of non-Hermitian Hamiltonians. Our last comment here is that the abstract evolution operator given by its spectral decomposition

$$U(t) = \sum_{n=0}^{\infty} |\phi_n\rangle e^{-iE_n t} \langle\widetilde{\phi}_n| \tag{2.2.76}$$

written in the coordinate representation $K_c(x, y, t) = \langle x|U(t)|y\rangle$ is just the propagator (2.2.72).

We would like to emphasis that conditions (2.2.70) and (2.2.71) have almost the usual form, only the complex conjugation is absent. Therefore they coincide with the corresponding equations for the Hermitian Hamiltonians in case when their eigenfunctions are real.

The final assumption we make is that the Hamiltonian h_c is a SUSY partner of a Hermitian Hamiltonian h_0 with a purely discrete spectrum and a complete set of eigenfunctions ψ_n which always can be chosen real

$$h_0 = -\frac{\partial^2}{\partial x^2} + V_0(x)\,, \quad h_0\psi_n(x) = E_n\psi_n(x)\,, \quad \psi_n(x) = \psi_n^*(x)\,, \quad n = 0, 1, \ldots$$

so that both the completeness and normalization conditions are given by equations (2.2.71) and (2.2.70) respectively with the replacement $\phi_n \to \psi_n$.

According to the general scheme of SUSY QM (see section 1.2.1) operators h_0 and h_c are (1-)SUSY partners if and only if there exists a first order differential operator L such that

$$Lh_0 = h_c L\,. \tag{2.2.77}$$

Operator L has the form (1.2.11) where the function $u(x)$ is a complex solution to equation

$$h_0 u(x) = \alpha u(x)\,. \tag{2.2.78}$$

The potential V_c is calculated with the aid of formula (1.2.14).

Together with operator L we need also its 'transposed form' (instead of L^+) which we define as follows:

$$L^t = -u'(x)/u(x) - \partial_x\,. \tag{2.2.79}$$

Then, just like in the usual SUSY QM the following factorizations take place:

$$L^t L = h_0 - \alpha\,, \qquad LL^t = h_c - \alpha \tag{2.2.80}$$

which can easily be checked by the direct calculation.

The spectrum of h_c may either **(iii)** coincide with the spectrum of h_0 or **(ii)** may differ from it by one (real) level which is absent in the spectrum of h_0. The case **(iii)** may be realized only with a complex parameter α which is called the factorization constant. The case **(ii)** may be realized only for a real factorization constant since $E = \alpha$ is just the discrete level of h_c missing in the spectrum of h_0 and we want that h_c has a real spectrum. Therefore in this case one has to choose $u(x)$ as a linear combination of two real linearly independent solutions to equation (2.2.78).

One of the main features of the method is that for the most physically interesting Hamiltonians h_0 operator (1.2.11) has the property $L\psi_E(\pm\infty) = 0$ provided $\psi_E(\pm\infty) = 0$ (conservative SUSY). As a result the set of functions

$$\phi_n = N_n L\psi_n\,, \qquad n = 0, 1, \ldots \tag{2.2.81}$$

is complete in the space $\mathcal{L}^2(\mathbb{R})$ in case **(iii)**. In case **(ii)** we have to add to this set the function $\phi_\alpha = N_\alpha/u$. The normalization coefficients N_n may be found by integration by parts in equation (2.2.70) and with the help of factorization property (2.2.80) which yields

$$N_n = (E_n - \alpha)^{-1/2}\,. \tag{2.2.82}$$

The main result of the present section is given by the following

Theorem 10. *The propagator $K_c(x, y; t)$ of the Schrödinger equation with the Hamiltonian h_c related with h_0 by a SUSY transformation is expressed in terms of the propagator $K_0(x, y; t)$ of the same equation with the Hamiltonian h_0 and the Green's function $G_0(x, y; E)$ of the stationary equation with the same Hamiltonian as follows:*
in case **(i)** $K_c(x, y, t) = K_L(x, y, t)$
in case **(ii)** $K_c(x, y, t) = K_L(x, y, t) + \phi_\alpha(x)\phi_\alpha(y)e^{-i\alpha t}$
where $K_L(x, y, t)$ is the 'transformed' propagator

$$K_L(x, y, t) = L_x L_y \int_{-\infty}^{\infty} K_0(x, z, t)G_0(z, y, \alpha)dz\,. \tag{2.2.83}$$

Here L_x is defined by (1.2.11) and L_y is the same operator where x is replaced by y.

Proof. The proof follows the same line as in the theorem 5 with obvious modifications coming from (2.2.69), (2.2.71) and (2.2.72) □

Further we will use the obtained relations to calculate some new propagators to stationary, non-stationary and complex potentials.

2.3 Explicit expressions for Green functions and propagators

2.3.1 Particle in a box

As first application, we consider a free particle in a box, i.e. the Schrödinger equation with $V_0(x) \equiv 0$ and Dirichlet BCs at the ends of the finite interval $(0,1)$. The eigenfunctions of this problem are the well known $\psi_{n-1}(x) = \sqrt{2}\sin(n\pi x)$, $n \in \mathbb{Z}_+$, with energies $E_{n-1} = n^2\pi^2$. The Green function of the particle in a box may be easily calculated by its definition (1.1.16)

$$G_{box}(x,y,E) = \frac{\sin(kx)\sin[k(y-1)]}{k\sin k}\,, \quad x<y\,, \quad E=k^2\,. \tag{2.3.1}$$

Poles of G_{box} coincide with the points of the discrete spectrum.

The corresponding propagator reads [33]

$$K_{box0}(x,y,t) = \frac{1}{2}\left[\vartheta_3^-(x,y;t) - \vartheta_3^+(x,y;t)\right]$$

with

$$\vartheta_3^-(x,y;t) := \vartheta_3\left(\frac{x-y}{2}\middle| -\frac{\pi t}{2}\right)\,, \quad \vartheta_3^+(x,y;t) := \vartheta_3\left(\frac{x+y}{2}\middle| -\frac{\pi t}{2}\right)$$

and $\vartheta_3(q|\tau)$ denoting the third theta function [140].

As SUSY partner problem we choose a model which we derive by removing the ground state level E_0 by a linear (one-step) SUSY-mapping with $u = \psi_0 = \sin\pi x$ as transformation function[3]. This leads to the Schrödinger equation with potential $V_1(x) = 2\pi^2/\sin^2(\pi x)$, i.e. a singular Sturm-Liouville problem. The propagator of this problem can be represented via (2.2.6) as

$$K_{box1}(x,y,t) = -\frac{1}{2\sin\pi y}L_x\int_0^y \left[\vartheta_3^-(x,z;t) - \vartheta_3^+(x,z;t)\right]\sin(\pi z)dz \tag{2.3.2}$$

or after explicit substitution of $L_x = -\pi\cot(\pi x) + \partial_x$ as

$$\begin{aligned} K_{box1}(x,y,t) = {}& \frac{\pi\cot(\pi x)}{2\sin(\pi y)}\int_0^y \left[\vartheta_3^-(x,z;t) - \vartheta_3^+(x,z;t)\right]\sin(\pi z)dz \\ -\frac{\pi}{2\sin(\pi y)}\int_0^y & \left[\vartheta_3^-(x,z;t) + \vartheta_3^+(x,z;t)\right]\cos(\pi z)dz + \frac{1}{2}\left[\vartheta_3^-(x,y;t) + \vartheta_3^+(x,y;t)\right]. \end{aligned} \tag{2.3.3}$$

Here after using the property $\partial_x\theta_3^\pm(x,z,t) = \pm\partial_z\theta_3^\pm(x,z,t)$ we integrated in (2.3.2) by parts.

We see that both the initial and the transformed propagators are expressed in terms of the third theta function $\vartheta_3(q|\tau)$, whereas the initial Green function contains only simple trigonometric functions. Therefore in the case of finite interval it is more convenient to work with the Green function. In the rest of this section we calculate closed expressions for the Green functions generated by different types of SUSY transformations.

In section 1.2.1 we demonstrated that there is only one possibility for the first order conservative SUSY transformation. To enlarge the possible choice of transformation function we first consider the example of a non-conservative SUSY transformation. Let $u = \mathrm{sh}(cx)$ be the transformation function. This function violates BCs at $x = 1$, therefore according to the general discussion in section 1.2.1 the spectrum of the transformed Hamiltonian radically differs from the spectrum of

[3]There exist other types of transformations leading to regular transformed Sturm-Liouville problems. But the solutions of the resulting Schrödinger equations will violate the Dirichlet BCs [4]. The special analysis of this case will be considered below.

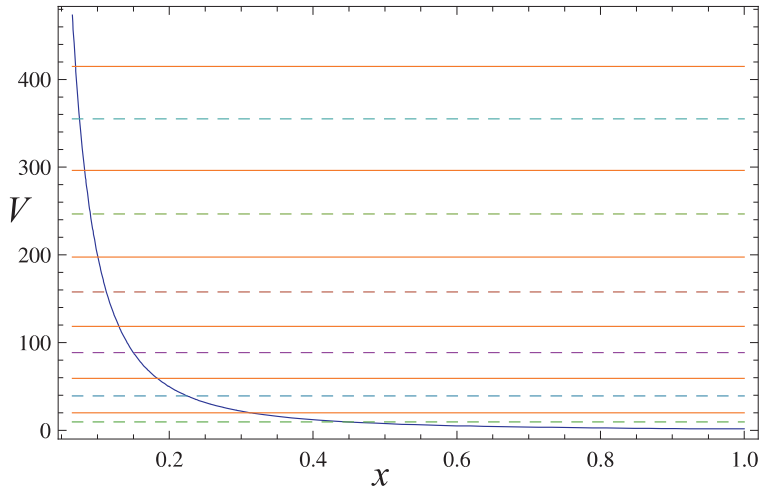

Figure 2.1: Non-conservative SUSY partner of the particle in box is presented, $V(x) = 2c^2/\sinh(cx)^2$, $c = 1/2$. Solid horizontal lines correspond to the transformed spectrum, dashed horizontal lines correspond to the spectrum of the particle in box.

the free particle in box. The transformation operator $L = -c\coth(cx) + \partial_x$ maps the eigenfunctions ψ_n to unphysical solutions $L\psi_n(1) = (-1)^n\pi$ which violate BCs at $x = 1$. Nevertheless, one may solve the spectral problem for the transformed Schrödinger equation. Acting by the transformation operator on the general solution $\Psi(x) = A\cos(kx) + B\sin(kx)$ of the initial equation we get the general solution $\Phi(x) = L\Psi(x)$ of the transformed equation for all $E \neq -c^2$. Imposing the Dirichlet BCs $\Phi(0) = 0$ and $\Phi(1) = 0$ we find that $A = 0$ and

$$k = c\coth c\tan k\,. \tag{2.3.4}$$

It is seen that the spectrum of the non-conservative SUSY partner is determined by the transcendent equation. Spectral points correspond to the intersections of line $y = k/(c\coth c)$ with tangents $y = \tan k$. We can change the spectrum of the model by varying parameter c. Note that the transformed spectrum approaches the initial one as $c \to +\infty$. Figure 2.1 shows an example of potential. First energy levels of the transformed model are compared with the energy levels of the initial spectrum.

Note, that in this case formula (2.1.1) fails. However, we can calculate the Green function using (1.1.16) and the general solution of the Schrödinger equation obtained through SUSY transformation:

$$G_1(x,y,E) = \frac{(k\sin k + c\coth c\cos k)\,(-c\coth(cx)\sin(kx) + k\cos(kx))}{k(c^2+k^2)(c\coth c\sin k - k\cos k)}\times$$
$$\times\left[\frac{c\coth c\sin k - k\cos k}{c\coth c\cos k + k\sin k}(c\coth(cy)\cos(ky) + k\sin(ky)) - c\coth(cy)\sin(ky) + k\cos(ky)\right],$$
$$x < y\,.$$

If the transformation function coincides with the ground state wave function $u = \sin(\pi x)$ then the SUSY transformation is conservative. The ground state level is removed and the spectrum is $E_n = (n\pi)^2$, $n = 2, 3, \ldots$. The transformed potential $V_1 = 2\pi^2\csc^2(\pi x)$ is shown in figure 2.2. Its Green function is given by (2.1.1)

$$G_1(x,y,E) = \frac{G_{box}(x,y,E)}{(E-\pi^2)}[k\,\mathrm{ctg}(kx) - \pi\,\mathrm{ctg}(\pi x)]\,[k\,\mathrm{ctg}(k(y-1)) - \pi\,\mathrm{ctg}(\pi y)]\,, \quad x < y\,.$$

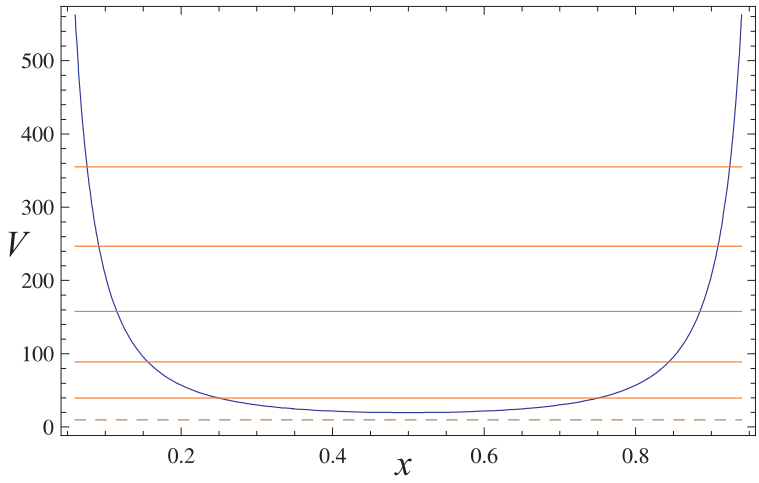

Figure 2.2: SUSY partner of the particle in box, $V(x) = 2\pi^2\csc^2(\pi x)$, which corresponds to the case **(i)** is shown. Solid horizontal lines correspond to the transformed spectrum, which coincides with the spectrum of the particle in box except one level $E_0 = \pi^2$.

It can be checked that $k = \pi$ ($E = \pi^2$) is a regular point of the transformed Green function. This is in agreement with the spectrum modification.

Our next step is to consider the second order SUSY transformation. To work with conservative transformations only we should impose on the transformation functions BCs discussed in section 1.2.2. In case (**V**) we can choose

$$u_1(x) = \sin(\pi x)\,, \quad u_2(x) = \sin(cx)\,, \quad 0 < c \le 2\pi\,.$$

From (4.3.74) we get the transformed potential

$$V_2 = (\pi^2 - c^2)\frac{c^2 - \pi^2 + \pi^2\cos(2cx) - c^2\cos(2\pi x)}{[\pi\cos(\pi x)\sin(cx) - c\cos(cx)\sin(\pi x)]^2}\,. \tag{2.3.5}$$

The bound state energy is shifted from $E_0 = \pi^2$ to $E_0' = c^2$. Potential (2.3.5) is plotted in figure (2.3). The transformed eigenfunctions are easily obtained from (1.2.29). Using (2.1.10) one can calculate the Green function:

$$G_2(x,y,E) = \frac{G_{box}(x,y,E)}{(E-\pi^2)(E-c^2)}(E + Z_1(x))(E + Z_2(y))\,, \quad x < y\,,$$

$$Z_j(x) = \frac{\pi c^2\cos(\pi x)\sin(cx) - a\pi^2\sin(\pi x)\cos(cx) + k(c^2-\pi^2)\sin(\pi x)\sin(cx)\,\mathrm{ctg}[k(c-\delta_{j2})]}{c\sin(\pi x)\cos(cx) - \pi\cos(\pi x)\sin(cx)}\,.$$

In case (**IV**) one may choose $u_1(x) = \mathrm{sh}(a_1 x)$ and $u_2(x) = \sin[a_2(x-1)]$, $0 < a_2 \le \pi$. The potential

$$V_2(x) = -(a_1^2 + a_2^2)\frac{a_1^2 + a_2^2 - a_1^2\cos[2a_2(x-1)] - a_2^2\cosh(2a_1 x)}{(a_1\cosh(a_1 x)\sin[a_2(x-1)] - a_2\sinh(a_1 x)\cos[a_2(x-1)])^2}\,, \tag{2.3.6}$$

corresponds to the irreducible second-order SUSY.

The intermediate Hamiltonian also determines a regular Sturm-Liouville problem, but its spectrum being defined by (2.3.4) radically differs from $\mathrm{spec}\, h_0$, whereas $\mathrm{spec}\, h_0 = \mathrm{spec}\, h_2$. It is

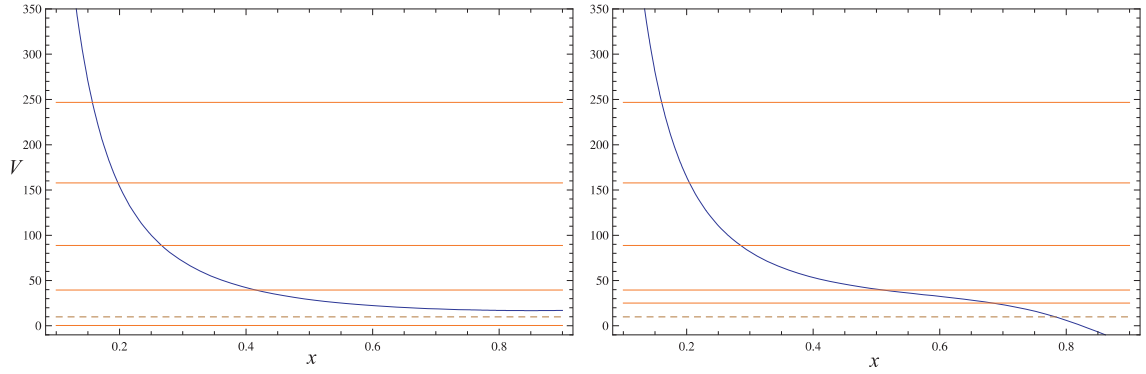

Figure 2.3: Potential (2.3.5) shifts the bound state energy only depending on c. Left/right part corresponds to $c = 0.6/c = 5$.

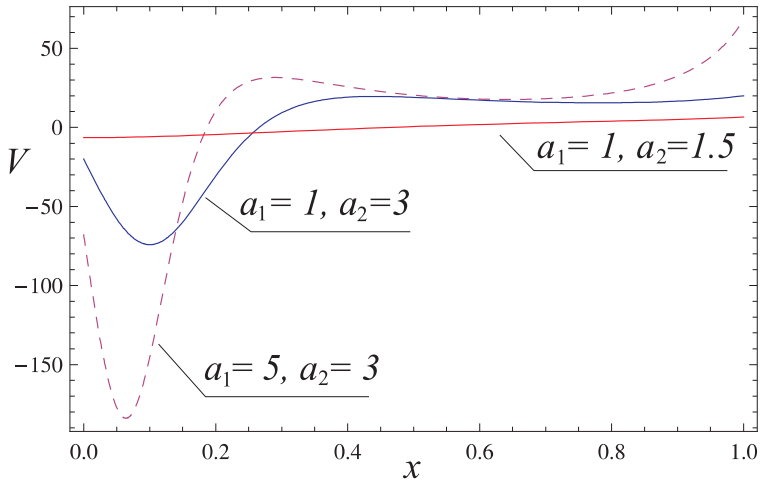

Figure 2.4: Potential (2.3.7). Parameters: $a_1 = 1, a_2 = 3$; $a_1 = 5, a_2 = 3$; $a_1 = 1, a_2 = 1.5$.

interesting that the value of the potential (2.3.6) at boundaries depends only on the factorization energies

$$V_2(0) = -2(a_1^2 + a_2^2)\,, \qquad V_2(1) = 2(a_1^2 + a_2^2)\ . \tag{2.3.7}$$

We plot potential (2.3.6) in figure 2.4 for several values of a_1 and a_2.

The Green function of potential (2.3.6) reads:

$$G_2(x,y,E) = \frac{G_{box}(x,y,E)}{(E-a_1^2)(E-a_2^2)}(E+Q_1(x))(E+Q_2(y)), \quad x<y\,,$$

$$Q_j(x) = \frac{a_1 a_2^2 \cosh(a_1 x)\sin[a_2(x-1)] - a_2 a_1^2 \sinh(a_1 x)\cos[a_2(x-1)]}{a_2 \sinh(a_1 x)\cos[a_2(x-1)] - a_1 \cosh(a_1 x)\sin[a_2(x-1)]} - \\ - \frac{k(a_2^2-a_1^2)\sinh(a_1 x)\sin[a_2(x-1)]\,\mathrm{ctg}[k(x-\delta_{j2})]}{a_2 \sinh(a_1 x)\cos[a_2(x-1)] - a_1 \cosh(a_1 x)\sin[a_2(x-1)]}\ .$$

Finally we note that the corresponding propagators can be calculated as follows [26]

$$K_N(x,y,t) = -\int\limits_{-\infty}^{\infty} \frac{dE}{2\pi} G_N(x,y,E)\mathrm{e}^{-iEt}\,. \tag{2.3.8}$$

2.3.2 Harmonic oscillator and its superpartners

Here we consider the Hamiltonian

$$h_0 = -\partial_{xx}^2 + \frac{x^2}{4}\,.$$

The propagator of the harmonic oscillator is expressed in elementary functions (see e.g. [26])

$$K_{osc}(x,y,t) = \frac{1}{\sqrt{4\pi i \sin t}}\,\mathrm{e}^{\frac{i[(x^2+y^2)\cos t - 2xy]}{4\sin t}}\,. \tag{2.3.9}$$

In a contrast, the expression for the Green function involves parabolic cylinder functions $D_\nu(x)$ [140]

$$G_{osc}(x,y,E) = \frac{1}{\sqrt{2\pi}}\Gamma\left(\frac{1}{2}-E\right) D_{E-\frac{1}{2}}(-x) D_{E-\frac{1}{2}}(y)\,, \qquad x<y\,. \tag{2.3.10}$$

Since the calculations of the transformed Green functions are rather straightforward, we will focus on the transformations of the propagator for several types of SUSY.

Using a two-fold transformation with transformation functions (see section 1.4.2)

$$u_2(x) = (x^2-1)\mathrm{e}^{-x^2/4} \qquad u_3(x) = x(x^2-3)\mathrm{e}^{-x^2/4}$$

corresponding to the second and third excited state eigenfunctions of h_0 we obtain a perturbed Harmonic oscillator potential [57]

$$V^{(2,3)}(x) = \frac{8x^2}{x^4+3} - \frac{96x^2}{(x^4+3)^2} + \frac{x^2}{4} + 2 \tag{2.3.11}$$

which for large $|x|$ behaves like the original harmonic oscillator potential, but for small $|x|$ shows two shallow minima (see figure 1.3). For completeness, we note that the transformation functions $u_2(x)$ and $u_3(x)$ have nodes, whereas their Wronskian $W(u_2,u_3) = (x^4+3)\mathrm{e}^{-x^2/2}$ is nodeless so that the corresponding second-order SUSY-transformation itself is well defined, but irreducible.

The propagator for the Schrödinger equation with Hamiltonian $h^{(2,3)} = -\partial_x^2 + V^{(2,3)}(x)$ can be constructed from propagator (2.3.9) via relation (2.2.34). The occurring integrals $\int_y^\infty K_{osc}(x,z,t)u_n(z)dz$ can be represented as derivatives with respect to the auxiliary current J of the generating function

$$\begin{aligned} S(J,x,y,t) &= \frac{1}{\sqrt{4\pi i\sin t}}\int_y^\infty \exp\left[\frac{i[(x^2+z^2)\cos t - 2xz]}{4\sin t} - \frac{z^2}{4} + Jz\right]dz \\ &= \frac{1}{2}\exp\left(\frac{-2it-x^2}{4} + (iJ^2\sin t + Jx)\exp(-it)\right) \\ &\times \left(1+\mathrm{erf}\left[\frac{-\sqrt{i}\exp(-\frac{it}{2})\,(2J\sin t + i(y\exp(it)-x))}{2\sqrt{\sin t}}\right]\right). \end{aligned}$$

As a result, we obtain

$$\begin{aligned} &K^{(2,3)}(x,y,t) \\ &= \mathrm{e}^{y^2/2} L_x\left(\frac{y(y^2-3)}{y^4+3}\left[\frac{\partial^2 S(J)}{\partial J^2} - S(J)\right] - \frac{y^2-1}{y^4+3}\left[\frac{\partial^3 S(J)}{\partial J^3} - 3\frac{\partial S(J)}{\partial J}\right]\right)_{J=0} \end{aligned}$$

in terms of obvious abbreviations.

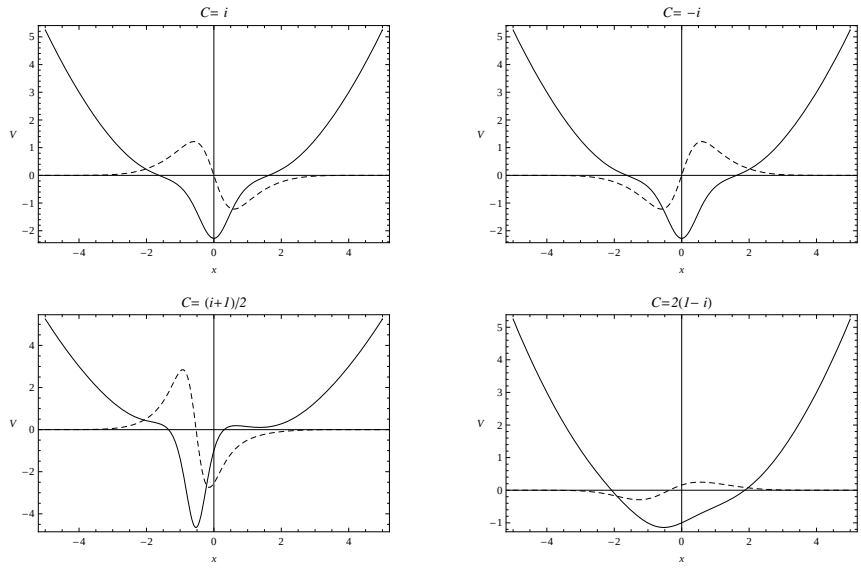

Figure 2.5: Potential (2.3.13) plotted at different values of parameter C. The solid curves correspond to the real part of the potential, the dashed curves correspond to the imaginary part of the potential.

The technique can be straightforwardly generalized to second-order SUSY-transformations built on any eigenfunction pair

$$u_k(x) = p_k(x)\mathrm{e}^{-x^2/4} \qquad u_{k+1}(x) = p_{k+1}(x)\mathrm{e}^{-x^2/4}$$

of the Hamiltonian h_0. The corresponding generalized potentials (1.4.13) have been considered in section 1.4.2.

With the help of (2.2.24) the propagator is obtained as

$$K^{(k,k+1)}(x,y,t) = \mathrm{e}^{y^2/2} L_x \left(\frac{p_{k+1}(y)}{Q_k(y)} \left[p_k\left(\partial_J\right) S(J) \right] - \frac{p_k(y)}{Q_k(y)} \left[p_{k+1}\left(\partial_J\right) S(J) \right] \right)_{J=0}$$

with $p_k\left(\partial_J\right)$ denoting the kth-order differential operator obtained from $p_k(x)$ by replacing $x^n \to \frac{\partial^n}{\partial J^n}$. Polynomials p_k and Q_k are defined in equations (1.4.9) and (1.4.12).

In the next example we consider the simplest complex deformation of the Harmonic oscillator with $\alpha = -1/2$ and

$$u(x) = e^{\frac{x^2}{4}} \left(C + \mathrm{erf}\left(x/\sqrt{2}\right) \right), \quad \mathrm{Im}\, C \neq 0$$

We need also the Green function of the oscillator Hamiltonian at $E = \alpha$. In this case we can avoid parabolic cylinder functions. We simply use the definition (1.1.18) of the Green function in terms of two special solutions $f_l(x,E)$ and $f_r(x,E)$. Functions f_l and f_r from (1.1.18) at $E = \alpha = -1/2$ read

$$f_l(x,-1/2) = \sqrt{\pi/2} e^{\frac{x^2}{4}} \left(1 + \mathrm{erf}\left(x/\sqrt{2}\right)\right), \quad f_r(x,-1/2) = \sqrt{\pi/2} e^{\frac{x^2}{4}} \left(1 - \mathrm{erf}\left(x/\sqrt{2}\right)\right). \qquad (2.3.12)$$

The spectrum of the complex-valued transformed potential

$$V_c(x) = \frac{x^2}{4} - 1 + 2xQ_1^{-1}(x)e^{-\frac{x^2}{2}} + 2Q_1^{-2}e^{-x^2}, \quad Q_1(x) = \sqrt{\frac{\pi}{2}}[C + \mathrm{erf}\left(x/\sqrt{2}\right)] \qquad (2.3.13)$$

consists of all oscillator energies $E_n = n + 1/2$, $n = 0, 1, \ldots$ and one additional level $E_{-1/2} = -1/2$ with the eigenfunction

$$\phi_{-1/2}(x) = (2\pi)^{-1/4} \sqrt{C^2 - 1} u^{-1}(x). \qquad (2.3.14)$$

It is not difficult to check by the direct calculation that

$$\int_{-\infty}^{\infty} \phi_{-1/2}^2(x)dx = 1\,. \tag{2.3.15}$$

Thus the transformed potential has the equidistant spectrum. We plot the real and the imaginary parts of this potential for different values of C in figure 2.5. Note, that in general this potential is not PT-symmetric and goes beyond the simplest realization of PT-scheme proposed by Bender [126].

Using theorem 10 and equations (1.1.18) and (2.3.12) we obtain the propagator for the Hamiltonian with potential (2.3.13)

$$K_c(x,y,t) = -\frac{\sqrt{\pi}(C+1)}{\sqrt{2}u(y)} L_x \int_{-\infty}^{y} K_{osc}(x,z,t) e^{\frac{z^2}{4}} (1+\mathrm{erf}\,(z/\sqrt{2}))dz$$
$$+\frac{\sqrt{\pi}(C-1)}{\sqrt{2}u(y)} L_x \int_{y}^{\infty} K_{osc}(x,z,t) e^{\frac{z^2}{4}} (1-\mathrm{erf}\,(z/\sqrt{2}))dz + \phi_{-1/2}(x)\phi_{-1/2}(y)e^{it/2}\,. \tag{2.3.16}$$

2.3.3 Transparent potentials

Here we apply our method to calculate propagators for the soliton potentials which are SUSY partners of the zero potential (see 1.4.1). The construction of the N-level soliton potential from the zero potential is given in section 1.4.1. Note that the propagator for a one-level transparent potential was previously calculated by Jauslin [77] for the Fokker-Planck equation. In one particular case when $b_n = 0$ and constants a_n are chosen in a special manner the corresponding propagator may be calculated using path-integral approach [34]. The propagator for a two-level potential can be found in [4] where the general form of the propagator for an N-level potential has been given as a conjecture. Here we will prove this conjecture [5].

The propagator K_0 and the Green function G_0 for the free particle are well-known [34]

$$K_0(x,y;t) = \frac{1}{\sqrt{4\pi i t}}\,\mathrm{e}^{\frac{i(x-y)^2}{4t}}\,, \tag{2.3.17}$$
$$G_0(x,y,E) = \frac{i}{2\kappa}\mathrm{e}^{i\kappa|x-y|}\,, \qquad \mathrm{Im}\kappa > 0\,, \qquad E = \kappa^2\,,$$

so that according to (2.2.22) the propagator of the transformed system can be calculated as

$$K_N(x,y,t) = \frac{L_x L_y}{\sqrt{4\pi i t}} \sum_{n=1}^{N} \left(\prod_{j=1, j\neq n}^{N} \frac{1}{\alpha_n - \alpha_j} \right) \int_{-\infty}^{\infty} \exp\left(\frac{i(x-z)^2}{4t} - a_n|z-y| \right) \frac{dz}{2a_n}$$
$$+ \sum_{n=1}^{N} \varphi_n(x)\varphi_n(y)\mathrm{e}^{-i\alpha_n t} =: K_{cN}(x,y,t) + K_{dN}(x,y,t)\,. \tag{2.3.18}$$

In the last line we separated contributions from the continuous spectrum, $K_{cN}(x,y,t)$, from contributions from the discrete spectrum, $K_{dN}(x,y,t)$.

The integral in $K_{cN}(x,y,t)$ can easily be calculated since the primitive of the integrand is well known (see e.g. integral 1.3.3.17 of Ref [124]). Using the well studied convergency conditions of the error-function erfc from [141] we find

$$I(a,x,y,t) := \frac{1}{\sqrt{4\pi i t}} \int_{-\infty}^{\infty} \exp\left(\frac{i(x-z)^2}{4t} - a|z-y| \right) \frac{dz}{2a}$$
$$= \frac{\mathrm{e}^{ia^2 t}}{4a} \left[\mathrm{e}^{a(x-y)}\mathrm{erfc}\left(a\sqrt{it} + \frac{x-y}{2\sqrt{it}} \right) + \mathrm{e}^{a(y-x)}\mathrm{erfc}\left(a\sqrt{it} - \frac{x-y}{2\sqrt{it}} \right) \right] \tag{2.3.19}$$
$$a > 0 \qquad t > 0$$

and with it

$$K_{cN}(x,y;t) = L_x L_y \sum_{n=1}^{N} \left(\prod_{m=1,m\neq n}^{N} \frac{1}{\alpha_n - \alpha_m} \right) I(a_n,x,y,t)\,. \tag{2.3.20}$$

Introducing the notation

$$\mathrm{erf}_{\pm}(a) := \mathrm{erf}\left(a\sqrt{it} \mp \frac{x-y}{2\sqrt{it}} \right)$$

and abbreviating the Wronskian of the $x-$dependent transformation functions $u_1,\ldots,u_N$ as $W(x)$ we formulate the final expression for the propagator as

Theorem 11. *The propagator for an N-level transparent potential has the form*

$$K_N(x,y;t) = \frac{1}{\sqrt{4\pi i t}}\, \mathrm{e}^{\frac{i(x-y)^2}{4t}}$$
$$+\sum_{n=1}^{N} \left(\frac{a_n}{4} \prod_{j=1,j\neq n}^{N} |a_n^2 - a_j^2| \right) \frac{W_n(x)W_n(y)}{W(x)W(y)}\, \mathrm{e}^{ia_n^2 t} \left[\mathrm{erf}_{+}(a_n) + \mathrm{erf}_{-}(a_n) \right]\,. \tag{2.3.21}$$

For the proof of this theorem we need the additional

Lemma 4. *Let $\{\alpha_i\}_{i=1}^{N}$ be a set of N non-coinciding complex numbers $a_i \neq a_{j\neq i} \in \mathbb{C}$ and[4] $n \in \mathbb{Z}^+$. Then the following identity holds:*

$$\sum_{i=1}^{N} \alpha_i^n \left(\prod_{j=1,j\neq i}^{N} \frac{1}{\alpha_i - \alpha_j} \right) = \delta_{n,N-1}\,. \tag{2.3.22}$$

Proof. Consider the auxiliary function

$$f(z) = \frac{z^n}{(z-\alpha_1)(z-\alpha_2)\ldots(z-\alpha_N)}$$

which is analytic in any finite part of the complex z-plane except for N simple poles $\alpha_1,\ldots,\alpha_N$. From the residue theorem follows

$$\sum_{i=1}^{N} \mathrm{res}\, f(\alpha_i) = \sum_{i=1}^{N} \alpha_i^n \left(\prod_{j=1,j\neq i}^{N} \frac{1}{\alpha_i - \alpha_j} \right) = -\mathrm{res}\, f(\infty)$$

what with the residue at infinity yields (2.3.22). □

As the next step we prove Theorem 11.

Proof. Without loss of generality we may set $b_j = 0$. We start with the propagator component $K_{cN}(x,y,t)$ in (2.3.20) related to the continuous spectrum. First we note that the function I in (2.3.20) depends only via the difference $x-y$ on the spatial coordinates so that the action of ∂_y in L_y can be replaced by $\partial_y^n \to (-1)^n \partial_x^n$. Hence, the composition of the two Nth-order transformation operators $L_x L_y$ acts as an effective $2N$th-order differential operator in x

$$L_x L_y = R_0 + R_1\partial_x + \ldots + R_{2N}\partial_x^{2N} \tag{2.3.23}$$

with coefficient functions $R_n(x,y)$. Accordingly, (2.3.20) takes the form

$$K_{cN}(x,y;t) = \sum_{n=1}^{N} \left(\prod_{m=1,m\neq n}^{N} \frac{1}{\alpha_n - \alpha_m} \right) [R_0 + R_1\partial_x + \ldots + R_{2N}\partial_x^{2N}] J_n \tag{2.3.24}$$

[4] We use the standard notation $\mathbb{Z}^+ = \{0,1,2,\ldots\}$ for the natural numbers with zero included.

where $J_n = I\,(a_n, x, y, t)$. From the explicit structure of the first derivatives of J_n

$$\begin{aligned}
\frac{\partial J_n}{\partial x} &= \frac{1}{4}\left[-\mathrm{e}^{-a_n(x-y)}\mathrm{erfc}_{\,+}(a_n) + \mathrm{e}^{a_n(x-y)}\mathrm{erfc}_{\,-}(a_n)\right]\mathrm{e}^{ia_n^2 t} \\
\frac{\partial^2 J_n}{\partial x^2} &= \frac{-1}{\sqrt{4\pi i t}}\,\mathrm{e}^{\frac{i(x-y)^2}{4t}} + a_n^2 I(a_n) \\
\frac{\partial^3 J_n}{\partial x^3} &= \frac{-1}{2t\sqrt{4\pi i t}}\,(x-y)\,\mathrm{e}^{\frac{i(x-y)^2}{4t}} \\
&+ \frac{a_n^2}{4}\left[-\mathrm{e}^{-a_n(x-y)}\mathrm{erfc}_{\,+}(a_n) + \mathrm{e}^{a_n(x-y)}\mathrm{erfc}_{\,-}(a_n)\right]\mathrm{e}^{ia_n^2 t}
\end{aligned} \tag{2.3.25}$$

we find (by induction) the general expression of an even-order derivative

$$\begin{aligned}
\frac{\partial^{2m} I}{\partial x^{2m}} &= \sum_{k=0}^{m-1} a_n^{2k} A_{km}(x,y,t)\mathrm{e}^{\frac{i(x-y)^2}{4t}} \\
&+ \frac{a_n^{m-1}}{4}\mathrm{e}^{ia_n^2 t}\left[\mathrm{e}^{-a_n(x-y)}\mathrm{erfc}_{\,+}(a_n) + \mathrm{e}^{a_n(x-y)}\mathrm{erfc}_{\,-}(a_n)\right]
\end{aligned} \tag{2.3.26}$$

and of an odd-order derivative

$$\begin{aligned}
\frac{\partial^{2m-1} I}{\partial x^{2m-1}} &= \sum_{k=0}^{m-2} a_n^{2k} A_{km}(x,y,t)\mathrm{e}^{\frac{i(x-y)^2}{4t}} \\
&- \frac{a_n^{m-1}}{4}\mathrm{e}^{ia_n^2 t}\left[\mathrm{e}^{-a_n(x-y)}\mathrm{erfc}_{\,+}(a_n) - \mathrm{e}^{a_n(x-y)}\mathrm{erfc}_{\,-}(a_n)\right].
\end{aligned} \tag{2.3.27}$$

It holds

$$A_{km}(x,y,t) \equiv 0 \qquad \Longleftrightarrow \qquad \left\{ \begin{array}{lll} m = 2l & \cap & k > l-1 \\ m = 2l+1 & \cap & k > l-1\,. \end{array} \right.$$

Subsequently we use the abbreviation

$$I_m(a_n) = \frac{1}{4a_n}\,\mathrm{e}^{ia_n^2 t}\left[(-1)^m \mathrm{e}^{-a_n(x-y)}\mathrm{erfc}_{\,+}(a_n) + \mathrm{e}^{a_n(x-y)}\mathrm{erfc}_{\,-}(a_n)\right] \tag{2.3.28}$$

and we will need the explicit form of the $a_n^{2(N-1)}$ and a_n^{2N} terms in the highest-order derivative

$$\frac{\partial^{2N} J_n}{\partial x^{2N}} = \ldots - a_n^{2(N-1)}\frac{1}{\sqrt{4\pi i t}}\,\mathrm{e}^{\frac{i(x-y)^2}{4t}} + a_n^{2N} I_{2N}\,. \tag{2.3.29}$$

The complete propagator component $K_{cN}(x,y;t)$ in (2.3.24) can now be rewritten as

$$\begin{aligned}
K_{cN}(x,y;t) &= \sum_{n=1}^{N}\left(\prod_{m=1,m\neq n}^{N}\frac{1}{\alpha_n-\alpha_m}\right) R_0 I_0(a_n) \\
&+ \sum_{n=1}^{N}\left(\prod_{m=1,m\neq n}^{N}\frac{1}{\alpha_n-\alpha_m}\right) a_n R_1 I_1(a_n) \\
&+ \sum_{n=1}^{N}\left(\prod_{m=1,m\neq n}^{N}\frac{1}{\alpha_n-\alpha_m}\right) R_2\left[-\frac{1}{\sqrt{4\pi i t}}\,\mathrm{e}^{\frac{i(x-y)^2}{4t}} + a_n^2 I_2(a_n)\right] + \ldots \\
&+ \sum_{n=1}^{N}\left(\prod_{m=1,m\neq n}^{N}\frac{1}{\alpha_n-\alpha_m}\right) R_{2N}\left[\sum_{k=0}^{N-1} a_n^{2k} A_{k,2N}(x,y,t)\,\mathrm{e}^{\frac{i(x-y)^2}{4t}} + a_n^{2N} I_{2N}(a_n)\right].
\end{aligned}$$

Comparison with Lemma 4 shows that due to $a_n^{2k} = (-\alpha_n)^k$ only a single term containing $\exp\left(i(x-y)^2/4t\right)$ does not vanish. It is the $k = N-1$ term in the very last sum which with $R_{2N} = (-1)^N$ and

$A_{N-1,2N}(x,y,t) = -(4\pi it)^{-1/2}$ yields exactly the propagator (2.3.17) of the free particle. All other terms containing $\exp\left(i(x-y)^2/4t\right)$, after interchanging the sums $\sum_{n=1}^{N}\ldots$ and $\sum_{k=0}^{N-1}\ldots$, cancel out due to Lemma 4. Thus, the above formula reduces to

$$K_{cN}(x,y;t) = \frac{1}{\sqrt{4\pi it}}\mathrm{e}^{\frac{i(x-y)^2}{4t}} + \sum_{n=1}^{N}\left(\prod_{m=1,m\neq n}^{N}\frac{1}{\alpha_n-\alpha_m}\right) \tag{2.3.30}$$
$$\times\left[R_0 I_0(a_n) + R_1 a_n I_1(a_n) + R_2 a_n^2 I_2(a_n) + R_3 a_n^3 I_3(a_n) + \ldots + R_{2N} a_n^{2N} I_{2N}(a_n)\right].$$

Expressing $I_m(a_n)$ via (2.3.28) in terms of erfc_+ and erfc_- one finds contributions

$$\frac{\mathrm{erfc}_+(a_n)}{4a_n}\mathrm{e}^{ia_n^2 t}(R_0 - a_n R_1 + a_n^2 R_2 - a_n^3 R_3 + \ldots + a_n^{2N} R_{2N})\mathrm{e}^{-a_n(x-y)}$$

$$\frac{\mathrm{erfc}_-(a_n)}{4a_n}\mathrm{e}^{ia_n^2 t}(R_0 + a_n R_1 + a_n^2 R_2 + a_n^3 R_3 + \ldots + a_n^{2N} R_{2N})\mathrm{e}^{a_n(x-y)}$$

which can be represented as

$$\frac{\mathrm{erfc}_+(a_n)}{4a_n}\mathrm{e}^{ia_n^2 t}(R_0 + R_1\partial_x + R_2\partial_x^2 + R_3\partial_x^3 + \ldots + R_{2N}\partial_x^{2N})\mathrm{e}^{-a_n(x-y)}$$

$$\frac{\mathrm{erfc}_-(a_n)}{4a_n}\mathrm{e}^{ia_n^2 t}(R_0 + R_1\partial_x + R_2\partial_x^2 + R_3\partial_x^3 + \ldots + R_{2N}\partial_x^{2N})\mathrm{e}^{a_n(x-y)}\,.$$

Comparison with (2.3.23) shows that the sums yield simply $L_x L_y \exp\left[\pm a_n(x-y)\right]$. Recalling furthermore that the transformation operators L_x and L_y are given by (1.2.6) and that the transformation functions have the form (1.4.2) we arrive after some algebra at[5]

$$L_x \mathrm{e}^{\pm a_n x} = (\mp 1)^n (-1)^{N+n-1} a_n \prod_{j=1,j\neq n}^{N}(a_j^2 - a_n^2)\frac{W_n(x)}{W(x)} \tag{2.3.31}$$

and, hence, at

$$L_x L_y \mathrm{e}^{\pm a_n(x-y)} = (-1)^n a_n^2 \prod_{j=1,j\neq n}^{N}(a_n^2 - a_j^2)^2 \frac{W_n(x)W_n(y)}{W(x)W(y)}\,. \tag{2.3.32}$$

Substituting (2.3.32) into (2.3.30) we obtain

$$K_{cN}(x,y;t) = \frac{1}{\sqrt{4\pi it}}\,\mathrm{e}^{\frac{i(x-y)^2}{4t}} + \frac{1}{4}\sum_{n=1}^{N}\mathrm{e}^{ia_n^2 t}a_n\left(\prod_{m=1,m\neq n}^{N}\frac{(-1)^n(a_n^2-a_m^2)^2}{\alpha_n-\alpha_m}\right)$$
$$\times\frac{W_n(x)W_n(y)}{W(x)W(y)}\left[\mathrm{erfc}_+(a_n) + \mathrm{erfc}_-(a_n)\right]. \tag{2.3.33}$$

A further simplification can be achieved by recalling that $\alpha_n = -a_n^2$ and that the parameters a_i are ordered as $a_1 < a_2 < \ldots < a_N$. Setting $(a_m^2 - a_n^2) = -(a_n^2 - a_m^2)$ in the denominator for $m = 1,\ldots,n-1$ gives an additional sign factor $(-1)^{n-1}$. The propagator sum $K_N = K_{cN} + K_{dN}$

[5]We note that equation (2.3.31) is compatible with (1.4.4). The function $\exp(-a_n x)$ is a solution of the initial Schrödinger equation related to one of the factorization constants and it is linearly independent from the corresponding factorization solution. Therefore $L_x\exp(-a_n x)$ up to a constant factor is one of the bound state functions of h_N given in (1.4.4).

resulting from continuous and discrete spectral components reads then

$$K_N(x,y;t) = \frac{1}{\sqrt{4\pi i t}}\, \mathrm{e}^{\frac{i(x-y)^2}{4t}} - \frac{1}{4}\sum_{n=1}^{N} \mathrm{e}^{ia_n^2 t} a_n \left(\prod_{m=1, m\neq n}^{N} |a_n^2 - a_m^2| \right) \times \frac{W_n(x) W_n(y)}{W(x) W(y)} \left[\mathrm{erfc}_{+}(a_n) + \mathrm{erfc}_{-}(a_n) \right] + \frac{1}{2}\sum_{n=1}^{N} \mathrm{e}^{ia_n^2 t} a_n \left(\prod_{m=1, m\neq n}^{N} |a_n^2 - a_m^2| \right) \frac{W_n(x) W_n(y)}{W(x) W(y)} \,. \tag{2.3.34}$$

and via the relation $\mathrm{erfc}(z) = 1 - \mathrm{erf}(z)$ it leads to the expression in the theorem. □

2.3.4 Deformed one-soliton potentials

In this section, we use theorems 9 and 10 to calculate propagators for the complex and time-dependent one-soliton potentials. These potentials may be interpreted as a deformation of the one-soliton potential obtained by varying parameters of the SUSY transformation.

Let us consider a complex one-soliton potential

$$V_c(x) = \frac{-2a^2}{\cosh^2(ax + c)} \,, \tag{2.3.35}$$

defined by the complex transformation function

$$u(x) = \cosh(ax + c) \,, \quad \alpha = -a^2 \,, \quad \mathrm{Im}\, c \neq 0 \,, \quad \mathrm{Im}\, a = 0 \,.$$

The Hamiltonian h_c with potential (2.3.35) has a bound state at $E_0 = -a^2$. The bound state wave function is

$$\phi_{-a^2}(x) = \sqrt{\frac{a}{2}}\, \frac{1}{u(x)} \,.$$

From theorem 10 one immediately gets:

$$K_c(x,y;t) = \frac{1}{\sqrt{4\pi i t}}\, \mathrm{e}^{\frac{i(x-y)^2}{4t}} + \frac{a \mathrm{e}^{ia^2 t}}{4u(x)u(y)} \left[\mathrm{erf}_{+}(a) + \mathrm{erf}_{-}(a) \right] , \tag{2.3.36}$$

where $c = \mathrm{arctanh}\, \frac{b^2 - a^2}{2iab}$, $\mathrm{Im}(b) = 0$.

In the case of the time-dependent soliton potential (1.4.6) the eigenfunctions of the symmetry operator $ig_0 = L^+ L + \alpha = (i\partial_x + \lambda)^2$ coincide with plane waves $\psi_k(x,t)$. Eigenfunctions of $ig_1 = LL^+ + \alpha$ are obtained as follows

$$\phi_k(x,t) = (1/\sqrt{k^2 + a^2}) L\psi_k(x,t) \,, \qquad \phi_\alpha(x,t) = N/u^*(x,t) \,.$$

We can decompose the transformed propagator in terms of the set $\{\phi(x,t)\}$ and rewrite this decomposition in terms of plane waves

$$K_{Ns}(x,y,t) = \int_{-\infty}^{\infty} \phi_k(x,t)\phi_k^*(y,0)dk + \phi_\alpha(x,t)\phi_\alpha^*(y)$$

$$= L_x L^*_{y,t=0} \int_{-\infty}^{\infty} \frac{\psi_k(x,t)\psi_k^*(y,0)}{k^2 + a^2} dk + \phi_\alpha(x,t)\phi_\alpha^*(y) \,.$$

Again we may identify the Green function and the propagator of the free particle thus obtaining

$$K_{Ns}(x,y,t) = L_x L^*_{y,t=0} I(x,y,t,a) + \phi_\alpha(x,t)\phi^*_\alpha(y)\,,$$

where integral I has been calculated already in section 2.3.3. The difference with the stationary case appears from the time-dependent transformation operators. After some algebra we get the following propagator

$$K_{Ns}(x,y;t) = \frac{1}{\sqrt{4\pi i t}}\,\mathrm{e}^{\frac{i(x-y)^2}{4t}} + \frac{a\mathrm{e}^{i(a^2-\lambda^2)t-i\lambda(x-y)}}{2\cosh[a(x+2\lambda)t]\cosh(ay)} -$$

$$\frac{\mathrm{erfc}_+(a)\mathrm{e}^{ia^2t}}{4\cosh[a(x+2\lambda)t]\cosh(ay)}\left((a-i\lambda)\mathrm{e}^{2a\lambda t} - i\lambda\cosh[a(x+y)+2a\lambda t] - \frac{\lambda^2}{a}\mathrm{e}^{-a(x-y)}\right) -$$

$$\frac{\mathrm{erfc}_-(a)\mathrm{e}^{ia^2t}}{4\cosh[a(x+2\lambda)t]\cosh(ay)}\left((a+i\lambda)\mathrm{e}^{2a\lambda t} + i\lambda\cosh[a(x+y)+2a\lambda t] - \frac{\lambda^2}{a}\mathrm{e}^{a(x-y)}\right)\,,$$

which approaches to the one-soliton propagator as $\lambda \to 0$.

Chapter 3

SUSY transformations for coupled channel problems with different thresholds [6–8]

3.1 Spectral properties of non-conservative multichannel SUSY partners of the zero potential

It was believed that the SUSY transformations can not introduce a non-trivial coupling between scattering channels if the initial system (1.1.20) is uncoupled. By trivially coupled scattering and Jost matrices, we mean non-diagonal matrices which may be diagonalized by energy-independent transformations. Similarly, a multichannel potential is nontrivially coupled if its matrix cannot be diagonalized by an r-independent transformation, where r is the radial coordinate. The argument comes from Amado's work [86] where the SUSY transformation of S-matrix was obtained. From the form of this transformation it is clear that matrices $S_0(k)$ and $S_1(k)$ are coupled or uncoupled simultaneously. Since there are only a few exactly solvable coupled-channel potentials (especially with non-trivially coupled channels) the usage of SUSY transformations was significantly limited. Fortunately, in [48] a new class of non-conservative SUSY transformations was proposed. These SUSY transformations may relate uncoupled and coupled potentials (and S-matrices) thus returning its power to the method. Recall that the non-conservative SUSY transformations modify the boundary behaviour of solutions thus radically changing the spectrum of the transformed Hamiltonian (see also the single-channel example in section 2.3.1).

To analyze this problem we use analytical expressions for the Jost matrix obtained by SUSY transformation. The zeros of the Jost-matrix determinant define positions of the bound/virtual states and resonances [22, 23]. Therefore, studying the zeros of the Jost-matrix determinant allows one to analyze the spectrum of the model. A closed analytical expression of the Jost matrix, as well as potential, resulting from a non-conservative SUSY transformation of the zero potential is obtained in [48]. The analysis of spectral properties for such potentials was not presented up to now despite the fact that the Jost matrix is well known [46]. This may be explained by the fact that the spectrum of the potential after a non-conservative SUSY transformation changes essentially and to

find these changes one has to find all the zeros of the Jost-matrix determinant.

The principal point of this section is to show that the qualitative behavior of the spectrum of the Cox potential constructed in the section 1.4.3 by the non-conservative SUSY transformation may be studied for an arbitrary number of channels, N. We think this is a very strong result, since even for the case $N = 2$ the full analysis of the spectrum is a very complicated problem [5, 6, 46]. The main reason for this is an extremely rapid growth of the order of an algebraic equation defining the spectrum with the growth of the number of channels. Fortunately, in the two channel case it is possible to find the exact solution of the spectral problem for the Cox potential [6].

The study of the spectrum for the non-conservative SUSY partner is reduced to the analysis of the Jost matrix determinant (1.1.31). According to (1.4.15), the roots of equation (1.1.31) are defined by the roots of

$$\det B(k) = 0\,, \qquad \kappa_j - ik_j \neq 0\,, \qquad j = 1, \ldots, N\,, \tag{3.1.1}$$

where

$$B(k) = w_0 - iK\,. \tag{3.1.2}$$

In what follows we concentrate on the analysis of the zeros of $\det B$ only keeping in mind that some of them may be cancelled in $\det F$ if $k_j = -i\kappa_j$. Also it is convenient to introduce special notations α_j for the diagonal and β_{jl} for the off-diagonal entries of w_0 (recall, that w_0 is the superpotential at the origin).

Our starting point is thus a system of algebraic equations (3.1.1) and (1.1.24) which reads, with certain coefficients a_i^j,

$$(-i)^N k_1 k_2 \ldots k_N + \sum_{j=1}^{N} a_{N-1}^j \prod_{l=1,\, l\neq j}^{N} k_l + \ldots + \sum_{j=1}^{N} a_1^j k_j + a_0 = 0\,, \tag{3.1.3}$$

$$k_j^2 - k_1^2 + \Delta_j = 0\,. \tag{3.1.4}$$

First we show that system (3.1.3), (3.1.4) can be reduced to an algebraic equation of the $N2^{N-1}$ degree with respect to one momentum, say k_1, only. Indeed, any momentum enters equation (3.1.3) only linearly. Therefore it can be rewritten in the form

$$k_N P_1(k_1, \ldots, k_{N-1}) = Q_1(k_1, \ldots, k_{N-1})\,, \tag{3.1.5}$$

where $P_1(k_1, \ldots, k_{N-1})$ and $Q_1(k_1, \ldots, k_{N-1})$ are polynomials of the first degree in each of the variables $k_1, \ldots, k_{N-1}$. It is important to note that given all momenta $k_1, \ldots, k_{N-1}$ this equation defines k_N in a unique way if P_1 does not vanish. On the other hand we can square the left- and right-hand sides of (3.1.5) thus obtaining an equation where k_N enters only in the second degree and polynomials P_1^2 and Q_1^2 are polynomials of the second degree with respect to their variables. But in the equation thus obtained using threshold condition (3.1.4) we can replace all second powers of the variables k_j, $j = 2, \ldots, N$ by $k_1^2 - \Delta_j$, which makes disappear both variable k_N and the second power of k_j, $j = 2, \ldots, N-1$ from the resulting equation and raises the power of k_1 till $2N$. We thus see that after these manipulations variable k_{N-1} enters in the resulting equation only in the first degree and the equation can be rewritten in form (3.1.5)

$$k_{N-1} P_2(k_1, \ldots, k_{N-2}) = Q_2(k_1, \ldots, k_{N-2})\,, \tag{3.1.6}$$

where $P_2(k_1, \ldots, k_{N-2})$ and $Q_2(k_1, \ldots, k_{N-2})$ are polynomials of the first degree in each of the variables $k_2, \ldots, k_{N-2}$. From (3.1.6), given $k_1, \ldots, k_{N-2}$, not a zero of P_{N-2}, we obtain k_{N-1} in

a unique way. We note that the system (3.1.6), (3.1.5) and (3.1.4) where from (3.1.4) the last equation $k_N^2 - k_1^2 + \Delta_N = 0$ should be excluded, is equivalent to the original system (3.1.3), (3.1.4).

It is clear that we can repeat the above process $N-3$ times more to get an equation

$$k_2 P_{N-1}(k_1) = Q_{N-1}(k_1) \tag{3.1.7}$$

and finally

$$P_N(k_1) = 0 \tag{3.1.8}$$

with P_N of order $N2^{N-1}$. Note, that the subscript in P_k and Q_k indicates nothing but the step in this procedure. It is evident that any k_1 which (together with $k_2, \ldots, k_N$) solves the system (3.1.3), (3.1.4) is a root of (3.1.8). The converse is also true. Indeed, given a root k_1 of (3.1.8), but not a root of P_{N-1}, we find from (3.1.7) a unique k_2. Once we know k_1 and k_2 we find k_3 from equation previous to (3.1.7) and so on till k_N which is found from (3.1.5). It is also clear that in this way we can get $N2^{N-1}$ number of sets $k_1, \ldots, k_N$ (some of them may coincide) each of which solves the system (3.1.3), (3.1.4) so that the same number $N2^{N-1}$ is the number of possible solutions of this system and the system (3.1.8), (3.1.7), ..., (3.1.5) is equivalent to the initial system (3.1.3), (3.1.4).

3.1.1 Number of bound states

Let us analyze the structure of solutions for equations (3.1.3), (3.1.4) in more details. The aim of this section is to count the number of the Jost determinant zeros corresponding to the bound states. Below, wave functions, entries of the Jost and the scattering matrices are considered as functions of k_1. Other momenta are expressed in terms of k_1 from the threshold conditions (1.1.24). Since in this section we are interested in the number of bound states we will consider only the negative energy semi-axis $E \in (-\infty, 0)$. It happens to be useful to change variables k_j in favor of $\bar{k}_j$ as $k_j = i\bar{k}_j$ and rewrite the threshold conditions (3.1.4) accordingly

$$\bar{k}_j = \sqrt{\bar{k}_1^2 + \Delta_j}\,, \tag{3.1.9}$$

where we have chosen only the positive value of the square root since in this section we analyze only the point spectrum of H, which restricts all momenta k_j to be purely imaginary with a positive imaginary part so that $\bar{k}_j = |k_j|$.

From (1.4.15) it is clear that all the zeros of $\det F$ are at the same time the zeros of the determinant of matrix B (3.1.2) and vice versa. This follows from (3.1.1) and the positive definiteness of matrix $\mathcal{K} - iK$ in the momenta region we consider so that neither of the roots of $\det B$ solves the equation $\det(\mathcal{K} - iK) = 0$.

Since $\det B = \prod_{j=1}^N \lambda_j$ where λ_j are the eigenvalues of B,

$$B(\bar{k}_1)\, x_j(\bar{k}_1) = \lambda_j(\bar{k}_1)\, x_j(\bar{k}_1)\,, \tag{3.1.10}$$

the equation $\det B(\bar{k}_1) = 0$ is equivalent to $\lambda_j(\bar{k}_1) = 0$, $j = 1, \ldots, N$. Matrix B is symmetric with real entries in the momenta region we consider, $B = w_0 + \bar{K} = B^T$, which implies the reality of both $\lambda_j(\bar{k}_1)$ and $x_j(\bar{k}_1)$. Here we introduced a diagonal matrix $\bar{K} = |K| = \mathrm{diag}(\bar{k}_1, \ldots, \bar{k}_N)$.

Another property of $\lambda_j(\bar{k}_1)$ important for the analysis is their monotony as functions of $\bar{k}_1$ that we prove below.

For a fixed $\bar{K}$ let us consider a deviation of $\lambda_j(\bar{k}_1)$ for a small increment of argument $\bar{k}_1$, i.e. $\lambda_j(\bar{k}_1 + \delta\bar{k}_1) = \lambda_j(\bar{k}_1) + \delta\lambda_j(\bar{k}_1)$ assuming $\delta\bar{K} = \mathrm{diag}(\delta\bar{k}_1, \ldots, \delta\bar{k}_N)$ real, positive definite (since $\delta\bar{k}_j > 0$, $\forall j$) and infinitesimal. From (3.1.10) one gets

$$B(\bar{k}_1 + \delta\bar{k}_1)x_j(\bar{k}_1 + \delta\bar{k}_1) = \lambda_j(\bar{k}_1 + \delta\bar{k}_1)x_j(\bar{k}_1 + \delta\bar{k}_1)\,. \tag{3.1.11}$$

Here according to (3.1.2) $B(\bar{k}_1 + \delta\bar{k}_1) = w_0 + \bar{K} + \delta\bar{K}$ and the increment of $B(\bar{k}_1)$ is just $\delta B = \delta\bar{K}$ which plays the role of a small perturbation of $B(\bar{k}_1)$. Therefore we may calculate the shifting of the eigenvalues produced by such a perturbation using a (Rayleigh-Schrödinger) perturbation theory. Thus, for a non-degenerate eigenvalue λ_j the first order correction reads

$$\delta\lambda_j = \langle x_j|\delta B|x_j\rangle > 0 \tag{3.1.12}$$

where the inequality follows from the positive definiteness of $\delta B = \delta\bar{K}$, which in turn implies monotony of the eigenvalues as functions of the momenta $\bar{k}_1$. For a degenerate eigenvalue corrections are obtained by diagonalizing the same perturbation operator δB restricted to a linear span of unperturbed eigenvectors corresponding to a given eigenvalue, which still leads to positive corrections because of positive definiteness of δB.

From here it follows that any eigenvalue $\lambda_j(\bar{k}_1)$ may vanish i.e. change its sign, only once. Moreover, $\lambda_j \to \bar{k}_j > 0$ as $\bar{k}_1 \to \infty$. Hence, the number of negative eigenvalues of B at $\bar{k}_1 = 0$, i.e. at the energy of the lowest threshold, is just the number of bound states. Thus, to count the number of bound states, n_b, one has to consider the eigenvalues $\lambda_j(\bar{k}_1)$, $j = 1, \ldots, N$ of matrix $B(\bar{k}_1)$ at $\bar{k}_1 = 0$,

$$B(0) \equiv w_0 - i\ \mathrm{diag}\ (i\sqrt{\Delta_j}) = w_0 + \mathrm{diag}(\sqrt{\Delta_j}) \tag{3.1.13}$$

so that

$$n_b = \frac{1}{2}(N - \Lambda)\,, \qquad \Lambda = \sum_{j=1}^{N} \Lambda_j\,, \qquad \Lambda_j = \frac{\lambda_j(0)}{|\lambda_j(0)|}\,. \tag{3.1.14}$$

To clarify this formula we notice that in the absence of bound states all $\Lambda_j = 1$, $\Lambda = N$ so that $n_b = 0$. Every bound state is responsible for the change of the sign of only one eigenvalue from positive to negative thus raising $-\Lambda$ by 2 units, i.e. $-\Lambda \to -\Lambda + 2$ with $n_b \to n_b + 1$. This justifies the factor $1/2$ in (3.1.14).

Summarizing, we see that the number of bound states is bounded by $0 \le n_b \le N$. Figure 3.1 shows the eigenvalues of matrix B as functions of $\bar{k}_1$ for the case $N = 3$. Two eigenvalues cross the axis which corresponds to the case of $n_b = 2$. The last comment in this section is devoted to equation (1.4.27). Now it can be seen that the factorization energy should be chosen lower than the ground-state energy for the transformed potential, $\mathcal{E} < E_g$, if any.

3.1.2 Number of virtual states

According to the definition of a virtual state [22, 23], in this section we will need to consider the channel wave numbers k_j lying both in the positive and the negative imaginary semi-axes of the corresponding momenta complex planes and consider the full imaginary axis for k_1, i.e. $\bar{k}_1 \in (-\infty, \infty)$. The other momenta, $k_2, \ldots, k_N$, belong to either the positive or to negative parts of their imaginary axes in agreement with the threshold conditions

$$\bar{k}_j = \sigma_j\sqrt{\bar{k}_1^2 + \Delta_j}\,, \qquad \sigma_j = \pm\,, \qquad j = 2, \ldots, N\,. \tag{3.1.15}$$

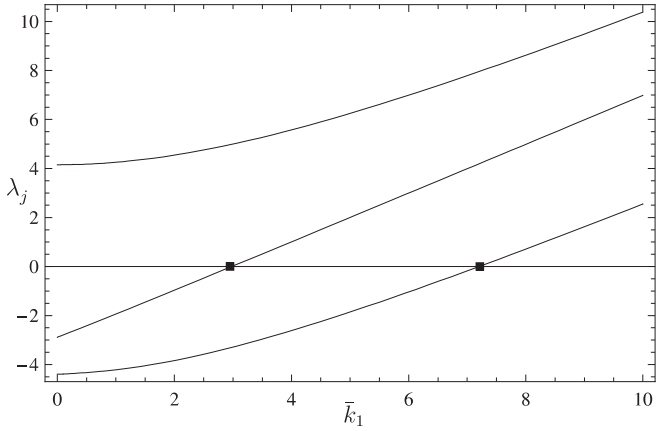

Figure 3.1: Typical behavior of B-matrix eigenvalues, $N = 3$. The case of two bound states with energies $E_1 = -51.8611$ and $E_2 = -8.8852$ is presented. The black squares show positions of these bound states. The corresponding parameters are $\alpha_1 = -3$, $\alpha_2 = -8$, $\alpha_3 = -1$, $\beta_{12} = 0.5$, $\beta_{13} = 0.4$, $\beta_{23} = 1$, $\Delta_2 = 15$, $\Delta_3 = 25$.

Since in (3.1.15) all combinations of signs are now possible it is convenient to introduce special notations for these combinations. Denote $\sigma = (+, \pm, \ldots, \pm)$ a string of N signs with σ_j being its j-th entry, which corresponds to the sign in (3.1.15) for the j-th momentum for $j > 1$. The first symbol "+" in σ indicates that all momenta $\bar{k}_j$ are expressed in terms of $\bar{k}_1$. Let $n_+(\sigma) + 1$ and $n_-(\sigma)$ be the numbers of "+" and "−" signs in this string. We notice the following evident combinatoric properties of $n_-(\sigma)$ and $n_+(\sigma)$. First, $n_+(\sigma) + n_-(\sigma) + 1 = N$ which implies

$$\sum_\sigma [n_+(\sigma) + n_-(\sigma) + 1] = N 2^{N-1} . \tag{3.1.16}$$

Here and in what follows the summation over σ includes all 2^{N-1} possible sign combinations. Next, a symmetry between "+" and "−" leads to the following relation

$$\sum_\sigma n_-(\sigma) = \sum_\sigma n_+(\sigma) = (N-1) 2^{N-2} . \tag{3.1.17}$$

According to (3.1.2) every sign combination leads to its own B matrix defined by the corresponding K matrix so that both K and B should carry an additional information about this combination. Therefore

$$B^\sigma = w_0 + \bar{K}^\sigma , \qquad \bar{K}^\sigma = \mathrm{diag}(\bar{k}_1, \sigma_2 \bar{k}_2, \ldots, \sigma_N \bar{k}_N) \tag{3.1.18}$$

and we denote $\lambda_j^\sigma(\bar{k}_1)$, $j = 1, \ldots, N$ the eigenvalues of B^σ.

In order to find the zeros of the Jost-matrix determinant corresponding to the virtual states we should find the purely real solutions of the equations $\lambda_j^\sigma(\bar{k}_1) = 0$, $j = 1, \ldots, N$ for all 2^{N-1} matrices B^σ. Although the $\bar{k}_j$'s are real, but bearing in mind our replacement $k_j = i\bar{k}_j$, throughout the text we call these zeros purely imaginary. Finally we note that since matrix $\mathcal{K} - iK$ in (1.4.15) is not positive definite for an arbitrary σ anymore, in some particular cases some of the zeros of B may be cancelled by the zeros of $\det(\mathcal{K} - iK)$ and will not correspond to virtual states. Nevertheless, omitting these particular cases, we will concentrate on an analysis of the zeros of $\det B$ only.

Eigenvalues $\lambda_j^\sigma(\bar{k}_1)$ are monotonous functions of $\bar{k}_1$ in two cases only: (i) $\sigma = (+, +, \ldots, +)$ and $\bar{k}_1 > 0$; (ii) $\sigma = (+, -, \ldots, -)$ and $\bar{k}_1 < 0$. In general, an eigenvalue $\lambda_j^\sigma(\bar{k}_1)$ may have minima/maxima for $\bar{k}_1 \lessgtr 0$ which may lead to two or even more roots in equation $\lambda_j^\sigma(\bar{k}_1) = 0$.

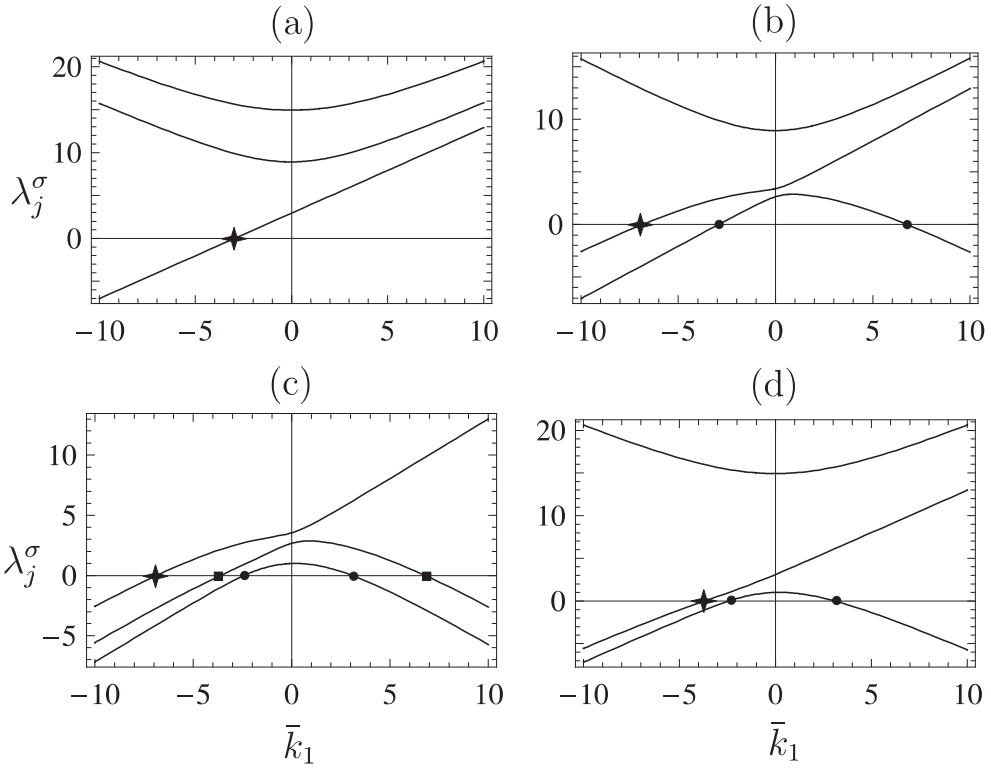

Figure 3.2: Typical behavior of the eigenvalues $\lambda_j^\sigma(\bar{k}_1)$, $N = 3$, is shown. Each plane corresponds to a particular choice of string σ: (a) $\sigma = (+++)$, (b) $\sigma = (++-)$, (c) $\sigma = (+--)$, (d) $\sigma = (+-+)$. Stars, squares and circles correspond to the virtual states. Virtual states are denoted by the identical symbol if they belong to the same eigenvalue $\lambda_j^\sigma(\bar{k}_1)$. The corresponding parameters are $\alpha_1 = 3$, $\alpha_2 = 5$, $\alpha_3 = 9$, $\beta_{12} = 0.5$, $\beta_{13} = 0.4$, $\beta_{23} = 0.2$, $\Delta_2 = 15$, $\Delta_3 = 35$.

We illustrate this behavior for $N = 3$ in figure 3.2. The monotonous lines in the right/left part of figure 3.2(a)/(c). correspond to case (i)/(ii). The position of the zeros of the eigenvalues is shown by stars, squares and circles. It is clearly seen that the total number of the roots of all equations $\lambda_j^\sigma(\bar{k}_1) = 0$ is $(N2^{N-1})|_{N=3} = 12$ which all correspond to virtual states.

A change of parameters may result in shifting the position of the virtual states only without changing the number of zeros (i.e. virtual states). For instance, in the simplest case we may shift all diagonal entries of w_0 by a number λ_0, $w_0 \to w_0 + \lambda_0 I$, thus shifting all eigenvalues of B by the same number, $\lambda_j^\sigma(\bar{k}_1) \to \lambda_j^\sigma(\bar{k}_1) + \lambda_0$.

Let us consider a specific eigenvalue defined by a string σ_0, with a local maximum at $\bar{k}_1 = \bar{k}_{1,max}$, $\lambda_j^{\sigma_0}(\bar{k}_{1,max}) = \lambda_{j,max}$. One can always shift all the eigenvalues by the value $\lambda_{j,max}$ such that the curve $\lambda_j^{\sigma_0}(\bar{k}_1)$ touches the $\bar{k}_1$ axis at the point $\bar{k}_1 = \bar{k}_{1,max}$ meaning that $\bar{k}_{1,max}$ not only becomes a root of the equation $\lambda_j^{\sigma_0}(\bar{k}_1) = 0$ but this root is multiple (of multiplicity 2) and by a small additional change of other parameters it can be split into two simple but complex roots. This is just in this way two virtual states collapse producing a resonance; a subject which deserves a special discussion (see the next section). Pairs of virtual states which may collapse are shown in figure 3.2 by squares and circles.

It is not difficult to convince oneself that for any given β_{jl} the situation when all the zeros of the Jost-matrix determinant are purely imaginary may be realized by a proper choice of α_j. To see that let us consider the asymptotic behavior of λ_j^σ for $|\bar{k}_1| \to \infty$, when all off-diagonal entries of B become negligibly small,

$$\lambda_1^\sigma \simeq \bar{k}_1 + \alpha_1\,, \tag{3.1.19}$$

$$\lambda_j^\sigma \simeq \sigma_j\sqrt{\bar{k}_1^2 + \Delta_j} + \alpha_j = \sigma_j\left(|\bar{k}_1| + \frac{\Delta_j}{2\bar{k}_1} + \dots\right) + \alpha_j\,. \tag{3.1.20}$$

$$|\bar{k}_1| \to \infty\,. \tag{3.1.21}$$

Numbers $n_+(\sigma)$ and $n_-(\sigma)$ determine the corresponding numbers of increasing and decreasing eigenvalues at positive infinity. The eigenvalue λ_1^σ increases both at negative and positive infinity. Now if we choose all α_j sufficiently large in absolute values and negative we can always guaranty the location of a root of the equation $\lambda_1^\sigma(\bar{k}_1) = 0$ near the point $\bar{k}_1 = \alpha_1$ and at the same time the location of two roots of the equation $\lambda_j^\sigma(\bar{k}_1) = 0$ with corresponding $\sigma_j = +$ near the points $\bar{k}_1 = \pm\alpha_j$. Thus, for each σ we can obtain $2n_+(\sigma) + 1$ zeros. The total number n_v of these zeros may be calculated by formulas (3.1.16) and (3.1.17)

$$n_v = \sum_\sigma [2n_+(\sigma) + 1] = N2^{N-1}\,, \tag{3.1.22}$$

which coincides with the total number of all possible roots of the system (3.1.3), (3.1.4) and is just the maximal possible number of virtual states. Hence, in this case all the roots are purely imaginary. In the next section we consider the case when some of the zeros may merge, become complex and produce resonances.

3.1.3 Number of resonances

For simplicity, independently on whether or not it can be seen in scattering data, we call any pair of complex zeros $k = \pm k_r + ik_i$ of the Jost-matrix determinant a resonance keeping in mind

that to be really visible in a scattering a resonance behavior of the corresponding cross-section should be narrow and sharp enough.

Conservation of the number of zeros of an n-th order algebraic equation under a variation of parameters included in its coefficients, which keeps unchanged its order (in our case this is equation (3.1.8) obtained from the system (3.1.3), (3.1.4)) applied to our case leads to the following relation $n_b + n_v + 2n_r = N2^{N-1}$, where n_b, n_v and n_r are number of bound states, virtual states and resonances respectively. The aim of this section is to establish the maximal number of possible resonances accepted by a non-conservative SUSY-partner of the vanishing potential.

Evidently, the maximal number of resonances corresponds to the minimal number of bound n_b and virtual n_v states. These numbers would both become zero if no one of the B matrix eigenvalues intersected the $\bar{k}_1$ axis. But as it was noticed in the previous section there always exists an eigenvalue λ_1^σ with the asymptotic behavior given in (3.1.19), i.e. ranging from $-\infty$ to $+\infty$ and, hence, it always intersects the $\bar{k}_1$ axis for all possible values of σ. We thus see that the minimal number of real zeros that all eigenvalues may take is achieved if all eigenvalues $\lambda_j^\sigma(\bar{k}_1)$, $j > 1$ are nodeless and curves $\lambda_1^\sigma(\bar{k}_1)$ intersect $\bar{k}_1$ axis only once for every given sign combination σ. To realize this case, we should choose parameters included in w_0 in a such way that the global minimum $\lambda_{j,min}^\sigma$ of every eigenvalue $\lambda_j^\sigma(\bar{k}_1)$ with $\sigma_j = +$ (they tend to $+\infty$ when $|\bar{k}_1| \to \infty$) be positive $\lambda_{j,min}^\sigma > 0$ and, respectively, the global maximum $\lambda_{j,max}^\sigma$ of every eigenvalue $\lambda_j^\sigma(\bar{k}_1)$ with $\sigma_j = -$ (they tend to $-\infty$ when $|\bar{k}_1| \to \infty$) be negative $\lambda_{j,max}^\sigma < 0$. Under these conditions only eigenvalues $\lambda_1^\sigma(\bar{k}_1)$ have zeros. The possibility that these eigenvalues have only one zero can always be realized. This can be demonstrated for small enough values of β_{ij} (the so called weak coupling approximation, see the next section) which in the limit $\beta_{ij} = 0$ for all i, j gives a very simple behavior of the eigenvalues. For instance, for $\Delta_{j+1} - \Delta_j$ large enough and $\min_j(\sqrt{\Delta_j} + \alpha_j) > \max_j(-\sqrt{\Delta_j} + \alpha_j)$, the straight line $\lambda_1^\sigma(\bar{k}_1)$ never intersects with the hyperbolas $\lambda_j^\sigma(\bar{k}_1)$ so that small perturbations coming from small non-zero β_{jl}-values (in a physical terminology, these perturbations shift the zero width resonances from the real energy axis to the complex plane) do not change the monotonous behavior of $\lambda_1^\sigma(\bar{k}_1)$ and, hence, do not bring additional roots to the equation $\lambda_1^\sigma(\bar{k}_1) = 0$.

Thus, we see that the minimal value of virtual states with the absence of bound states is equal to all possible sign combinations of σ which is $n_{vmin} = \sum_\sigma 1 = 2^{N-1}$. Hence, the maximal possible number of resonances is obtained by subtracting this number from the total number of solutions, i.e.

$$2n_{r,max} = N2^{N-1} - 2^{N-1} = (N-1)2^{N-1}\,. \tag{3.1.23}$$

3.1.4 Weak coupling approximation

For the number of channels $N > 2$ there is no way to get analytical solutions of system (3.1.3), (3.1.4), but if the coupling parameters β_{ij} are small enough, assuming the analyticity of the roots of the Jost-matrix determinant as functions of β_{ij}, a perturbation technique may be developed. In this section, we demonstrate this possibility by obtaining first order corrections to unperturbed values of the roots of the Jost-matrix determinant corresponding to $\beta_{ij} = 0$.

For the zero coupling, matrix w_0 becomes diagonal $w_0 = \mathrm{diag}(\alpha_1, \alpha_2, \ldots, \alpha_N)$ and the system

(4.1.15), (1.1.24) reduces to

$$(\alpha_1 - ik_{0,1})(\alpha_2 - ik_{0,2})\dots(\alpha_N - ik_{0,N}) = 0\,, \tag{3.1.24}$$

$$k_{0,j}^2 - k_{0,1}^2 + \Delta_j = 0\,, \qquad j = 2,\dots,N\,, \tag{3.1.25}$$

where the additional subscript 0 corresponds to the uncoupled case. Its solutions have the form

$$\begin{aligned}
k_{0,1}^{(1,\sigma)} &= -i\alpha_1\,, \quad k_{0,m}^{(1,\sigma)} = \sigma_m\sqrt{-\alpha_1^2 - \Delta_m}\,, \quad m \neq 1\,,\\
k_{0,2}^{(2,\sigma)} &= -i\alpha_2\,, \quad k_{0,m}^{(2,\sigma)} = \sigma_m\sqrt{-\alpha_2^2 + \Delta_2 - \Delta_m}\,, \quad m \neq 2\,,\\
&\dots\\
k_{0,N}^{(N,\sigma)} &= -i\alpha_N\,, \quad k_{0,m}^{(N,\sigma)} = \sigma_m\sqrt{-\alpha_N^2 + \Delta_N - \Delta_m}\,, \quad m \neq N\,,
\end{aligned} \tag{3.1.26}$$

where $m = 1,\dots,N$. Let us explicitly indicate the meaning of sub- and superscripts in (3.1.26): the second subscript m in $k_{0,m}^{(j,\sigma)}$ corresponds to the channel, the first superscript j indicates a row number in (3.1.26) and σ indicates one of all 2^{N-1} combinations of signs. Thus, we see once again that the total number of solutions of the system is $N2^{N-1}$ and it does not depend on whether or not the coupling is absent. Note that every energy level $E_j = -\alpha_j^2 + \Delta_j$ corresponding to a row in (3.1.26) is 2^{N-1} fold degenerate. Below we show that under a small coupling every degenerate level E_j splits in 2^{N-1} sub-levels and we will find approximate values of the splitting. But the unperturbed j-th momentum corresponding to this level simply equals $k_{0,j}^{(j,\sigma)} = -i\alpha_j$. Therefore, instead of our previous convention to express all quantities in terms of k_1, it is convenient here to express corrections to the j-th momentum produced by a perturbation in terms of unperturbed j-th momentum $\bar{k}_{0,j}^{(j,\sigma)}$. This is always possible due to the fact that all momenta have equal rights. But now we have to change our signs convention introduced in section 3.1.2, where the first momentum $\bar{k}_1$ entered in the string σ always with the positive sign ($\sigma_1 = +$). Now we have the j-th momentum $\bar{k}_j \in (-\infty, \infty)$ and $\sigma_j = +$ in string σ.

From (3.1.26) we learn that no coupling implies no finite-width resonances but as we discuss below the zeros lying above the first threshold may be associated with zero-width resonances which acquire a non-zero width under a small coupling.

From the first row of (3.1.26) we conclude that the corresponding 2^{N-1} zeros with $E_1 = -\alpha_1^2$ are always below the first threshold (bound or virtual states). Energy $E_n = -\alpha_n^2 + \Delta_n$, $n = 2,\dots,N$, may be positive with respect to the first threshold and only these $(N-1)2^{N-1}$ zeros are associated with zero-width resonances. According to our convention a resonance corresponds to a pair of complex zeros. Here we can easily compute the number of the zero-width resonances, n_{zwr}, which is $n_{zwr} = (N-1)2^{N-2}$ which agrees with the maximal number of possible resonances obtained in the previous section.

The unperturbed B^σ matrix, we denote B_0^σ is diagonal

$$B_0^\sigma = \mathrm{diag}(\alpha_1 + \sigma_1\bar{k}_1, \alpha_2 + \sigma_2\bar{k}_2, \dots, \alpha_N + \sigma_N\bar{k}_N) \tag{3.1.27}$$

and its eigenvalues $\lambda_{0,j}^\sigma$ coincide with its diagonal entries

$$\lambda_{0,j}^\sigma(\bar{k}_j) = \alpha_j + \bar{k}_j\,, \qquad \lambda_{0,l}^\sigma(\bar{k}_j) = \alpha_l + \sigma_l\sqrt{\bar{k}_j^2 + \Delta_l - \Delta_j}\,, \tag{3.1.28}$$

$$l = 1,\dots,N\,, \qquad l \neq j\,. \tag{3.1.29}$$

For simplicity we assume all coupling parameters β_{ij} proportional to the same small parameter β so that the perturbed B^σ matrix reads

$$B^\sigma = B_0^\sigma + \beta\mathcal{B}\,, \quad \mathcal{B} = ||b_{jl}||\,, \quad b_{jj} = 0\,, \quad j = 1,\dots,N\,. \tag{3.1.30}$$

Now, as it was mentioned above, assuming the analyticity of eigenvalues of this matrix as functions of β, we can develop them in a Taylor series with respect to β,

$$\tilde{\lambda}_j^\sigma = \lambda_{0,j}^\sigma + \lambda_{1,j}^\sigma + \lambda_{2,j}^\sigma + \dots\,, \tag{3.1.31}$$

where the first subscript number is just the power of β. First we notice that the perturbation $\mathcal{B}$ has zero diagonal entries which results in $\lambda_{1,j}^\sigma = 0$. To get the second order correction we are using the usual Rayleigh-Schrödinger perturbation approach which leads to

$$\lambda_{2,j}^\sigma(\bar{k}_j) = \beta^2 \sum_{l=1,\, l\neq j}^{N} \frac{b_{jl}^2}{\lambda_{0,j}^\sigma(\bar{k}_j) - \lambda_{0,l}^\sigma(\bar{k}_j)}\,. \tag{3.1.32}$$

In what follows we also assume that we can neglect the higher-order corrections to the eigenvalues.

Actually, our aim is to find corrections to the unperturbed degenerate j-th Jost-matrix determinant zero given in (3.1.26). Assuming a Taylor series expansions for this root over the small parameter β indicating it now explicitly

$$\bar{k}_j = \bar{k}_{0,j}^{(j,\sigma)} + \beta c_1 + \beta^2 c_2 + \dots \tag{3.1.33}$$

we find coefficients c_1 and c_2 from the equation

$$\tilde{\lambda}_j^\sigma(\bar{k}_j) = \lambda_{0,j}^\sigma(\bar{k}_j) + \lambda_{2,j}^\sigma(\bar{k}_j) = 0\,. \tag{3.1.34}$$

For that we develop $\tilde{\lambda}_j^\sigma(\bar{k}_j)$ in a Taylor series in β parameter considering its β dependence as given through $\bar{k}_j$ and (3.1.33). The term (3.1.32) contains the factor β^2, therefore in its denominator we simply put $\bar{k}_{0,j}^{j,\sigma}$ instead of $\bar{k}_j$. The $\bar{k}_j$-dependence of the term $\lambda_{0,j}^\sigma(\bar{k}_j)$ is given by (3.1.28) and its β-dependence is obtained via (3.1.33). Thus, the left hand side of equation (3.1.34) is presented as a series over the powers of β where every coefficient should vanish. This leads to $c_1 = 0$ and

$$c_2 = \sum_{l=1,\, l\neq j}^{N} \frac{b_{jl}^2}{\alpha_l + \sigma_l\sqrt{\alpha_j^2 + \Delta_l - \Delta_j}}\,. \tag{3.1.35}$$

Finally up to the second order in β we obtain the roots of system (3.1.26)

$$\begin{aligned}
k_1^{(1,\sigma)} &= -i\alpha_1 + i\sum_{l=2}^{N} \tfrac{\beta^2 b_{1l}^2}{\alpha_l+\sigma_l\sqrt{\alpha_1^2+\Delta_l}}\,, \quad k_m^{(1,\sigma)} = \sigma_m\sqrt{\left(k_1^{(1,\sigma)}\right)^2 - \Delta_m}\,,\\
k_2^{(2,\sigma)} &= -i\alpha_2 + i\sum_{l=1,\, l\neq 2}^{N} \tfrac{\beta^2 b_{2l}^2}{\alpha_l+\sigma_l\sqrt{\alpha_2^2+\Delta_l-\Delta_2}}\,, \quad k_m^{(2,\sigma)} = \sigma_m\sqrt{\left(k_2^{(2,\sigma)}\right)^2 + \Delta_2 - \Delta_m}\,,\\
&\dots\\
k_N^{(N,\sigma)} &= -i\alpha_N + i\sum_{l=1}^{N-1} \tfrac{\beta^2 b_{Nl}^2}{\alpha_l+\sigma_l\sqrt{\alpha_N^2+\Delta_l-\Delta_N}}\,, \quad k_m^{(N,\sigma)} = \sigma_m\sqrt{\left(k_N^{(N,\sigma)}\right)^2 + \Delta_N - \Delta_m}\,.
\end{aligned}$$

Here each row is obtained by applying equations (3.1.32), (3.1.33), (3.1.34) and (3.1.35) for $j = 1,\dots,N$, respectively, and $m = 1,\dots,N$, $m \neq j$ for each j. The square roots in the last column of (3.1.36) should be expanded in Taylor series up to β^2.

From here it is easily seen that, when $\alpha_m^2 < \Delta_m$, purely imaginary unperturbed zeros $k_m = -i\alpha_m$ move from the axes to the complex plane due to the real part of corrections. For instance for k_2, the real part reads $\pm\beta^2\sqrt{\Delta_2 - \alpha_2^2}/(\alpha_1^2 - \alpha_2^2 + \Delta_2)$. We thus confirmed the previous statement that zero width resonances acquire non-zero widths.

3.2 General properties of the 2×2 Cox potential

3.2.1 Explicit expression of the potential

The two-channel case deserves an additional attention because some analytical results may be obtained. For $N = 2$, the arbitrary parameters entering the Cox potential are the entries of the superpotential matrix at the origin,

$$w_0 = \begin{pmatrix} \alpha_1 & \beta \\ \beta & \alpha_2 \end{pmatrix} \tag{3.2.1}$$

and the factorization energy $\mathcal{E}$. The corresponding factorization wave number, $\kappa = (\kappa_1, \kappa_2)$, is made of two positive parameters κ_1 and κ_2 which are not independent of each other: they should satisfy the "threshold condition" [see Eq. (1.1.24)]

$$\kappa_2^2 - \kappa_1^2 = \Delta. \tag{3.2.2}$$

Here and in what follows we put for convenience $\Delta_1 = 0$, $\Delta_2 = \Delta > 0$.

In terms of these parameters, the necessary and sufficient condition for a regular potential, i.e., $\mathcal{K} + w_0$ positive definite, can be written for instance

$$\kappa_1 > -\alpha_1, \tag{3.2.3a}$$

$$\kappa_2 > \frac{\beta^2}{\kappa_1 + \alpha_1} - \alpha_2. \tag{3.2.3b}$$

This puts an upper limit on the factorization energy in terms of the parameters appearing in w_0.

Two explicit expressions for the superpotential are given in Ref. [49]. Using Eqs. (1.2.21) and (1.4.21), one gets what is probably the simplest possible explicit expression for the potential itself:

$$V_{1;11} = -8\kappa_1 e^{-2\kappa_1 r} \times \tag{3.2.4a}$$
$$\frac{x_{11}\kappa_1 + \left[2x_{11}x_{22}\kappa_1 - x_{12}^2\left(\kappa_1 + \kappa_2\right)\right] e^{-2\kappa_2 r} + x_{22}\left(x_{11}x_{22} - x_{12}^2\right)\kappa_1 e^{-4\kappa_2 r}}{\left[1 + x_{11}e^{-2\kappa_1 r} + x_{22}e^{-2\kappa_2 r} + \left(x_{11}x_{22} - x_{12}^2\right) e^{-2(\kappa_1+\kappa_2)r}\right]^2},$$

$$V_{1;12} = -4x_{12}\sqrt{\kappa_1\kappa_2}e^{-(\kappa_1+\kappa_2)r} \times \tag{3.2.4b}$$
$$\frac{\kappa_1 + \kappa_2 + x_{11}(\kappa_2 - \kappa_1)e^{-2\kappa_1 r} + x_{22}(\kappa_1 - \kappa_2)e^{-2\kappa_2 r} - \left(x_{11}x_{22} - x_{12}^2\right)(\kappa_1 + \kappa_2)e^{-2(\kappa_1+\kappa_2)r}}{\left[1 + x_{11}e^{-2\kappa_1 r} + x_{22}e^{-2\kappa_2 r} + \left(x_{11}x_{22} - x_{12}^2\right) e^{-2(\kappa_1+\kappa_2)r}\right]^2}.$$

The element $V_{1;22}$ is obtained from Eq. (3.2.4a) by the replacement $\kappa_1 \leftrightarrow \kappa_2$ and $x_{11} \leftrightarrow x_{22}$. Here, we have used the symmetric matrix

$$X_0 = \begin{pmatrix} x_{11} & x_{12} \\ x_{12} & x_{22} \end{pmatrix}, \tag{3.2.5}$$

which is related to matrix (3.2.1) by Eqs. (1.4.17) and (1.4.18).

3.2.2 Zeros of the Jost-matrix determinant

The particular case of two coupled channels is important both from the practical and theoretical point of views. Let us recall the following inequalities for the number of the bound/virtual states and resonances obtained in sections 3.1, 3.1.2 and 3.1.3: $0 \leq n_b \leq 2$, $0 \leq n_r \leq 1$, $0 \leq n_v \leq 4$. The same inequalities are obtained for $N = 2$ in [5, 6] from another approach. The two-channel problem is the only one where one is able to get analytic expressions for the Jost-determinant roots, i.e. to solve the direct problem consisting in finding the positions of the bound/virtual states and resonances. This possibility is based on the fact that the roots of an algebraic equation of the fourth, $(N2^{N-1})|_{N=2} = 4$, order may be expressed in radicals. Thus we obtain zeros as functions of parameters defining the potential. One may be interested in solving the inverse problem: to express parameters of the potential from the knowledge about positions of zeros of the Jost-matrix determinant. In principle, one may try to inverse radicals, but we propose a more elegant way below.

The Jost matrix for the Cox potential reads (see also Refs. [46, 48, 49])

$$F_1(k,p) = \begin{pmatrix} \frac{k_1+i\alpha_1}{k_1+i\kappa_1} & \frac{i\beta}{k_1+i\kappa_1} \\ \frac{i\beta}{k_2+i\kappa_2} & \frac{k_2+i\alpha_2}{k_2+i\kappa_2} \end{pmatrix}. \tag{3.2.6}$$

The determinant of the Jost matrix coincides with the Fredholm determinant of the corresponding integral equation [23]; it reads here

$$f(k_1,k_2) \equiv \det F(k_1,k_2) = \frac{(k_1+i\alpha_1)(k_2+ia_2)+\beta^2}{(k_1+i\kappa_1)(k_2+i\kappa_2)}. \tag{3.2.7}$$

In this case, the system of equations (3.1.3), (3.1.4) is significantly simplified

$$k_1^2 - k_2^2 = \Delta, \tag{3.2.8}$$

$$(k_1+i\alpha_1)(k_2+i\alpha_2)+\beta^2 = 0 \tag{3.2.9}$$

and may be reduced to a single fourth order algebraic equation in k_1

$$k_1^4 + ia_1k_1^3 + a_2k_1^2 + ia_3k_1 + a_4 = 0\,. \tag{3.2.10}$$

Coefficients a_i, $i = 1, \ldots, 4$ (see [6], (33a-d)) read

$$a_1 = 2\alpha_1, \tag{3.2.11a}$$

$$a_2 = \alpha_2^2 - \alpha_1^2 - \Delta, \tag{3.2.11b}$$

$$a_3 = 2[\alpha_1(\alpha_2^2-\Delta) - \alpha_2\beta^2], \tag{3.2.11c}$$

$$a_4 = -\alpha_1^2(\alpha_2^2-\Delta) + 2\alpha_2\beta^2\alpha_1 - \beta^4. \tag{3.2.11d}$$

Taking into account (3.2.9) one can express momentum k_2 from the following equation

$$k_2(ik_1-\alpha_1) = \alpha_2(k_1+i\alpha_1) - i\beta^2\,. \tag{3.2.12}$$

Equations (3.2.10) and (3.2.12) are nothing but system (3.1.8), (3.1.7), ..., (3.1.5) for $N = 2$ (see section 3.1).

We notice that after substitution $k_1 = i\lambda$, Eq. (3.2.10) becomes an algebraic equation in λ with real coefficients. Its four roots are thus either real numbers, which correspond to real negative

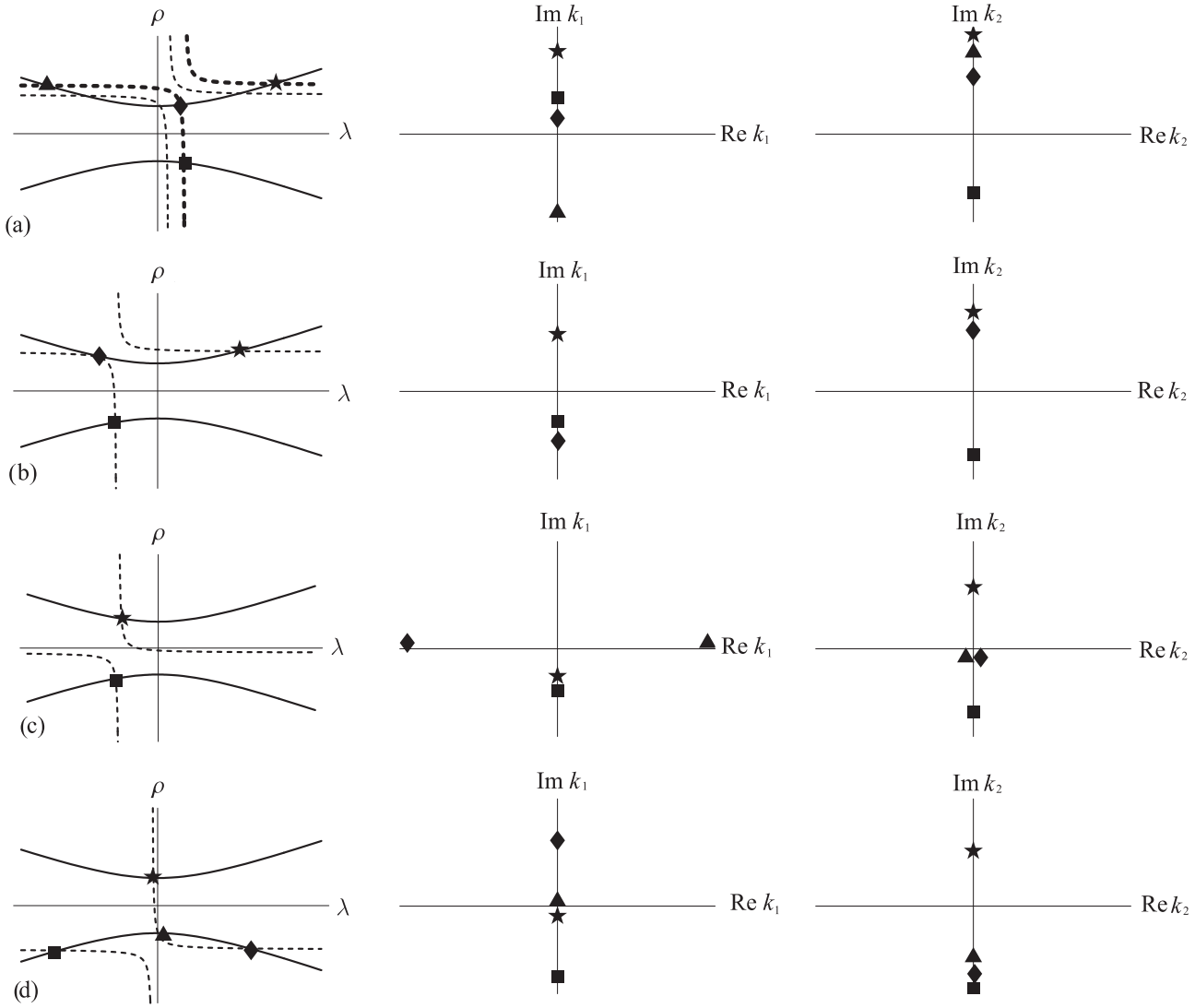

Figure 3.3: Geometrical representation of Eqs. (3.2.13a) (first column, solid lines) and (3.2.13b) (first column, dashed lines), and positions of the corresponding roots of system (3.2.8) in the complex k (second column) and p (third column) planes. Various values of the parameters α_1, α_2 are chosen, which imply various numbers of bound, virtual and resonant states: (a) $\alpha_1 < 0$, $\alpha_2 < -\sqrt{\Delta}$, two bound states (star and diamond), two virtual states (square and triangle), no resonance; (b) $\alpha_1 > 0$, $\alpha_2 < -\sqrt{\Delta}$, one bound state (star), one virtual state (square), appearance of a resonance (diamond); (c) $\alpha_1 > 0$, $\alpha_2 > 0$, no bound state, two virtual states (star and square), one resonance (triangle and diamond, not seen in the first column); (d) $\alpha_1 > 0$, $\alpha_2 > \sqrt{\Delta}$, no bound state, no resonance, four virtual states. Increase of either α_1 or α_2 leads to: (a) (thin dashed lines) disappearance of a bound state; (b) appearance of the resonance.

energies (bound or virtual states), or mutually-conjugated complex numbers, which correspond to mutually-conjugated complex energies (resonant states). Basing on this property, we will use in what follows a geometric representation of the system of equations which allows for a visualization of the zeros of $f(k_1, k_2)$ in the parameter space.

Let us first consider bound and virtual states, which correspond to solutions of system (3.2.8) with k_1 and k_2 purely imaginary. After substitution $k_1 = i\lambda$, $k_2 = i\rho$, with λ and ρ real, equations (3.2.8)-(3.2.9) define two hyperbolas in the (λ, ρ)-plane,

$$\rho^2 - \lambda^2 = \Delta\,, \tag{3.2.13a}$$

$$(\lambda + \alpha_1)(\rho + \alpha_2) = \beta^2, \tag{3.2.13b}$$

the positions of which are defined by the values of the parameters α_1, α_2, β and Δ. The roots of system (3.2.13) that correspond to bound and virtual states are the intersection points of these hyperbolas. Different possibilities of hyperbola locations are shown in figure 3.3. The solid-line hyperbola corresponds to the threshold condition (3.2.13a); its semi-major axis is $\sqrt{\Delta}$ and its slant asymptotes are given by $\rho = \pm\lambda$. The dashed-line hyperbola corresponds to Eq. (3.2.13b); its asymptotes are given by $\lambda = -\alpha_1$ and $\rho = -\alpha_2$. The abscissa (resp., ordinate) of a crossing point in the (λ, ρ)-plane gives the position of the corresponding zero on the imaginary axis in the k_1-plane (resp., k_2-plane), as shown in the second (resp., third) column of figure 3.3. Bound states correspond to $\lambda, \rho > 0$, i.e., to intersection points laying in the first quadrant of the (λ, ρ)-plane, while virtual states correspond to intersections in the second, third and fourth quadrants. In both cases, their energy with respect to the first threshold is given by

$$E = k_1^2 = -\lambda^2\,. \tag{3.2.14}$$

It is clearly seen on figure 3.3 that the two hyperbolas (3.2.13a) and (3.2.13b) cross in either two or four points. Moreover, they can have zero, one or two intersections in the first quadrant, which means that the potential has either zero, one or two bound states. This contradicts Ref. [46], where it is said that the potential does never support bound states. Since Eq. (3.2.10) is fourth order, when the hyperbolas cross in four points, the Jost determinant does not have any other zero; on the other hand, when the hyperbolas cross in only two points, the Jost determinant has two other zeros, which have to form a mutually-conjugated complex pair, as seen above. This last case corresponds to a resonance, as illustrated by figure 3.3(c), where the hyperbolas only have two intersection points in the (λ, ρ)-plane and a pair of complex roots appears in the complex k_1 and k_2 planes. The potential thus has either zero or one resonance. The intermediate case of three intersection points for the hyperbolas [figure 3.3(b)] corresponds to the presence of a multiple root of Eq. (3.2.10), which lies in an unphysical sheet ($\mathrm{Im}k_1 < 0$, $\mathrm{Im}k_2 > 0$ or $\mathrm{Im}k_1 > 0$, $\mathrm{Im}k_2 < 0$) of the Riemann energy surface; this case corresponds to a transition between a one-resonance and a two-virtual-state situation.

One sees that the parameters α_1 and α_2 determine the position of hyperbola (3.2.13b) and, hence, the number of bound states n_b (0, 1 or 2) and of resonances n_r (0 or 1). Let us now determine, for fixed values of β and Δ, the domains in the plane of parameters $\mathbb{A} = (\alpha_1, \alpha_2)$ with constant values of n_b and n_r. To find domains in $\mathbb{A}$ where system (3.2.13) has two complex conjugated roots (one resonance), we consider the case where the hyperbolas have a common tangent point, as illustrated by figure 3.3(b). One can see that the decrease of either α_1 or α_2 leads to the disappearance of the resonance, while the increase of either α_1 or α_2 leads to the appearance

of the resonance. We define the parametric curves $[\alpha_1(\lambda_0,\rho_0),\alpha_2(\lambda_0,\rho_0)]$ in plane $\mathbb{A}$ by shifting the tangent point (λ_0,ρ_0) along the hyperbola $\rho^2-\lambda^2=\Delta$. These curves limit domains in $\mathbb{A}$ with either zero or two complex roots. To find them, we use the two conditions corresponding to the common tangent point (λ_0,ρ_0)

$$\rho_0 = \frac{\beta^2}{\lambda_0+\alpha_1} - \alpha_2 = \pm\sqrt{\lambda_0^2+\Delta}, \tag{3.2.15a}$$

$$\left.\frac{d\rho}{d\lambda}\right|_{\lambda=\lambda_0} = -\frac{\beta^2}{(\lambda_0+\alpha_1)^2} = \pm\frac{\lambda_0}{\sqrt{\lambda_0^2+\Delta}}\,. \tag{3.2.15b}$$

The upper signs correspond to $\lambda_0<0$ (tangent point in the second quadrant) while the lower signs correspond to $\lambda_0>0$ (tangent point in the fourth quadrant). We can solve system (3.2.15) with respect to α_1 and α_2:

$$\alpha_1(\lambda_0) = \pm\frac{\beta}{\sqrt{|\lambda_0|}}(\lambda_0^2+\Delta)^{1/4} - \lambda_0\,, \tag{3.2.16a}$$

$$\alpha_2(\lambda_0) = \pm\frac{\beta\sqrt{|\lambda_0|}}{(\lambda_0^2+\Delta)^{1/4}} + \mathrm{sign}(\lambda_0)\sqrt{\lambda_0^2+\Delta}\,. \tag{3.2.16b}$$

It should be noted that the Schrödinger equation with the Cox potential has the following scale invariance:

$$\alpha_{1,2} \to \gamma\alpha_{1,2}\,, \qquad \Delta\to\gamma^2\Delta\,, \tag{3.2.17a}$$

$$\kappa_{1,2} \to \gamma\kappa_{1,2}\,, \qquad \beta\to\gamma\beta\,, \tag{3.2.17b}$$

$$r \to r/\gamma\,, \tag{3.2.17c}$$

which leaves $\Delta_d=\Delta/\beta^2$ invariant. Hence, we may put $\Delta=1$ without losing generality. This choice is equivalent to measuring energies in units of Δ. It is convenient to express equations (3.2.16) in terms of dimensionless variables α_i/β, $\Delta_d=\Delta/\beta^2$, $\lambda_0\to\lambda_0/\beta$:

$$\frac{\alpha_1}{\beta}(\lambda_0) = \pm\frac{1}{\sqrt{|\lambda_0|}}(\lambda_0^2+\Delta_d)^{1/4} - \lambda_0\,, \tag{3.2.18a}$$

$$\frac{\alpha_2}{\beta}(\lambda_0) = \pm\frac{\sqrt{|\lambda_0|}}{(\lambda_0^2+\Delta_d)^{1/4}} + \mathrm{sign}(\lambda_0)\sqrt{\lambda_0^2+\Delta_d}. \tag{3.2.18b}$$

These four solutions [taking into account $\mathrm{sign}(\lambda_0)$] can be considered as four parametric curves in plane $\widetilde{\mathbb{A}}=(\alpha_1/\beta,\alpha_2/\beta)$, which separate the plane in five regions (one inner region and four outer regions, see figure 3.4).

In the inner region, the Jost determinant has two complex roots $k_{1,2}=\pm k_r+ik_i$ and, hence, these values of parameters α_1,α_2 correspond to one resonance ($n_r=1$). In this case, we define the resonance energy with respect to the first threshold, E_r, and the resonance width, Γ, by

$$k_{1,2}^2 = E_r \pm i\Gamma/2\,. \tag{3.2.19}$$

In the four outer regions, the Jost determinant has purely-imaginary roots, hence $n_r=0$. The curves in figure 3.4 tend asymptotically to straight lines which are defined as the limits for $\lambda_0\to 0$ and $\lambda_0\to\pm\infty$. As a result, one finds for all branches two horizontal asymptotes $\alpha_2/\beta=\pm\sqrt{\Delta_d}$ and three slant asymptotes defined by $\alpha_2/\beta=-\alpha_1/\beta$ (for the curves in the second and fourth quadrants) and $\alpha_2/\beta=-\alpha_1/\beta\pm 2$ (for the curves in the first and third quadrants, respectively).

Consider now the case where the hyperbolas cross at the point $\lambda_0=0$, $\rho_0=\sqrt{\Delta}$ [see the thin dashed lines in figure 3.3(a)]. After a small decrease of either α_1 or α_2, the number of positive

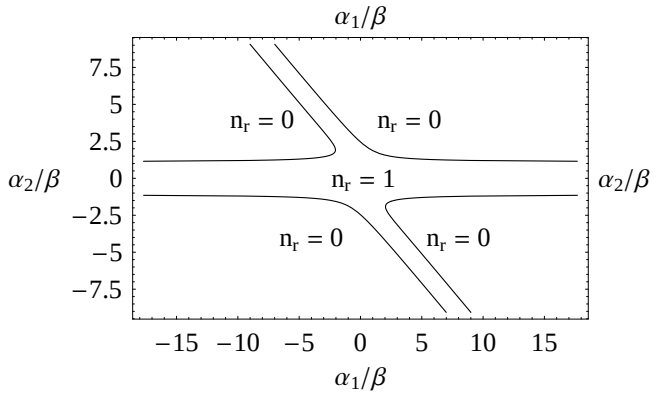

Figure 3.4: Parametric curves in terms of dimensionless parameters defined by Eqs. (3.2.18) in plane $\widetilde{\mathbb{A}} = (\alpha_1/\beta, \alpha_2/\beta)$ for $\Delta/\beta^2 = 1.2$. The left-hand-side curves correspond to the lower signs in the equations, while the right-hand-side curves correspond to the upper signs. The number of resonances, n_r, is indicated in each domain of the plane.

roots, i.e., of bound states, increases by one unit. Hence, assuming $\lambda_0 = 0$ and $\rho_0 = \sqrt{\Delta}$ in system (3.2.13), we get the curves

$$\alpha_1 \left(\alpha_2 + \sqrt{\Delta}\right) - \beta^2 = 0, \tag{3.2.20}$$

which define three domains in the plane of parameters $\mathbb{A}$, where Eqs. (3.2.13) have different number of positive roots (see figure 3.5).

One can directly check that the number n_b of bound states may be calculated as a function of the parameters as

$$n_b = 1 + \frac{1}{2}\,(I_1 - 1)\, I_2, \tag{3.2.21}$$

where the quantities

$$I_1 = \text{sign}\left(\beta^2 - \alpha_1\sqrt{\Delta} - \alpha_1\alpha_2\right) \cdot 1, \tag{3.2.22a}$$

$$I_2 = \text{sign}(\alpha_2 + \sqrt{\Delta}) \cdot 1 \tag{3.2.22b}$$

may be considered as invariants. For $n_b = 0$, one has $I_1 = -1$ and $I_2 = 1$; for $n_b = 1$, one has $I_1 = 1$ and $I_2 = \pm 1$; for $n_b = 2$, one has $I_1 = I_2 = -1$.

Let us now summarize our findings on the number of bound states and resonances of the 2×2 Cox potential, by combining Figs. 3.4 and 3.5 in figure 3.6, where both n_b and n_r are given for all the possible regions of plane $\widetilde{\mathbb{A}}$. The border lines of these regions, as already discussed, correspond to the parametric curves defined by Eqs. (3.2.16), (3.2.18), and to the curves given by Eq. (3.2.20). From the asymptotic behavior of these curves, it is easy to see the global structure of the zones. For instance, for the case of two bound states, the hyperbolas in figure 3.3 have to have four intersection points, which implies that no resonance is present. This is the reason why the boundary lines between the zones of bound and resonant states do not cross in the lower-half $\widetilde{\mathbb{A}}$-plane. Moreover, one can see that the topological structure of these zones does not depend on a particular choice of the parameter $\Delta_d = \Delta/\beta^2$. A change of this parameter only leads to a

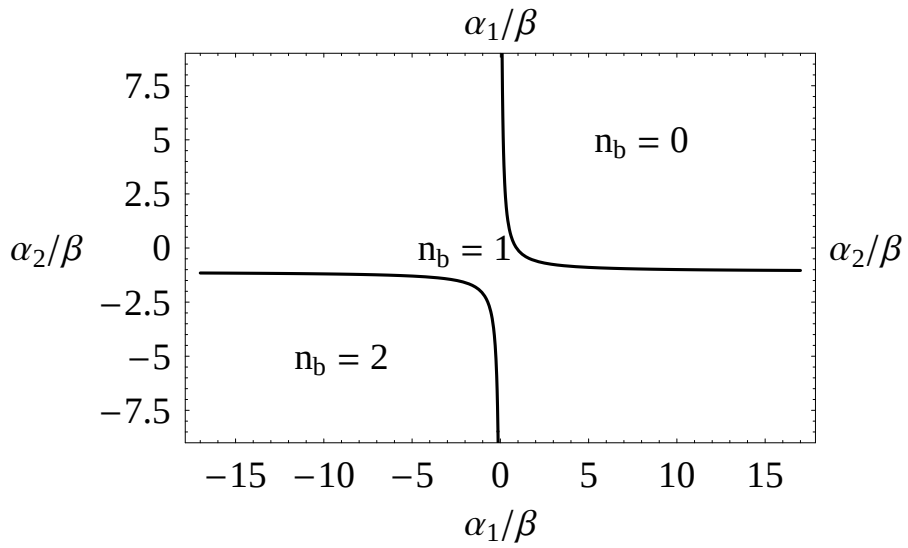

Figure 3.5: Curves (3.2.20) in plane $\widetilde{\mathbb{A}}$ in terms of dimensionless parameters for $\Delta/\beta^2 = 1.2$. The number of bound states, n_b, is indicated in each domain of the plane.

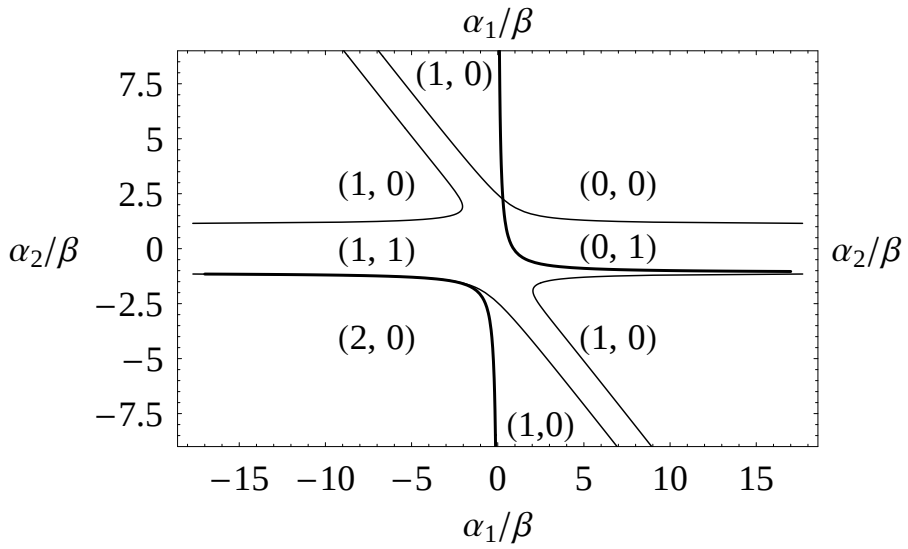

Figure 3.6: Regions of the $\widetilde{\mathbb{A}}$-plane with different numbers of bound states and resonances, (n_b, n_r), for the Cox potential with $\Delta/\beta^2 = 1.2$.

deformation of zones, namely, the distance between horizontal asymptotes changes, but does not make any new intersection point or new boundary line appear.

The case of $\beta = 0$, $\Delta_d = \infty$ corresponds to uncoupled channels. In this case there are no resonances. Only bound or virtual states located in different channels may appear (see section 3.4).

Up to now, we have excluded the factorization energy from our analysis because Eqs. (3.2.13) are independent of $\kappa_{1,2}$, but conditions (3.2.3) put an upper limit on κ_1 (resp. κ_2). The allowed values of κ_1 should be such that $\kappa_1 > \sqrt{|E_g|}$, where E_g is the ground state energy if it is present and $E_g = 0$ otherwise (for details see Ref. [5]). The necessary and sufficient condition for a regular potential can thus be simply stated as: the factorization energy should be negative and lower than the ground state energy, if any.

To conclude our consideration of the zeros of the Jost matrix determinant we note that for solving a realistic two-channel scattering inverse problem, it is necessary to express the Cox potential in terms of physical data such as the threshold energy, bound-state energies, resonance energy and width, or scattering data. While the threshold energy explicitly appears in the expression of the Cox potential as parameter Δ, the other data are directly related to the positions of the zeros of the Jost-matrix determinant, as seen above. Ideally, one would thus like to directly express parameters α_1, α_2, β, and $\mathcal{E}$, which define the Cox potential, in terms of the roots of Eq. (3.2.10). Certainly, there exist general formulas for the roots of the fourth-order algebraic equation (3.2.10), but they are very involved and cannot help much in realizing the above program. Therefore, we propose an intermediate approach (for detail see Ref. [5]) and with the cold atom in mind, prefer to focus on the low-energy scattering in the following section.

Let us assume we have found two of the roots of system (3.2.8), (3.2.9) we denote $(k_1^{(1)}, k_2^{(1)})$ and $(k_1^{(2)}, k_2^{(2)})$, which clearly are functions of parameters α_1 and α_2. Their dependence on parameters β and Δ is not important for the moment, since both β and Δ assumed to be fixed. Being put back to (3.2.9) the equation reduces twice to identity for any values of α_1 and α_2, which we write as

$$(k_1^{(1)} + i\alpha_1)(k_2^{(1)} + i\alpha_2) + \beta^2 = 0\,, \tag{3.2.23}$$

$$(k_1^{(2)} + i\alpha_1)(k_2^{(2)} + i\alpha_2) + \beta^2 = 0\,. \tag{3.2.24}$$

The reason why we replaced the identity sign by the equality sign is that these equations may be considered as an implicitly written inverted dependence of $\alpha_{1,2}$ on the set of parameters $k_{1,2}^{(1,2)}$. We may thus fix arbitrary values for $k_{1,2}^{(1,2)}$ and find from (3.2.23), (3.2.24) α_1 and α_2 in terms of $k_{1,2}^{(1,2)}$ which is a much easier task than finding an explicit dependence of $k_{1,2}^{(1,2)}$ on α_1 and α_2. For that we have to solve, e.g. for α_1, the following second order equation

$$\alpha_1^2 - \alpha_1 i(k_1^{(1)} + k_1^{(2)}) - k_1^{(1)}k_1^{(2)} + \beta^2\frac{R_1}{R_2} = 0\,, \tag{3.2.25}$$

with $R_1 = k_1^{(2)} - k_1^{(1)}$ and $R_2 = k_2^{(2)} - k_2^{(1)}$ which easily follows from (3.2.23) and (3.2.24). From here we find

$$\alpha_1 = \frac{1}{2}\left[i(k_1^{(1)} + k_1^{(2)}) \pm \sqrt{-R_1^2 - 4\beta^2 R_1/R_2}\right], \tag{3.2.26}$$

$$\alpha_2 = \frac{1}{2}\left[i(k_2^{(1)} + k_2^{(2)}) \mp \sqrt{-R_2^2 - 4\beta^2 R_2/R_1}\right]. \tag{3.2.27}$$

The upper (resp., lower) sign in (3.2.27) corresponds to the upper (resp., lower) sign in (3.2.26). The values of $k_1^{(1,2)}$ and $k_2^{(1,2)}$ should be chosen so as to warranty the reality of parameters $\alpha_{1,2}$.

Table 3.1: Possible mappings between some experimental data and the Cox potential parameters.

Experimental data	Fixed parameters	Free parameters	Restrictions
$\Delta\,, E_r\,, E_i$	$\alpha_1\,, \alpha_2$	κ_1, β	$\beta \geq \sqrt{-k_r p_r}$
$\Delta\,, E_b = -\lambda_b^2\,, E_r\,, E_i$	$\alpha_1\,, \alpha_2\,, \beta$	κ_1	$\kappa_1 > \lambda_b$
$\Delta\,, E_{1,2} = -\lambda_{1,2}^2$	$\alpha_1\,, \alpha_2$	κ_1, β	$\kappa_1 > \lambda_2 > \lambda_1$
$\Delta\,, E_b = -\lambda_b^2$	α_2	$\kappa_1\,, \beta\,, \alpha_1$	$\kappa_1 > \lambda_b$

Once two roots are fixed, (3.2.10) reduces to a second-order algebraic equation $\mathcal{Q}_2(k_1) = 0$ for the two other roots $k_1^{(3)}$ and $k_1^{(4)}$ thus providing an implicit but rather simple mapping between the roots of system (3.2.8), (3.2.9) and the set of parameters $(\alpha_1, \alpha_2, \beta)$. Polynomial $\mathcal{Q}_2(k_1)$ is the ratio of the polynomial appearing in (3.2.10) and $\mathcal{P}_2(k_1) = k_1^2 - k_1(k_1^{(2)} + k_1^{(1)}) + k_1^{(2)}k_1^{(1)}$, i.e.,

$$k_1^4 + ia_1k_1^3 + a_2k_1^2 + ia_3k_1 + a_4 = \mathcal{P}_2(k_1)\mathcal{Q}_2(k_1)\,.$$

From here we find, with the explicit expression for coefficients a_i, $i = 1, \ldots, 4$ [5],

$$\mathcal{Q}_2(k_1) = (k_1 + i\alpha_1)^2 + k_1(k_1^{(2)} + k_1^{(1)}) + \\ (2i\alpha_1 + k_1^{(2)} + k_1^{(1)})(k_1^{(2)} + k_1^{(1)}) + \alpha_2^2 - \Delta - k_1^{(1)}k_1^{(2)}$$

and, hence,

$$k_1^{(3)} = \frac{1}{2}\left[\mp i\sqrt{-R_1^2 - 4\beta^2 R_1/R_2} + \sqrt{D_1}\right], \tag{3.2.28}$$

$$k_1^{(4)} = \frac{1}{2}\left[\mp i\sqrt{-R_1^2 - 4\beta^2 R_1/R_2} - \sqrt{D_1}\right], \tag{3.2.29}$$

where $D_1 = R_1^2 + 4\beta^2\frac{R_2}{R_1} + 4k_1^{(2)}k_1^{(1)}$. The sign before the first square root in (3.2.28) and (3.2.29) should be chosen in accordance with the signs in (3.2.26) and (3.2.27).

To find $k_2^{(3,4)}$ we do not need to solve any equation. We simply notice that the equation $\det F(k_1, k_2) = 0$ is invariant under the transformation $k_1 \leftrightarrow k_2$, $\alpha_1 \leftrightarrow \alpha_2$, $\Delta \leftrightarrow -\Delta$. This means that being transformed according to these rules equations (3.2.28) and (3.2.29) give us the k_2 values:

$$k_2^{(3)} = \frac{1}{2}\left[\mp i\sqrt{-R_2^2 - 4\beta^2 R_2/R_1} - \sqrt{D_2}\right], \tag{3.2.30}$$

$$k_2^{(4)} = \frac{1}{2}\left[\mp i\sqrt{-R_2^2 - 4\beta^2 R_2/R_1} + \sqrt{D_2}\right], \tag{3.2.31}$$

where $D_2 = R_2^2 + 4\beta^2\frac{R_1}{R_2} + 4k_2^{(2)}k_2^{(1)}$.

Two initial zeros $(k_1^{(1)}, k_2^{(1)})$, $(k_1^{(2)}, k_2^{(2)})$ and threshold difference Δ are assumed to be known from the experiment. For instance, these zeros may correspond to a visible Feshbach resonance or two bound states. The possible cases for initial data are summarized in Table 3.1. The first row of Table 3.1 corresponds to the case where the position of the resonance is known (see section 3.3.1 below). The second row corresponds to the case where the positions of both the resonance and one bound state are known, which allows one to fix a maximal number of parameters. The third row corresponds to the case where the positions of two bound states are known (see section 3.3.2 below). The last row corresponds to the special case when only one zero may be fixed from experimental

data. The free parameters in Table 3.1 allow either isospectral deformations of the potential or fits of additional experimental data as, e.g., scattering lengths (see e.g. [5, 6]). The restriction on the factorization energy is deduced from the regularity condition of the potential (1.4.27). The restriction on the coupling parameter β is explained below (see (3.3.5) in section 3.3.1). Let us now consider the scattering properties of the Cox potential.

3.2.3 Low-energy scattering matrix for the Cox potential, $N = 2$

In this section, we analyze the S-matrix given by Eq. (1.1.33) for energies close to the lowest threshold, the energy of which we have chosen equal to zero. From Eqs. (3.2.6) and (3.2.7), one finds the Cox-potential S-matrix

$$\mathbf{S}(k_1, k_2) = \frac{1}{f(k_1, k_2)} \begin{pmatrix} f(-k_1, k_2) & \frac{-2i\beta\sqrt{k_1 k_2}}{k_1^2+\kappa_1^2} \\ \frac{-2i\beta\sqrt{k_1 k_2}}{k_2^2+\kappa_2^2} & f(k_1, -k_2) \end{pmatrix}. \tag{3.2.32}$$

When the second channel is closed, i.e., for energies $0 < E < \Delta$, the physical scattering matrix is just a function $S(k, p)$, which coincides with the first diagonal element of S-matrix (3.2.32). It reads

$$S(k_1) = \frac{k_1 + i\kappa_1}{k_1 - i\kappa_1} \frac{[i(k_1 - i\alpha_1)(\sqrt{\Delta - k_1^2} + \alpha_2) - \beta^2]}{[i(k_1 + i\alpha_1)(\sqrt{\Delta - k_1^2} + \alpha_2) + \beta^2]}. \tag{3.2.33}$$

From here one finds the scattering amplitude $A(k) = [S(k) - 1]/2ik$, which reads

$$A(k_1) = \frac{(\alpha_2 + \sqrt{\Delta - k_1^2}\,)\,(\alpha_1 - \kappa_1) - \beta^2}{i\,(k_1 - i\kappa_1)\left[i(k_1 + i\alpha_1)\left(\sqrt{\Delta - k_1^2} + \alpha_2\right) + \beta^2\right]}. \tag{3.2.34}$$

and the scattering length $a = -A(0)$, which reads

$$a = \frac{1}{\kappa_1} + \frac{\sqrt{\Delta} + \alpha_2}{\beta^2 - \alpha_1\left(\sqrt{\Delta} + \alpha_2\right)}. \tag{3.2.35}$$

From the argument of $S(k) = e^{2i\delta(k)}$, one deduces the phase shift $\delta(k)$, which reads

$$\delta(k_1) = -\arctan\frac{k_1}{\kappa_1} - \arctan\frac{k_1\left(\sqrt{\Delta - k_1^2} + \alpha_2\right)}{\beta^2 - \alpha_1\left(\sqrt{\Delta - k_1^2} + \alpha_2\right)}. \tag{3.2.36}$$

One can check on Eqs. (3.2.35) and (3.2.36) that the scattering length is the slope of the phase shift at zero energy, as it should be. Note that Eq. (3.2.36) is equivalent to

$$-k_1 \cot\delta(k_1) = \frac{a_\beta(k_1)\kappa_1 + k_1^2}{\kappa_1 - a_\beta}, \tag{3.2.37}$$

where $a_\beta(k_1) = \alpha_1 - \beta^2/\left(\sqrt{\Delta - k_1^2} + \alpha_2\right)$. In the uncoupled case ($\beta = 0$), this expression reduces to the phase shifts of the simplest Bargmann potential (see e.g. Ref. [23]), which depends on the parameters κ_1 and $a_B \equiv a_{\beta=0} = \alpha_1$. Therefore, the Cox potential may be considered as a coupled-channel deformation of the Bargmann potential, resulting in an energy dependence of one of its parameters, a_B.

The scattering length is an important physical quantity. In many-body theories for instance, it is often used to describe interactions in the s-wave regime. Let us thus study in detail the scattering length of the Cox potential, as given by Eq. (3.2.35). When considered as a function of $\alpha_{1,2}$, it has

a singularity located at the boundary of the single-bound-state region provided by Eq. (3.2.20). Such infinite values of the scattering length happen when a zero of the Jost determinant, which corresponds to an S-matrix pole, crosses the first threshold: a bound state is then transformed into a virtual state, in agreement with the general theory [23].

3.3 Examples of Cox potentials

Now we use all the information about the Cox potential to present several exactly solvable examples which correspond to the different possibilities listed in table 3.1.

3.3.1 Single resonance

A resonance corresponds to a pair of complex roots $k_1^{(1)}$ and $k_1^{(2)}$ of the Jost-matrix determinant such that $ik_1^{(1)}$ and $ik_1^{(2)}$ are mutually complex conjugate. Therefore we assume equations (3.2.8) and (3.2.9) to have two complex roots. Let us define their first-channel components as

$$k_1^{(1)} = k_r + ik_i\,, \quad k_1^{(2)} = -k_r + ik_i\,, \quad k_i \in \mathbb{R}\,, \quad k_r \in \mathbb{R}\,, \quad k_r > 0\,, \tag{3.3.1}$$

and write the corresponding energies, $\left(k_1^{(1,2)}\right)^2$, as $E_r \pm iE_i$, where we also assume $E_i > 0$ (which means that the upper sign corresponds to $k_1^{(1)}$ or $k_1^{(2)}$, depending on the sign of k_i). We would like to choose as parameters the threshold difference Δ, as well as the real and imaginary parts of the resonance complex energy, E_r, E_i. As exemplified below, these can correspond to physical parameters of a visible resonance in some (but not all) cases. In terms of these parameters, k_r and k_i are expressed as

$$k_r = \frac{E_i}{\sqrt{2}}\left[\sqrt{E_r^2+E_i^2} - E_r\right]^{-1/2}, \quad k_i = \pm\frac{1}{\sqrt{2}}\left[\sqrt{E_r^2+E_i^2} - E_r\right]^{1/2}. \tag{3.3.2}$$

In the second channel the roots

$$k_2^{(1)} = p_r + ip_i\,, \quad k_2^{(2)} = -p_r + ip_i\,,$$

can be found from the threshold condition yielding

$$p_r = -\frac{1}{\sqrt{2}}\left[\sqrt{E_i^2+(E_r-\Delta)^2} + E_r - \Delta\right]^{1/2}, \tag{3.3.3}$$

$$p_i = \mp\frac{E_i}{\sqrt{2}}\left[\sqrt{E_i^2+(E_r-\Delta)^2} + E_r - \Delta\right]^{-1/2}. \tag{3.3.4}$$

The upper (resp., lower) sign in (3.3.2) corresponds to the upper (resp., lower) sign in (3.3.4), which means that, for a given zero, the signs of k_i and p_i are opposite. Moreover, equations (3.3.2) and (3.3.3) show that, for a given zero, the signs of k_r and p_r are also opposite. This implies that, for the Cox potential, the complex resonance zeros (or scattering-matrix poles) are always in opposite quadrants in the complex k_1 and k_2 planes. This has important consequences for physical applications: for a resonance to be visible, one of the corresponding zero has to lie close to the physical positive-energy region, i.e., close to the real positive k_1 axis and close to the region made of the real positive k_2 axis and of the positive imaginary k_2 interval: $[0, i\sqrt{\Delta}]$. Consequently, the only possibility for a visible resonance with the Cox potential is that of a Feshbach resonance, only visible in the channel with lowest threshold, with an energy lying below threshold Δ. At higher resonance energies, the corresponding zero is either close to the k_1-plane physical region (and far from the k_2-plane one) or close to the k_2-plane physical region (and far from the k_1-plane one); it cannot be close to both physical regions at the same time, hence it cannot have a visible impact on the coupled scattering matrix. Here, we illustrate the case of a visible resonance, which is the most

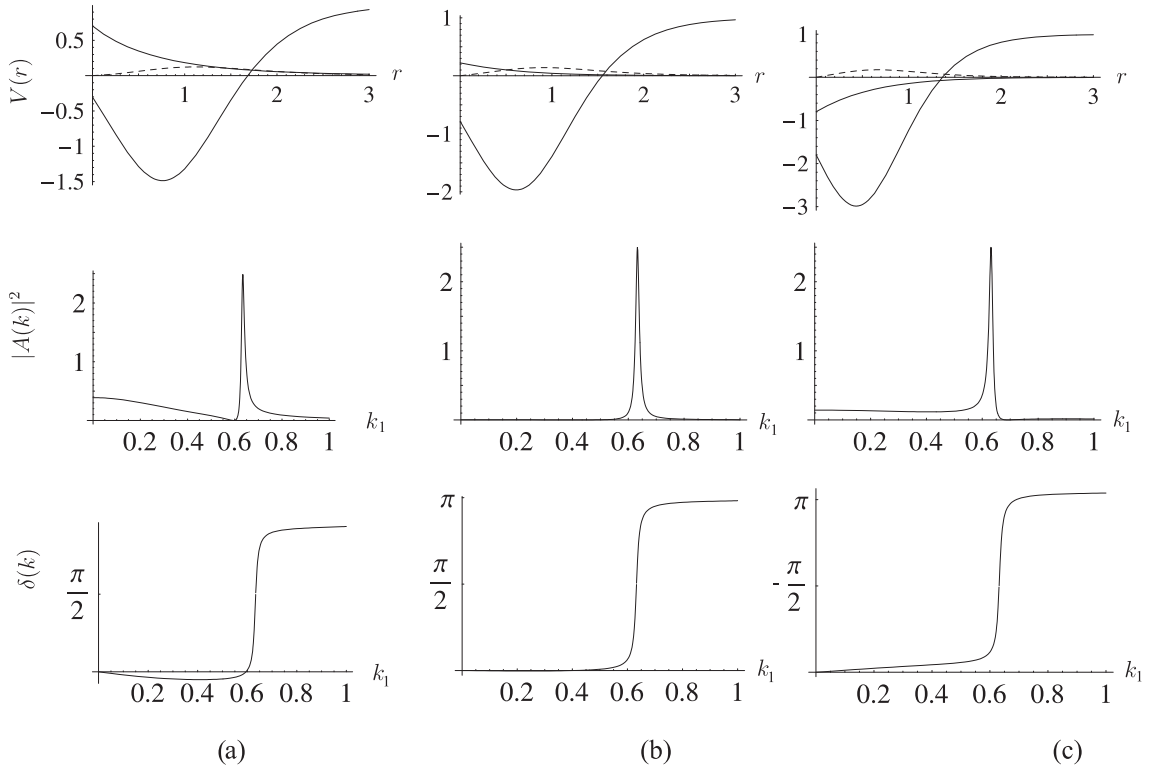

Figure 3.7: The Cox potential without bound state and with one visible resonance of energy $E_r = 0.4$ and width $\Gamma = 0.02$, for $\Delta = 1$ and $\beta = 0.1$ (first row, solid lines for V_{11} and $V_{22} + \Delta$, dashed line for V_{12}), with the corresponding partial cross section (second row) and phase shifts (third row) for (a) $\kappa_1 = 0.5$; (b) $\kappa_1 = 0.7$; (c) $\kappa_1 = 1$.

interesting from the physical point of view. It corresponds to the lower signs in (3.3.2) and (3.3.4), with a resonance energy E_r such that $0 < E_r < \Delta$, and a resonance width $\Gamma = 2E_i$ such that $E_i < E_r$.

Note, that for non-zero values of the parameters k_r and p_r (which have opposite signs), the coupling parameter β cannot be infinitesimal: because α_1 and α_2 have to be real, β is restricted to satisfy the inequality

$$\beta \geq \sqrt{-k_r p_r}\,. \tag{3.3.5}$$

To get a potential with one bound state at energy $-\lambda_b^2$, we choose the lower signs in (3.2.26), (3.2.27). We then get for $k_1^{(3)}(\beta)$ an expression similar to (3.2.28), (3.2.29), from which the value of β can be found by solving the bi-squared equation $k_1^{(3)}(\beta) = i\lambda_b$.

Let us now choose explicit parameters. First, we put $\Delta = 1$. To get a visible resonance, we put $E_r = 0.4$, $E_i = 0.01$ (which corresponds to a resonance width $\Gamma = 0.02$), and $\beta = 0.1$. Using (3.2.26), (3.3.1) and (3.3.2), one finds $\alpha_1 = 0.76938$ and $\alpha_2 = -0.766853$ (we choose the upper signs (3.2.26), (3.2.27)). The factorization energy, $\mathcal{E}$, is not constrained in this case: it just has to be negative. The Cox potential with one resonance and two virtual states $E_{v1} = -0.560473$, $E_{v2} = -0.599544$ is shown in the first row of figure 3.7.

The diagonal elements of the potentials, V_{11} and $V_{22} + \Delta$, are plotted with solid lines, while V_{12} is plotted with dashed lines. Parameter κ_1 is responsible for the isospectral deformation of the potential which results in the behavior of the phase shifts. The second row of figure 3.7 shows the corresponding partial cross sections, where the resonance behavior is clearly seen, as well as the evolution of the low-energy cross section, which is related to the scattering length. The last row of

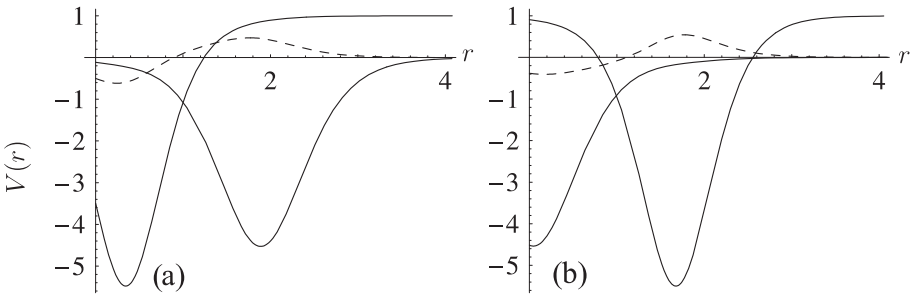

Figure 3.8: The Cox potential (solid lines for V_{11} and $V_{22}+\Delta$, dashed line for V_{12}) with two bound states at energies $E_1 = -0.01$ and $E_2 = -2.25$, for $\Delta = 1$, $\beta = 0.1$ and $\kappa_1 = 1.51$. The left (resp., right) graphic corresponds to the upper (resp., lower) signs in (3.2.26) and (3.2.27).

figure 3.7 shows the corresponding phase shifts for the open channel, where a typical Breit-Wigner behavior (see e.g. Ref. [22]) is seen for the resonance, as well as the evolution of the zero-energy phase-shift slope, which is also related to the scattering length.

3.3.2 Two bound states

Let us now construct a Cox potential with two bound states, and hence no resonance (see figure 3.6). We choose $k_1^{(1)} = 0.1i$ and $k_1^{(2)} = 1.5i$ for these bound states and, as in the previous example, we put $\Delta = 1$ and $\beta = 0.1$. We thus have $k_2^{(1)} = \sqrt{1.01}i$ and $k_2^{(2)} = \sqrt{3.25}i$, which defines R_2 in (3.2.26), (3.2.27). Choosing the upper signs in these equations, we find $\alpha_1 = -0.112649$ and $\alpha_2 = -1.79557$, while for the lower signs, we get $\alpha_1 = -1.48735$ and $\alpha_2 = -1.0122$. The corresponding Cox potentials are shown in figure 3.8.

3.4 Two-channel model of alkali-metal atom-atom collisions in the presence of a magnetic field

3.4.1 Magnetic Feshbach resonance

Ultra-cold collisions of alkali-metal atoms play a key role in applications of laser cooling such as Bose-Einstein condensation and BEC-BCS crossover [12–14, 142]. The analysis of such collisions is commonly based on the coupled-channel method [143], i.e., on solving numerically a set of coupled differential equations.

In this section we reduce the low-energy scattering problem of two alkali-metal atoms to an effective two-channel problem with a single Feshbach resonance, as in Ref. [142]. The model consists of a single closed channel Q containing a bound state, which interacts with the scattering continuum in the open channel P, so that the whole scattering problem is reduced to the two-channel scattering described by the 2×2 Hamiltonian

$$H = -\frac{d^2}{dr^2} + \begin{pmatrix} V_P(r) & V_{int}(r) \\ V_{int}(r) & V_Q(r) \end{pmatrix}, \tag{3.4.1}$$

where V_P is the uncoupled open-channel potential, V_Q is the uncoupled closed-channel potential, and potential V_{int} describes the coupling between the open and closed channels P and Q. These channels describe atoms placed in a magnetic field and occupying different energy sub-levels which can be shifted with respect to each other with the change of the magnetic field (Zeeman effect). For each value of the magnetic field, the zero of energy is chosen as the energy of the dissociated atoms in channel P.

Even in the simplest case of a homogeneous magnetic field, the potential-energy matrix of Hamiltonian (3.4.1) depends on the magnetic field. We will assume that the external field changes slowly enough so that we can take advantage of the adiabatic approximation, assuming that the stationary Schrödinger equation may be applied for describing the scattering process and the magnetic field enters the Hamiltonian as a parameter only. Moreover, the known observation that, when the scattering length is much larger than the range of the interaction, the general behavior of the system is nearly independent of the exact form of the potential [144], suggests us to use the Cox potential with large scattering length for describing the interatomic scattering. We thus replace the potential matrix in Eq. (3.4.1) by the Cox potential. In this case, the parameters of the Cox potential should carry a dependence on the magnetic field. Below, we show that, to get a good agreement with available experimental data, it is sufficient to impose a linear field dependence on the threshold difference Δ only, keeping all other parameters field independent. Thus, inverting known scattering experimental data, one can find all the parameters defining the Cox potential, obtaining in this way a simple analytical model of the atom-atom scattering process in the presence of a magnetic field.

The position of the highest bound (or virtual) state is crucial in describing the resonance phenomena of interatomic collisions. In an s-wave single-channel system, the scattering process becomes resonant at low energy when a bound state or virtual state is located near the threshold, a phenomenon known as "potential resonance". In a multichannel system, the incoming channel (which is always open) may be coupled during the collision process to other open or closed

channels, corresponding to different spin configurations. When a bound state in a closed channel lies near the collision energy continuum, a Feshbach resonance [145, 146] may occur, giving rise to scattering properties that are tunable by an external magnetic field. In Ref. [147], some interesting examples of the interplay between a potential resonance and a Feshbach resonance are considered. Below, we adjust the analytically-solvable model based on the Cox potential for describing the same phenomena.

Typically, the coupling between the closed and open channels is rather small; we thus consider first an uncoupled limit of the Cox potential, i.e., $V_{int}(r) \to 0$, which corresponds to $\beta \to 0$. In this case, the Jost determinant (3.2.7) has the following zeros:

$$k_1^{(1)} = -i\alpha_1 \tag{3.4.2}$$

and

$$k_2^{(2)} = -i\alpha_2. \tag{3.4.3}$$

According to Eq. (3.2.14), the energies of these unperturbed (i.e., with zero coupling) states (called bare molecular states in Ref. [147]) with respect to the first threshold are

$$E_1 = -\alpha_1^2 \tag{3.4.4}$$

and

$$E_2 = -\alpha_2^2 + \Delta\,. \tag{3.4.5}$$

It should be noted that in this case E_P belongs to channel P while E_Q belongs to channel Q. Hence, α_1 is associated with the potential resonance, while α_2 is associated with the Feshbach resonance. Due to the Zeeman effect, the difference between the thresholds is a linear function of the magnetic field,

$$\Delta(B) = \Delta_0 + \mu_{mag}(B - B_0), \tag{3.4.6}$$

where B_0 can be arbitrarily chosen in the domain of interest and Δ_0 is the value of the threshold corresponding to B_0. If $\alpha_{1,2} < 0$ and the coupling is absent, then the two bound states cross at $\Delta = \alpha_2^2 - \alpha_1^2$. Note that E_Q crosses the threshold at $\Delta = \alpha_2^2$. When there is a coupling between channels, the levels E_P and E_Q avoid crossing (see below).

Let us consider the behavior of the scattering length in the presence of the Feshbach resonance. It is described by the following formula [15]:

$$a = a_{bg}\left(1 - \frac{\Gamma_B}{B - B_0}\right). \tag{3.4.7}$$

Here, B_0 is the position of the magnetic Feshbach resonance and Γ_B is its width (in terms of magnetic field).

In particular, Eq. (3.2.35) shows that such an infinite value of the scattering length occurs for the Cox potential at a threshold Δ_0 defined by:

$$\sqrt{\Delta_0} = \frac{\beta^2 - \alpha_1\alpha_2}{\alpha_1}\,. \tag{3.4.8}$$

Let us now assume for the Cox potential a threshold difference given by Eq. (3.4.6) with such a value of Δ_0. Expanding Eq. (3.2.35) near this resonance one gets

$$\begin{aligned} a &= \frac{\alpha_1 - \kappa_1}{\alpha_1\kappa_1} \\ &\times \left(1 + \frac{2\left[1 + \frac{\Delta-\Delta_0}{2\Delta_0} + \ldots\right]\kappa_1\sqrt{\Delta_0}\left(\sqrt{\Delta_0} + \alpha_2\right)}{(\alpha_1 - \kappa_1)\,(\Delta_0 - \Delta)}\right). \end{aligned} \tag{3.4.9}$$

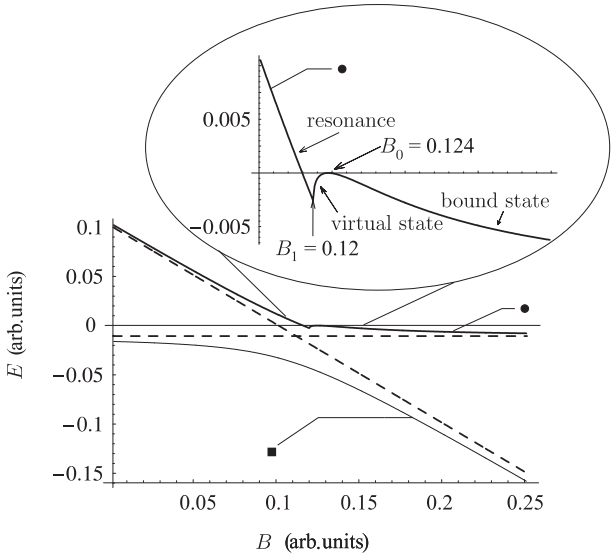

Figure 3.9: Energies of bare (dashed lines) and dressed (solid lines) states as functions of the magnetic field B for the Cox potential defined by parameters (3.4.12). The transition between a Feshbach resonance, a virtual state, and a bound state is shown in the inset for the • solid line. The dressed ground state is shown by the ■solid line.

$$\Gamma_B = \frac{2\kappa_1\sqrt{\Delta_0}\left(\sqrt{\Delta_0}+\alpha_2\right)}{\mu_{mag}\left(\alpha_1-\kappa_1\right)}\,. \tag{3.4.10}$$

As shown in Ref. [147], the background scattering length a_{bg} is due to the open-channel potential. Indeed, equations (3.4.7) and (3.4.9) show that, for our model, $a_{bg} = \lim_{\beta\to 0} a$. When there is a bound state or virtual state close to threshold, it can be further decomposed as a sum of two contributions: a standard potential part, which depends on the potential range, and a potential-resonance part, which depends on the bound/virtual-state energy. This decompostion clearly appears in our model:

$$a_{bg} = \frac{1}{\kappa_1} - \frac{1}{\alpha_1}, \tag{3.4.11}$$

where the first term is proportional to $1/\kappa_1$, the parameter which defines the range of the open-channel potential [see Eqs. (3.2.4)]; it may thus be considered as the standard potential part of the background scattering length. The second term is associated with the P-channel bound (or virtual) state in the uncoupled limit. Hence, it may be interpreted as the potential-resonance part of the background scattering length. Let us further consider two different possibilities giving rise to a large (either positive or negative) background scattering length. By that we want to study, with the exactly solvable model, examples of general phenomena described in [147].

3.4.2 Interplay between a bound state and the Feshbach resonance

The first possibility occurs when the highest bound state is located near the threshold, i.e., when $\alpha_1 \lesssim 0$. In figure 3.9, we show energies as functions of the magnetic field when channel P

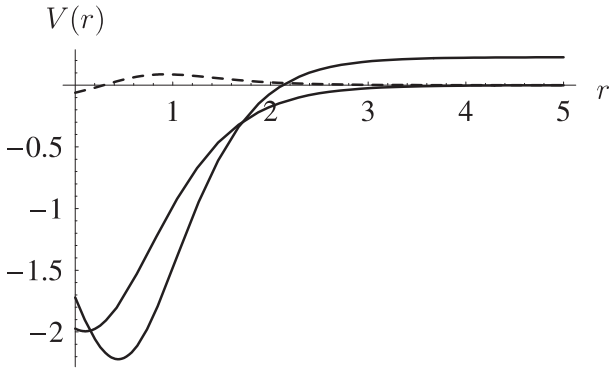

Figure 3.10: The Cox potential defined by parameters (3.4.12) for $B = 0.1$; V_P and $V_Q + \Delta$ are represented by solid lines, V_{int} by a dashed line.

has a bound state just below the threshold, for

$$\beta = 0.05, \tag{3.4.12a}$$

$$\alpha_1 = -\lambda_b = -0.103, \tag{3.4.12b}$$

$$\alpha_2 = -0.5, \tag{3.4.12c}$$

$$\kappa_1 = 1. \tag{3.4.12d}$$

Without coupling between the channels ($\beta = 0$), the energies $E = k_1^2$ of the bare bound states with respect to the first threshold are shown in figure 3.9 by the dashed horizontal [see Eq. (3.4.4)] and slanted [see Eq. (3.4.5)] lines respectively, as functions of the magnetic field B. We are using arbitrary units and choose $\Delta(B) = 0.35 - B$ in Eq. (3.4.6).

For the coupled case, the B-behavior of the (dressed) ground state is shown by the ■ solid line and it now avoids crossing with the (dressed) excited state (cf. [147]) which is shown by the • solid line.

For the fields $B > 0$ and till a value $B = B_1$ (which we define below), the excited bare state in Q-space becomes a resonance and the corresponding Jost determinant zero shifts from the real axis in k-plane to the lower half of the complex k-plane and from the imaginary axis in p-plane it shifts to the upper half plane. Recall that, according to our convention (3.2.19) we show the real part of k^2 for the resonance in figure 3.9, which may be negative. For any complex zero of the Jost determinant there exists another zero with the opposite sign of the real part. With the growth of B these two zeros move towards each other approaching the imaginary axis from different sides where they merge thus defining the point $B = B_1 = 0.12$. At this point the zeros become purely imaginary [• and ∘ in figure 3.11 (c), (d), (e)] which corresponds to appearance of two virtual states and the discontinuous slope of the real part of the energy clearly visible in figure 3.9. With further increasing of the magnetic field, one of these virtual states (• solid line in figure 3.9 and • in figure 3.11) tends to the threshold, while the other virtual state (not represented in figure 3.9, ∘ in figure 3.11) goes down along the imaginary axis. At $B_0 = 0.124$, the virtual state crosses the threshold and becomes a bound state; the scattering length thus goes through infinite values at that field: this is the magnetic-Feshbach-resonance phenomenon itself. Above B_0, the model has two bound states, the energies of which tend to the bare-state energies when the field continues to increase.

Following Ref. [147], we stress that, although the behavior of the dressed states shows some resemblance with the two-level Landau-Zener description [148], this model does not include the

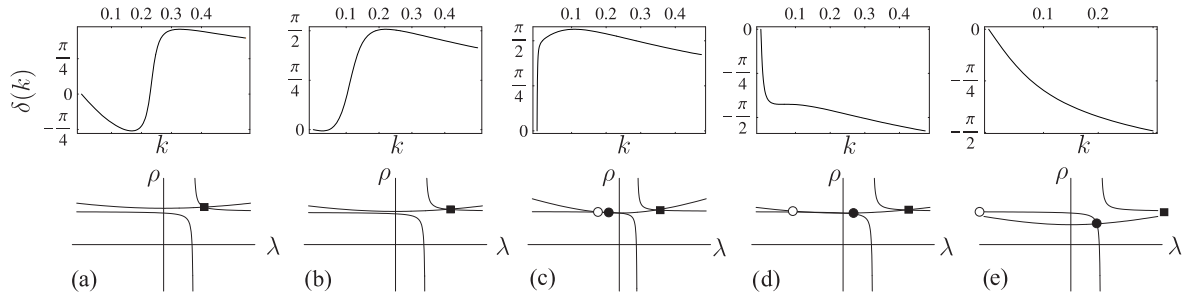

Figure 3.11: Phase shifts and graphical representation of Eqs. (3.2.13) for the Cox potential defined by parameters (3.4.12). The ■ corresponds to the position of the dressed ground state. The • corresponds to the virtual state which transforms into a bound state. The ∘ corresponds to the virtual state. The columns correspond to different values of the magnetic field: (a) $B = 0.05$; (b) 0.1; (c) 0.1235; (d) 0.125; (e) 0.24.

threshold effects shown in figure 3.9 and, hence, cannot be used to properly describe the interplay between a potential resonance and a Feshbach resonance. With respect to Ref. [147], our model displays a slightly more sophisticated behavior for the state energies (compare our figure 3.9 with their figure 4). A more significant novelty of our description is the direct knowledge of the coupled-channel potential corresponding to these energies. This potential is shown in figure 3.10 for $B = 0.1$. The potential form factor changes slowly with the change of the magnetic field, which is mainly responsible for the variation of Δ.

The value of κ_1 chosen in Eq. (3.4.12d) is arbitrary. However, the necessary and sufficient condition to get a Cox potential without singularity imposes then that the bound-state energies of the model should be larger than -1. Figure 3.9 shows that this condition will be satisfied for a limited range of magnetic field only. For higher fields, a larger κ_1 should be chosen.

The phase shifts of the same Cox potential, as well as a graphical representation of Eqs. (3.2.13), are shown in figure 3.11 for different values of B. The first and the last columns correspond to a large positive background scattering length ($a_{bg} \sim 1/\lambda_b \approx 10$), due to a bound state close to the threshold.

Physically, this occurs for the ^{133}Cs atom-atom interaction [149], for instance. Figure 3.11(b) illustrates the case where the scattering length is close to zero. The calculation or measurement of the zero of the scattering length plays an important role in determining the resonance width [150]. The phase-shift behavior for the virtual state and bound state close to threshold is shown in figures 3.11(c) and 3.11(d), respectively. In this case, the scattering length is very large and its sign changes while the energy of the zero of the Jost-matrix determinant crosses the threshold. Recalling that the intersection points in the graphical representation of Eqs. (3.2.13), shown in the second row of figure 3.11, give the positions of bound and virtual states, one may establish a correspondence between the second row of figure 3.11 and the motion of the corresponding zeros in the complex plane described above.

3.4.3 Interplay between a virtual state and the Feshbach resonance

Another interesting possibility occurs when there is a virtual state close to the threshold, i.e., when $\alpha_1 \gtrsim 0$. This is the case of the ^{85}Rb atom-atom interaction, for example. We will use rubidium scattering data [147, 151] in this example, and work with units $\hbar = 2\mu = 1$, where μ is the reduced mass of the two atoms. The length unit is chosen as the Bohr radius a_0; energies

are thus expressed in units of a_0^{-2}. According to Ref. [147], the bare virtual state is located at $\lambda_v = -1.78 \cdot 10^{-3} a_0^{-1}$, but this value is associated with the model they used in their calculations. We just consider $\lambda_v \sim -10^{-3} a_0^{-1}$ and set Eq. (3.4.11) as a constraint between $\alpha_1 = -\lambda_v$ and κ_1. In order to fit the scattering-length behavior (3.4.7) with $a_{bg} = -443\, a_0$, $B_0 = 15.5041$ mT and $\Gamma_B = 1.071$ mT, we use Eq. (3.2.35).

The value of β defines, in particular, the position of the Feshbach resonance, i.e., the magnetic field B_0 for which the bound state crosses the threshold. According to Eq. (3.2.20), one has

$$\beta = \sqrt{\alpha_1 \left(\alpha_2 + \sqrt{\Delta_0}\right)}, \tag{3.4.13}$$

where Δ_0 is the value of the threshold corresponding to B_0. The value of α_2, defining the width of the Feshbach resonance Γ_B, should be found from the condition $a(B_0 + \Gamma_B) = 0$. Then, according to Eq. (3.2.35), we find

$$\alpha_2 = \frac{\alpha_1 \left[\sqrt{\Delta(B_0 + \Gamma_B)} - \sqrt{\Delta_0}\right]}{\kappa_1} - \sqrt{\Delta(B_0 + \Gamma_B)}, \tag{3.4.14}$$

where $\Delta_0 = 2471.386$ MHz and $\mu_{mag} = -36.4$ MHz/mT [147]. To get that value of Δ_0, we have used the known value of the threshold at zero magnetic field [151] and assumed that Eq. (3.4.6) is valid down to that field.

From Eq. (3.4.11), we may fix $\kappa_1 = \alpha_1/(1 + \alpha_{bg}\kappa_1)$ at $a_{bg} = -443\, a_0$ and find the values of all parameters defining the potential at the given position of the Feshbach resonance and with the given value of the background scattering length:

$$\begin{aligned}
\beta &= 0.0202366\, a_0^{-1}, && \text{(3.4.15a)}\\
\alpha_1 &= -\lambda_v = 2.2 \cdot 10^{-3}\, a_0^{-1}, && \text{(3.4.15b)}\\
\alpha_2 &= -0.239343\, a_0^{-1}, && \text{(3.4.15c)}\\
\kappa_1 &= 0.0866\, a_0^{-1}, && \text{(3.4.15d)}\\
\kappa_2 &= \sqrt{\kappa_1^2 + \Delta} = \sqrt{0.0789668 - 0.856899 B}\, a_0^{-1}. && \text{(3.4.15e)}
\end{aligned}$$

The value $\alpha_1 = 2.2 \cdot 10^{-3}\, a_0^{-1}$ was chosen to get a smooth potential V_P without repulsive core. This potential is shown in figure 3.12 and, once again, has a form factor rather independent of the field, except for the threshold.

In figure 3.13, we show that, with these parameters, the Cox-potential scattering length (3.2.35) reproduces the Feshbach-resonance scattering length (3.4.7) with good precision.

The behavior of the phase shifts in the region with the resonant and virtual states is shown in the first row of figure 3.14. A similar discussion to that of figure 3.11 can be made here, except that here the large negative background scattering length results in a large positive slope for the phase shift at the origin.

Exactly at $B_0 = 15.5041$ mT, when the bound state transforms into a virtual state, the phase shift starts from $\pi/2$. The second row of figure 3.14 shows the corresponding behavior of the bound- and virtual-state zeros on the wave-number imaginary axes, confirming the above analysis.

Similarly to the interplay between the ground state and the Feshbach resonance discussed in detail in the previous section, figure 3.15 shows the interplay between the virtual state and the Feshbach resonance, where the corresponding energies $E = k^2$ are plotted as functions of the magnetic field B (as in the previous section, for the resonance we show $\mathrm{Re}\, k^2$ in figure 3.15). The

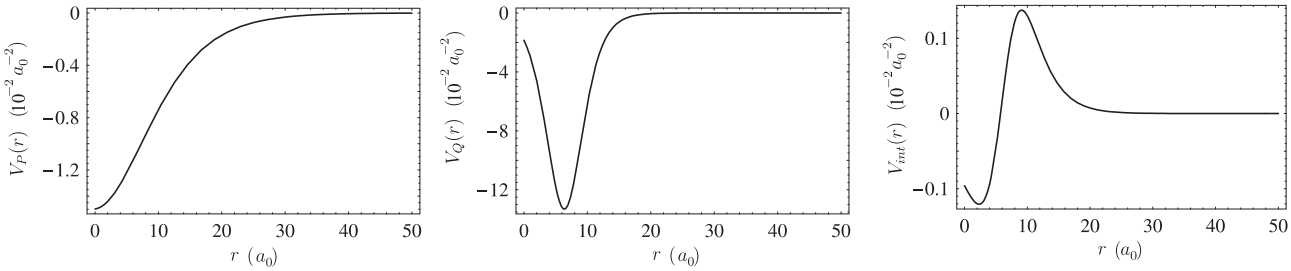

Figure 3.12: The Cox potential describing the Feshbach resonance in ^{85}Rb, defined by parameters (3.4.15), plotted at $B = 14.5$ mT ($\Delta = 0.0590363\,a_0^{-2}$).

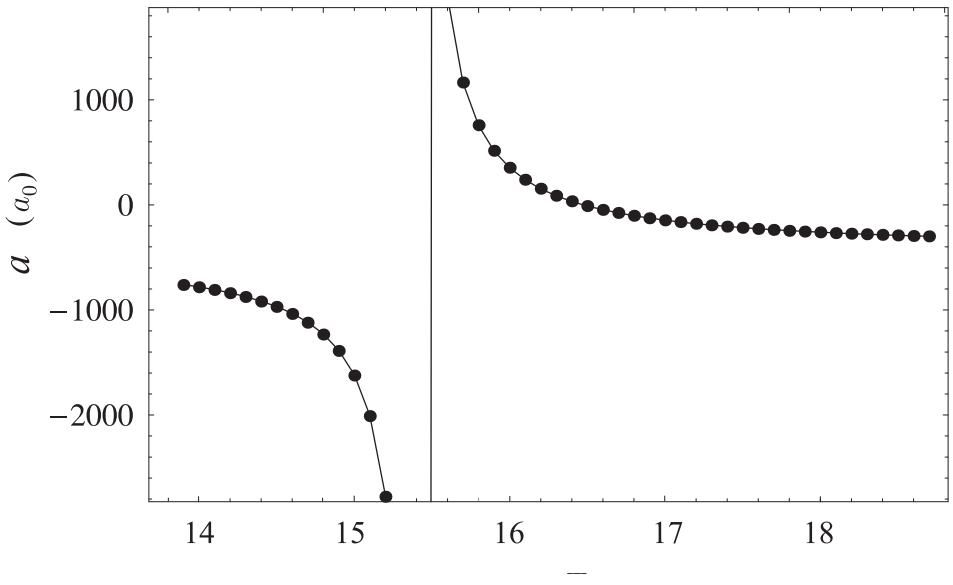

Figure 3.13: Solid line: Feshbach-resonance scattering length (3.4.7) for the ^{85}Rb parameters [147, 151]. Dots: Cox-potential scattering length (3.2.35) for the parameters (3.4.15).

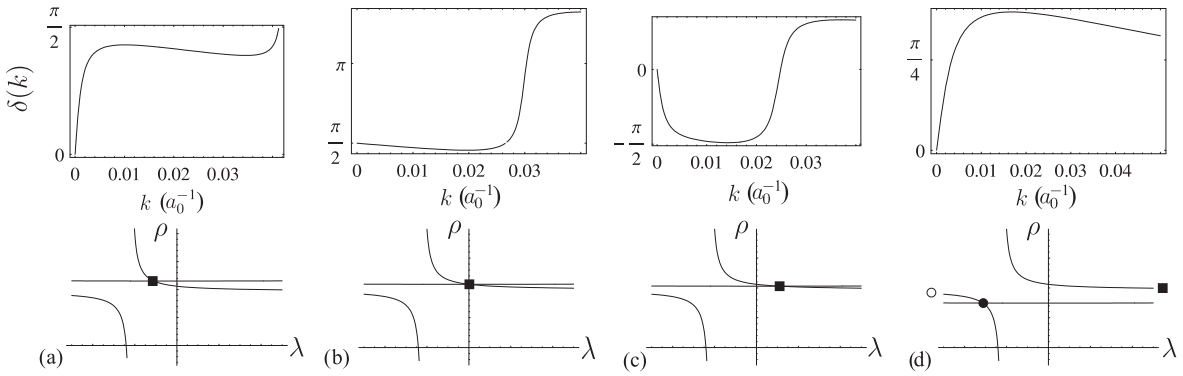

Figure 3.14: Phase shifts and graphical representation of Eqs. (3.2.13) for the Cox potential defined by parameters (3.4.15). The symbols •, ∘ and ■ label positions of the Jost-determinant zeros. The columns correspond to different values of the magnetic field: (a) $B = 14.454$ mT; (b) 15.504 mT; (c) 15.854 mT ; (d) 19.0 mT. In the last column, ∘ and ■correspond to the zeros which are not visible in that scale.

bare bound state of channel Q is represented by the slanted dashed line. The bare virtual state of channel P, which is located at $\lambda_v = -2.2 \cdot 10^{-3}\, a_0^{-1}$, is not shown in figure 3.15. The dressed states are indicated by solid lines. When $B < B_0 = 15.5041$ mT, there exist both a virtual state [■ in figure 3.14 (a)] and a Feshbach resonance, the energies of which tend to the bare-state energies for small B. The virtual state becomes a bound state at $B = B_0$ [see ■ solid line in the inset in figure 3.15 and figure 3.14 (b)]. With increasing B, the real part of the resonance energy decreases and at $B = 16.657$ mT it crosses the threshold. Finally, at $B = 16.9$ mT, the two resonance zeros collapse and produce two virtual states, one of which stabilizes at $\lambda_v = -2.2 \cdot 10^{-3}\, a_0^{-1}$ (• in figure 3.14, the other one has a much larger negative energy and is not represented, as it does not affect the low-energy scattering properties). The behavior of the curves in figure 3.15 is very similar to those of figure 3.9, in particular regarding the transformation of the Feshbach resonance into a virtual state. The only difference between the present case (avoided crossing between a virtual state and a Feshbach resonance) and the previous case (avoided crossing between a bound state and a Feshbach resonance) is that here a virtual state transforms into a bound state before the crossing, while there a virtual state transforms into a bound state after the crossing. Another interesting comparison is between our figure 3.15 and figure 5 of Ref. [147]; it would be instructive to perform a detailed comparison of the two models to explain the differences between these two figures.

As for the interplay with a bound state, figure 3.15 also shows some limit on the range of magnetic field on which our model can be used: since κ_1 is fixed in Eq. (3.4.15d) and the bound-state energy should be larger than $-\kappa_1^2 \approx -0.0075 a_0^{-2}$ (otherwise the potential becomes singular for some value of r), the field should be lower than 24.5 mT.

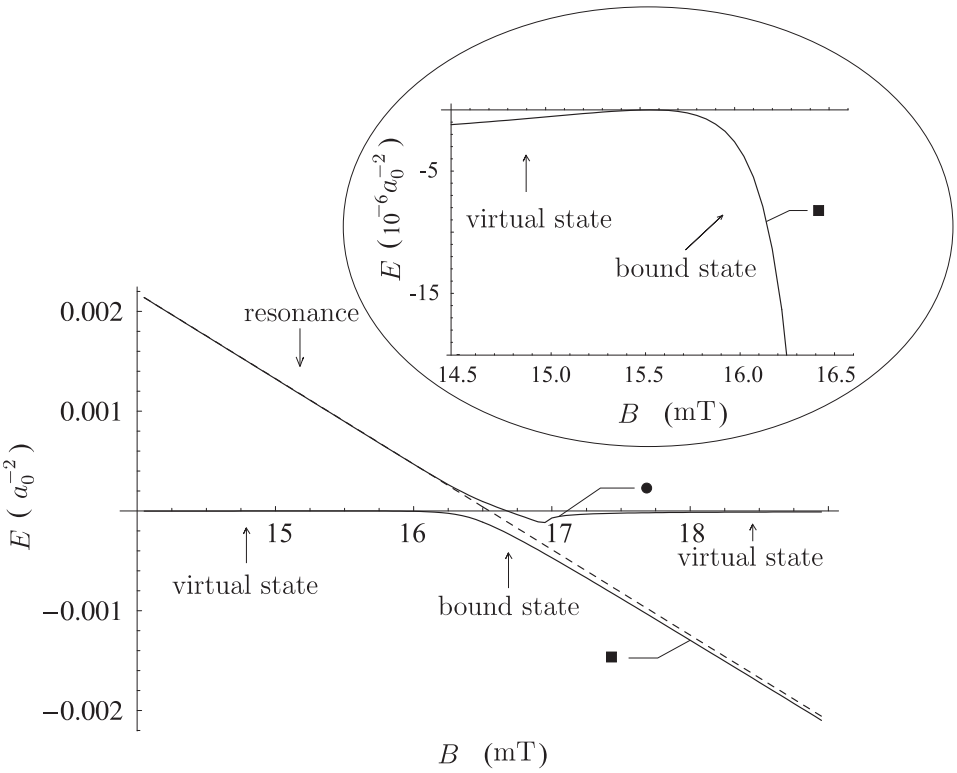

Figure 3.15: B-dependence of the energies of the bare (dashed lines) and dressed (solid lines) states for the Cox potential defined by parameters (3.4.15). The ■solid line corresponds to the transformation from the virtual into the bound state. The • solid line corresponds to the transformation from the resonance into the virtual state.

Chapter 4

SUSY transformations for coupled channel problems with equal thresholds [9, 10]

The exactly solvable two-channel potentials with equal thresholds are of interest due to their possible applications. For instance, following two-channel sectors appear in the neutron-proton scattering: ${}^3S_1 - {}^3D_1, {}^3P_2 - {}^3F_2, \ldots$, [152]. There are two possible strategies to restore the interaction potential from the scattering data. Using some conjectures about the possible shape of the potential one may fit some free parameters to reproduce the scattering data. Obviously, a high accuracy of the fitting procedure requires a sufficiently large number of free parameters. An alternative way is to use the inverse scattering method which allows one to construct the interaction directly from the scattering data. In particular, using the integral transformations (Gelfand-Levitan approach) Newton and Fulton [152] constructed a three-parameter phenomenological neutron-proton potential fitting low-energy ${}^3S_1 - {}^3D_1$ scattering data. It would be interesting to extend this result by enlarging the number of parameters to fit scattering data on a wider energy range; however, the method based on integral transformations is rather involved and therefore quite difficult to generalize. Using the Marchenko equation, the results of Newton and Fulton were nevertheless partially reproduced and improved by von Geramb et al [44]. More precisely, the potential constructed in [44] reproduces the same scattering matrix as the Newton-Fulton potential. Nevertheless, the two potentials differ from each other. Other potentials constructed by Marchenko inversion, which are compatible with modern scattering data, contain a large number of parameters.

Our hope that the SUSY technique may be efficient for the multichannel Schrödinger equation is based on the well known equivalence between SUSY transformations and the integral transformations of the inverse scattering method for single-channel problems [81, 85, 153, 154]. Due to this equivalence, one can use chains of first-order SUSY operators for constructing a Hamiltonian with given scattering properties [83,84]. In particular, we believe (and argue why in the present chapter) that the inverse scattering problem may be treated by the conservative SUSY transformations only. As in the case of different thresholds the initial potential is restricted to be the zero potential for simplicity.

Zero potential is, of course, decoupled, therefore coupling should follow from the inversion procedure. In the current chapter, with the equal threshold inverse problem in mind, we firstly concentrate on the necessary ingredients for a single conservative SUSY transformation to generate coupled scattering matrices, starting from a decoupled potential. We will show that, such a transformation introduces bound and virtual states at the same energy and we calculate their degeneracy. Next, we discuss the possibility to get a trivially or non trivially coupled scattering matrix when both the potential and Jost matrix are non trivially coupled. We will be able to answer the following questions: does a non trivial coupling of the potential imply a non trivial coupling of the scattering matrix? Does a non trivial coupling of the Jost matrix imply a non trivial coupling of the scattering matrix?

4.1 First order SUSY transformations

4.1.1 Coupling SUSY transformation

In the most general case the transformation function may be expressed in terms of the Jost solutions as follows

$$u_c(r) = f_d(-i\kappa, r)C + f_d(i\kappa, r)D\,, \tag{4.1.1}$$

where the real constant matrices C and D should satisfy to equation (1.2.25). Their canonic form is given in (1.2.26). Here and in what follows subscripts d and c stand for quantities related with diagonal (uncoupled) and non-diagonal (coupled) matrices, respectively.

We need the asymptotic behaviour of the superpotential $w_{c\infty} := \lim_{r\to\infty} w_c(r)$ to find the transformed Jost solution and, hence, the Jost and scattering matrices. As it was shown in [49] for different thresholds, this behaviour of the superpotential depends crucially on matrix C. Below we shortly discuss the method developed in [49] while making necessary changes to adjust it for the case of equal thresholds.

The asymptotic matrix $w_{c\infty}$ is determined by the behaviour of transformation function (4.1.1) at large distances

$$u_c(r\to\infty) \to A \begin{pmatrix} I_M e^{\kappa r} & 0 \\ 0 & I_{N-M} e^{-\kappa r} \end{pmatrix}, \qquad A = \begin{pmatrix} I_M & -Q^T \\ Q & I_{N-M} \end{pmatrix}. \tag{4.1.2}$$

From (1.2.23) and (4.1.2) we obtain

$$w_{c\infty} = \kappa A \begin{pmatrix} I_M & 0 \\ 0 & -I_{N-M} \end{pmatrix} A^{-1} \tag{4.1.3}$$

with

$$A^{-1} = A^T \begin{pmatrix} I_M + Q^T Q & 0 \\ 0 & I_{N-M} + QQ^T \end{pmatrix}^{-1}. \tag{4.1.4}$$

Comparing this result with that obtained in [49], we conclude that the main difference between equal and different thresholds is the non-diagonal character of the superpotential at infinity. Note that superpotential $w_{c\infty}$ has a richer structure than that previously reported by Amado et al [87]. Their result corresponds to the choice $M = 1$ when $w_{c\infty}$ is expressed in terms of a single $(N-1)$-vector $Q = (q_1, \ldots, q_{N-1})^T$.

Once $w_{c\infty}$ is determined one can calculate the Jost solution $f_c(k, r)$ and the Jost matrix $F_c(k)$ for the transformed potential V_c using (1.2.27) and (1.1.28), respectively.

In order to find the Jost matrix, we first consider the behaviour of the superpotential in a vicinity of $r = 0$ which depends on the character of the transformation solution (4.1.1). Below we will assume that there is no bound state at the factorization energy, $\det F_d(i\kappa) \neq 0$, and each column of the transformation solution is singular at the origin. Using the property

$$f_d(-k, r\to 0) = f_d(k, r\to 0)F_d(-k)F_d^{-1}(k) + \mathrm{o}(r^\nu) \tag{4.1.5}$$

which follows from (1.1.28) and the invertibility of $F_d(i\kappa)$, one finds the behaviour of the transformation solution at the origin,

$$u_c(r\to 0) = f_d(i\kappa, r)[F_d(-i\kappa)F_d^{-1}(i\kappa)C + D] + \mathrm{o}(r^\nu)\,. \tag{4.1.6}$$

We assume

$$\det\left(F_d(-i\kappa)F_d^{-1}(i\kappa)C+D\right)\neq 0\,, \tag{4.1.7}$$

which can always be provided by a proper choice of matrices C and D. The leading term of the superpotential at $r\to 0$ reads

$$w_c(r\to 0)=-r^{-1}\nu+\mathrm{o}(1)\,,\qquad \nu_j>0\,, \tag{4.1.8}$$

where we used the Laurent series for the Jost solution

$$f(k,r)=r^{-\nu}(2\nu-1)!!F^T(k)+r^{-\nu+1}b_1(k)+\mathrm{o}(r^{-\nu+1})\,. \tag{4.1.9}$$

It follows from (1.1.23) and the Schrödinger equation that $b_1(k)=0$. We note the diagonal character of superpotential (4.1.8) at the origin. The singularity at the origin of the transformed potential,

$$V_c(r\to 0)\to r^{-2}\tilde\nu(\tilde\nu+1)=(V_d-2w_c')|_{r\to 0}=r^{-2}\nu(\nu-1), \tag{4.1.10}$$

decreases by one unit, $\nu\to\tilde\nu=\nu-1$. Hence we can apply our coupling transformation to potentials for which matrix ν is positive definite, $\nu>0$, a property we will assume to hold throughout the paper.

The Jost matrix can be obtained from expression (1.1.27) of the regular solution $\varphi_c(k,r)$ corresponding to V_c. The regular solution of the transformed potential $\varphi_c(k,r)$ is determined by (1.1.25) with the singularity parameter $\tilde\nu$. To derive it, we act on both sides of expression (1.1.27) of the regular solution $\varphi_d(k,r)$ for potential V_d with the transformation operator L_c. From (1.1.25), (1.2.20) and (4.1.8), it follows that

$$L_c\varphi_d(k,r)=-\varphi_c(k,r). \tag{4.1.11}$$

Taking into account (1.2.27), we rewrite (4.1.11) as

$$\varphi_c(k,r)=-\frac{i}{2k}\left[f_c(-k,r)(w_{c\infty}+ikI_N)F_d(k)-f_c(k,r)(w_{c\infty}-ikI_N)F_d(-k)\right]\,. \tag{4.1.12}$$

Comparing (1.1.27) and (4.1.12) we find a relation between the initial and transformed Jost matrices

$$F_c(k)=-(ikI_N+w_{c\infty})F_d(k)\,. \tag{4.1.13}$$

For $M=0$ and $M=N$, Q is absent and $A=I_N$ in (4.1.3). When $M=N$, the superpotential at infinity (4.1.3) becomes proportional to the identity matrix, $w_{c\infty}=\kappa I_N$. The transformed Jost matrix (4.1.13) becomes diagonal. Similarly, the case $M=0$ leads to $w_{c\infty}=-\kappa I_N$. From here we draw an important conclusion. The necessary (but not sufficient) condition for a non-trivial coupling in the Jost and hence scattering matrices is $0<M<N$. This will be assumed in the following.

As already mentioned, a non-trivial coupling in the Jost matrix requires not only a non-diagonal Jost matrix, but also the impossibility to diagonalize this matrix by a k-independent transformation. It is clear that matrix $ikI_N+w_{c\infty}$ from (4.1.13) can be diagonalized by a k-independent transformation. When F_d is not proportional to the identity matrix, channels in $F_c(k)$ are coupled in a non-trivial way. Nevertheless, this property does not guarantee the non-triviality of the S-matrix. As it follows from definition (1.1.33), the S-matrix will be trivially coupled when the product $F_d(-k)F_d^{-1}(k)$ is proportional to the identity matrix, i.e. when

$$F_{d;j}(k)=|F_{d;j}(k)|\mathrm{e}^{-i\delta(k)}\;\Rightarrow\;S_{d;j}(k)=(-1)^{l_j}\mathrm{e}^{2i\delta(k)}\,,\qquad j=1,\dots,N\,. \tag{4.1.14}$$

In particular, if all single-channel potentials have the same S-matrix, i.e. if they are phase equivalent [94] or isophase [96], the S-matrix resulting from a SUSY transformation keeps being trivially coupled. When the initial S-matrix is not proportional to the identity matrix, one may expect non-trivially coupled channels.

The analytic expression (4.1.13) for the Jost matrix allows us to study the spectral properties of the transformed potential (1.2.21) [7]. The positions of the bound/virtual states and resonances are defined as the solutions of $\det F_c(k) = 0$. As it follows from (4.1.13) and (4.1.3), the Jost-matrix determinant is given by

$$\det F_c(k) = (-1)^N (ik+\kappa)^M (ik-\kappa)^{N-M} \det F_d(k) \tag{4.1.15}$$

since $w_{c\infty}$ has the M fold degenerate eigenvalue κ and the $N-M$ fold degenerate eigenvalue $-\kappa$. Therefore, if $\det F_d(k)$ has no pole at $k = \pm i\kappa$ (this property is assumed to hold in the rest of the paper), the SUSY transformation leads to a new M fold degenerate bound state with $k_b = i\kappa$, $E_b = -\kappa^2$ and an $N-M$ fold degenerate virtual state with $k_v = -i\kappa$, $E_v = -\kappa^2$.

Now we continue to compare our method with the approach developed by Amado et al [87]. For that, we calculate the asymptotic behaviour of matrix $\Phi(r) = [u_c(r)^\dagger]^{-1}$, which upon using (4.1.2) reads

$$\Phi(r\to\infty) \to \left(A^T\right)^{-1} \begin{pmatrix} I_M e^{-\kappa r} & 0 \\ 0 & I_{N-M} e^{\kappa r} \end{pmatrix}. \tag{4.1.16}$$

The M first columns of $\Phi(r)$ are vectors decreasing at infinity. According to (4.1.6) and (4.1.9), $\Phi(r)$ is a regular solution, $\Phi(0) = 0$. Therefore these vectors correspond to the bound state wave functions of the coupled system appeared after the SUSY transformation. This confirms that the energy level of this bound state is M fold degenerate. All the other columns in $\Phi(r)$ correspond to virtual states. For the particular case $M = 1$ this asymptotic form just corresponds to the transformation function used by the authors of [87] for decoupling a coupled problem. We thus conclude that their transformation corresponds to a particular case of our transformation when realized in the opposite direction.

Another useful remark is that although the superpotential $w_c(r)$ depends on parameters X_0, the Jost matrix $F_c(k)$ and, hence, the S-matrix are X_0-independent. This means that the superpotential $w_c(r)$ leads to a family of potentials, parameterized by the entries of X_0, having the same scattering properties.

Below we concentrate on the two-channel case with equal thresholds and arbitrary partial waves. The coupling SUSY transformation produces in this case one bound state and one virtual state. First we will analyze the long range behaviour of the transformed potential.

4.1.2 Long range behaviour of the transformed potential

In the two-channel case, according to (1.1.22), the initial diagonal potential has the following long-range behaviour

$$V_d(r\to\infty) \to \frac{1}{r^2} \begin{pmatrix} l_1(l_1+1) & 0 \\ 0 & l_2(l_2+1) \end{pmatrix}. \tag{4.1.17}$$

The Jost solution at large distances is expressed in terms of third kind Bessel functions $H_l^{(1)}(z)$, also called first Hankel functions (see [140] for a definition)

$$f_d(k, r\to\infty) = \mathrm{diag}\left[h_{l_1}(kr), h_{l_2}(kr)\right], \qquad h_l(z) = i^{l+1}(\pi z/2)^{\frac{1}{2}} H_l^{(1)}(z). \tag{4.1.18}$$

The recurrence relations for $h_l(z)$ and its asymptotic behaviour

$$h_l(kr) = e^{ikr}\left(1 + \frac{il(l+1)}{2kr} + \mathrm{o}(r^{-1})\right), \tag{4.1.19}$$

follow from those for $H_l^{(1)}(z)$ [140].

For the coupling transformation, according to our previous discussion, we choose transformation function (4.1.1) with matrices

$$C = \begin{pmatrix} 1 & 0 \\ q & 0 \end{pmatrix}, \qquad D = \begin{pmatrix} x & -q \\ 0 & 1 \end{pmatrix}, \tag{4.1.20}$$

which contain only two independent parameters x and q. The restriction on the parameters

$$x + F_{d,1}(-i\kappa)F_{d;1}^{-1}(i\kappa) - q^2 F_{d,2}(-i\kappa)F_{d;2}^{-1}(i\kappa) \neq 0 \tag{4.1.21}$$

follows from (4.1.7). Transformation solution (4.1.1) reads

$$u_c(r) = \begin{pmatrix} f_{d;1}(-i\kappa r) + x f_{d;1}(i\kappa r) & -q f_{d;1}(i\kappa r) \\ q f_{d;2}(-i\kappa r) & f_{d;2}(i\kappa r) \end{pmatrix}. \tag{4.1.22}$$

Let us consider the first two terms in the asymptotic behaviour of the superpotential (1.2.23), $w_c(r \to \infty) = w_{c\infty} + w_{-1}r^{-1} + \mathrm{o}(r^{-1})$. The first term $w_{c\infty}$ has been calculated for an arbitrary number of channels in Section 4.1.1. Thus from (4.1.3) we obtain

$$w_{c\infty} = \frac{\kappa}{1+q^2}\begin{pmatrix} 1-q^2 & 2q \\ 2q & q^2-1 \end{pmatrix}. \tag{4.1.23}$$

Another parametrization for $w_{c\infty}$ is useful,

$$w_{c\infty} = \kappa\begin{pmatrix} \cos\alpha & \sin\alpha \\ \sin\alpha & -\cos\alpha \end{pmatrix}, \qquad q = \tan\frac{\alpha}{2}. \tag{4.1.24}$$

Note that a non-zero value of w_{-1} will lead to a modification of the long range behaviour of potential (1.2.21) with $w_c'(r \to \infty) = -w_{-1}r^{-2} + \mathrm{o}(r^{-2})$.

In order to establish the asymptotic behaviour of the potential $V_c(r) = V_d(r) - 2w_c'(r)$, we replace $f_{d,j}(\pm i\kappa r)$ in (4.1.22) by its asymptotic form given in (4.1.18) and neglect in (1.2.21) and (1.2.23) all exponentially decreasing terms such as $h_{l_1}(i\kappa r)h_{l_2}(i\kappa r)$. Taking into account

$$h_{l_1}(i\kappa r)h_{l_2}(-i\kappa r) = 1 + \frac{1}{2\kappa r}\left[l_1(l_1+1) - l_2(l_2+1)\right] + \mathrm{o}(r^{-1}), \quad r \to \infty, \tag{4.1.25}$$

combining (1.2.21) with (4.1.17) and using parametrization (4.1.24), one finally gets

$$\begin{aligned} V_c(r \to \infty) = {} & \frac{1}{r^2}\begin{pmatrix} l_1(l_1+1) & 0 \\ 0 & l_2(l_2+1) \end{pmatrix} \\ & + \frac{[l_2(l_2+1) - l_1(l_1+1)]\sin\alpha}{r^2}\begin{pmatrix} \sin\alpha & -\cos\alpha \\ -\cos\alpha & -\sin\alpha \end{pmatrix}. \end{aligned} \tag{4.1.26}$$

A similar asymptotic behaviour of the matrix potential is obtained from the Gelfand-Levitan equation in [43].

From (4.1.26) we conclude that, for $l_1 \neq l_2$, the transformed potential has a non-zero long range coupling, $V_{c;12} \neq 0$. Moreover, it is impossible to associate diagonal entries of V_c given in (4.1.26)

with usual centrifugal terms. The only way to avoid this inconvenience is to fix $\alpha = \pm\pi/2$ (or equivalently $q = \pm 1$), which leads to a physically reasonable long range behaviour

$$V_c(r \to \infty, q = 1) = \frac{1}{r^2} \begin{pmatrix} l_2(l_2+1) & 0 \\ 0 & l_1(l_1+1) \end{pmatrix} . \tag{4.1.27}$$

Having compared (4.1.17) and (4.1.27) we find the modification of the corresponding angular momentum quantum numbers under the SUSY transformation $l = \mathrm{diag}(l_1, l_2) \to \tilde{l} = \mathrm{diag}(l_2, l_1)$. For short, this unusual property of the SUSY transformation will be called the exchange of the channels angular momenta. Summarizing, we get an additional constraint $q = 1$ (the dual case $q = -1$ leads to the same transformed potential except $V_{c;12} \to -V_{c;12}$) to consider only physically reasonable potentials in the case $l_2 \neq l_1$.

4.1.3 Transformed Jost and scattering matrices, eigenphase shifts and mixing angle

In the two-channels case, introducing $w_{c\infty}$ as given in (4.1.24) into (4.1.13) provides an explicit relation between the transformed Jost matrix $F_c(k)$ and the initial diagonal Jost matrix $F_d(k)$,

$$F_c(k) = -\begin{pmatrix} ik + \kappa\cos\alpha & \kappa\sin\alpha \\ \kappa\sin\alpha & ik - \kappa\cos\alpha \end{pmatrix} F_d(k) . \tag{4.1.28}$$

From (4.1.15), we obtain $\det F_c = (k^2 + \kappa^2)\det F_d$. The coupling transformation produces one bound state and one virtual state, in agreement with the general properties of the transformed Jost matrix analyzed in Section 4.1.1.

Once the transformed Jost matrix $F_c(k)$ (4.1.28) is found, the S-matrix may be obtained according to its definition (1.1.33), where we have to take into account the change of attribution of the angular momenta $l \to \tilde{l}$ by the coupling transformation,

$$S_c(k) = e^{i\tilde{l}\frac{\pi}{2}}(-ikI_2 + w_{c\infty})(-1)^l S_d(k)(ikI_2 + w_{c\infty})^{-1} e^{i\tilde{l}\frac{\pi}{2}} . \tag{4.1.29}$$

The diagonal matrix

$$S_d(k) = \mathrm{diag}(e^{2i\delta_{d;1}(k)}, e^{2i\delta_{d;2}(k)}) \tag{4.1.30}$$

is obtained from the diagonal Jost matrix $F_d(k)$ before the transformation. One can see that for the particular case of identical partial waves, $l \propto I_2$, our result (4.1.29) reproduces the corresponding relation (17a) from [87]. For different partial waves however, the modification of the angular momenta leads to the appearance of additional phase factors $e^{i\tilde{l}\frac{\pi}{2}}$ and $(-1)^l$.

Let us now find the transformed eigenphase shifts $\delta_{c;j}(k)$, $j = 1, 2$, and the mixing angle $\epsilon(k)$ (see (1.1.34), (1.1.35) and (1.1.36)). One can distinguish three essentially different cases:
(a) the difference between the angular momenta is odd, $l_2 = (l_1 + 1) \,(\mathrm{mod}\, 2)$;
(b) the difference between the angular momenta is even, $l_2 \neq l_1$, $l_2 = l_1 \,(\mathrm{mod}\, 2)$;
(c) the angular momenta coincide, $l_2 = l_1$.

Note that case **(a)** does not correspond to any reduction of the rotationally invariant three-dimensional scattering problem, since in this case any nontrivial coupling means a parity breakdown (see e.g. [22]). For the sake of completeness we will analyze this case also although the corresponding system of coupled equations has no direct relation to a scattering problem. Moreover, we will use the usual scattering theory terminology in this case also, although from the point of view of a

three-dimensional scattering it bears only a formal character. In cases **(a)** and **(b)**, we should put $\alpha = \pi/2$, which is not necessary in the third case (see (4.1.26)).

Definition (4.1.30) allows writing

$$S_{d;1}(k) + S_{d;2}(k) \equiv e^{2i\delta_{d;1}(k)} + e^{2i\delta_{d;2}(k)} = 2\mathrm{e}^{i(\delta_{d;1}+\delta_{d;2})}\cos\Delta\,, \qquad \Delta = \delta_{d;2} - \delta_{d;1}\,, \tag{4.1.31}$$

and (1.1.36) leads to expressions for the mixing angle in the three cases as

$$(\mathbf{a}):\ \tan 2\epsilon(k) = \frac{2(-1)^{(l_2-l_1-1)/2}\kappa\sin\alpha\,(\kappa\cos\alpha\cos\Delta - k\sin\Delta)}{2\kappa k\cos\alpha\cos\Delta - (k^2-\kappa^2)\sin\Delta}\,, \tag{4.1.32}$$

and

$$(\mathbf{b}),(\mathbf{c}):\ \tan 2\epsilon(k) = \frac{2(-1)^{(l_2-l_1)/2}\kappa\sin\alpha\,(\kappa\cos\alpha\sin\Delta + k\cos\Delta)}{2\kappa k\cos\alpha\cos\Delta - \sin\Delta\,(k^2-\kappa^2\cos 2\alpha)}\,. \tag{4.1.33}$$

Since $q = 1$ and $\alpha = \pi/2$ in cases **(a)** and **(b)**, expressions (4.1.32) and (4.1.33) are simplified to

$$(\mathbf{a}):\ \epsilon(k) = (-1)^{(l_2-l_1+1)/2}\arctan\frac{k}{\kappa}\,, \tag{4.1.34}$$

$$(\mathbf{b}):\ \tan 2\epsilon(k) = (-1)^{(l_2-l_1+2)/2}\frac{2\kappa k}{k^2+\kappa^2}\cot\Delta. \tag{4.1.35}$$

We will assume below that the scattering matrix of the transformed potential satisfies the effective range expansion (see e.g. [155]), which implies

$$\begin{aligned}\cot\delta_{c;1,2}(k\to 0) &= a_{1,2}k^{-(2l_{1,2}+1)} + \mathrm{o}\left(k^{-(2l_{1,2}+1)}\right),\\ \epsilon(k\to 0) &= \epsilon_0 k^{|l_2-l_1|} + \mathrm{o}\left(k^{|l_2-l_1|}\right).\end{aligned} \tag{4.1.36}$$

Since there are rather simple analytical expressions for the mixing angle, we will analyze restrictions on parameters of the SUSY transformation which follow from the second equation in (4.1.36).

In case **(a)**, (4.1.34) satisfies the effective range expansion (4.1.36) when $|l_2-l_1| = 1$ and violates (4.1.36) when $|l_2 - l_1| > 1$. The important property of the coupling transformation in case **(a)** is that the transformed phase shifts coincide with the initial phase shifts, i.e.,

$$R_c^T(k)S_c(k)R_c(k) = \begin{pmatrix} e^{2i\delta_{d;2}(k)} & 0\\ 0 & e^{2i\delta_{d;1}(k)}\end{pmatrix}. \tag{4.1.37}$$

Therefore, one may separately fit the phase shifts for the l_1 and l_2 waves before the coupling transformation.

In case **(b)**, the effective range expansion for mixing angle (4.1.35) leads to the restriction $\cot\Delta = 0$ or $\delta_{d,2}(0) - \delta_{d,1}(0) = (n+1/2)\pi$. According to the Levinson theorem (see e.g. [23]) this means that the potential V_d supports a bound state at zero energy.

Finally, in case **(c)** there is no any additional constraint since $\epsilon(k\to 0) = \mathrm{const}$.

Having established properties of the transformed phase shifts and the mixing angle, we will consider in the next section some schematic examples of scattering for the $s-s$, $s-p$ and $s-d$ coupled channels.

4.2 Examples of exactly solvable two-channels potentials with equal thresholds

To illustrate the difference between couplings in potential, Jost and scattering matrices, we construct in this section nontrivially coupled potentials having trivially coupled S-matrices and both trivially and non-trivially coupled Jost matrices. After that we exemplify SUSY transformations leading to non-trivially coupled S-matrices.

4.2.1 Coupled potentials with uncoupled S-matrices

Let us consider the 1-channel potential expressed in terms of a Wronskian as

$$V(r;\beta) = -2\frac{d}{dr^2}\ln W\left[\sinh(\kappa_0 r), \sinh(\kappa_2 r), \exp(\kappa_1 r) + \beta\exp(-\kappa_1 r)\right], \qquad \kappa_0 < \kappa_1 < \kappa_2\,, \qquad \beta < -1\,, \tag{4.2.1}$$

which can easily be obtained from the zero potential with the help of the usual (i.e. 1-channel) SUSY transformations. This potential has one bound state at energy $E = -\kappa_1^2$ and its Jost function has the form

$$F(k) = i(k - i\kappa_1)\left[(k + i\kappa_0)(k + i\kappa_2)\right]^{-1}\,. \tag{4.2.2}$$

All potentials from the β-family (4.2.1) have the same Jost and scattering matrices. Therefore, we can construct a diagonal potential $V_d(r) = \mathrm{diag}\left[V(r;\beta_1), V(r;\beta_2)\right]$ with a two fold degenerate bound state at energy $E = -\kappa_1^2$. Both its Jost and scattering matrices are proportional to the identity matrix

$$F_d(k) = F(k)I_2\,, \qquad S_d(k) = F(-k)F^{-1}(k)I_2\,. \tag{4.2.3}$$

As a result, the Jost matrix (4.1.13) obtained after the coupling transformation can be diagonalized by the same k-independent transformation as the superpotential $w_{c\infty}$. This just corresponds to a trivial coupling in both Jost and scattering matrices.

For the coupling transformation we choose the transformation function (4.1.22) where Jost solutions $f_d(i\kappa, r)$ of the Schrödinger equation (4.1.9) with potential V_d are used. To avoid a singularity at finite distance in the transformed potential we impose the restriction $\kappa > \kappa_2 > \kappa_1$. Such a transformed potential is shown in figure 4.1(a). The function $\sigma(r) = V_{c;12}/(V_{c;22} - V_{c;11})$ demonstrates the non-triviality of the transformed potential matrix. If σ is a constant, the potential matrix is globally diagonalizable. As we see from figure 4.1 (b), a non constant σ means that the transformed potential has a non-trivial coupling. At the same time, the mixing angle (4.1.33) in the scattering matrix is just a constant for $\Delta = 0$

$$\epsilon(k) = \frac{\alpha}{2}\,. \tag{4.2.4}$$

The phase shifts for this potential read

$$\delta_{c;1}(k) = 2\pi - \sum_{j=0}^{2}\arctan\frac{k}{\kappa_j} + \arctan\frac{k}{\kappa}\,, \tag{4.2.5}$$

$$\delta_{c;2}(k) = \pi - \sum_{j=0}^{2}\arctan\frac{k}{\kappa_j} - \arctan\frac{k}{\kappa}\,. \tag{4.2.6}$$

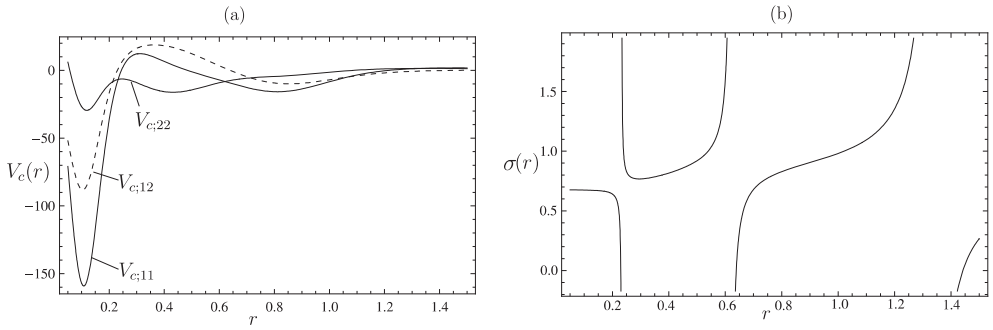

Figure 4.1: (a) Exactly solvable potential $\bar{V}_c = V_c$ obtained from two uncoupled potentials (4.2.1) ($\beta_1 = -2\,, \beta_2 = -1.5\,, \kappa_0 = 1\,, \kappa_1 = 2.5\,, \kappa_2 = 3.5$) by the coupling transformation with parameters $q = 0.5$, $\kappa = 6$, $x = 25$. (b) Ratio $\sigma(r) = V_{c;12}(r)/\left(V_{c;22}(r) - V_{c;11}(r)\right)$.

From here one can see that after the coupling transformation the additional bound state increases the value of the phase shifts at zero energy in agreement with the Levinson theorem.

To show the restrictive character of the requirement for the S matrix to be non-trivially coupled, we construct below a potential with non-trivially coupled potential and Jost matrices but a trivially coupled S-matrix. This possibility is based on the fact that in the single-channel case two different Jost functions may correspond to the same scattering matrix [95, 96]. In this case, the two Jost functions differ from each other by a real factor for real k's (see (4.1.14)). Therefore if we apply our coupling transformation to the following uncoupled system

$$V_d(r) = \mathrm{diag}\left[V_1(r), V_2(r)\right], \quad F_d(k) = \mathrm{diag}\left[F_1(k), F_2(k)\right], \quad S_d(k) = S(k)I_2\,, \tag{4.2.7}$$

from (4.2.7), (1.2.21), (4.1.13) and (4.1.29) we can see that the transformed potential and Jost matrices cannot be diagonalized by a constant rotation whereas the scattering matrix becomes diagonal after the same k-independent rotation which diagonalizes $w_{c\infty}$.

An example in which we get a non-diagonal Jost matrix and a trivially coupled S-matrix after applying the coupling transformation follows from (4.2.7) where we choose

$$F_d(k) = \mathrm{diag}\left[\frac{i(k-i\kappa_0)}{(k+i\kappa_1)(k+i\kappa_2)}, \frac{-i}{(k+i\kappa_0)(k+i\kappa_1)(k+i\kappa_2)}\right], \tag{4.2.8}$$

$$S_d(k) = \frac{(k+i\kappa_0)(k+i\kappa_1)(k+i\kappa_2)}{(k-i\kappa_0)(k-i\kappa_1)(k-i\kappa_2)} I_2\,. \tag{4.2.9}$$

Here κ_0, κ_1 and κ_2 are arbitrary real parameters. Matrix ν for the corresponding potential

$$V_d(r) = \mathrm{diag}\left[V(r, \beta < -1), V(r, \beta = -1)\right]\,, \tag{4.2.10}$$

is $\nu = \mathrm{diag}(1, 3)$ meaning that $\nu - 1 > 0$ and we can apply the coupling transformation. Here the non-trivially coupled transformed Jost matrix (4.1.13) with F_d as given in (4.2.8) leads to the following trivially coupled S-matrix

$$S_c(k) = (ikI_2 - w_{c\infty})^2 \frac{(k+i\kappa_0)(k+i\kappa_1)(k+i\kappa_2)}{(k-i\kappa_0)(k-i\kappa_1)(k-i\kappa_2)(k^2+\kappa^2)}\,. \tag{4.2.11}$$

The corresponding phase shifts are given by (4.2.5) where $\delta_{c;2} \to \delta_{c;2} - \pi$ and the mixing angle is given by (4.2.4).

4.2.2 Coupled $s-s$ partial waves

Using our general scheme described in section 4.1.3, we can study the behaviour of the phase shifts for the $s-s$ coupled potential. Since the angular momenta in both channels coincide, we have here the case **(c)** discussed above. Parameter q is not fixed from the long-range behaviour of the potential and the mixing angle is given by (4.1.33). The analysis of this expression is based on the low-energy behaviour of the phase shifts $\delta_{d;1,2}$ before the coupling transformation

$$e^{2i\delta_{d;1,2}} = 1 - 2ia_{1,2}k + \mathrm{o}(k)\,, \tag{4.2.12}$$

where a_1 and a_2 are the scattering lengths for each channel. Combining (4.1.33) and (4.2.12) we get

$$\tan 2\epsilon(k\to 0) = \frac{2(1+(a_1-a_2)\kappa\cos\alpha)\sin\alpha}{2\cos\alpha+(a_1-a_2)\kappa\cos 2\alpha} + \mathrm{o}(k)\,. \tag{4.2.13}$$

The expansion of the eigenvalues of the transformed scattering matrix at low energies reads

$$e^{2i\delta_{c;1,2}} = 1 - ik\left[(a_1+a_2) \pm \sqrt{(a_2-a_1)^2 + 4\left(1/\kappa - (a_2-a_1)\cos\alpha\right)/\kappa}\right] + \mathrm{o}(k)\,. \tag{4.2.14}$$

An important result from the point of view of inverse scattering corresponds to a coupling vanishing at low energies, i.e. when $\epsilon(0)=0$. This leads to an additional link between the parameters,

$$\cos\alpha = \frac{1}{(a_2-a_1)\kappa}\,, \tag{4.2.15}$$

where we have used (4.2.13) and (4.1.36). Hence (4.2.14) simplifies into

$$e^{2i\delta_{c;1,2}} = 1 - 2ia_{2,1}k + \mathrm{o}(k)\,. \tag{4.2.16}$$

In this case, the scattering lengths for the transformed potential coincide with the initial scattering lengths a_1 and a_2. This property allows us to fit low energy scattering data for uncoupled channels thus simplifying essentially the inverse problem. Let us illustrate this property in a schematic example.

We start from the zero potential with a transformation which introduces poles at the origin, $\nu = \mathrm{diag}(0,0) \to \nu = \mathrm{diag}(1,1)$. In each channel we realize the usual (i.e. 1-channel) SUSY transformation with transformation functions $\mathrm{sh}(\kappa_1 r)$ and $\mathrm{sh}(\kappa_2 r)$. This leads to the uncoupled superpotential

$$w_d(r) = \mathrm{diag}\left[\kappa_1\coth(\kappa_1 r), \kappa_2\coth(\kappa_2 r)\right] \tag{4.2.17}$$

and the potential (see (1.2.21))

$$V_d(r) = 2\mathrm{diag}\left[\kappa_1^2\mathrm{cosech}^2(\kappa_1 r), \kappa_2^2\mathrm{cosech}^2(\kappa_2 r)\right]\,, \tag{4.2.18}$$

with the Jost solution

$$f_d(k,r) = e^{ikr}\begin{pmatrix} k+i\kappa_1\coth(\kappa_1 r) & 0 \\ 0 & k+i\kappa_2\coth(\kappa_2 r)\end{pmatrix}\begin{pmatrix} k+i\kappa_1 & 0 \\ 0 & k+i\kappa_2\end{pmatrix}^{-1} \tag{4.2.19}$$

and the Jost matrix

$$F_d(k) = (w_{d\infty} - ikI_2)^{-1}\,, \quad w_{d\infty} = \lim_{r\to\infty} w_d(r) = \mathrm{diag}\,(\kappa_1,\kappa_2)\,. \tag{4.2.20}$$

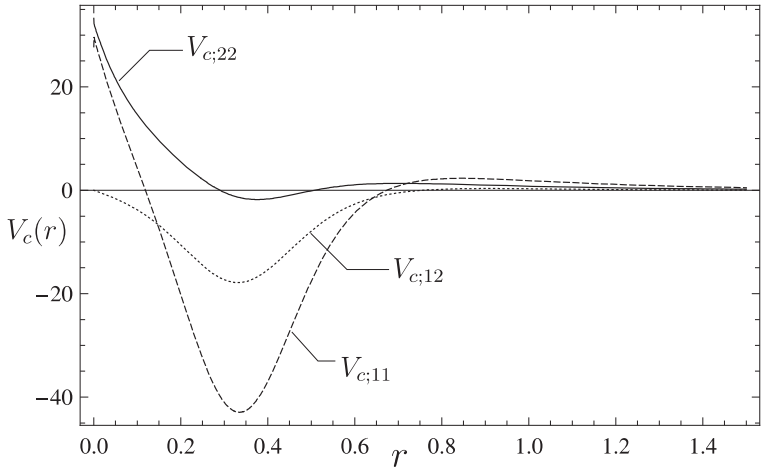

Figure 4.2: Exactly solvable $s-s$ potential $\bar{V}_c = V_c$ with parameters $\kappa_1 = 1.5$, $\kappa_2 = 1$, $q = 0.4$, $\kappa = 4.14286$, $x = 15$.

As coupling transformation we choose transformation function (4.1.1) with matrices C and D given by (4.1.20). The explicit expression for $u_c(r)$ coincides with (4.1.22) where

$$f_{d;1}(i\kappa, r) = \frac{\kappa + \kappa_1 \coth(\kappa_1 r)}{\kappa + \kappa_1}\, e^{-\kappa r}\,, \qquad f_{d;2}(i\kappa, r) = \frac{\kappa + \kappa_2 \coth(\kappa_2 r)}{\kappa + \kappa_2}\, e^{-\kappa r}\,. \tag{4.2.21}$$

The parameter x from (4.1.20) should be chosen in order to avoid any singularity in the transformed potential. As can easily be seen from the analysis of $\det u_c$, it is sufficient to choose x large enough. The asymptotic behaviour of the superpotential is given by (4.1.23) or (4.1.24).

The Jost matrix $F_c(k)$ may be found from (4.1.13). Its explicit expression is rather involved and we omit it. More important is its determinant (4.1.15), the expression of which is extremely simple,

$$\det F_c(k) = \frac{k^2 + \kappa^2}{(k + i\kappa_1)(k + i\kappa_2)}\,. \tag{4.2.22}$$

From here we find the location of the bound state at $k_b = i\kappa$ and the virtual state at $k_v = -i\kappa$.

The chain of two SUSY transformations with parameters $\kappa_{1,2} = a_{1,2}^{-1}$ and κ, q, x described above leads to the mixing angle (4.2.13). The corresponding potential ($q = 0.4$) is shown in figure 4.2. The factorization constant κ is fixed from (4.2.15). As a result, the mixing angle takes the form

$$\tan 2\epsilon(k) = \frac{2k^2\kappa_1\kappa_2 \tan\alpha}{\kappa_1^2\kappa_2^2 \sec^2\alpha + k^2(\kappa_1^2 + \kappa_2^2)}\,. \tag{4.2.23}$$

Parameters κ_1 and κ_2 are related with 1-channel transformations and allow us to fit the scattering lengths. The mixing angle $\epsilon(k)$ depends on parameter α, which allows one to fit its experimental behaviour at low energies. The mixing angle at large energies tends to a constant value, $\tan 2\epsilon(k \to \infty) = -2\kappa_1\kappa_2 \tan\alpha/(\kappa_1^2 + \kappa_2^2)$ which can also be fitted using corresponding experimental data (if available). Figure 4.3 shows the phase shifts and mixing angle for two coupled $s-s$ potentials.

The phase shifts of the diagonal potential V_d are shown as dotted lines in figure 4.3(a). The phase shifts of the transformed potential V_c are shown as dashed ($q = 0.4$) and solid ($q = 1.2$) lines respectively. One can see that the slopes of these curves coincide at the origin. The mixing angles of the transformed potential are plotted in figure 4.3(b).

According to (4.2.22) this potential has one bound state at the factorization energy $E_g = -\kappa^2$. Note that the normalization constant of the bound state wave function is determined by parameter q as follows from (4.1.16).

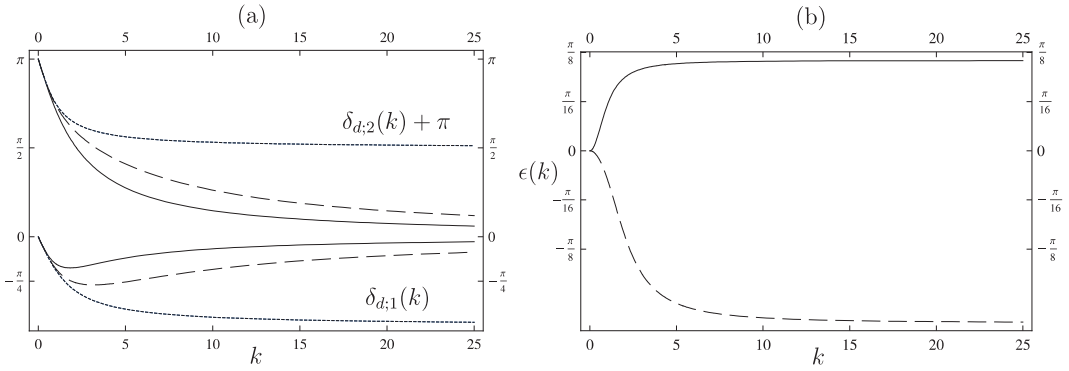

Figure 4.3: The scattering matrix for the coupled $s-s$ potential. (a) The eigenphases are shown as dotted lines for V_d and as dashed and solid lines for V_c. The parameters are: solid lines - $\kappa_1 = 1.5$, $\kappa_2 = 1$, $q = 0.4$, $\kappa = 4.14286$, $x = 15$, dashed lines - $\kappa_1 = 1.5$, $\kappa_2 = 1$, $q = 1.2$, $\kappa = 13.6667$, $x = 15$. (b) Mixing angle ϵ.

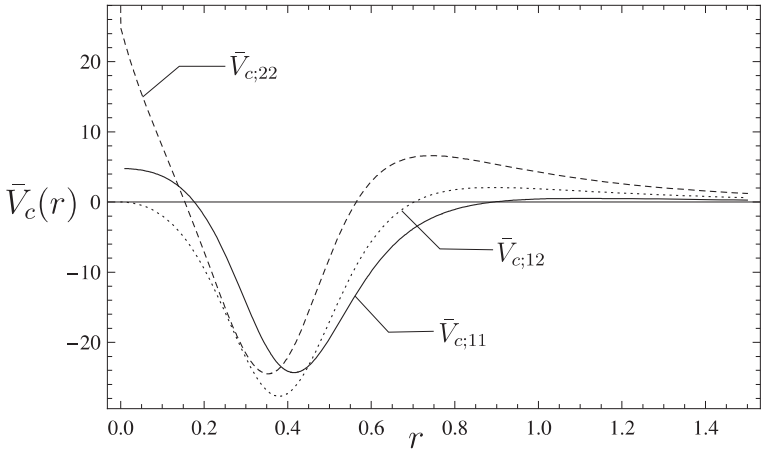

Figure 4.4: Exactly solvable $s-p$ potential $\bar{V}_c = V_c - \tilde{l}(\tilde{l}+1)r^{-2}$ with parameters $\kappa_0 = 1.5$, $\kappa_1 = 1.75$, $\kappa = 3.53$, $q = 1$, $x = 1$.

4.2.3 Coupled $s-p$ partial waves

In this section we consider the simplest $s-p$ coupled potential. This potential is characterized by $\tilde{l} = \tilde{\nu} = \mathrm{diag}(1,0)$. The coupling transformation acts as follows:

$$l = \mathrm{diag}(l_1, l_2) \to \tilde{l} = \mathrm{diag}(l_2, l_1)\,, \qquad \nu = \mathrm{diag}(\nu_1, \nu_2) \to \tilde{\nu} = \mathrm{diag}(\nu_1 - 1, \nu_2 - 1)\,. \tag{4.2.24}$$

Therefore the initial diagonal potential should have $l = \mathrm{diag}(0,1)$, $\nu = (2,1)$. These properties are satisfied for the initial potential of the form

$$V_d(r) = \mathrm{diag}\left[-2\frac{d^2}{dr^2}\ln W[\sinh(\kappa_0 r), \sinh(\kappa_1 r)], 2r^{-2}\right], \tag{4.2.25}$$

where the potential in the s-channel is obtained from the zero potential after two consecutive SUSY transformations with κ_0 and κ_1 as factorization constants. The potential in the p-channel is just the centrifugal term. The Jost solution in the s-channel is expressed in terms of the Wronskian of factorization solutions $\sinh(\kappa_j r)$, $j = 0, 1$,

$$f_d(k,r) = \mathrm{diag}\left[\frac{W\left[\sinh(\kappa_0 r), \sinh(\kappa_1 r), e^{ikr}\right]}{(k+i\kappa_0)(k+i\kappa_1)W\left[\sinh(\kappa_0 r), \sinh(\kappa_1 r)\right]}, \frac{(i+kr)\mathrm{e}^{ikr}}{kr}\right]. \tag{4.2.26}$$

The uncoupled Jost matrix reads

$$F_d(k) = \mathrm{diag}\left[-\left[(k+i\kappa_0)(k+i\kappa_1)\right]^{-1}, ik^{-1}\right]. \tag{4.2.27}$$

The next step is to apply the coupling transformation with the transformation function (4.1.1) where the Jost solution is replaced by (4.2.26). An example of potential curves is shown in figure 4.4. The Jost matrix (4.2.27) is transformed according to (4.1.13) and the scattering matrix is given by (4.1.29).

Since the transformed eigenphase shifts coincide with the initial phase shifts, we may fit the phase shifts for the s and p waves separately before the coupling transformation. In our example the phase shifts read

$$\delta_{c;1}(k) = 0\,, \qquad \delta_{c;2}(k) = \pi - \arctan\frac{k}{\kappa_0} - \arctan\frac{k}{\kappa_1}\,. \tag{4.2.28}$$

Parameters κ_0 and κ_1 allow one to fit the s-channel phase shifts. Parameter κ may be used to fit the slope of the mixing angle (4.1.34) at zero energy. If necessary, one may use arbitrary chains of 1-channel transformations to get the best fit of the phase shifts.

4.2.4 Coupled $s-d$ partial waves

The simplest $s-d$ coupled potential is characterized by $\tilde{l} = \tilde{\nu} = \mathrm{diag}(2,0)$. Therefore the initial diagonal potential should have $l = \mathrm{diag}(0,2)$ and $\nu = (3,1)$. Moreover, as we established in section 4.1.3, $\delta_{d;2}(0) - \delta_{d;1}(0) = (n+1/2)\pi$ which for $n=0$ leads to the following initial phase shifts $\delta_{d;2}(0) = \pi/2$ and $\delta_{d;1}(0) = 0$.

We start with the initial s-wave potential

$$V_0(r) = \frac{-2\kappa_0^2}{\cosh^2(\kappa_0 r)} \tag{4.2.29}$$

having a zero energy virtual state [23] which follows from its Jost function

$$F_0(k) = \frac{k}{k+i\kappa_0}\,. \tag{4.2.30}$$

Note that this potential and the solutions of the corresponding Schrödinger equation may be obtained by a SUSY transformation. This is a regular potential. To be able to apply the coupling transformation, we increase its singularity at the origin using three SUSY transformations with the transformation functions

$$u(\kappa_i, r) = \kappa_i \sinh(\kappa_i r) + \kappa_0 \cosh(\kappa_i r)\tanh(\kappa_0 r)\,, \qquad i = 1,2,3\,. \tag{4.2.31}$$

The potential and the Jost function in the s-channel after these transformations read

$$V_{d;1}(r) = \frac{-2\kappa_0^2}{\cosh^2(\kappa_0 r)} - 2\left(\ln W\left[u(\kappa_1,r), u(\kappa_2,r), u(\kappa_3,r)\right]\right)''\,, \tag{4.2.32}$$

$$F_{d;1}(k) = \frac{-ik}{(k+i\kappa_0)(k+i\kappa_1)(k+i\kappa_2)(k+i\kappa_3)}\,. \tag{4.2.33}$$

The potential in the d-channel

$$V_{d;2}(r) = \frac{6}{r^2} - 2\ln v''(\kappa_4, r) = \frac{6(3+6\kappa_4 x + 6\kappa_4^2 r^2 + 4\kappa_4^3 r^3 + \kappa_4^4 r^4)}{r^2(3+3\kappa_4 r + \kappa_4^2 r^2)^2}\,, \tag{4.2.34}$$

$$v(\kappa_4, r) = \mathrm{e}^{-\kappa_4 r}\left(1 + 3\kappa_4 r + \frac{3}{(\kappa_4 r)^2}\right), \tag{4.2.35}$$

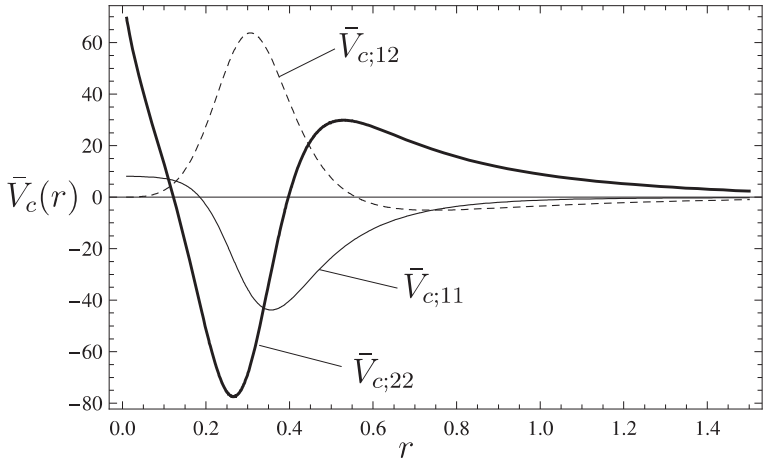

Figure 4.5: Exactly solvable $s-d$ potential $\bar{V}_c = V_c - \tilde{l}(\tilde{l}+1)r^{-2}$ with parameters $\kappa_0 = 1$, $\kappa_1 = 1.5$, $\kappa_2 = 1.75$, $\kappa_3 = 2$, $\kappa_4 = 3$ $q = -1$, $x = 15$, $\kappa = 5.53$.

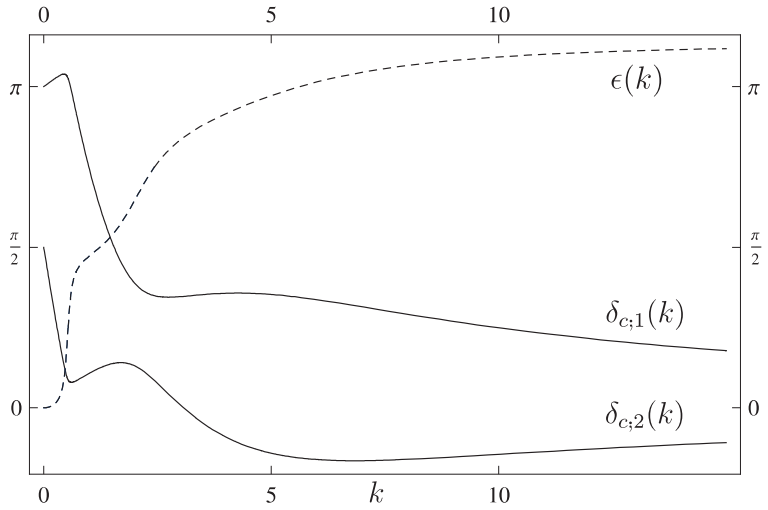

Figure 4.6: The scattering matrix for the coupled $s-d$ potential. The phase shifts $\delta_{c;1}(k)$ and $\delta_{c;2}(k)$ are plotted by solid lines. The mixing angle $\epsilon(k)$ is plotted by the dashed line. The corresponding parameters are $\kappa_0 = 1$, $\kappa_1 = 1.5$, $\kappa_2 = 1.75$, $\kappa_3 = 2$, $\kappa_4 = 3$ $q = 1$, $x = 15$, $\kappa = 5.53$.

is obtained from the centrifugal term $6/r^2$ by the SUSY transformation with $v(r,\kappa_4)$ as the transformation function, which decreases the singularity of the potential at the origin.

The Jost solution in the s-channel is expressed in terms of the Wronskian of factorization solutions (4.2.31)

$$f_{d;1}(k,r) = \frac{W\left[u(\kappa_1,r),u(\kappa_2,r),u(\kappa_3,r),f_0(k,r)\right]}{(k+i\kappa_1)(k+i\kappa_2)(k+i\kappa_3)W\left[u(\kappa_1,r),u(\kappa_2,r),u(\kappa_3,r)\right]}\,, \tag{4.2.36}$$

$$f_0(k,r) = \mathrm{e}^{ikr}\frac{k+i\kappa_0\tanh(\kappa_0 r)}{k+i\kappa_0}\,. \tag{4.2.37}$$

The Jost solution in the d-channel is

$$f_{d;2}(k,r) = i\frac{W\left[v(\kappa_4,r),h_2(kr)\right]}{(k-i\kappa_4)v(\kappa_4,r)}\,, \qquad h_2(kr) = \mathrm{e}^{ikr}\left(1+3i\kappa_4 r-\frac{3}{(\kappa_4 r)^2}\right). \tag{4.2.38}$$

The uncoupled Jost matrix reads

$$F_d(k) = \mathrm{diag}\left[\frac{-ik}{(k+i\kappa_0)(k+i\kappa_1)(k+i\kappa_2)(k+i\kappa_3)},\frac{ik-\kappa_4}{k^2}\right], \tag{4.2.39}$$

which produces the eigenphase shifts

$$\delta_{d;1}(k) = \frac{\pi}{2}-\sum_{j=0}^{3}\arctan\frac{k}{\kappa_j}\,, \qquad \delta_{d;2}(k) = \arctan\frac{k}{\kappa_4}\,. \tag{4.2.40}$$

Next we apply the coupling transformation with the transformation function (4.1.1) where the Jost solution $f_d = \mathrm{diag}(f_{d;1}, f_{d;2})$ is combined from (4.2.36) and (4.2.38). An example of potential curves thus obtained is shown in figure 4.5. The Jost matrix (4.2.39) is transformed according to (4.1.13) and the scattering matrix is given by (4.1.29).

The corresponding phase shifts and mixing angle are plotted in figure 4.6. The mixing parameter $\epsilon(k)$ is determined by (4.1.35) which, in the current case, reduces to

$$\tan 2\epsilon(k) = \frac{2\kappa k}{(k^2+\kappa^2)}\tan\left(\sum_{j=0}^{4}\arctan\frac{k}{\kappa_j}\right). \tag{4.2.41}$$

We were not able to find simple expressions for the eigenphase shifts in this case. One can see that the mixing parameter satisfies the effective range expansion (4.1.36) (see (4.2.41) and figure 4.6). Unfortunately, this is not the case for the phase shifts (see figure 4.6).

4.3 Second order SUSY transformations

In the previous section, we saw that the first order SUSY transformations can introduce a non-trivial coupling but in the physically interesting case of partial waves with the same parity there is the serious drawback (see subsection 4.2.4). It is impossible to get the transformed phase shifts and the mixing parameter which satisfy to the effective range expansion. This is a signal that the transformed potential may be unphysical. The simplest possible way to avoid this obstacle is to use a pair of first order transformations. Thus we obtain additional free parameters which can be used to satisfy the requirements appearing from the effective range expansion. In this way, analyzing the most general second order SUSY transformation we have found a new type of SUSY transformations for two channel problems.

4.3.1 Eigenphase preserving SUSY transformations

Two-fold SUSY transformations lead to a number of interesting quantum models with unusual properties [63]. In particular, the corresponding superalgebra is nonlinear. The case of two transformations is less restrictive since the intermediate Hamiltonian may be chosen unphysical. In particular, one may use as transformation functions complex-valued solutions of the Schrödinger equation corresponding to complex factorization constants. It is natural to consider the two-fold SUSY transformation of the Schrödinger equation (1.1.20) as a chain of usual (i.e. one-fold) SUSY transformations. As we show below, a chain of two such transformations may preserve the eigenphase shifts.

The chain of two SUSY transformations, $H_0 \to H_1 \to H_2$, emerges from the following intertwining relations:

$$L_1 H_0 = H_1 L_1 \,, \qquad L_2 H_1 = H_2 L_2 \,, \tag{4.3.1}$$

where the operators L_j map solutions of the Schrödinger equations to each other as $\psi_1 = L_1\psi_0$ and $\psi_2 = L_2\psi_1$. These operators can be combined into an operator L defining the two-fold SUSY transformation

$$L H_0 = H_2 L \,, \qquad L = L_2 L_1 \,, \tag{4.3.2}$$

directly mapping solutions of the initial Schrödinger equation to solutions of the transformed Schrödinger equation as $\psi_2 = L\psi_0$.

The operators L_j are first-order differential operators,

$$L_1 = w_1(r) - \partial_r \,, \qquad L_2 = \tilde{w}_2(r) - \partial_r \,. \tag{4.3.3}$$

We use the standard notation for the superpotentials

$$w_j(r) = u_j'(r) u_j^{-1}(r) \,, \qquad j = 1, 2 \,, \tag{4.3.4}$$

$$\tilde{w}_2(r) = \tilde{u}_2'(r) \tilde{u}_2^{-1}(r) \,, \tag{4.3.5}$$

which are expressed in terms of the matrix factorization solutions u_j and $\tilde{u}_2 = L_1 u_2$. These solutions satisfy the following Schrödinger equations:

$$H_0 u_j = E_j u_j \,, \qquad H_1 \tilde{u}_2 = E_2 \tilde{u}_2 \,, \tag{4.3.6}$$

with E_1, E_2 being factorization constants. Operator L then has a nontrivial kernel space, Ker L, spanned by the set of transformation functions u_1 and u_2:

$$\mathrm{Ker}\, L = \mathrm{span}\{u_1, u_2\}\,. \tag{4.3.7}$$

In the following, we will only consider self-conjugate factorization solutions, i.e. solutions with a vanishing self-Wronskian $\mathrm{W}[u,u]=0$, where the Wronskian of two matrix functions u, v is defined by (1.1.29). For factorization solutions we get

$$\mathrm{W}[u_1,u_2](r) = u_1^T(r)\left[w_2(r) - w_1^T(r)\right] u_2(r). \tag{4.3.8}$$

Hence, self-conjugate solutions correspond to symmetric superpotentials. Solution $\tilde{u}_2$ then reads

$$\tilde{u}_2(r) = L_1 u_2(r) = [w_1(r) - w_2(r)]u_2(r) = -\left[u_1^T(r)\right]^{-1}\mathrm{W}[u_1,u_2](r)\,, \tag{4.3.9}$$

where the last expression has been obtained using (4.3.8) and the symmetry of w_1.

The Hamiltonians in (4.3.1) correspond to potentials related to each other through superpotentials

$$V_1(r) = V_0(r) - 2w_1'(r)\,, \qquad V_2(r) = V_1(r) - 2\tilde{w}_2'(r)\,. \tag{4.3.10}$$

The sum of the two superpotentials w_1 and $\tilde{w}_2$ defines the two-fold superpotential W_2, which directly connects V_0 to V_2:

$$W_2(r) \equiv w_1(r) + \tilde{w}_2(r)\,, \qquad V_2(r) = V_0(r) - 2W_2'(r)\,. \tag{4.3.11}$$

Using the Schrödinger equation twice, one sees that the derivative of Wronskian (4.3.8) reads

$$\mathrm{W}[u_1,u_2]'(r) = (E_1 - E_2)u_1^T(r)u_2(r)\,. \tag{4.3.12}$$

Hence, using (4.3.5) and (4.3.9), one can rewrite W_2 in the compact forms

$$\begin{aligned} W_2(r) &= (E_1 - E_2)\left[w_2(r) - w_1(r)\right]^{-1} &(4.3.13)\\ &= (E_1 - E_2)u_2(r)\mathrm{W}[u_1,u_2]^{-1}(r)u_1^T(r). &(4.3.14)\end{aligned}$$

As will be seen below, the second expression is more general than the first one, as it may be used in cases where the individual superpotentials w_1 or w_2 are singular.

Similarly, expressing the second derivative of the matrix solution $\psi_0(k,r)$ from (1.1.20) and defining the logarithmic derivative

$$w_k(r) = \psi_0'(k,r)\psi_0^{-1}(k,r)\,, \tag{4.3.15}$$

one can rewrite the action of the second order transformation operator L on $\psi_0(k,r)$,

$$\psi_2(k,r) = (\tilde{w}_2 - \partial_r)\,(w_1 - \partial_r)\,\psi_0(k,r)\,, \tag{4.3.16}$$

in the following form

$$\psi_2(k,r) = \left[(-k^2 + E_1)\mathbf{1} + W_2(r)(w_1 - w_k)\right]\psi_0(k,r)\,. \tag{4.3.17}$$

A more symmetric form of this formula

$$\psi_2(k,r) = \left[\left(-k^2 + \frac{E_2+E_1}{2}\right)\mathbf{1} + W_2(r)\left(\frac{w_1+w_2}{2} - w_k\right)\right]\psi_0(k,r) \tag{4.3.18}$$

may also be useful.

4.3.2 Main theorem

Let us now particularize the above results to two consecutive SUSY transformations with mutually conjugated complex matrix factorization solutions corresponding to imaginary factorization energies. We will prove that such a second order transformation modifies the mixing parameters without affecting the eigenphase shifts. We will consider the case of two partial waves l_1 and l_2 with identical parity,

$$l_2 = l_1 + 2m, \qquad m \in \mathbb{Z}. \tag{4.3.19}$$

To construct eigenphase preserving transformations, we need solutions of the Schrödinger equation (1.1.20) with a special behaviour both at large distances and near the origin. Thus, we first prove that the necessary solutions exist.

Lemma 5. *For any momentum k such that* Im $k > 0$, det $F_0(k) \neq 0$, *and for any constants $c_{1,2}, d_{1,2} \in \mathbb{C}$, there exist two vector solutions $\vec{u}(k,r)$ and $\vec{v}(k,r)$ of the Schrödinger equation* (1.1.20) *which behave at large distances as*

$$\vec{u}(k, r \to \infty) = \mathrm{e}^{-ikr}(c_1, c_2)^T(1 + \mathrm{o}(1))\,, \tag{4.3.20}$$

$$\vec{v}(k, r \to \infty) = \mathrm{e}^{ikr}(d_1, d_2)^T(1 + \mathrm{o}(1))\,, \tag{4.3.21}$$

and near the origin as

$$\vec{u}(k, r \to 0) = (a_1 r^{\nu_1+1}, a_2 r^{\nu_2+1})^T(1 + \mathrm{o}(r))\,, \tag{4.3.22}$$

$$\vec{v}(k, r \to 0) = (b_1 r^{-\nu_1}, b_2 r^{-\nu_2})^T(1 + \mathrm{o}(r))\,, \tag{4.3.23}$$

where $a_{1,2}, b_{1,2} \in \mathbb{C}$.

Proof. To obtain the behaviour (4.3.21), $\vec{v}(k,r)$ can be expressed in terms of the Jost solution

$$\vec{v}(k,r) = f_0(k,r)(d_1, d_2)^T. \tag{4.3.24}$$

Formula (4.3.23) follows from the behaviour of the Jost solution near the origin (see, e.g., [22]).

Taking into account that Im $k > 0$, one gets from (1.1.27)

$$\varphi_0(k, r \to \infty) \to \frac{i}{2k} f_0(-k,r) F_0(k)\,. \tag{4.3.25}$$

Here, we omit the second term in (1.1.27) since it becomes negligible at large distances with respect to the first term. Thus, solution $\vec{u}(k,r)$ may be obtained as

$$\vec{u}(k,r) = \frac{2k}{i}\varphi_0(k,r)F_0^{-1}(k)(c_1, c_2)^T. \tag{4.3.26}$$

Formula (4.3.22) follows from (1.1.25). □

Theorem 12. *Consider a complex matrix solution u of the coupled-channel Schrödinger equation* (1.1.20)-(1.1.23)*, with imaginary energy $E_1 = k_1^2 \equiv 2i\chi^2$ and complex wave number $k_1 = \chi(i+1)$, $\chi > 0$, behaving at large distances as*

$$u(r \to \infty) \to \begin{pmatrix} h_{l_1}(-k_1 r) & \pm i h_{l_1}(k_1 r) \\ \mp i h_{l_2}(-k_1 r) & h_{l_2}(k_1 r) \end{pmatrix}, \tag{4.3.27}$$

and near the origin as

$$u(r \to 0) = \begin{pmatrix} a_1 r^{\nu_1+1} & b_1 r^{-\nu_1} \\ a_2 r^{\nu_2+1} & b_2 r^{-\nu_2} \end{pmatrix} [1 + \mathrm{o}(r)]. \tag{4.3.28}$$

The two-fold SUSY transformation defined by (4.3.2)-(4.3.6) *with matrix factorization solutions* $u_1 = u$, $u_2 = u^*$ *corresponding to the imaginary factorization constants* E_1, $E_2 = E_1^* = -2i\chi^2$ *and complex wave numbers* k_1, $k_2 = \chi(i-1)$, *possesses the following properties:*

A. *The resulting potential* V_2 *defined in* (4.3.11) *is real, symmetric and regular* $\forall r$. *The two-fold superpotential* W_2 *reads*

$$W_2(r) = 4i\chi^2 \left[w^*(r) - w(r)\right]^{-1}, \qquad w(r) = u'(r)u^{-1}(r), \tag{4.3.29}$$

$$= 4i\chi^2 u^*(r)\mathrm{W}[u, u^*]^{-1}(r)u^T(r), \tag{4.3.30}$$

where only the second expression can be used when the superpotential w *is singular.*

B. *The long range behaviour of* V_2,

$$V_2(r \to \infty) = \bar{l}(\bar{l} + \mathbf{1})r^{-2} + \mathrm{o}(r^{-2}), \qquad \bar{l} = \mathrm{diag}(l_2, l_1), \tag{4.3.31}$$

corresponds to a re-ordering of partial waves with respect to channels.

C. *The scattering matrix* S_2 *of the transformed Schrödinger equation is expressed from the initial scattering matrix* S_0 *as follows:*

$$S_2(k) = O(k)S_0(k)O^T(k), \tag{4.3.32}$$

where the real orthogonal matrix O *reads*

$$O(k) = e^{i\bar{l}\frac{\pi}{2}} \frac{1}{\sqrt{k^4 + 4\chi^4}} \begin{pmatrix} -k^2 & \mp 2\chi^2 \\ \pm 2\chi^2 & -k^2 \end{pmatrix} e^{-il\frac{\pi}{2}}. \tag{4.3.33}$$

D. *The eigenphase shifts of the transformed scattering matrix* S_2 *coincide with the initial ones. With the permutation*

$$\delta_{2;1}(k) = \delta_{0;2}(k), \tag{4.3.34}$$

$$\delta_{2;2}(k) = \delta_{0;1}(k), \tag{4.3.35}$$

the mixing parameter transforms as

$$\epsilon_2(k) = \epsilon_0(k) \pm (-1)^m \arctan \frac{k^2}{2\chi^2}. \tag{4.3.36}$$

Proof. First, we note that Lemma 5 implies that solution u exists. It reads

$$u(r) = \frac{2k_1}{i}\varphi_0(k_1, r)F_0^{-1}(k_1) \begin{pmatrix} 1 & 0 \\ \mp i & 0 \end{pmatrix} + f_0(k_1, r) \begin{pmatrix} 0 & \pm i \\ 0 & 1 \end{pmatrix}. \tag{4.3.37}$$

Using (4.1.19) and (4.3.27), one may write the leading terms of the asymptotic behaviour of this factorization solution as

$$u(r \to \infty) \to \begin{pmatrix} e^{-ik_1 r}\left(1 - \frac{i\Lambda_1}{2k_1 r}\right) & \pm ie^{ik_1 r}\left(1 + \frac{i\Lambda_1}{2k_1 r}\right) \\ \mp ie^{-ik_1 r}\left(1 - \frac{i\Lambda_2}{2k_1 r}\right) & e^{ik_1 r}\left(1 + \frac{i\Lambda_2}{2k_1 r}\right) \end{pmatrix}. \tag{4.3.38}$$

A. According to the choice of transformation functions and factorization constants, the one-fold superpotentials w_1 and w_2 are mutually complex conjugated, $w_1 = w$, $w_2 = w^*$. Therefore, one can use $w = u'u^{-1}$ and its complex conjugated form w^* in (4.3.4), (4.3.5) and (4.3.9), thus obtaining

$$\tilde{w}_2(r) = \tilde{w}^*(r) = (\tilde{u}^*)'(\tilde{u}^*)^{-1}, \qquad \tilde{u}^*(r) = L_1 u^*(r) = (w - w^*)u^*. \tag{4.3.39}$$

In this case, (4.3.29) and (4.3.30) directly follow from (4.3.13) and (4.3.14).

From (4.3.29), it is seen that W_2, and thus the transformed potential (4.3.11), are real. The symmetry of matrix V_2 (i.e. $V_2^T = V_2$) follows from the symmetry of superpotential w, which can be established by considering the self-Wronskian $\mathrm{W}[u,u]$. Since (4.3.12) implies that this self-Wronskian is constant with respect to r and (4.3.38) implies that it vanishes at large distances, $\mathrm{W}[u,u](\infty) = 0$, one has $\mathrm{W}[u,u](r) = 0, \forall r$. According to (4.3.8), this is equivalent to the symmetry $w^T(r) = w(r), \forall r$.

Let us now prove that V_2 is regular. According to (4.3.11) and (4.3.30), this is the case if and only if the Wronskian $\mathrm{W}[u,u^*]$ is invertible $\forall r$. From (1.1.29) follows that $\mathrm{W}[u,u^*]$ is an anti-Hermitian matrix, i.e. $\mathrm{W}[u,u^*] = -\mathrm{W}^\dagger[u,u^*]$. Moreover, using (4.3.12), the derivative of this Wronskian reads

$$\mathrm{W}[u,u^*]'(r) = 4i\chi^2 u^T(r)u^*(r)\,. \tag{4.3.40}$$

Its diagonal entries can thus be integrated using (4.3.28) and (4.3.38) respectively. One gets finally

$$\mathrm{W}[u,u^*](r) = \begin{pmatrix} 4i\chi^2 \int_0^r (|u_{11}(t)|^2 + |u_{21}(t)|^2)dt & \mathrm{W}_{12}[u,u^*](r) \\ -\mathrm{W}_{12}^*[u,u^*](r) & -4i\chi^2 \int_r^\infty (|u_{12}(t)|^2 + |u_{22}(t)|^2)dt \end{pmatrix}, \tag{4.3.41}$$

where u_{ij} and $\mathrm{W}_{ij}[u,u^*]$ label the entries of the factorization solution and of the Wronskian, respectively. This result implies that $\det \mathrm{W}[u,u^*] > 0, \forall r$, which proves the regularity of V_2 stated in the theorem. Let us stress that this proof holds even in cases where superpotential w and the intermediate potential V_1 are singular, which shows that expression (4.3.30), though more complictaed, is more general than (4.3.29).

B. Let us first consider the case $l_1 \neq l_2$. From the asymptotic behaviour (4.3.38), it follows that the determinant of the transformation solution u tends to zero as $r \to \infty$ like the Laurent series

$$\det u(r \to \infty) = \frac{(\Lambda_2 - \Lambda_1)}{\chi(1-i)r} + \mathrm{o}(r^{-2})\,. \tag{4.3.42}$$

Hence, the superpotential w behaves asymptotically as

$$w(r \to \infty) = \frac{4\chi^2 r}{\Lambda_1 - \Lambda_2} \begin{pmatrix} i & \pm 1 \\ \pm 1 & -i \end{pmatrix} + \mathrm{O}(1)\,, \tag{4.3.43}$$

from which, using (4.3.29), we find the asymptotic behaviour of W_2,

$$W_2(r \to \infty) = \frac{\Lambda_2 - \Lambda_1}{2r} \begin{pmatrix} 1 & 0 \\ 0 & -1 \end{pmatrix} + \mathrm{o}(r^{-1})\,. \tag{4.3.44}$$

It should be emphasized that from (4.3.44) follows the exchange of the centrifugal terms in V_2 with respect to V_0 [see (4.3.11)]. This effect of coupling SUSY transformations was previously described in [9]. Note that the scattering properties of the transformed system crucially depend on the exchange of centrifugal terms because of the presence of l-dependent factors in the S-matrix definition (1.1.33).

In the case of coinciding partial waves, $l_1 = l_2$, (4.3.44) is still valid but cannot be established through (4.3.43): instead, $W_2(r)$ can be calculated from the Wronskian representation (4.3.30). This allows us to avoid manipulations with singular quantities which appear in (4.3.43) when $l_1 = l_2$. It is convenient to rewrite the asymptotic behaviour of the transformation solution in the form

$$u(r \to \infty) \to \left(2Q_\mp - \frac{i}{\xi_1}\Lambda Q_\mp \sigma_z\right) \mathrm{e}^{-i\xi_1\sigma_z}\,, \qquad Q_\mp = (\mathbf{1} \mp \sigma_y)/2\,, \qquad \xi_1 = k_1 r, \tag{4.3.45}$$

where $\Lambda = \mathrm{diag}(\Lambda_1, \Lambda_2)$, σ_x, σ_y and σ_z are the Pauli matrices, and the projection matrices $Q_\mp$ satisfy

$$Q_\pm^T = Q_\mp\,, \qquad Q_\pm Q_\mp = 0\,, \qquad Q_\pm^2 = Q_\pm\,, \tag{4.3.46}$$

$$Q_\pm \sigma_z = \sigma_z Q_\mp\,, \qquad Q_\pm \sigma_x = \sigma_x Q_\mp. \tag{4.3.47}$$

Here and in what follows we will only retain terms of order r^{-1} or lower. Let us first calculate the Wronskian asymptotics at large distances. Definition (1.1.29) leads to

$$\mathrm{W}(r\to\infty) \to 4i\chi \mathrm{e}^{-i\xi_1\sigma_z}(\sigma_z \pm \sigma_x)\left[1 - \frac{(1-i)}{4\chi r}(\Lambda_1+\Lambda_2)\sigma_z Q_\mp\right]\mathrm{e}^{i\xi_1^*\sigma_z}\,, \tag{4.3.48}$$

which can be inverted (up to r^{-1}) to give

$$\begin{aligned}\mathrm{W}^{-1}(r\to\infty) &\to \frac{1}{8i\chi}\mathrm{e}^{-i\xi_1^*\sigma_z}\left[1 + \frac{(1-i)}{4\chi r}(\Lambda_1+\Lambda_2)\sigma_z Q_\mp\right](\sigma_z \pm \sigma_x)\mathrm{e}^{i\xi_1\sigma_z} &(4.3.49)\\ &= \frac{1}{8i\chi}\mathrm{e}^{-i\xi_1^*\sigma_z}\left[\sigma_z \pm \sigma_x + \frac{1}{2\chi r}(\Lambda_1+\Lambda_2)Q_\pm\right]\mathrm{e}^{i\xi_1\sigma_z}\,. &(4.3.50)\end{aligned}$$

We can now calculate the two-fold superpotential up to r^{-1}

$$\begin{aligned}W_2 &= 4i\chi^2 u^* \mathrm{W}^{-1} u^T &(4.3.51)\\ &\to \chi\left(\frac{i}{\xi_1^*}\Lambda Q_\pm \sigma_z(\sigma_z\pm\sigma_x)Q_\pm + \frac{1}{\chi r}(\Lambda_1+\Lambda_2)Q_\pm - \frac{i}{\xi_1}Q_\pm(\sigma_z\pm\sigma_x)\sigma_z Q_\pm \Lambda\right), &(4.3.52)\end{aligned}$$

where (4.3.46) and (4.3.47) have been used. To further simplify this expression, we also use the decomposition $\Lambda = \mathbf{1}(\Lambda_1+\Lambda_2)/2 + \sigma_z(\Lambda_1-\Lambda_2)$, which leads finally to

$$W_2(r\to\infty) \to \frac{1}{2r}(\Lambda_2 - \Lambda_1)\sigma_z\,. \tag{4.3.53}$$

This expression is valid for any l_1 and l_2; it is thus also valid for the case of coinciding partial waves. The fact that the two-fold superpotential vanishes at large distances faster than r^{-1} implies that the centrifugal tails are not affected by the SUSY transformations and that the partial waves are unchanged.

C. To establish the modification of the scattering matrix, we have to look at the way the Jost solutions and the regular solutions transform in the two-fold transformation.

Once again, let us start with the simpler case $l_1 \neq l_2$. Without loss of generality we may apply the general transformation of solutions (4.3.18) to the Jost solution, which now takes the form

$$Lf_0(k,r) = \left[-k^2\mathbf{1} + W_2(r)\left(\frac{w+w^*}{2} - w_k\right)\right] f_0(k,r) \equiv U(k,r) f_0(k,r). \tag{4.3.54}$$

As we will see below, the matrix $U_\infty(k) = \lim_{r\to\infty} U(k,r)$ determines the transformed Jost and scattering matrices. Using (4.3.43), (4.3.44) and the fact that $W_2 w_k$ vanishes at large distances, one obtains a simple expression for this matrix,

$$U_\infty(k) = \begin{pmatrix} -k^2 & \mp 2\chi^2 \\ \pm 2\chi^2 & -k^2 \end{pmatrix}. \tag{4.3.55}$$

From the dominant term of (1.1.26) and (4.1.19), it follows that the function

$$f_2(k,r) = Lf_0(k,r)U_\infty^{-1}(k) \tag{4.3.56}$$

is the transformed Jost solution.

As in the previous part, the case $l_1 = l_2$ requires additional attention since the product $W_2(w + w^*)$ gives at large distances the uncertainty $0 \cdot \infty$. Again we use the Wronskian representation (4.3.30) of the two-fold superpotential W_2 and the asymmetrical form of transformation (4.3.17) thus obtaining

$$Lf_0(k,r) \underset{r\to\infty}{\to} \left[(-k^2 + 2i\chi^2)\mathbf{1} + 4i\chi^2 u^* \mathrm{W}[u,u^*]^{-1} u^{T\prime}\right] f_0(k,r)\,. \tag{4.3.57}$$

Using (4.3.45) and (4.3.50) in this expression leads to the same matrix $U_\infty(k)$ as in (4.3.55).

Let us now find how the SUSY transformation modifies the behaviour of the potential at the origin. From (4.3.28), one gets

$$\det u(r \to 0) \to a_1 b_2 r^{\nu_1 - \nu_2 + 1} - a_2 b_1 r^{\nu_2 - \nu_1 + 1}, \tag{4.3.58}$$

which suggests that the discussion will depend on the relative values of ν_1 and ν_2.

For $\nu_2 = \nu_1$, excluding the case $a_1 b_2 = a_2 b_1$ (which requires higher order expansions), one can expand the superpotential $w(r)$ in a Laurent series near $r = 0$,

$$w(r \to 0) = \frac{1}{(a_1 b_2 - a_2 b_1) r} \begin{pmatrix} a_1 b_2 (\nu_1 + 1) + a_2 b_1 \nu_1 & -a_1 b_1 (2\nu_1 + 1) \\ a_2 b_2 (2\nu_2 + 1) & -a_2 b_1 (\nu_2 + 1) - a_1 b_2 \nu_2 \end{pmatrix} + \mathrm{o}(1), \tag{4.3.59}$$

which implies with (4.3.29) that the lowest-order term in W_2 is linear in r. Consequently, (4.3.11) implies that the singularity indices are not modified by the two-fold SUSY transformation. Note however that (4.3.10) implies that the intermediate potential V_1 displays in general off-diagonal singular terms at the origin.

For $\nu_2 > \nu_1$, one gets instead of (4.3.59)

$$w(r \to 0) = \frac{1}{r} \begin{pmatrix} \nu_1 + 1 & 0 \\ 0 & -\nu_2 \end{pmatrix} + \mathrm{o}(1). \tag{4.3.60}$$

To find the behaviour of W_2 at the origin, a higher-order expansion would thus be necessary. It is simpler in this case to study the two first-order transformations separately. From (4.3.10) and (4.3.60), we conclude that the intermediate potential V_1 has the following singularity indices $\nu \to \tilde{\nu} = \mathrm{diag}(\nu_1 + 1, \nu_2 - 1)$. For $\nu_2 < \nu_1$, one gets $\nu \to \tilde{\nu} = \mathrm{diag}(\nu_1 - 1, \nu_2 + 1)$ by symmetry.

Let us now analyze the behaviour of the transformation function $\tilde{u}^* = L_1 u^*$ which determines operator L_2. Using (4.3.3) and (4.3.60) [or (4.3.59) when $\nu_1 = \nu_2$] one can find that a regular/singular vector solution transforms into a regular/singular vector solution of the new equation. Such transformations are called conservative SUSY transformations [48]. As a result the behaviour of $\tilde{u}^*$ near the origin is given by the conjugate of (4.3.28) with different values of constants $a^*_{1,2}$ and $b^*_{1,2}$, i.e., $a^*_{1,2} \to \tilde{a}^*_{1,2}$ and $b^*_{1,2} \to \tilde{b}^*_{1,2}$, and shifted singularity indices $\tilde{\nu} = \mathrm{diag}(\nu_1 + 1, \nu_2 - 1)$ (to fix ideas, we consider the case $\nu_2 > \nu_1$)

$$\tilde{u}^*(r \to 0) = \begin{pmatrix} \tilde{a}^*_1 r^{\nu_1 + 2} & \tilde{b}^*_1 r^{-\nu_1 - 1} \\ \tilde{a}^*_2 r^{\nu_2} & \tilde{b}^*_2 r^{-\nu_2 + 1} \end{pmatrix} [1 + \mathrm{o}(r)]. \tag{4.3.61}$$

We have to split the discussion into two subcases, once again. For $\tilde{\nu}_2 = \tilde{\nu}_1$, i.e. $\nu_2 = \nu_1 + 2$, an equation similar to (4.3.59) implies that $\tilde{w}^*$ behaves like r^{-1} multiplied by a non-diagonal matrix close to the origin. Consequently, the final potential V_2 will be unphysical in general, with non-diagonal singular terms at the origin; therefore, we will not consider this case any further. For $\tilde{\nu}_2 > \tilde{\nu}_1$, i.e. $\nu_2 > \nu_1 + 2$, the same reasoning as above implies that the transformed potential V_2 has

the following singularity indices: $\tilde{\nu} \to \bar{\nu} = \mathrm{diag}(\tilde{\nu}_1 + 1, \tilde{\nu}_2 - 1) = \mathrm{diag}(\nu_1 + 2, \nu_2 - 2)$. Finally, for $\tilde{\nu}_2 < \tilde{\nu}_1$, which is the case for $\nu_2 = \nu_1 + 1$, the second transformation restores the initial singularity indices $\tilde{\nu} \to \bar{\nu} = \mathrm{diag}(\tilde{\nu}_1 - 1, \tilde{\nu}_2 + 1) = \mathrm{diag}(\nu_1, \nu_2)$.

The modification rules for the singularity indices of the potential may thus be summarized as follows in the physical cases:

$$(\nu_1, \nu_1) \xrightarrow{L} (\nu_1, \nu_1)\,, \tag{4.3.62}$$

$$(\nu_1, \nu_1 + 1) \xrightarrow{L} (\nu_1, \nu_1 + 1)\,, \tag{4.3.63}$$

$$(\nu_1, \nu_1 + m) \xrightarrow{L} (\nu_1 + 2, \nu_1 + m - 2)\,, \qquad m > 2. \tag{4.3.64}$$

From here it is seen that in all cases $\mathrm{Tr}\nu = \mathrm{Tr}\bar{\nu}$.

We are now ready to construct the regular solution of the transformed Schrödinger equation. For $\nu_2 \neq \nu_1$ superpotentials w and $\tilde{w}^*$ have the structure given by (4.3.59) or (4.3.60) depending on the singularity indices. Therefore the first-order transformations L_1 and L_2 are conservative. Thus, the result of the two-fold SUSY transformation applied to $\varphi_0(k, r)$ in the most general form can be written as follows

$$L\varphi_0(k, r) = \varphi_2(k, r)U_0(k)\,, \tag{4.3.65}$$

where U_0 is a constant matrix with respect to r. Matrix $U_0(k)$ is invertible $\forall k \neq k_{1,2}$, which can be seen from (4.3.7). In the case $\nu_2 = \nu_1$, the conservativeness of the two-fold SUSY transformation can be established by considering (4.3.54) where ψ_0 is replaced by a regular solution. Note that $\varphi_{0,2}(k, r) = \varphi_{0,2}(-k, r)$; therefore, matrix U_0 is an even matrix function of wave number k, $U_0(k) = U_0(-k)$. The precise value of U_0 is not important for the following.

Using the relation between the Jost solutions and the regular solution (1.1.27), which in view of (4.3.56) and (4.3.65) we rewrite as

$$\varphi_2(k, r)U_0(k) = \frac{i}{2k}\left[f_2(-k, r)U_\infty(-k)F_0(k) - f_2(k, r)U_\infty(k)F_0(-k)\right], \tag{4.3.66}$$

we find the transformed Jost matrix

$$F_2(k) = U_\infty(-k)F_0(k)U_0^{-1}(k)\,. \tag{4.3.67}$$

The transformation of the scattering matrix then follows from its definition (1.1.33),

$$S_2(k) = e^{i\bar{l}\frac{\pi}{2}}U_\infty(k)e^{-il\frac{\pi}{2}}S_0(k)e^{-il\frac{\pi}{2}}U_\infty^{-1}(k)e^{i\bar{l}\frac{\pi}{2}}\,, \tag{4.3.68}$$

and is equivalent to (4.3.32) and (4.3.33). Note that the transformed S-matrix does not depend on U_0. To prove that matrix O is real and orthogonal, one has to remember that l_1, l_2, $\bar{l}_1$, $\bar{l}_2$ all have the same parity, as implied by (4.3.19) and (4.3.31).

D. Diagonalizing S_2 in the same way as S_0 in (1.1.34),

$$R_2^T(k)S_2(k)R_2(k) = \mathrm{diag}\left(e^{2i\delta_{2;1}(k)}, e^{2i\delta_{2;2}(k)}\right), \tag{4.3.69}$$

and remembering that matrices R_0 and O both belong to $SO(2)$, one sees that S_0 and S_2 have the same eigenvalues. By choosing

$$R_2(k) = O(k)R_0(k)\begin{pmatrix} 0 & 1 \\ -1 & 0 \end{pmatrix}, \tag{4.3.70}$$

one inverts the order of these eigenvalues, in agreement with (4.3.31), hence (4.3.34). This allows to keep parametrization (1.1.35) with a modification of mixing parameter given by (4.3.36) and vanishing at zero energy, $\epsilon_2(0) - \epsilon_0(0) = 0$. □

These eigenphase preserving transformations may be considered as a generalization of those in the case of different parities (see (4.1.37)). Let us finally note that the transformed potential V_2 can be used as a starting point for a next eigenphase preserving transformation. This means that the two-fold SUSY transformation considered above can be iterated as long as desirable. A chain of n such transformations over the initial potential V_0 will lead to the following mixing parameter:

$$\epsilon_{2n}(k) = \epsilon_0(k) \pm (-1)^m \sum_{j=0}^{n} \arctan \frac{k^2}{2\chi_j^2} \tag{4.3.71}$$

leaving the eigenphase shifts unchanged.

4.3.3 Phenomenological neutron-proton interaction potential

An important consequence of the theorem 12 is the possibility to use the single channel SUSY transformations fitting the experimental values of the eigenphase shifts. Afterwards, the mixing parameter can be fitted without further modification of the eigenphase shifts by the eigenphase preserving SUSY transformations. Thus, the main advantage of our approach consists in splitting the inversion problem into two independent parts: (1) fitting eigenphase shifts to experimental values independently for each channel and (2) fitting the mixing parameter between these channels. As a result, one can construct a potential which gives rise to the desirable scattering matrix using a chain of SUSY transformations.

Let us consider how this strategy works in the ${}^3S_1 - {}^3D_1$ coupled-channel case of the neutron-proton scattering. We first build the simplest possible potential, valid at low energy only, in the spirit of Ref. [156]. Next, we generalize this result to get a potential that fits scattering data with better accuracy on the whole elastic region.

The scattering matrix in Ref. [156] was chosen in the following form

$$S(k) = \frac{1}{k^4 + 4\chi^4} \begin{pmatrix} 2\chi^2 & k^2 \\ -k^2 & 2\chi^2 \end{pmatrix} \begin{pmatrix} \frac{(k+i\kappa_1)(k+i\kappa_2)}{(k-i\kappa_1)(k-i\kappa_2)} & 0 \\ 0 & 1 \end{pmatrix} \begin{pmatrix} 2\chi^2 & -k^2 \\ k^2 & 2\chi^2 \end{pmatrix}. \tag{4.3.72}$$

We will present two possible chains *SUSY 1* and *SUSY 2* of SUSY transformations leading to S-matrix (4.3.72). The difference between these chains consists in the different ways to introduce the bound state.

SUSY 1

To reproduce s-wave eigenphase shift and the deuteron binding energy we use the Bargman potential [157], which can also be obtained by two supersymmetric transformations of the zero potential. It reads [156]

$$V_{bg}(r) = -2\frac{d^2}{dr^2} \ln W[\exp(\kappa_1 r), \sinh(\kappa_2 r)] \tag{4.3.73}$$

$$= \frac{2\kappa_2^2(\kappa_1^2 - \kappa_2^2)}{[\kappa_2 \cosh(\kappa_2 r) - \kappa_1 \sinh(\kappa_2 r)]^2}, \tag{4.3.74}$$

where W is a Wronskian determinant. As in [156] we choose

$$\kappa_1 = 0.232\,, \qquad \kappa_2 = 0.944\,. \tag{4.3.75}$$

We reproduce zero phase shift in d-wave choosing the centrifugal term $V_d = 6/r^2$ as the second potential .

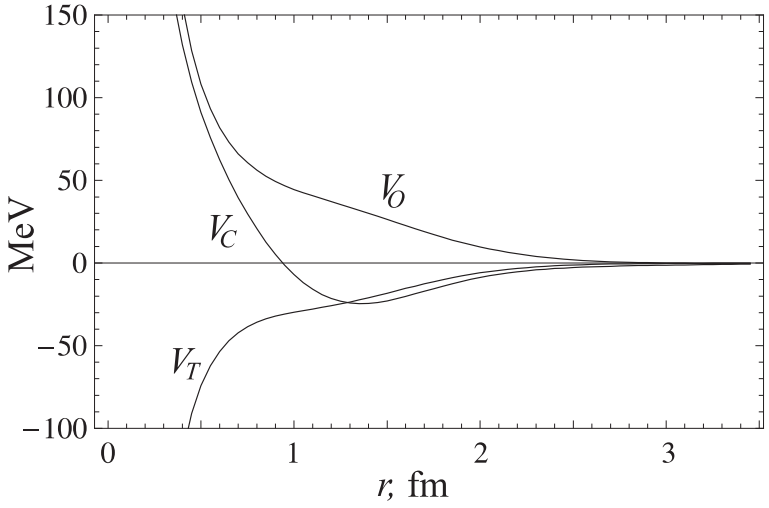

Figure 4.7: *SUSY 1.* Exactly solvable potential curves obtained from two uncoupled potentials with parameters $\kappa_1 = 0.232\,, \kappa_2 = 0.944$ by the eigenphase preserving transformation with $\chi = 1.22$.

The following regular and Jost solutions are used to construct the factorization solution for the eigenphase preserving SUSY transformation

$$\varphi_s(k,r) = \frac{2i\left[(k^2+\kappa_1^2)\kappa_2\sin(kr) - (k(\kappa_1^2-\kappa_2^2)\cos(kr) + \kappa_1(k^2+\kappa_2^2)\sin(kr))\tanh(\kappa_2 r)\right]}{(k-\kappa_1)(k-\kappa_2)(\kappa_2-\kappa_1\tanh(\kappa_2 r))}\,, \tag{4.3.76}$$

$$\varphi_d(k,r) = \frac{2i\left[(3-k^2r^2)\sin(kr) - 3kr\cos(kr)\right]}{k^2r^2}\,, \tag{4.3.77}$$

$$f_s(k,r) = \frac{\left[(k-i\kappa_1)\kappa_2 + (i\kappa_2^2 - k\kappa_1)\tanh(\kappa_2 r)\right]}{(k+i\kappa_2)(\kappa_2-\kappa_1\tanh(\kappa_2 r))}\,\mathrm{e}^{ikr}\,, \tag{4.3.78}$$

$$f_d(k,r) = \mathrm{e}^{ikr}\left(1 + 3ikr - \frac{3}{(kr)^2}\right)\,. \tag{4.3.79}$$

According to the theorem 12 factorization solution $u(r)$ [in the case $V_0 = \mathrm{diag}(V_{bg}, V_d)$] reads

$$u(r) = \begin{pmatrix} \varphi_s(k_1,r) & if_s(k_1,r) \\ -i\varphi_d(k_1,r) & f_d(k_1,r) \end{pmatrix}, \qquad -u'' + V_0 u = k_1^2 u\,, \qquad k_1 = \chi(1+i)\,, \tag{4.3.80}$$

and the transformed potential is calculated as follows

$$V_2 = V_0 + 4\chi^2\frac{d}{dr}\left(\mathrm{Im}u'u^{-1}\right)^{-1}\,. \tag{4.3.81}$$

The transformed potential (4.3.81) with $u(r)$ defined in (4.3.80) and $\chi = 1.22$ is shown in figure 4.7. We extract central, tensor and spin-orbital potential curves

$$V_C = V_{2;2,2}\,, \quad V_T = V_{2;1,2}/\sqrt{8}\,, \quad V_O = (V_{2;2,2} - V_{2;1,2}/\sqrt{2} - V_{2;1,1} + 6/r^2)/3\,, \tag{4.3.82}$$

taking into account the exchange of the partial waves under the eigenphase preserving SUSY.

These potential curves are similar to ones shown in figure 13 in Ref. [45]. Ratio of asymptotic amplitudes of the bound state wave function $\eta = A_d/A_s = \kappa_1^2/(2\chi^2) = 0.018081$ coincides with the ratio obtained from S-matrix residue

$$\eta = \frac{\mathrm{res}S_{2,1}(k=i\kappa_1)}{\mathrm{res}S_{1,1}(k=i\kappa_1)} \tag{4.3.83}$$

Table 4.1: Deuteron observables of the studied cases.

parameter	SUSY 1	Kohlhoff (b)	SUSY 2(input)	SUSY 2 (num)	[Newton-Fulton]
E_b	2.2321394	2.2321399	2.2321394	2.2321206	2.2321394
P_d	6.76633	6.77		1.875	2.09
A_s	0.875296	0.8753	$a_s = 0.0584957$	0.8310	0.8269
η	0.0180812	0.018081	0.0393192	0.03949	**-0.018081**

by construction. These potential curves are singular at the origin. Thus this potential significantly differs from the original Newton-Fulton potential.
SUSY 2

We can obtain a potential which is more similar to the Newton-Fulton potential using the initial diagonal potential without bound states

$$V_0(r) = \mathrm{diag}\left(-2\Big(\ln \mathrm{W}\left[v_1, v_2\right](r)\Big)'', \frac{6}{r^2}\right). \tag{4.3.84}$$

The d-wave potential is purely centrifugal, while the s-wave potential is obtained from the zero potential by a second order one-channel SUSY transformation with the factorization solutions $v_1(r) = \sinh(\kappa_1 r)$ and $v_2(r) = \sinh(\kappa_2 r)$. This s-wave potential has no bound state but a singular repulsive core at the origin [83]. Potential V_0 is thus characterized by the singularity and centrifugal indices

$$\nu = \mathrm{diag}(2,2)\,, \quad l = \mathrm{diag}(0,2)\,. \tag{4.3.85}$$

The Jost solution corresponding to potential V_0 reads

$$f_0(k,r) = \mathrm{diag}\Big(f_{0s}(k,r), f_{0d}(k,r)\Big), \tag{4.3.86}$$

where

$$f_{0s}(k,r) = \mathrm{e}^{ikr}\left(1 + \frac{3i}{kr} - \frac{3}{(kr)^2}\right), \tag{4.3.87}$$

$$f_{0d}(k,r) = \left(\frac{\tilde{v}_2'(r)}{\tilde{v}_2(r)} - \partial_r\right)\left(\frac{v_1'(r)}{v_1(r)} - \partial_r\right)\mathrm{e}^{ikr} N_1 N_2\,, \tag{4.3.88}$$

with $\tilde{v}_2 = [(\ln v_1)' - \partial_r]v_2$ and the normalization constants $N_j = (ik - \kappa_j)^{-1}$. The regular solution φ_0 is expressed from (1.1.27) with the Jost matrix

$$F_0(k) = \mathrm{diag}\,(-N_1 N_2, 1)\,. \tag{4.3.89}$$

Using these expressions for the Jost and regular solutions, one may construct with (4.3.37) a transformation solution u with asymptotics (4.3.27) and (4.3.28), according to Lemma 5. The eigenphase preserving transformation described in Theorem 12 leads to a singular potential V_2 without bound state and with

$$\bar{\nu} = \mathrm{diag}(2,2)\,, \quad \bar{l} = \mathrm{diag}(2,0)\,. \tag{4.3.90}$$

The eigenphase shifts of the transformed S-matrix coincide with the initial eigenphase shifts,

$$\delta_s(k) = -\arctan\frac{k}{\kappa_1} - \arctan\frac{k}{\kappa_2}\,, \tag{4.3.91}$$

$$\delta_d(k) = 0\,. \tag{4.3.92}$$

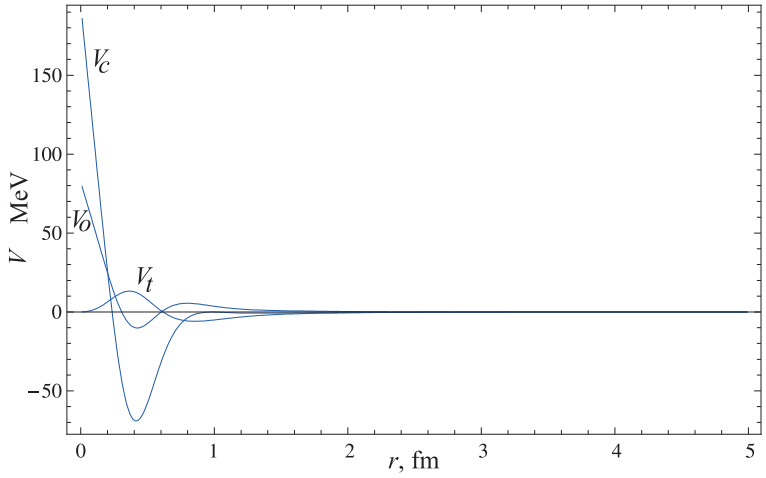

Figure 4.8: *SUSY 2.* Exactly solvable potential curves obtained by the eigenphase preserving SUSY transformation and phase equivalent bound state addition, $\kappa_1 = 0.232\,, \kappa_2 = 0.944$, $\chi = 1.22$.

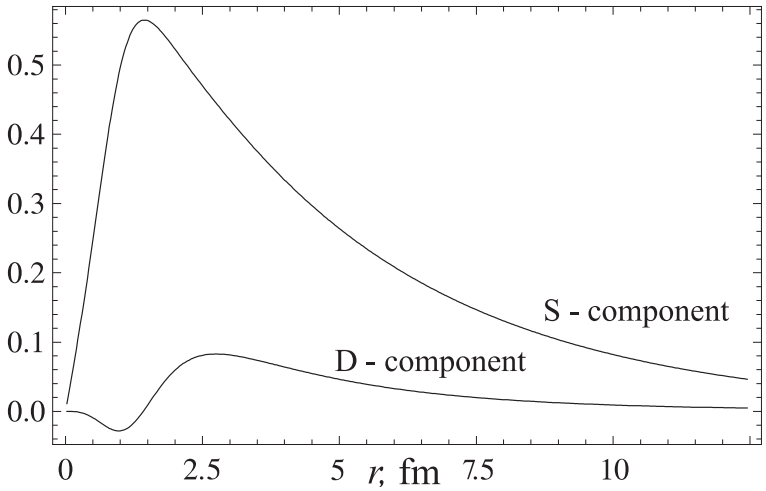

Figure 4.9: (a) Wave function with the following asymptotic constants $A_s = 0.833$, $A_d = 0.0856$.

The mixing angle is given by (4.3.36) with $\epsilon_0 = 0$ and positive sign. Note that due to the exchange of centrifugal terms after the eigenphase preserving SUSY the first channel corresponds to d-wave and the second channel corresponds to s-wave. The Newton-Fulton potential differs from the potential constructed above because it has one bound state.

In the contrast with *SUSY 1* the bound state is introduced by phase-equivalent bound state addition for coupled channels [91]. The corresponding transformed potential may be defined in terms of the vector solution

$$\psi_p(r) = f_2(i\kappa_1, r)\vec{a}_1\,, \qquad \vec{a}_1 = (a_d^2 + a_s^2)^{-1/2}(a_d, a_s)^T\,, \tag{4.3.93}$$

as follows

$$V = V_2 - 2\frac{d}{dr}w_p\,, \qquad w_p = -\frac{\psi_p\psi_p^+}{(a_s^2 + a_d^2)^{-1} + \int\limits_r^\infty \psi_p^+\psi_p dt}\,. \tag{4.3.94}$$

Here f_2 is the Jost solution of the Schrödinger equation with potential V_2, a_d and a_s are arbitrary constants. These constants are proportional to the asymptotic amplitudes A_d and A_s of the bound state, $A_d/A_s = a_d/a_s$.

Table 4.2: Factorization constants

s_j, fm^{-1}	d_j, fm^{-1}	Modulus χ, fm^{-2}	Argument α
0.2315380	0.671119	0.134547	3.09823
1.752295	3.39537	11.3097	4.01335
2.173204	0.401557	10.1828	0.742398

Since Newton-Fulton potential is finite at the origin we impose this requirement to the potential $V(r)$ thus obtaining a link between asymptotic amplitudes

$$\frac{A_s}{A_d} = \frac{8\chi^3 + 8\chi^2\kappa_1 + 4\chi\kappa_1^2 + \kappa_1^3}{2\chi^2\kappa_1}\,, \tag{4.3.95}$$

The resulting potential and the corresponding wave function are shown in figures 4.8 and 4.9, respectively. The shape of the potential curves is similar to one presented in [156]. Note that the finiteness of the potential at the origin was not reproduced in [45]. This shows that the method of SUSY transformations is more flexible.

In table 4.1 we compare deuteron observables obtained by *SUSY 1* with respect to the case (b) in Ref. [45] and results of *SUSY 2* with respect to original results of Newton and Fulton [156]. It can be seen that our results are in agreement with Ref. [45]. The chain *SUSY 2* contains two two-fold coupled channel SUSY transformations thus making analytical calculations to complicated. The bound state observables for the resulting potential were obtained numerically. Therefore we provide in Table 4.1 both input data and numerical values.

We believe that quantitative difference with Ref. [156] is explained by a somewhat different input parameters. It should be stressed, that ratio $\eta = -0.018081$ reported in [156] do not correspond to the ratio of asymptotic normalization constants. Apparently, Newton and Fulton did not realize that their potential has long-ranged tails (see figure 4.17), thus A_s/A_d cannot be determined from (4.3.83). It is determined from (4.3.95).

SUSY 3

At the end of this chapter, we present more sophisticated example which combines all ingredients of SUSY inversion. In this example, we start from Reid93 potential [158] and fit its phase shifts and mixing parameter as follows

$$\delta_s(k) = \pi - \arctan\left(\frac{k}{s_1}\right) - \arctan\left(\frac{k}{s_2}\right) - \arctan\left(\frac{k}{s_3}\right)\,, \tag{4.3.96}$$

$$\delta_d(k) = \delta_{d0}(k) - \arctan\frac{k}{d_1} - \arctan\frac{k}{d_2} - \arctan\frac{k}{d_3}\,, \tag{4.3.97}$$

$$\delta_{d0}(k) = \arctan\frac{3kx_0^2}{3x_0 - k^2(x_0^3 + c)}\,, \tag{4.3.98}$$

$$\epsilon_1 = \sum_{j=1}^{3} \arctan\left(\frac{E}{\chi_j \sin(\alpha_j)} + \tan\left(\alpha_j - \frac{\pi}{2}\right)\right)\,. \tag{4.3.99}$$

This fit corresponds to the three single channel SUSY transformations in the s wave applied to the zero potential and to the three single channel SUSY transformations in the d wave applied to the following potential

$$V(r) = \frac{6(r+x_0)((r+x_0)^3 - 2c)}{[c + (r+x_0)^3]^2}\,, \tag{4.3.100}$$

Table 4.3: Deuteron observables for the Reid93 inversion.

parameter	Reid93	SUSY (input/num)
E_b, MeV	-2.224575	-2.224575/-2.224572
P_d,	5.699	/7.035
A_s	0.8853	/0.8658
η	0.02514	0.02863/0.02902
Q, fm^2	0.2703	/0.2935
$< r >$, fm	1.969	/1.939

where additional constraints

$$x_0 = \sum_{j=1}^{3} \frac{1}{d_j}\,, \qquad c = -\sum_{j=1}^{3} \frac{1}{\kappa_j^3}\,,$$

are imposed to provide a correct effective range expansion. The coupling is introduced by the three two-fold eigenphase preserving transformations. The factorization energies are $-s_j^2$, $-d_j^2$ and $\chi_j \exp(i\alpha_j)$ for the s wave, d wave and coupling, respectively. Note that s_1 is fixed from the deuteron binding energy. The eigenphase preserving transformations involve complex factorization energies, whereas in our theorem 12 only purely imaginary factorization energies were used. As it turns, the method works in more general case, but we skip these technical details. Using standard fitting algorithms available in the packet of analytical calculations Mathematica, we found the following values of parameters listed in table 4.2.

In figures 4.10, 4.11 and 4.12 we compare the phase shifts of the Reid93 potential and ones given by (4.3.96), (4.3.97) and (4.3.99) in the whole elastic region ($T_{lab} < 350$ Mev). The transition between Mev and fm^{-2} may be done by coefficient $\hbar/(2\mu) = 41.471$ Mev fm^{-2}, where μ is the reduced mass. Potential curves are compared in figures 4.13, 4.14 and 4.15. The potential generated by SUSY transformation has several wells which indicates that the choice of the factorization constants is not correct. We should stress, that diagonal potential generated by single-channel SUSY transformations does not have such drawback. Hence, we can conclude, that the problem may be in the complex factorization constants responsible for coupling (see figure 4.16). Finally, in table 4.3 we compare deuteron observables for the Reid93 potential and for its SUSY inversion. The eigenphase preserving transformations were made numerically. As a starting point, we used analytical expressions for the initial diagonal potential with eigenphase shifts (4.3.96) and (4.3.97). There is a difference between input and output parameters due to numerical errors.

Finally, to compare the asymptotic behaviour of three potentials (*SUSY 1, 2, 3*) and the asymptotics of the Reid93 potential we plot $\log|V_{i,j}|$ in figure 4.17. Potential *SUSY 1* related with the von Geramb results decreases to fast, whereas *SUSY 2* has long-range tails. This comparison with the one-pion-exchange asymptotics may be useful to improve potential *SUSY 3* in future work.

Note that our aim in this example is to show that we can improve phase shifts fit and values of deuteron observables of the simplest Newton-Fulton model by using SUSY transformations. It seems that this aim has been reached. We hope that a fine tuning of the factorization constants may improve the shape of the potential and agreement with the deuteron parameters significantly. The main difference here is that there are several inequivalent configurations of complex factorization energies leading to similar mixing parameters.

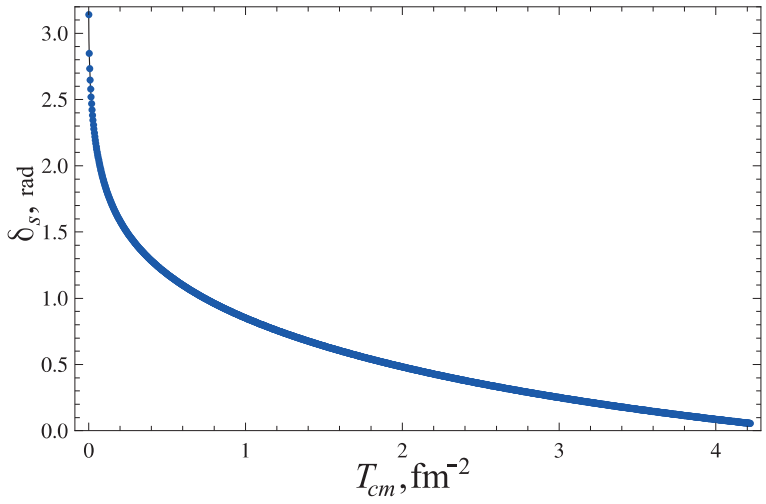

Figure 4.10: s-wave phase shifts. Solid curve corresponds to the Reid93 potential, dots correspond to (4.3.96).

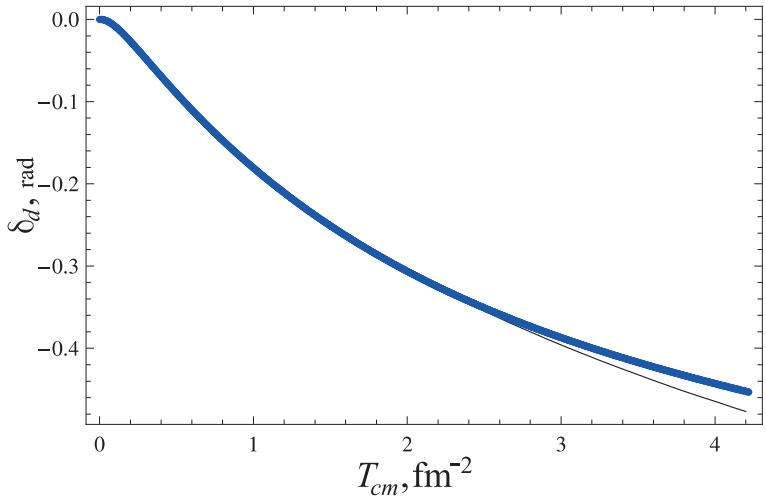

Figure 4.11: d-wave phase shifts. Solid curve corresponds to the Reid93 potential, dots correspond to (4.3.97).

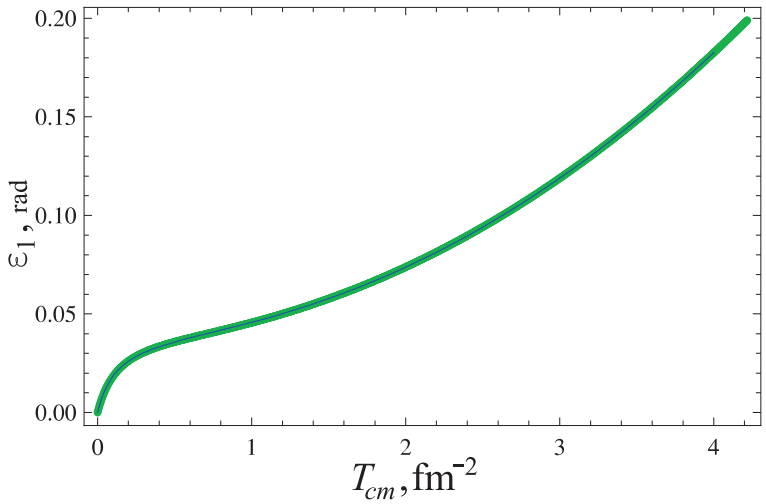

Figure 4.12: Mixing parameter. Solid curve corresponds to the Reid93 potential, dots correspond to (4.3.99).

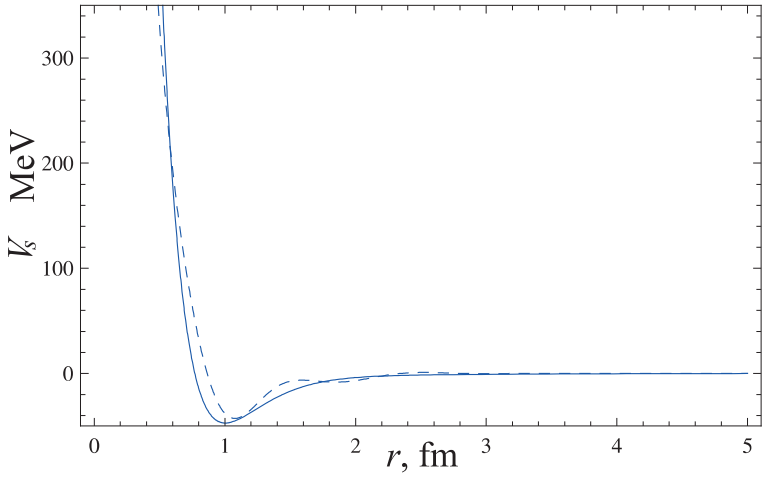

Figure 4.13: *SUSY 3*, s-wave potential. Solid curve corresponds to the Reid93 potential, Dashed curve corresponds to the potential generated by SUSY transformations.

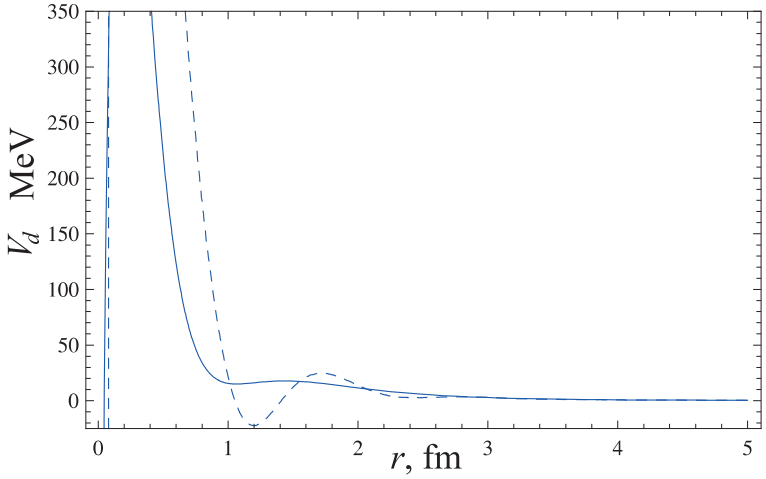

Figure 4.14: *SUSY 3*, d-wave potential. Solid curve corresponds to the Reid93 potential, Dashed curve corresponds to the potential generated by SUSY transformations.

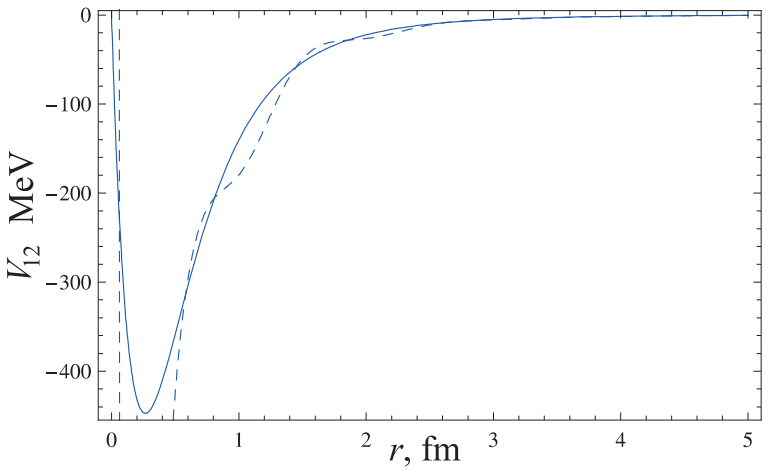

Figure 4.15: *SUSY 3*, sd-coupling potential. Solid curve corresponds to the Reid93 potential, Dashed curve corresponds to the potential generated by SUSY transformations.

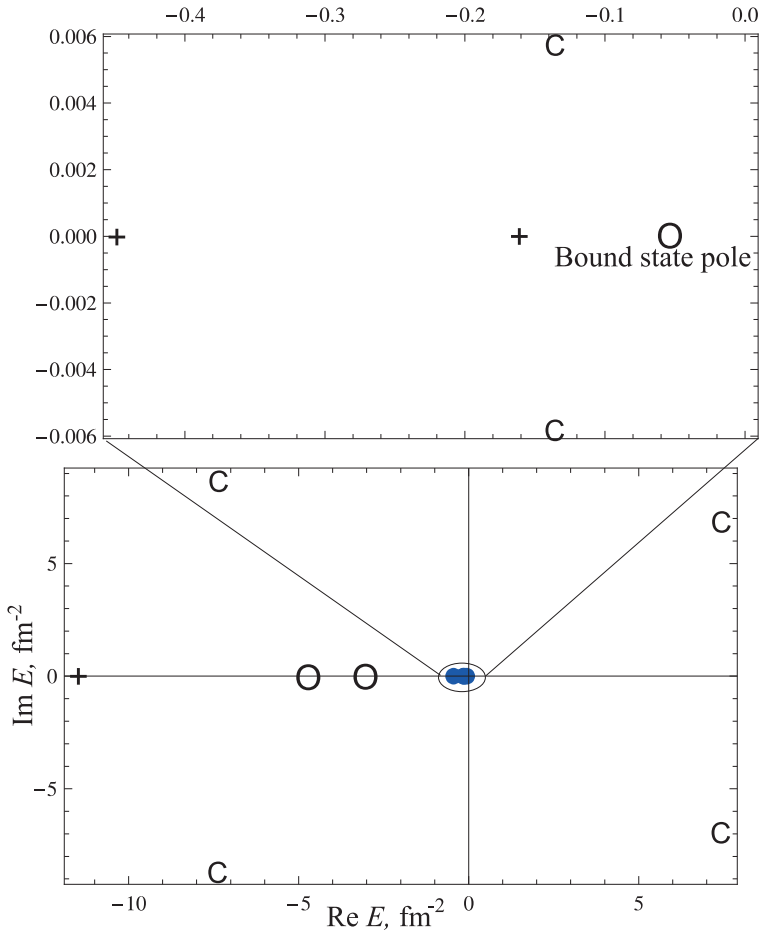

Figure 4.16: Position of S-matrix poles (factorization constants). Poles responsible for the coupling are shown by C, S-wave poles are shown by O and D-wave poles are shown by +.

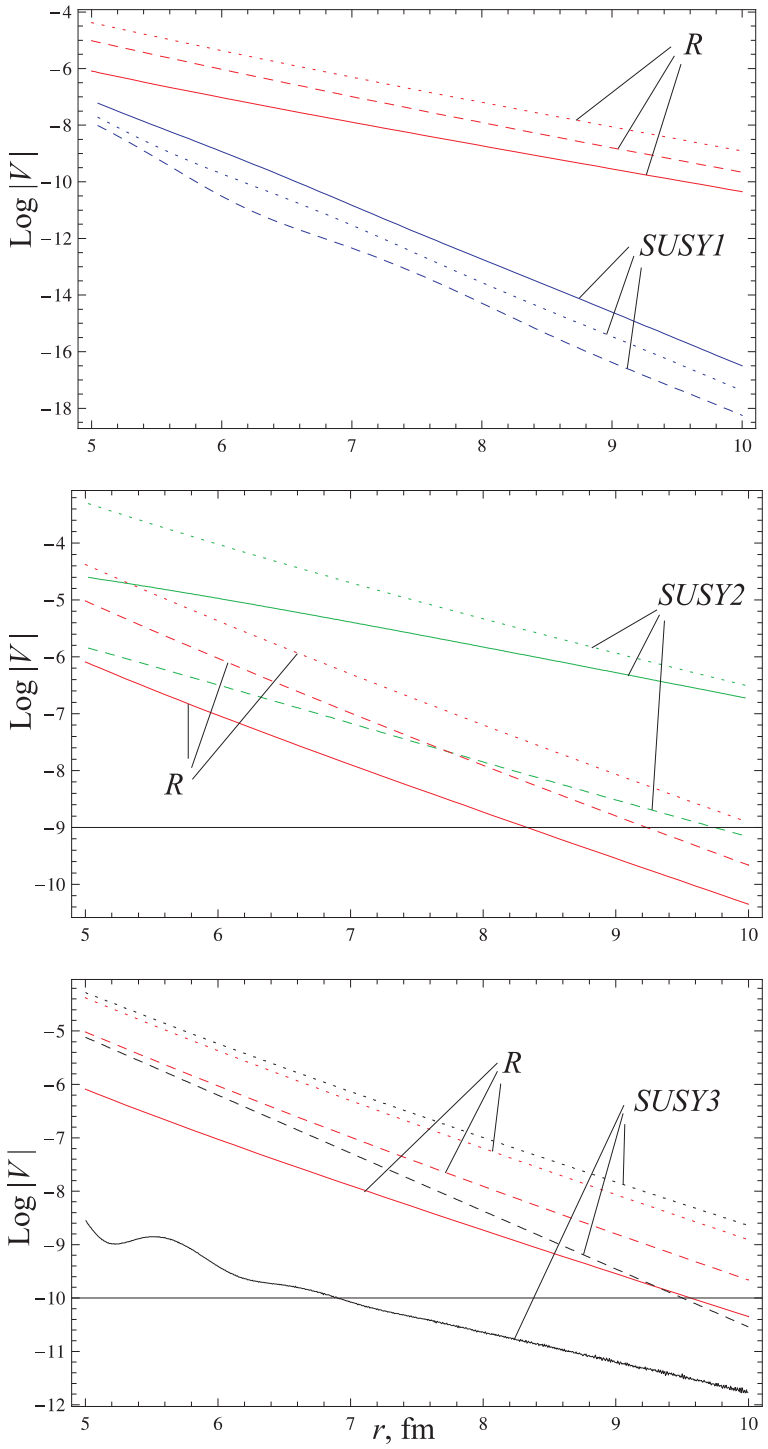

Figure 4.17: Asymptotic behaviour of $\log|V_{i,j}|$. Solid lines correspond to $V_{1,1}$ (S wave), dashed lines correspond to $V_{2,2}$ (D wave), dotted lines correspond to $V_{1,2}$. R – asymptotics of Reid93 potential.

Conclusion

In the case of the single-channel Schrödinger equation, a careful study of propagators and Green functions for SUSY partner Hamiltonians has been made. We have shown that it is possible to establish a relation between the traces of the Green functions for the two partner Hamiltonians for the cases of the deletion of the ground state, the addition of a new ground state and when the two Hamiltonians are isospectral. The formulas derived in this work are valid for the general case of Hamiltonians having both discrete and continuous spectra. Our results show that when a continuous spectrum is present, each of the traces of the Green functions for the SUSY partners may diverge but the difference between the traces remains finite. We have illustrated our results by considering the case of the free motion on the full line. We would like to note that the difference of the traces of the Green functions of the two SUSY partner Hamiltonians appears as the trace (actually super-trace) of the Green function of the supersymmetric Schrödinger equation (supersymmetric Green function). Thus, our results reveal the possibility of divergence of the component traces of the supersymmetric Green function while its super-trace remains finite.

Assuming the partner Hamiltonians to be linked by polynomial supersymmetry of a general type, we have derived user friendly expressions interrelating the corresponding associated propagators. Since the propagators may also be defined in terms of continual integrals, the results should be useful in exploring new classes of continual integrals. We have applied our general technique to derive propagators for transparent potentials and for a family of SUSY partner potentials of the harmonic oscillator. The generalization to time-dependent and complex potentials has also been presented.

In the case of the coupled-channel Schrödinger equation, basing on the exactly-solvable N-channel Cox potential derived from a non-conservative supersymmetric transformation of the vanishing potential, we have established different parameterizations of this potential, as well as a necessary and sufficient condition for its regularity. A careful study of the spectral properties of the N-channel Cox potential has been given. Our treatment is based on the analysis of the Jost-matrix determinant zeros. We have shown that the zeros of the Jost-matrix determinant are the roots of an $N2^{N-1}$th-order algebraic equation. The number of bound states n_b is restricted by the number of channels, $0 \leq n_b \leq N$. The upper bound for the number of resonances is $(N-1)2^{N-2}$. The generalization is based on the analysis of the behavior of the Jost-matrix eigenvalues. In the $N = 2$ case, a full analysis of the corresponding Jost matrix has been carried out. In particular, the structure of the zeros of the Jost determinant has been presented geometrically.

With ultracold gases in mind, we have also studied the low energy S-matrix and the scattering length of the 2×2 Cox potential. Using the independence of scattering properties from interaction details in the regime with a large scattering length, a model of alkali-metal atom-atom scattering has been constructed. This provides interesting exactly-solvable schematic models for the interplay of a magnetically-induced Feshbach resonance with a bound state or a virtual state close to threshold.

We consider the development of supersymmetric transformations as a very promising tool for the multi-channel inverse scattering problem with threshold difference and for the construction of more advanced exactly-solvable coupled-channel models. In particular, iterations or chains of transformations might lead to more complicated Jost functions, with arbitrary number of bound states and resonances, hopefully still with a tractable connection between potential parameters and physical observables.

As far as physical applications are concerned, atom-atom interactions are both very interest-

ing today, due to the active research field of ultracold gases, and rather simple with respect to supersymmetric quantum mechanics, as only s-waves have to be considered and as the interaction is short ranged (no Coulomb term). We foresee to apply the present model to other systems presenting these simple features, namely coupled s-wave baryon-baryon interactions, with at least one neutral baryon. In the longer term, we hope to generalize our method to higher partial waves and to Coulomb interactions. This should allow us to construct useful models in the context of low-energy nuclear reactions, the field which first motivated the work of Feshbach [145,146] on coupled-channel resonances, leading to possible applications in nuclear astrophysics and exotic-nuclei low-energy reactions.

In the case of coinciding thresholds, coupling SUSY transformations have been studied. In particular, we have formulated conditions imposed on the transformation function to get a nontrivially coupled scattering matrix resulting from the first order SUSY transformation. A careful analysis of N-channel SUSY transformations between uncoupled potentials with equal thresholds but arbitrary partial waves and coupled ones has been made. A family of iso-phase potentials generated by a first order coupling SUSY transformation has been obtained. The analysis of the zeros of the Jost-matrix determinant for these potentials has shown that the SUSY transformation creates a new M fold degenerate bound state energy $E_b = -\kappa^2$ and an $N - M$ fold degenerate virtual state energy $E_v = -\kappa^2$.

In the most important practical case, the two-channel case, we have analyzed the behaviour of the superpotential and potential at large distances in details. We have found an unusual effect, i.e. a modification of the long-range behaviour of the potential under a coupling SUSY transformation, which consists in an exchange of the partial waves between the channels. The analysis of the phase shifts and mixing angle has demonstrated how scattering properties change after a SUSY transformation.

As an illustration of our approach, several simple examples have been presented. First, to emphasize the difference between couplings in the potential, Jost and scattering matrices, we presented examples of a trivially coupled scattering matrix corresponding to non trivially coupled potential and Jost matrices. These examples answer the general questions raised in the beginning of chapter 4: situations may exist where a non trivially coupled potential leads to a trivially coupled S-matrix, with either a trivially or non trivially coupled Jost matrix. Thus, the requirement that an S-matrix be non trivially coupled is more restrictive than the similar requirement for a potential matrix or the Jost matrix. Afterwards, a non trivial coupling has been introduced in the $s-s$, $s-p$ and $s-d$ channels. In both $s-s$ and $s-p$ examples, we have shown how to fit the low-energy behaviour of the phase shifts and mixing angle using parameters of the transformation. In the $s-d$ case, to satisfy the effective range expansion for the mixing parameter, we used an initial potential with a zero energy virtual state. Nevertheless, the obtained phase shifts of the coupled $s-d$ potential do not satisfy the correct effective range expansion. Moreover, the presence of the zero energy virtual state strongly restricts possible applications of our method to the inversion in this case.

A careful analysis of the first order SUSY transformations indicates the significant drawback of this transformations and gives us a hint of how to avoid this drawback. We have developed the technique of the second-order transformations. In this way we have introduced an "eigenphase preserving" two-fold SUSY transformation for the two-channel Schrödinger equation with partial waves of the same parity (e.g. $s-d$). This transformation alters the mixing parameter between channels without modifying the eigenphase shifts (as the first order coupling transformation in the $s-p$ case). Chains of such transformations lead to coupling between channels in the scattering ma-

trix which correspond to nontrivial k-dependences of the mixing angle (4.3.71). With a reasonably small number of parameters, such mixing angles are probably able to fit experimental data, in a similar way to the usual phase shift fitting used in one-channel SUSY inversion [84, 91]. Combining both techniques, we obtain a complete method of coupled-channel scattering data inversion based on SUSY transformations. As a first application of this method, we have reproduce simple model presented in [156] and its revision in [45]. We also have constructed an example of the potential obtained from the inversion of Reid93 scattering data, thus showing how SUSY inversion may work in the coupled-channel case.

Acknowledgements

This work was supported by the International Cooperation Funds of the Université Libre de Bruxelles and by the Russian 'Dynasty' foundation. I would like to thank my PhD directors. It was Boris Samsonov who involved me into the serious scientific work and gave me the first lessons in this activity. Jean-Marc Sparenberg showed me how mathematical physics may be related with real physical problems. Moreover, he tried to explain me the importance of clear and logical presentations of ideas and results. I would also like to thank Daniel Baye for very interesting discussions and Vladislav Bagrov with whom I started to work in SUSY QM.

My stays in Brussels were fruitful due to the friendly and creative atmosphere of PNTPM. I appreciated the assistance of my friends in Moscow (P. Inzhelevskij, I. Chernov) in obtaining my visa. Many thanks to my parents, who inspired me to begin and to finish this work.

Bibliography

[1] B. F. Samsonov, C. V. Sukumar, and A. M. Pupasov. SUSY transformation of the Green function and a trace formula. *J. Phys. A: Math. Gen.*, 38:7557–7565, 2005.

[2] B. F. Samsonov and A. M. Pupasov. Darboux transformation of the Green's function of a regular Sturm-Liouville problem. *Rus. Phys. J*, 48:1020–1028, 2005.

[3] A. M. Pupasov and B. F. Samsonov. Exact propagators for complex SUSY partners of real potentials. *Phys. Lett. A*, 356:210–214, 2006.

[4] A. M. Pupasov and B. F. Samsonov. Exact propogators for soliton potentials. *Symm. Integrabil. Geom.: Meth. Appl.*, 1:020 (7pp), 2005.

[5] A. M. Pupasov, B. F. Samsonov, and U. Guenther. Exact propagators for SUSY partners. *J. Phys. A: Math. and Theor.*, 40:10557–10587, 2007.

[6] A. M. Pupasov, B. F. Samsonov, and J.-M. Sparenberg. Exactly-solvable coupled-channel potential models of atom-atom magnetic Feshbach resonances from supersymmetric quantum mechanics. *Phys. Rev. A*, 77:012724 (14pp), 2008.

[7] A. M. Pupasov, B. F. Samsonov, and J.-M. Sparenberg. Spectral properties of non-conservative multichannel SUSY partners of the zero potential. *J. Phys. A: Math. and Theor.*, 41:175209 (17pp), 2008.

[8] A. M. Pupasov, B. F. Samsonov, J.-M. Sparenberg, and D. Baye. Exactly-solvable coupled-channel models from supersymmetric quantum mechanics. *Mod. Phys. Lett. B*, 22:2277–2286, 2008.

[9] A. M. Pupasov, B. F. Samsonov, J.-M. Sparenberg, and D. Baye. Coupling between scattering channels with SUSY transformations for equal thresholds. *J. Phys. A: Math. Theor.*, 42:195303 (19pp), 2009.

[10] A. M. Pupasov, B. F. Samsonov, J.-M. Sparenberg, and D. Baye. Eigenphase preserving two-channel SUSY transformations. *J. Phys. A: Math. Theor.*, 43:155201 (15pp), 2010.

[11] M. H. Anderson, J. R. Ensher, M. R. Matthews, C. E. Wieman, and E. A. Cornell. Observation of Bose-Einstein condensation in a dilute atomic vapor. *Science*, 269:198–201, 1995.

[12] H. T. C. Stoof, M. Houbiers, C. A. Sackett, and R. G. Hulet. Superfluidity of spin-polarized ^{6}Li. *Phys. Rev. Lett.*, 76:10–13, 1996.

[13] M. Houbiers, R. Ferwerda, H. T. C. Stoof, W. I. McAlexander, C. A. Sackett, and R. G. Hulet. Superfluid state of atomic ^{6}Li in a magnetic trap. *Phys. Rev. A*, 56:4864–4878, 1997.

[14] M. Bartenstein, A. Altmeyer, S. Riedl, R. Geursen, S. Jochim, C. Chin, J. Hecker Denschlag, R. Grimm, A. Simoni, E. Tiesinga, C. J. Williams, and P. S. Julienne. Precise determination of ^{6}Li cold collision parameters by radio-frequency spectroscopy on weakly bound molecules. *Phys. Rev. Lett.*, 94:103201 (4pp), 2005.

[15] A. J. Moerdijk, B. J. Verhaar, and A. Axelsson. Resonances in ultracold collisions of ^{6}Li, ^{7}Li, and ^{23}Na. *Phys. Rev. A*, 51:4852–4861, 1995.

[16] H. Kamano, B. Julia-Diaz, T.-S. H. Lee, A. Matsuyama, and T. Sato. Dynamical coupled-channels study of π N $\to \pi\pi$ N reactions. *Phys. Rev. C*, 79:025206 (11pp), 2009.

[17] H. Esbensen. Coupled-channels calculations of ^{16}O+^{16}O fusion. *Phys. Rev. C*, 77:054608 (7pp), 2008.

[18] C. Beck, N. Keeley, and A. Diaz-Torres. Coupled-channels effects in elastic scattering and near-barrier fusion induced by weakly bound nuclei and exotic halo nuclei. *Phys. Rev. C.*, 75:054605 (11pp), 2007.

[19] V. I. Zagrebaev and V. V. Samarin. Near-barrier fusion of heavy nuclei: Coupling of channels. *Phys. Atom. Nucl.*, 67:1462–1477, 2004.

[20] M. O. Scully and M. S. Zubairy. *Quantum Optics*. Cambridge University Press, Cambridge, 1997.

[21] M. Hirvensalo. *Quantum computing*. Springer-Verlag, New York, 2001.

[22] J. R. Taylor. *Scattering Theory: The Quantum Theory on Nonrelativistic Collisions*. Wiley, New York, 1972.

[23] R. G. Newton. *Scattering Theory of Waves and Particles*. Springer, New York, second edition, 1982.

[24] R. Dum, A. Sanpera, K.-A. Suominen, M. Brewczyk, M. Kus', K. Rzazewski, and M. Lewenstein. Wave packet dynamics with Bose-Einstein condensates. *Phys. Rev. Lett.*, 80:3899–3902, 1998.

[25] L. Zhou, X. Huang, and C. T. Chan. A time-dependent Green's function approach to study the transient phenomena in metamaterial lens focusing. *Photonics Nanost. Fund. Appl.*, 3:100–106, 2005.

[26] R. P. Feynman and A. R. Hibbs. *Quantum Mechanics and Path Integrals*. McGraw-Hill, New York, 1965.

[27] R. P. Feynman. Space-time approach to non-relativistic quantum mechanics. *Rev. Mod. Phys.*, 20:367–403, 1948.

[28] K. Chadan and P. C. Sabatier. *Inverse Problems in Quantum Scattering Theory*. Springer, New York, second edition, 1989.

[29] O. Chuluunbaatar, A. A. Gusev, A. G. Abrashkevich, A. Amaya-Tapia, M. S. Kaschiev, S. Y. Larsen, and S. I. Vinitsky. A program for computing energy levels, reaction matrix and radial wave functions in the coupled-channel hyperspherical adiabatic approach. *Comp. Phys. Comm.*, 177:649–675, 2007.

[30] V. Ledoux, M. Van Daele, and G. V. Berghe. CPM{P,N} methods extended for the solution of coupled channel Schrödinger equations. *Comp. Phys. Comm.*, 174:357–370, 2006.

[31] L. Gr. Ixaru. Exactly solvable coupled-channel Schrödinger equation. *Phys. Rev. A*, 77:064102 (4pp), 2008.

[32] F. A. Berezin and M. A. Shubin. *The Schrödinger equation*. Kluwer, Dordrecht, 1991.

[33] V. V. Dodonov and V. I. Man'ko. Evolution of multidimensional systems. Magnetic properties of ideal gases of charged particles. *Proc. Lebedev Phys. Inst.*, 183:182–286, 1987.

[34] C. Grosche and F. Steiner. *Handbook of Feynman path integrals*. Springer, Berlin, 1998.

[35] V. V. Dodonov, I. A. Malkin, and V. I. Man'ko. Integrals of the motion, Green functions, and coherent states of dynamical systems. *Int. J. Theor. Phys.*, 14:37–54, 1975.

[36] A. del Campo and J. G. Muga. Exact propagators for atom-laser interactions. *J. Phys. A: Math. Gen.*, 39:14079–14088, 2006.

[37] M. Doumica, F. Duboc, and F. Golsec. Simulation of laser beam propagation with a paraxial model in a tilted frame. *J. Comput. Phys.*, 228:861–880, 2009.

[38] W. van Dijk and Y. Nogami. Analytical approach to the wave function of a decaying quantum system. *Phys. Rev. C*, 65:024608 (14pp), 2002.

[39] A. I. Baz', Ya. B. Zel'dovich, and A. M. Perelomov. *Scattering, Reactions and Decay in Nonrelativistic Quantum Mechanics*. IPST, Jerusalem, 1969. Translated from Russian by Z. Lerman.

[40] I. M. Gelfand and B. M. Levitan. On the determination of a differential equation from its spectral function. *Izvest. Akad. Nauk. SSSR Math. Series*, 15:309–360, 1951.

[41] V. A. Marchenko. On reconstruction of the potential energy from phases of the scattered waves. *Dokl. Akad. Nauk SSSR*, 104:695–698, 1955.

[42] R. G. Newton and R. Jost. The construction of potentials from the s-matrix for systems of differential equations. *Nuovo Cim.*, 1:590–622, 1955.

[43] T. Fulton and R. G. Newton. Explicit non-central potentials and wave functions for given s-matrices. *Nuovo Cim.*, 3:677–717, 1956.

[44] H. V. von Geramb and H. Kholhoff. Nucleon-nucleon potentials from phase shifts and inversion. In von Geramb [159], pages 285–313.

[45] H. Kohlhoff and H. V. von Geramb. Coupled channels Marchenko inversion for nucleon-nucleon potentials. In von Geramb [159], pages 314–341.

[46] J. R. Cox. Many-channel Bargmann potentials. *J. Math. Phys.*, 5:1065–1069, 1964.

[47] F. Vidal and J. LeTourneux. Multichannel scattering with nonlocal and confining potentials. i. General theory. *Phys. Rev. C*, 45:418–429, 1992.

[48] J.-M. Sparenberg, B. F. Samsonov, F. Foucart, and D. Baye. Multichannel coupling with supersymmetric quantum mechanics and exactly-solvable model for Feshbach resonance. *J. Phys. A*, 39:L639–L645, 2006.

[49] B. F. Samsonov, J.-M. Sparenberg, and D. Baye. Supersymmetric transformations for coupled channels with threshold differences. *J. Phys. A*, 40:4225–4240, 2007.

[50] E. Witten. Dynamical breaking of supersymmetry. *Nucl. Phys. B*, 188:513–554, 1981.

[51] G. Darboux. Sur une proposition relative aux equations lineaires. *C. R. Acad. Sc. Paris*, 94:1343, 1882. Quoted in Ref. [160].

[52] L. Infeld and T. E. Hull. The factorization method. *Rev. Mod. Phys.*, 23:21–67, 1951.

[53] B. Mielnik and O. Rosas-Ortiz. Factorization: little or great algorithm? *J. Phys. A*, 37:10007–10035, 2004.

[54] A. A. Andrianov, N. V. Borisov, and M. V. Ioffe. Factorization method and Darboux transformation for multidimensional Hamiltonians. 61:1078–1088, 1984.

[55] A. A. Andrianov, N. V. Borisov, and M. V. Ioffe. The factorization method and quantum systems with equivalent energy spectra. *Phys. Lett.*, 105A:19–22, 1984.

[56] F. Cooper, A. Khare, and U. Sukhatme. *Supersymmetry in Quantum Mechanics*. World Scientific, Singapore, 2001.

[57] V. G. Bagrov and B. F. Samsonov. Darboux transformations, factorization, and supersymmetry in one-dimensional quantum mechanics. *Theor. Math. Phys.*, 104:1051–1060, 1995.

[58] B. F. Samsonov and I. N. Ovcharov. Darboux transformations and non-classical orthogonal polynomials. *Russ. Phys. J*, 38:58–65, 1995.

[59] I. Aref'eva, D. J. Fernández, V. Hussin, J. Negro, L. M. Nieto, and B. F. Samsonov, editors. *Progress in Supersymmetric Quantum Mechanics*, *special issue of J.Phys. A: Math. Gen.*, 37:10007-10458, 2004.

[60] B. N. Zakhariev and V. M. Chabanov. *Submissive Quantum Mechanics : New Status of the Theory in Inverse Problem Approach*. Nova Science, New York, 2008.

[61] A. A. Andrianov and A. V. Sokolov. Factorization of nonlinear supersymmetry in one-dimensional quantum mechanics i: general classification of reducibility and analysis of third order algebra. *J. Math. Sci.*, 143:2707–2722, 2007.

[62] A. A. Andrianov and A. V. Sokolov. Nonlinear supersymmetry in quantum mechanics: Algebraic properties and differential representation. *arXiv:hep-th/0301062*, 2003.

[63] A. A. Andrianov, M. V. Ioffe, and D. N. Nishnianidze. Polynomial SUSY in quantum mechanics and second derivative Darboux transformation. *Phys. Lett. A*, 201:103–110, 1995.

[64] A. Das, H. Falomir, J. Gamboa, and F. Mendez. Non-commutative supersymmetric quantum mechanics. *Phys. Lett. B*, 670:407–415, 2009.

[65] S. M. Klishevich and M. S. Plyushchay. Nonlinear supersymmetry, quantum anomaly and quasi-exactly solvable systems. *Nucl. Phys. B*, 606:583–612, 2001.

[66] A. A. Andrianov, M. V. Ioffe, and F. Cannata. Higher-order derivative SUSY in quantum mechanics with large energy shifts. *Mod. Phys. Lett. A*, 11:1417–1428, 1996.

[67] F. Cannata, M. V. Ioffe, and D. N. Nishnianidze. Two-dimensional Schrödinger Hamiltonians with effective mass in SUSY approach. *Ann. Phys.*, 323:2624–2632, 2008.

[68] L. E. Gendenshtein. Derivation of exact spectra of the Schrodinger equation by means of supersymmetry. *JETP Lett.*, 38:299–302, 1983.

[69] A. A. Andrianov, N. V. Borisov, M. V. Ioffe, and M. I. Eides. Supersymmetric mechanics: A new look at the equivalence of quantum systems. *Theor. Math. Phys.*, 61:965–972, 1984.

[70] B. F. Samsonov. SUSY transformations between digonalizable and non-diagonalizable Hamiltonians. *J. Phys. A: Math. Gen.*, 38:L397–L403, 2005.

[71] B. F. Samsonov and V. V. Shamshutdinova. Quadratic pseudosupersymmetry in two-level systems. *J. Phys. A: Math. Gen.*, 38:4715–4725, 2005.

[72] B. F. Samsonov. Spectral singularities of non-hermitian Hamiltonians and SUSY transformations. *J. Phys. A: Math. Gen.*, 38:L571L579, 2005.

[73] A. A. Andrianov, F. Cannata, and A. V. Sokolov. Non-linear supersymmetry for non-hermitian, non-diagonalizable Hamiltonians: I. general properties. *Nucl. Phys. B*, 773:107–136, 2007.

[74] A. A. Andrianov, F. Cannata, J.-P. Dedonder, and M. Ioffe. SUSY quantum mechanics with complex superpotentials and real energy spectra. *Int. J. Mod. Phys. A.*, 14:2675–2688, 1999.

[75] F. Cannata, G. Junker, and J. Trost. Schrödinger operators with complex potential but real spectrum. *Phys. Lett. A.*, 246:219–226, 1998.

[76] A. V. Sokolov, A. A. Andrianov, and F. Cannata. Non-hermitian quantum mechanics of non-diagonalizable Hamiltonians: puzzles with self-orthogonal states. *J. Phys. A: Math. Gen.*, 39:10207–10228, 2006.

[77] H. R. Jauslin. Exact propagator and eigenfunctions for multistable models with arbitrarily prescribed n lowest eigenvalues. *J. Phys. A: Math. Gen.*, 21:2337–2350, 1988.

[78] A. Inomata and G. Junker. Quasi-clasical path integral aproach to supersymmetric quantum mechanics. *Phys. Rev. A*, 50:3638–3649, 1994.

[79] D. S. Fine and S. F. Sawin. A rigorous path integral for supersymmetic quantum mechanics and the heat kernel. *Comm. Math. Phys.*, 284:79–91, 2008.

[80] C. V. Sukumar. Green's function, sum rules and matrix element for SUSY partners. *J. Phys. A: Math. Gen.*, 37:10287–10295, 2004.

[81] C. V. Sukumar. Supersymmetric quantum mechanics and the inverse scattering method. *J. Phys. A*, 18:2937–2955, 1985.

[82] A. A. Andrianov, F. Cannata, J.-P. Dedonder, and M. V. Ioffe. Second order derivative supersymmetry and scattering problem. *Int. J. Mod. Phys. A*, 10:2683–2702, 1995.

[83] J.-M. Sparenberg and D. Baye. Inverse scattering with singular potentials: A supersymmetric approach. *Phys. Rev. C*, 55:2175–2184, 1997.

[84] B. F. Samsonov and F. Stancu. Phase shift effective range expansion from supersymmetric quantum mechanics. *Phys. Rev. C*, 67:054005, 2003.

[85] D. Baye and J.-M. Sparenberg. Inverse scattering with supersymmetric quantum mechanics. *J. Phys. A*, 37:10223–10249, 2004.

[86] R. D. Amado, F. Cannata, and J.-P. Dedonder. Coupled-channel supersymmetric quantum mechanics. *Phys. Rev. A*, 38:3797–3800, 1988.

[87] R. D. Amado, F. Cannata, and J.-P. Dedonder. Formal scattering theory approach to S-matrix relations in supersymmetric quantum mechanics. *Phys. Rev. Lett.*, 61:2901–2904, 1988.

[88] R. D. Amado, F. Cannata, and J.-P. Dedonder. Supersymmetric quantum mechanics, coupled channels, scattering relations. *Int. J. Mod. Phys. A*, 5:3401, 1990.

[89] F. Cannata and M. V. Ioffe. Solvable coupled channel problems from supersymmetric quantum mechanics. *Phys. Lett. B*, 278:399–402, 1992.

[90] F. Cannata and M. V. Ioffe. Coupled-channel scattering and separation of coupled differential equations by generalized Darboux transformations. *J. Phys. A*, 26:L89–L92, 1993.

[91] J.-M. Sparenberg and D. Baye. Supersymmetry between phase-equivalent coupled-channel potentials. *Phys. Rev. Lett.*, 79:3802–3805, 1997.

[92] H. Leeb, S. A. Sofianos, J.-M. Sparenberg, and D. Baye. Supersymmetric transformations in coupled-channel systems. *Phys. Rev. C*, 62:064003 (5pp), 2000.

[93] B. F. Samsonov and A. A. Pecheritsin. Chains of Darboux transformations for the matrix Schrödinger equation. *J. Phys. A: Math. Gen.*, 37:239–250, 2004.

[94] D. Baye. Supersymmetry between deep and shallow nucleus-nucleus potentials. *Phys. Rev. Lett.*, 58:2738–2741, 1987.

[95] J.-M. Sparenberg and D. Baye. Supersymmetry between deep and shallow optical potentials for ^{16}O+^{16}O scattering. *Phys. Rev. C*, 54:1309–1321, 1996.

[96] B. F. Samsonov and F. Stancu. Phase equivalent chains of Darboux transformations in scattering theory. *Phys. Rev. C*, 66:034001 (12pp), 2002.

[97] A. Mostafazadeh. Pseudo-unitary operators and pseudo-unitary quantum dynamics. *J. Math. Phys.*, 45:932–946, 2004.

[98] B. M. Levitan and I. S. Sargsyan. *Introduction to spectral theory: selfadjoint ordinary differential operators.* American Mathematical Society, Providence, Rhode Island, 1975.

[99] B. M. Levitan. *Inverse Sturm-Liouville Problems.* Nauka, Moscow, 1984.

[100] A. G. Kostyuchenko and I. S. Sargsyan. *Distribution of eigenvalues. Selfadjoint ordinary differential operators.* Nauka, Moscow, 1979.

[101] P. Morse and H. Feshbach. *Methods of Theoretical Physics.* McGraw-Hill, New York, 1953.

[102] S. A. Rakityanskyy and S. A. Sofianos. Jost function for coupled partial waves. *J. Phys. A: Math. Gen.*, 31:51495175, 1998.

[103] C. V. Sukumar. Supersymmetric quantum mechanics of one-dimensional systems. *J. Phys. A*, 18:2917–2936, 1985.

[104] A. A. Andrianov, M. V. Ioffe, and V. P. Spiridonov. Higher-derivative supersymmetry and Witten index. *Phys. Lett. A*, 174:273–279, 1993.

[105] A. A. Andrianov and F. Cannata. Nonlinear supersymmetry for spectral design in quantum mechanics. *J. Phys. A: Math. Gen.*, 37:10297–10321, 2004.

[106] M. G. Krein. On a continual analogue of the Christoffel formula from the theory of orthogonal polynomials. *Dokl. Akad. Nauk SSSR*, 113:970–973, 1957.

[107] M. M. Crum. Associated Sturm-Louville systems. *Quarterly Journal of Mathematics*, 6:121–127, 1955.

[108] B. F. Samsonov. New possibilities for supersymmetry breakdown in quantum mechanics and second-order irreducible Darboux transformations. *Phys. Lett. A*, 263:274–280, 1999.

[109] B. K. Bagchi. *Supersymmetry in classical and quantum mechanics.* Monographs and surveys in pure and applied mathematics. Chapman and Hall/CRC, Boca Raton, 2001.

[110] A. V. Sokolov. *Quantum mechanics with nonlinear supersymmetry for one-dimensional Hermitian and non-Hermitian Hamiltonians.* PhD thesis, St.Petersburg State University, 2008. unpublished.

[111] V. G. Bagrov and B. F. Samsonov. On irreducible second-order Darboux transformations. *Russ. Phys. J*, 45:27–33, 2002.

[112] B. F. Samsonov. New features in supersymmetry breakdown in quantum mechanics. *Mod. Phys. Lett. A*, 11:1563–1567, 1996.

[113] F. Cannata, M. Ioffe, G. Junker, and D. Nishnianidze. Intertwining relations of non-stationary Schrödinger operators. *J. Phys. A: Math. and Gen.*, 32:35833598, 1999.

[114] V. Matveev and M. Salle. *Darboux transformations and solitons.* Springer, New York, 1991.

[115] A. R. Its and V. B. Matveev. Schrödinger operators with finite-gap spectrum and n-soliton solutions of the Korteweg-de-Vries equation. *Teoret. Mat. Fiz.*, 23:5168, 1975.

[116] F. Calogero and A. Degasperis. *Spectral Transform and Solitons. Tools to Solve and Investigate Nonlinear Evolution Equations.* North-Holland, Amsterdam, 1982.

[117] Yu. V. Pershin and B. F. Samsonov. Quantum dots created through spherically polarized nuclear spins. *Phys. E: Low Dim. Syst. Nanostru.*, 28:134–140, 2005.

[118] B. Dubrovin, I. Krichever, T. Malanuyk, and V. Makhankov. Exact solutions of non-stationary Schrödinger equation with self-consistent potentials. *Phys. Elem. Part. Nucl.*, 19:579621, 1988.

[119] B. F. Samsonov. Coherent states of potentials of soliton origin. *JETP*, 87:1046–1052, 1998.

[120] V. G. Bagrov, B. F. Samsonov, and L. A. Shekoyan. Coherent states of nonstationary soliton potentials. *Russ. Phys. J*, 41:60–66, 1998.

[121] S. Y. Dubov, V. M. Eleonskii, and N. E. Kulagin. Equidistant spectra of anharmonic oscillators. *JETP*, 102:814–825, 1992.

[122] I. S. Gradshteyn and I. M. Ryzhik. *Table of Integrals, Series, and Products*. Academic Press, New York, 6th edition, 2000.

[123] I. M. Gelfand and G. E. Shilov. *Generalized functions*. Academic press, New York, 1964.

[124] A. P. Prudnikov, Yu. A. Brychkov, and O. I. Marichev. *Integrals and series*. Nauka, Moscow, 1981.

[125] M. Znojil, editor. *Pseudo-Hermitian Hamiltonians in Quantum Physics*, *Czech. J. Phys.*, 55:1049-1192, Netherlands, 2005. Springer.

[126] C. M. Bender, J.-H. Chen, and K. A. Milton. PT-symmetric versus hermitian formulations of quantum mechanics. *J. Phys. A: Math. Gen.*, 39:16571668, 2006.

[127] D. Baye, G. Lévai, and J.-M. Sparenberg. Phase-equivalent complex potentials. *Nucl. Phys.*, A599:435–456, 1996.

[128] M. A. Naimark. *Linear differential operators*. Ungar, New York, 1967.

[129] M. V. Keldysh. On the eigenvalues and eigenfunctions of certain classes of nonselfadjoint equations. *Dokl. Akad. Nauk SSSR*, 77:11–14, 1951.

[130] V. B. Lidskiy. Summability of series in the eigenvectors of non-selfadjoint operators. *Dokl. Akad. Nauk SSSR*, 132:275–278, 1960.

[131] P. A. M. Dirac. Bakerian lecture. The physical interpretation of quantum mechanics. *Proc. Roy. Soc. A.*, 180:1–40, 1942.

[132] W. Pauli. On Dirac's new method of field quantization. *Rev. Mod. Phys.*, 15:175–207, 1943.

[133] T. D. Lee and G. C. Wick. Negative metric and the unitarity of the S-matrix. *Nucl. Phys. B.*, 9:209–243, 1969.

[134] L. Solombrino. Weak pseudo-hermiticity and antilinear commutant. *J. Math. Phys.*, 43:5439 (7pp), 2002.

[135] G. Scolarici and L. Solombrino. On the pseudo-hermitian nondiagonalizable Hamiltonians. *J. Math. Phys.*, 44:4450 (10pp), 2003.

[136] A. Mostafazadeh. Pseudo-hermiticity versus PT symmetry: The necessary condition for the reality of the spectrum of a non-hermitian Hamiltonian. *J. Math. Phys.*, 43:205 (10pp), 2002.

[137] T. Curtright and L. Mezincescu. Biorthogonal quantum systems. *J. Math. Phys.*, 48:092106 (35pp), 2007.

[138] B. F. Samsonov and P. Roy. Is the CPT norm always positive? *J. Phys. A: Math. Gen.*, 38:L249–L255, 2005.

[139] N. K. Nikolskiy. *Lectures on a shift operator*. Nauka, Moscow, 1980.

[140] A. Erdélyi, W. Magnus, F. Oberhettinger, and F. G. Tricomi. *Higher Transcendental Functions*. McGraw-Hill, New York, 1953.

[141] M. Abramowitz and I. A. Stegun. *Handbook of mathematical functions.* National Bureau of standards, Washington DC, 1964.

[142] N. Nygaard, B. I. Schneider, and P. S. Julienne. Two-channel R-matrix analysis of magnetic-field-induced Feshbach resonances. *Phys. Rev. A*, 73:042705 (10pp), 2006.

[143] H. T. C. Stoof, J. M. V. A. Koelman, and B. J. Verhaar. Spin-exchange and dipole relaxation rates in atomic hydrogen: rigorous and simplified calculations. *Phys. Rev. B*, 38:4688–4697, 1988.

[144] J. J. Sakurai. *Modern Quantum Mechanics*. Addison-Wesley, Reading, 1994.

[145] H. Feshbach. Unified theory of nuclear reactions. *Ann. Phys. (N. Y.)*, 5:357–390, 1958.

[146] H. Feshbach. A unified theory of nuclear reactions. II. *Ann. Phys. (N. Y.)*, 19:287–313, 1962.

[147] B. Marcelis, E. G. M. van Kempen, B. J. Verhaar, and S. J. J. M. F. Kokkelmans. Feshbach resonances with large background scattering length: interplay with open-channel resonances. *Phys. Rev. A*, 70:012701 (15pp), 2004.

[148] C. Zener. Non-adiabatic crossing of energy levels. *Proc. Roy. Soc. London A*, 137:696–702, 1932.

[149] P. J. Leo, C. J. Williams, and P. S. Julienne. Collisions properties of ultracold ^{133}Cs atoms. *Phys. Rev. Lett.*, 85:2721 (4pp), 2000.

[150] K. M. O'Hara, S. L. Hemmer, S. R. Granade, M. E. Gehm, J. E. Thomas, V. Venturi, E. Tiesinga, and C. J. Williams. Measurement of the zero crossing in a Feshbach resonance of fermionic ^{6}Li. *Phys. Rev. A*, 66:041401 (4pp), 2002.

[151] E. Arimondo, M. Inguscio, and P. Violino. Experimental determination of the hyperfine structure in the alkali atoms. *Rev. Mod. Phys.*, 49:31–75, 1977.

[152] R. G. Newton and R. Jost. The constructions of potentials from the s-matrix for systems of differential equations. *Nuovo Cim.*, 1:590–622, 1955.

[153] D. Baye. Phase-equivalent potentials for arbitrary modifications of the bound spectrum. *Phys. Rev. A*, 48:2040–2047, 1993.

[154] B. F. Samsonov. On the equivalence of the integral and the differential exact solution generation methods for the one-dimensional Schrödinger equation. *J. Phys. A: Math. Gen.*, 28:6989–6998, 1995.

[155] L. M. Delves. Effective range expansion of the scattering matrix. *Nucl. Phys.*, 8:358–373, 1958.

[156] R. G. Newton and Th. Fulton. Phenomenological neutron-proton potentials. *Phys. Rev.*, 107:1103–1111, 1957.

[157] V. Bargmann. Remarks on the determination of a central field of force from the elastic scattering phase shifts. *Phys. Rev.*, 75:301–303, 1949.

[158] V. G. J. Stoks, R. A. M. Klomp, C. P. F. Terheggen, and J. J. de Swart. Construction of high-quality NN potential models. *Phys. Rev. C*, 49:2950–2962, 1994.

[159] H. V. von Geramb, editor. *Quantum Inversion Theory and Applications*, volume 427 of *Lecture Notes in Physics*, Berlin, 1994. Springer.

[160] B. F. Samsonov. Distorsion of a phase space under the Darboux transformation. *J. Math. Phys.*, 39:967–975, 1998.